IMMUNOTHERAPY ON TRIPLE NEGATIVE BREAST CANCER

A University Thesis Presented to the Faculty

of

California State University, East Bay

In Partial Fulfillment

of the Requirements For the Degree

Master of Science in Biological Sciences

By

Golzar Hemmati

March, 2016

Abstract

The purpose of this research is to identify Triple Negative Breast Cancer (TNBC) therapeutic agents. Recent statistics showed that 20% of the breast cancer patients in the U.S. have been diagnosed with subtype TNBC (92736). Unfortunately, no promising therapeutic targets have been identified for its treatment. Our laboratory has previously shown that there is a correlation between high levels of MYC oncogene expression and poor prognosis. Pharmaceutical inhibition of MYC, a transcription factor that is thought to drive tumor development, is technically difficult, which excludes it as a direct therapeutic target.

This study focuses on an immunotherapeutic approach to treat or control TNBC tumor progression. In this study, we focus on the immune inhibitory checkpoint blockade of PD-L1, a promising anti-cancer therapeutic technique with the potential for more durable and objective response, higher efficacy, lower toxicity and lower risk of recurrence. This immunotherapeutic approach has recently been used in humans for treating various types of cancer, including melanoma, non-small cell lung carcinoma (NSCLC) and renal cell carcinoma (RCC).

The rationale of this approach is based on the ability of the immune system to attack tumor cells. Considering that tumor-infiltrating lymphocytes are one of the known clinical characteristics of TNBC, the inability of the immune system to fight against cancer is due to an immune resistance mechanism involved in cancer survival. The tumor-cancer cell interaction initiates an immunosuppressive pathway in infiltrating

lymphocytes, resulting in the inhibition of cytokine release and the attenuation of tumor specific T-cell activity. This effect is most likely mediated by immune inhibitory receptors expressed on TILs. Thus, targeting this immune inhibitory checkpoint is assumed to restore the patient's immune cell function and fight against breast tumors.

Programmed cell Death protein 1 (PD1) and its two best-characterized ligands, PD-L1and PD-L2 comprise one crucial immune checkpoint pathway. The PD-L1 is expressed in 50% of human solid tumors including melanoma, breast, lung, colon, ovarian, and likely accounts for immune tolerance. Moreover, recent studies show that this protein is highly expressed in TNBC. Despite these findings, the role of PD-L1 in TNBC immunosuppression and its corresponding molecular pathway are not yet clear. This research aimed to study the effect of PD1-PD-L mediated immunosuppression on TNBC tumor progression as well as recurrence. We also aimed to study the effect of secondary mutations on tumor progression, immune response, and immune inhibitory molecules expression.

In this study we unveiled the importance of PD-L1 expression on the myeloid cells for the effectiveness of anti-PD-L1 immune checkpoint blockade approach. We found that despite the lack of PD-L1 expression on MYC-driven tumor cells, anti PD-L1 treatment delayed tumor recurrence and primary tumor progression. We have shown that myeloid subpopulations, namely monocytes and PMNs, expressed PD-L1 and it is suggested that they exhaust tumor-specific $CD8^+$ T cells through the PD1immune inhibitory checkpoint pathway. Hence, the blockade of PD-L1 most likely restored the antitumor lymphocytes' function and caused the observed delay in tumor progression and

recurrence. We also found that line A tumor recruited neutrophils significantly more than line B and this population, after $CD4^+$ T cells, constituted the majority of the tumor-infiltrated immune cells in line A. Further analysis is required to ensure this difference in the neutrophil population is not due to the effect of secondary mutation(s).

We also found that PVR, another immune inhibitory ligand, was expressed significantly on the tumor cells as well as tumor-infiltrating myeloid cells and we postulate that PVR may be another candidate to be targeted alone or in combination with anti-PD-L1 to increase the effectiveness of an immunotherapy-based regiment for treatment of TNBC.

IMMUNOTHERAPY ON TRIPLE NEGATIVE BREAST CANCER

By

Golzar Hemmati

Approved: Date:

3/8/16

Andrei Goga, M.D, Ph. D.

3/11/16

Maria Gallegos, Ph.D.

2016 Mar. 11

Claudia Uhde-Stone, Ph.D.

Acknowledgments

First, I would like to thank Dr. Henok Eyob, a post-doctoral fellow, who helped provide this opportunity for me by initiating this project. Not only did he train me in the necessary techniques required for this project, including western blot and mouse handling, but he also sincerely supported and supervised me in times of need. His constructive discussions opened my horizon into the reality of science, which allowed me to experience in-depth thought and taught me to be patient in the path of science.

I would also like to thank, Drs. Julia Rohrberg, Andrew Beardsley and Olga Momcilovic for their continuous support, insightful conversations. I thank Dr. Dai Horiuchi for his critical and handy advice for troubleshooting. Finally, thanks to all members of the Andrei Goga and Mehrdad Matloubian labs for their assistance and support throughout the entire project.

Furthermore, I would like to thank Dr. Claudia Stone, my thesis committee member who enhanced my knowledge in cellular and molecular fields and facilitated the development of my abilities in analytical thinking.

I'm more grateful than ever for Dr. Maria Gallegos' support throughout my entire education in the U.S. She not only enriched my knowledge and taught me valuable skills but also assisted in acquiring this project. She constantly supported me and guided me through this project.

I believed the best opportunity I was given throughout my time in the U.S. was the chance of being mentored directly by Mehrdad. Learning from such a passionate and dedicated scientist who is not only always ready to train but also support in the times of need was paramount in my success. To name a few, I learned mouse-handling techniques and more importantly, all of the intricate details I learned about the FACS were because of Mehrdad. I never would have learned special ingenious techniques that I did unless I was ever trained directly by him.

Last but certainly not least; I would love to thank Andrei Goga, my major advisor, who graciously welcomed me into his lab. His support was always motivating. His passion and dedication for science inspired me. His fruitful discussion and leadership enlightened my scientific path.

Table of Contents

Abstract ii

Acknowledgments vi

List of Figures xi

List of Tables xvi

Chapter One Introduction 1
1.1 Neoplasm 1
1.1.1 Breast Cancer 2
1.1.1.1 Triple Negative Breast Cancer Subtype, Clinical Characteristics 4
1.1.1.2 Tumor-Infiltrating Lymphocytes (TIL) in TNBC 8
1.2 MYC and Breast Cancer Development 9
1.3 Cancer Immunotherapy 14
1.3.1 Immune Checkpoints 18
1.3.1.1 PD-L1 and Its Role in Immune Tolerance 21
1.3.2 Immune Checkpoints Blockade 24

Chapter Two Background Data 30
2.1 MYC-Driven MTB/TOM Mouse Model 30
2.2 MTB/TOM Tumor Development 32
2.3 MYC Expression Upon MYC Withdrawal 32
2.4 Tumor Growth Study in Lines A and B 33
2.5 Sequence Analysis 35

Chapter Three Materials and Methods 39
3.1 Studying The Tumor Progression And Recurrence of MTB/TOM Tumor Breast-Transplanted Mouse Models 39
3.1.1 Line B Tumor Recurrence 39
3.2 Leukocyte Isolation From Tumor-Burden Mice 40
3.2.1 Line A Tumor Progression and Recurrence upon Anti-PD-L1 Antibody Treatment 40
3.2.2 Tumor-Infiltrating Leukocyte Isolation From MYC-Induced Breast Tumors Using Density Gradient Centrifugation Technique 42
3.2.3 Spleen Leukocytes Isolation 44
3.3 Immunoinhibitory Ligands and Receptor Staining of Myeloid Cells 44
3.3.1 Isotype Control Antibody Staining 45
3.3.2 Immune Inhibitory Ligands' Antibody Staining 46

3.3.3 Immune Inhibitory Receptors' Antibody Staining 47
3.3.4 Compensation 48
3.3.4.1 Single-Color Antibody Staining for Compensation 49

Chapter Four Results 51
4.1 Aim 1: Determine Whether The PD-L1 Expression, If There Is Any, Is Regulated By MYC 51
4.1.1 Tumor Cells (Both A Line And B Line) Do Not Express PD-L1 And The Expression Of PD-L1 Is Not Regulated By Transcription Factor MYC 51
4.2 Aim 2: Targeting PD-L1 Ligand Through Anti-PD-L1 Antibody To Study The Effect Of PD1-PD-L1 Mediated Immunosuppression Pathway On TNBC Tumor Progression And Recurrence 56
4.2.1 Anti-PD-L1 Therapy Slowed MYC-Driven Breast Tumor Growth 56
4.2.2 Anti-PD-L1 Therapy Delayed Recurrence Of MYC-Driven Breast Tumor Growth 59
4.2.2.1 PD-L1 Was Expressed On Tumor-Associated Myeloid Cells Of Both Primary Tumors And Recurred Tumors But NOT On The Tumor Cells 63
4.2.2.2 Collagenase Treatment Had No Effect On Detected PD-L1 Expression On Tumor Cells 72
4.2.3 Kinetics Of The Immune Response Upon Acute MYC Withdrawal 75
4.2.3.1 FACS Data Analysis Showed Tumor Regression Four Days After MYC Withdrawal 76
4.2.3.2 Immune Cell Population Is Dynamic Within The Body And There Is A Correlation Between Lymphocyte Populations Of Spleen And Tumor: As One Change, The Other Changes 78
4.2.3.3 Both PD1 And TIGIT Are Significantly Expressed On Tumor-Infiltrating $CD8^+$ T Cells But Only The Level Of PD1 Expression Elevated In The Infiltrated $CD8^+$ T Cell Subset Upon Regression 83
4.3 Aim 3: Investigating Other Immune Checkpoints Expressed On Tumor Cells To Target In MYC-Driven TNBC. 86
4.3.1 PVR Is Highly Expressed On Tumor-Associated Myeloid Cells As Well As On The Tumor Cells 86
4.3.2 PVR Expression On Tumor Cells Is Not Regulated By MYC Induction *In Vitro* 89
4.3.3 PVR Was Also Expressed On Tumor-Associated Myeloid Cells Of Recurred Tumor Regardless Of The Tumor Type 91
4.4 Aim 4: Can Secondary Mutation In Primary Tumors Cooperate With MYC And Alter Immune Response To The Both Primary And Recurred Tumor? 95
4.4.1 Tumor Recurrence Pattern Was Different Between Line A And B 96
4.4.2 The Spleen In Line A And B Was Different In Terms Of Size And Total Number Of Immune Cells 98

4.4.3 Immune Phenotype Of Both Spleen And Tumor Of These Two Lines Showed Some Differences That Can Be Associated With Differences In The Immune Response 102
4.4.3.1 Immune Cell Composition Within The Spleen Changed Upon Tumor Response. These Changes Differed From Line To Line. 109
4.4.3.2 The Spleen Enlargement In Line A Is Due To The Increase In The Total Number Of All Immune Cells But Mostly PMNs And $CD4^+$ T Cells 112
4.4.4 Line A/B Tumor-Associated Myeloid Cells 122
4.4.4.1 Depending On The Stage Of The Growth And The Type Of The Tumor, Tumors Displayed Different Infiltrating Immune Cells Phenotypes. Line A Attracts PMNs More Than Line B At The Primary Stage 122
4.4.4.2 Line A Tumor Constituted Of More Immune Cells, Lymphocytes And Myeloid Cells Compared To Line B, Regardless Of The Stage Of The Tumor Growth. Line A Exclusively Had More PMNs And $CD4^+$ T Cells Than Line B At The Primary Stage. 125
4.4.5 The Tumor-Infiltrating T Cell Subsets Of Both Lines Displayed The Same Phenotype In Terms Of The Expression Of Immune Inhibitory Molecules Of TIM3, PD1 And TIGIT In The Primary Tumor. Both Lines Are Different At The Recurred Stage In Regards To The Level Of Expression Of These Receptors 136

Chapter Five Discussion and Conclusion 151
5.1 Conclusion 174
5.2 Future Directions 175

References 177

List of Figures

Figure 1. Estimated Number Of New Cancer Cases And Deaths By Sex Within The United States In 2015 4

Figure 2. Breast Cancer Subtypes And Their Prevalence Within The Population 5

Figure 3. Survival Rate Of Breast Cancer Subtypes. 7

Figure 4. The Tumor Lymphocytes' ($CD4^+$ And $CD8^+$ T Cells) Density Is Correlated Within The Overall Survival Of Breast Cancer Patients. 9

Figure 5. Myc Family Protein Structure. 10

Figure 6. MYC Induces Tumorigenesis Through Transcriptionally Activating A Wide Variety Of Tumor Promoting Genes 11

Figure 7. MYC Activated Cellular Functions Contribute To Tumor Development 12

Figure 8. MYC Overexpressed In Human TNBC Versus Receptor Positive Ones. 13

Figure 9. Cancer-Immunity Cycle 16

Figure 10. Effector T Cells Activation Upon Tumor Antigen Stimulation And Their Antitumor Immune Response 17

Figure 11. Immune Inhibitory Receptors Inhibit T Cells' Function Through Two Mechanisms 19

Figure 12. Immune Inhibitory And Stimulatory Receptors; Interaction With Their Ligands 20

Figure 13. PD1-PDL Mediated Pathway Induces T-Cell Attenuation And Immune Tolerance 23

Figure 14. The CTLA-4 Immunosuppressive Pathway And The Effect Of Its Blockages On Reactivation Of T Cells' Function 25

Figure 15. Targeting PD-L1 To Reactivate T Cells 27

Figure 16. TCGA Database Of Immune Inhibitory Checkpoints Ligands mRNA Expression In TNBC Versus Other Subtypes Of Cancer 28

Figure 17. Schematic Showing The Procedure To Develop Tet-Inducible MTB/TOM Transgenic Mouse Model 31

Figure 18. MYC Inducible MTB/TOM Mouse Model 31

Figure 19. MYC Expression In The Beast Tumor Of MTB/TOM Mouse Model 32

Figure 20. Tumor Progression Graphs Of Line A And B 34

Figure 21. PI3k / Akt Signaling Pathway 36

Figure 22. Kras-Mediated Signaling Pathway 38

Figure 23. Developing Breast Tumor In FVB Mouse Through Serial Transplantation Of MTB/TOM Breast Tumor Line A/B Into Their Mammary Fat Pad 40

Figure 24. Flow Cytometry Histograms Representative Of PD-L1 Expression On Epcam^{+} And Epcam^{-} Cells Of Line A Recurred Tumor Stained By Anti-PD-L1(Red) And Isotype Control Antibody (Grey) 52

Figure 25. The Quantified MFI Of PD-L1 Expression On Epcam^{+} Cells Of Both A Line And B Line 53

Figure 26. Flow Cytometry Histogram Representative Of PD-L1 Expression On Epcam^{+} CD45^{-} And Epcam$^{lo\text{-}Int}$ CD45^{-} Cells Of Line A Regressed Tumor Stained By Anti-PD-L1 (Green And Orange) And Isotype Control Antibody (Blue And Red) 55

Figure 27. Growth Curve Of Primary Tumor Of Line A 58

Figure 28. Survival Curve Of Primary Tumor-Bearing Mice 59

Figure 29. Growth Curve Of Primary Tumor Of Line A Upon MYC Withdrawal 61

Figure 30. Survival Curve Of Recurred Tumor-Bearing Mice. Red: primary tumor of A line treated with anti-PD-L1 62

Figure 31. Gating Procedure And Flow Cytometry Histogram Representative Of PD-L1 Expression On Different Myeloid Cell Populations As Well As Epcam^{+} And Epcam$^{lo\text{-}Int}$ Cells 64

Figure 32. Comparison Of The Level Of PD-L1Expression On Myeloid Subpopulations Between The Naïve Spleen, Spleen Of Primary Tumor And Primary Tumor Of Line A 68

Figure 33. Comparison Of The Level Of PD-L1Expression On Myeloid Subpopulations Between The Naïve Spleen, Spleen Of Recurred Tumor And Recurred Tumor Of Line A 71

Figure 34. Effect Of Collagenase Treatment On PD-L1 Expression On Different Myeloid Subpopulations 74

Figure 35. FACS Gating On Tumor Infiltrated Immune Cells, CD45+, And Tumor Cells, Epcam+, And Their Percentage On Primary Tumor And Regressed Tumor 76

Figure 36. The Total And Average Number Of Spleen Lymphocytes In The MYC-Driven Tumor And Regressed Tumor (Two Days And Four Days After MYC Withdrawal) 79

Figure 37. The Total And Average Number Of Tumor-Infiltrating Lymphocytes In The MYC-Driven Tumor And Regressed Tumor (Two Days And Four Days After MYC Withdrawal) 80

Figure 38. Total Number Of Tumor-Infiltrating Myeloid Populations In The Primary Tumor And Regressed Tumor, Two Days And Four Days After MYC Withdrawal 82

Figure 39. MFI Of PD1 Expression On Spleen/Tumor Infiltrating Lymphocytes On MYC-Driven Tumor And Regressed Tumor (2 Days And Four Days After MYC Withdrawal) 85

Figure 40. The Quantified MFI Of PD-L1 Expression On Tumor-Infiltrating Myeloid Populations At The Primary Tumor And Regressed Tumor, Two Days And our Days After MYC Withdrawal 86

Figure 41. The Quantified MFI Of PVR Expression On $Epcam^+$ Cells Of Both A Line And B Line At Their Recurred Stage Stained With Isotype Control Antibody And PVR Antibody 88

Figure 42. Flow Cytometry Histogram Representative Of PVR Expression On $Epcam^+$ And $Epcam^-$ Cells Of Line A Recurred Tumor Stained By Anti-PVR (Red) And Isotype Control Antibody (Grey) 89

Figure 43. Flow Cytometry Histogram Representative Of Epcam And PVR Expression On Isolated Tumor Cells Grown In Culture 90

Figure 44. Representative Flow Cytometry Histograms Of PVR Expression Of Tumor-Infiltrating Myeloid Cells (Monocytes And Dendritic Cells) 91

Figure 45. The Quantified MFI Of PVR Expression On Tumor-Infiltrated Myeloid Cells of Both A Line And B Line at Their Recurrent Stage Only 94

Figure 46. Tumor Recurrence of Lines A And B After Dox Withdrawal 97

Figure 47. Spleens Of Tumor-Bearing Mice Of Line A And B At Their Recurred Stage 99

Figure 48. Total Number Of Viable Cells In The Spleen Of Recurred Tumor Line A And B 100

Figure 49. Total Number Of Viable Cells In The Spleen Of Recurred Tumor Line A And B 101

Figure 50. Gating Procedures to Detect Myeloid Subsets of Spleen and Tumor on FACS 103

Figure 51. Gating Procedures To Detect Lymphocytes Subpopulations Of Spleen And Tumor On FACS 109

Figure 52. The Comparison of The Distribution of Immune Subpopulations in The Spleens 111

Figure 53. Total Number Of $CD4^+$ And $CD8^+$T Cells Isolated From Spleens Of Both A Line And B Line Tumor-Bearing Mice At Both The Recurred Stage And Primary Stage Of Tumor Growth 115

Figure 54. Total Number Of CD11b And CD11c Cells Isolated From Spleens Of Both A Line And B Line Tumor-Bearing Mice At Both The Recurred Stage And Primary Stage Of Tumor Growth..... 118

Figure 55. Total Number Of PMN And Monocytes Isolated From Spleens Of Both A Line And B Line Tumor-Bearing Mice At Both The Recurred Stage And Primary Stage Of Tumor Growth 121

Figure 56. The Comparison Of Demography Of Immune Subpopulations Of Tumors . 124

Figure 57. Total Number Of $CD4^+$ And $CD8^+$ T Cells Isolated From Tumors Of Both A Line And B Line Tumor-Bearing Mice At Both The Recurred Sage And Primary Stage Of Tumor Growth 128

Figure 58. Total Number Of CD11b And CD11c Isolated From Tumors Of Both A Line And B Line Tumor-Bearing Mice At Both The Recurred Stage And Primary Stage Of Tumor Growth 131

Figure 59. Total Number of PMN and Monocytes Isolated from Tumors of both A Line and B Line Tumor-Bearing Mice at both The Recurred Stage and Primary Stage of Tumor Growth..... 134

Figure 60. TCGA Database Of Immune-Inhibitory Checkpoints Ligands mRNA Expression In TNBC Versus Other Subtypes Of Cancer 139

Figure 61. Flow Cytometry Histogram Representative Of PD1, TIM3 And TIGIT Expression On $CD4^+$ T Cells And $CD8^+$T Cells By Anti-PD1, Anti-TIM3 And Anti-TIGIT (Green), Respectively 140

Figure 62. Comparing The TIGIT Inhibitory Receptor Expression On Lymphocytes' Population Of $CD4^+$ And $CD8^+$ T Cells Between Line A And B 143

Figure 63. Comparing The TIM3 Inhibitory Receptor Expression On Lymphocytes' Population Of $CD4^+$ And $CD8^+$ T Cells Between Line A And B 146

Figure 64. Comparing The PD1 Inhibitory Receptor Expression On Lymphocytes' Population Of $CD4^+$ And $CD8^+$ T Cells Between Line A And B 149

Figure 65. Schematic Of Different Cancer Immunotherapy Approaches According To The Tumor Characteristics 160

Figure 66. The Suggested Molecular Mechanism Underlying The TIGIT-Mediated TIL Inhibition..... 162

Figure 67. The Model For Monocyte Recruitment To The Solid Tumor Hypoxic Areas 165

Figure 68. The Mechanism Of Neutrophil-Mediated Tumor Progression And Metastasis..... 170

List of Tables

Table 1. Next generation sequencing data analysis of lines A and B……35

Table 2. The wells with seeded cells and their applied staining set per sample……48

Table 3. The spleen cells stained with different antibodies for compensation……..50

Chapter One

Introduction

1.1 Neoplasm

Neoplasm or cancer is the abnormal proliferation of cells, which then poses the capability of spreading to distant locations other than the primary site. Cancer is initiated by transformation of at least one single cell from its normal state to the neoplastic state. The transition to neoplastic state is a multistage process in which the cell aberrantly grows and skips the cell cycle checkpoints and apoptosis (Cooper and Hausman 2007). The underlying reason for cancer development hasn't been discovered yet, however, a myriad of studies have characterized cancer with both the loss of cell cycle regulators and the accumulation of gene mutations (Tian et al. 2011).

Going through these evolutionary steps from normal state to the cancerous one, the cell acquires eight capabilities that enable the cells to become tumorigenic. These hallmark capabilities are: sustaining proliferative signaling, resisting cell death, evading growth suppressors, inducing angiogenesis, activating invasion and metastasis, enabling replicative immortality, reprogramming of energy metabolism, and evading immune destruction (Hanahan and Weinberg 2011).

To gain each of these eight traits, the cancer cell takes several different approaches. For example, to sustain proliferative signaling, the cancer cell up-regulates growth factor receptors to become hyper responsive to the limited number of growth factors' signaling or to stimulate adjacent normal cells to release growth factors to feed cancer cells (Cheng et al. 2008; Bhowmick, Neilson, and Moses 2004). To resist cell death, tumor cells up-regulate anti-apoptotic regulators such as Bcl-2 and Bcl-xL or down regulating pro-apoptotic factors including Bax, Bim, Puma (Hanahan and Weinberg 2011).

1.1.1 Breast Cancer

Cancer can be classified into a wide variety of types based on the original tissue and compartment of the tissue from which the cancerous cells originate. Breast cancer is caused, specifically, by the abnormal growth of breast tissue compartments, the epithelial cells of ducts or lobules. This leads to the advent of ductal carcinoma or lobular carcinoma respectively (Alteri, Rick; Barnes, Cammie MBA; Adriane Burke, MPH; Ted Gansler, MD, MPH; Susan Gapstur, PhD; Mia Gaudet, PhD; Joan Kramer, MD; Lisa A Newman, MD, MPH; Dearell Niemeyer, MPH; Cheri Richards, MS; Carolyn Runowicz, MD; Debbie Saslow, PhD; Scott Simpson 2014).

Other than the histology of the original cancer cell, breast cancer itself may also be subcategorized into five different subtypes according to the expression of cell receptors. Each receptor is responsive to one hormone that stimulates the growth within the targeted cell (Sotiriou and Pusztai 2009).

1) Estrogen receptor-positive (ER^+) is a subtype of breast cancer that expresses estrogen receptors

2) Progesterone receptor-positive (PR^+), is a subtype of breast cancer that expresses progesterone receptors

3) HER2/neu receptor-positive, is a subtype of breast cancer that displays human Receptor tyrosine-protein kinase erbB-2

4) Triple negative (TN) is a subtype that does not express any of the receptors for estrogen, progesterone and HER2 and

5) Triple positive is a subtype that expresses all three receptors of estrogen, progesterone and HER2.

Breast cancer is one of the most common types of cancer among women in the United States. According to the American Cancer Society, in 2015, approximately 231,840 (29%) of new cases of breast cancer were estimated to be diagnosed solely among women. Having one of the highest fatality rates among all cancer types, in 2015 breast cancer alone is estimated to lead to over 40,000 deaths (Figure 1) (DeSantis, Siegel, and Jemal 2013).

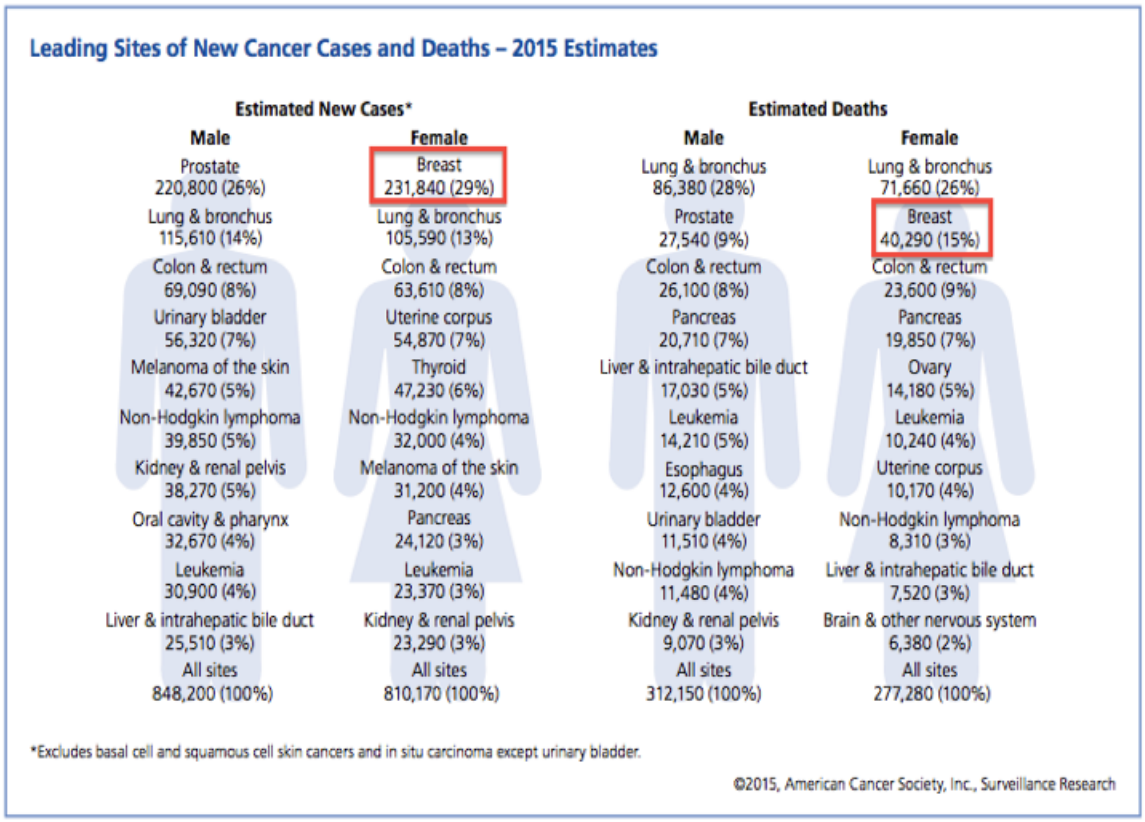

Figure 1. Estimated Number Of New Cancer Cases And Deaths By Sex Within The United States In 2015 (DeSantis, Siegel, and Jemal 2013).

1.1.1.1 Triple Negative Breast Cancer Subtype, Clinical Characteristics

Among all subtypes of breast cancer, TNBC is one of the most challenging subtypes in regards to finding a promising therapeutic approach. Firstly, because other subtypes of breast cancers display at least one hormonal receptors that is overexpressed. This overexpressed hormone receptor causes an influx of hormonal signals to the cell to proliferate. The overexpressed hormone-dependent receptors in breast tumor cells are generally used as biomarkers, candidate molecules, for identifying and successfully

developing an effective targeted therapy against them (i.e. anti-hormonal therapy, or inhibitory monoclonal antibodies). However, TNBC cannot be treated through the receptor targeting approach due to the lack of the expression of the receptors (Livasy et al. 2006; Sierra et al. 1999).

Second, this subtype of cancer is the second most common type of breast cancer and constitutes 15-20% of the all diagnosed breast cancer cases (Figure 2). Third, this subtype of cancer is characterized by high metastatic rate, high aggressiveness and invasiveness as well as poorest outcomes compared to other types of breast cancers. All of these important features about the TNBC highlight the urgency in finding a promising therapeutic target for this subtype of breast cancer (D. Horiuchi et al. 2012).

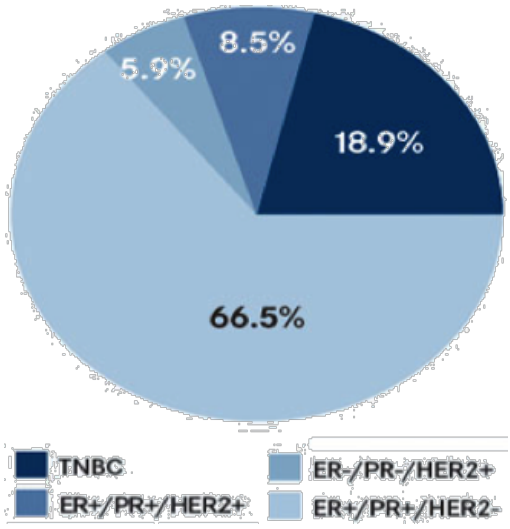

Figure 2. Breast Cancer Subtypes And Their Prevalence Within The Population (Voduc et al. 2010; Cheang et al. 2009).

One of the important characteristics of TNBC is its overall poor outcome that worsens as the tumor progresses from stage one to four. There are four main stages through which breast cancer progresses. If the cancer only grows in the local breast tissues from which it is originates the cancer is at stage 1. As the cancer spreads beyond the local breast tissue (i.e. to the lymph node), the breast cancer is staged as 2 or 3, depending on the level of progression. Eventually, the cancer reaches stage 4, the most advanced form, when the tumor undergoes metastasis. Among all types of the breast cancer, TNBC has the poorest outcome if it is at stage 4 (Bauer et al. 2007; Dent et al. 2007).

Additionally, another important distinguishing feature of TNBC is the correlation between the stage of the cancer and survival rates of the cancer patients. As the cancer progresses from stage one to four, the five-year overall survival rate of the patient will decrease. TNBC has one of the lowest five-year survival rates amongst other subtypes that drop sharply from 100% to 22% within five years if it is diagnosed at stage 4 (Figure 3A) (Bauer et al. 2007; Dent et al. 2007). Studies show that in the first 5 years, TNBC and HER^{+} subtypes have a sharp decrease in their overall survival rate and an increased risk of death, whereas the survival rate for other subtypes of the breast cancer drop only 5% within the first five years of treatment (Figure 3B) (Steward et al. 2014).

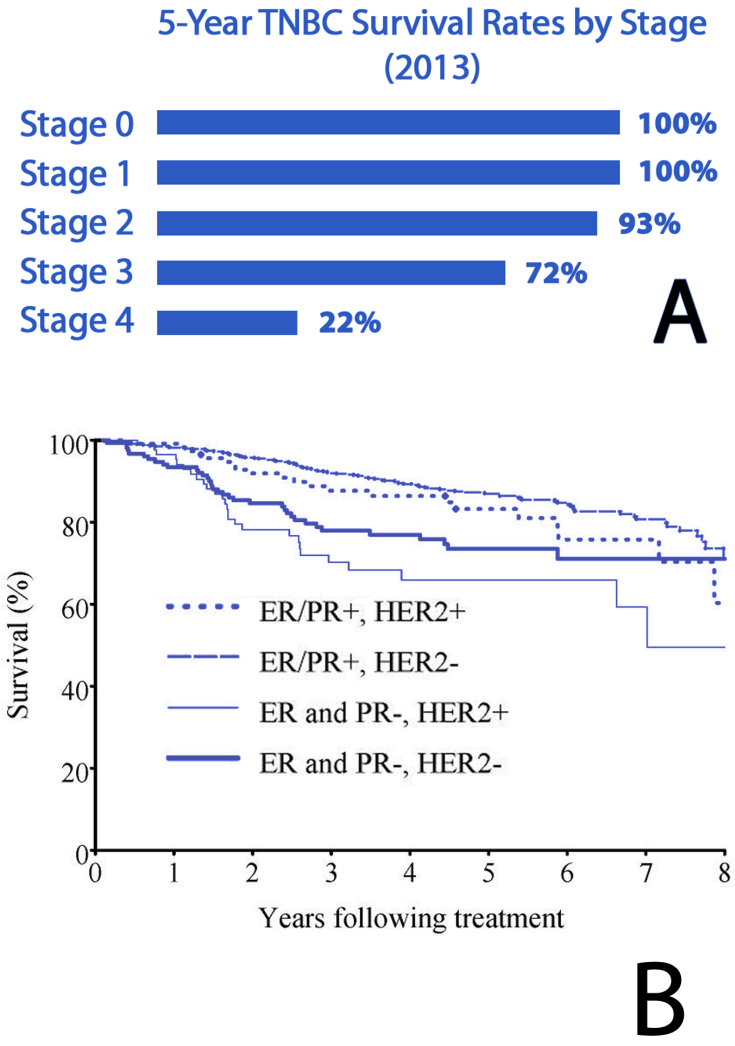

Figure 3. Survival Rate Of Breast Cancer Subtypes. A: Comparison of survival rate in five different subtypes of breast cancer. TNBC and $HER2^{+}$ have the lowest survival rate in the first five-years among others. B: Five-year survival rate of TNBC according to the stage at time of diagnosis (Carey et al. 2006; Legouy et al. 1987; Zimmerman et al. 1990, Onitilo et al. 2009).

TNBC is also characterized by its higher rate of recurrence in the first three years of diagnosis (Carey et al. 2006). Although patients with TNBC do respond to

neoadjuvant chemotherapy effectively, no complete pathological response can be achieved because of high metastatic rate. About 25% of TNBC patients will experience tumor recurrence, which will result in a death rate of 75% after treatment (Steward et al. 2014).

Therefore, understanding the molecular pathways of TNBC is of fundamental importance, enabling us to identify therapeutic targets with profound clinical implications.

1.1.1.2 Tumor-Infiltrating Lymphocytes (TIL) in TNBC

Tumor-infiltrating lymphocytes, the immune cells within the tumor tissue, is a well-known characteristic of TNBC and is employed as a prognostic factor for studying TNBC therapeutic efficiency (Fridman et al. 2011). A recent study on TNBC patients has shown the correlation between the abundance of intratumoral $CD4^+$ and $CD8^+$ T cell population and better clinical outcomes (Figure 4) (Liu, Lachapelle, and Leung 2012). Taken together, these studies suggest that among all subtypes of breast cancer, TNBC appears to be the most responsive subtypes to immunotherapies (Stagg and Allard 2013). Knowing the immune infiltrated profile of the TNBC tumor more easily enables us to recognize the immune events within the tumor's microenvironment. It also helps us learn how to harness the immune system to improve the TNBC prognosis and response to therapeutics.

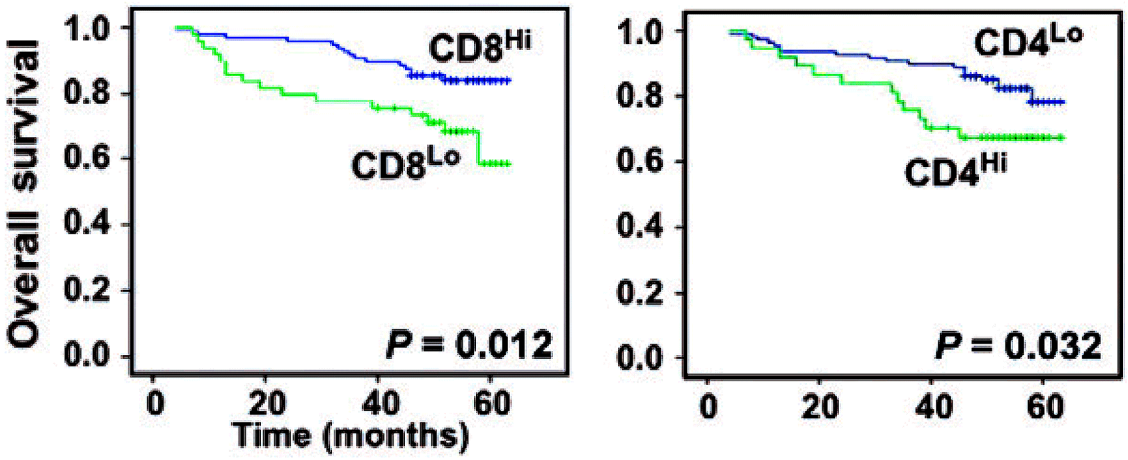

Figure 4. The Tumor Lymphocytes' ($CD4^+$And $CD8^+$ T Cells) Density Is Correlated With The Overall Survival Of Breast Cancer Patients. Patients with high rate of tumor-infiltrating $CD8^+$ T cells and low density of $CD4^+$ T cells survived longer. The overall survival of the breast cancer patients with high density of TILs decreased by only 10 % in the first five years while it decreased by 30-40 % for the breast cancer patients with low density TILs (DeNardo, 2011).

1.2 MYC and Breast Cancer Development

MYC is an oncoprotein transcription factor that can be expressed by three distinct gene family members in mammalian cells namely: c-MYC, n-MYC, l-MYC (Tansey 2014). While these three types of MYC protein have almost the same function, their level of expression and their patterns are different from one cell to another (Strieder and Lutz 2002).

MYC protein structure, similar to many other transcription factors, contains three main domains including, Transcriptional activator domain, DNA binding domain (DBD) and canonical nuclear localization sequence (N). MYC needs to interact with MAX

protein, to be able to bind to DNA and act as a transcription factor (Figure 5) (Tansey 2014). This heterodimerization is also important for oncogenicity of MYC (Amati, Littlewood, et al. 1993; Amati, Brooks, et al. 1993).

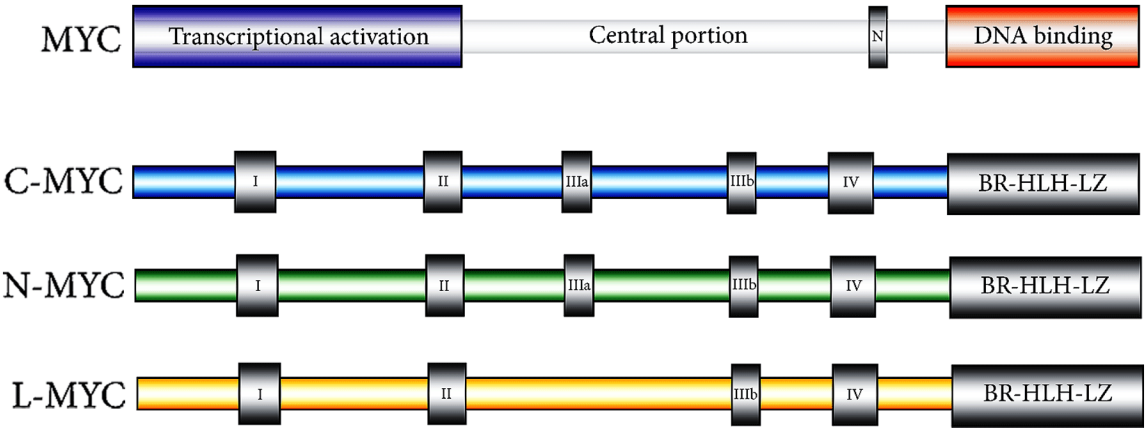

Figure 5. Myc Family Protein Structure. The top image shows four main domains that are common in mammalian MYC protein, including the transcriptional activation domain, the central portion, the nuclear localization sequence (N), and the DNA binding which is needed to interact with MAX. Images below are a representation of conserved regions in C-MYC, N-MYC, and L-MYC family members (Tansey 2014).

MYC as a transcription factor can regulate the expression of hundreds of genes directly or indirectly (up to 15% of the human genes) (Dang et al. 2006). The functionally critical genes in turn coordinate a wide variety of cellular functions as well as intracellular signaling pathways including DNA replication, protein transcription and even regulation of gene expression. Consequently, MYC is directly or indirectly involved in proliferation, apoptosis, differentiation, self-renewal and senescence, metabolism, angiogenesis, cell survival and cell growth (Figure 6) (Felsher 2010).

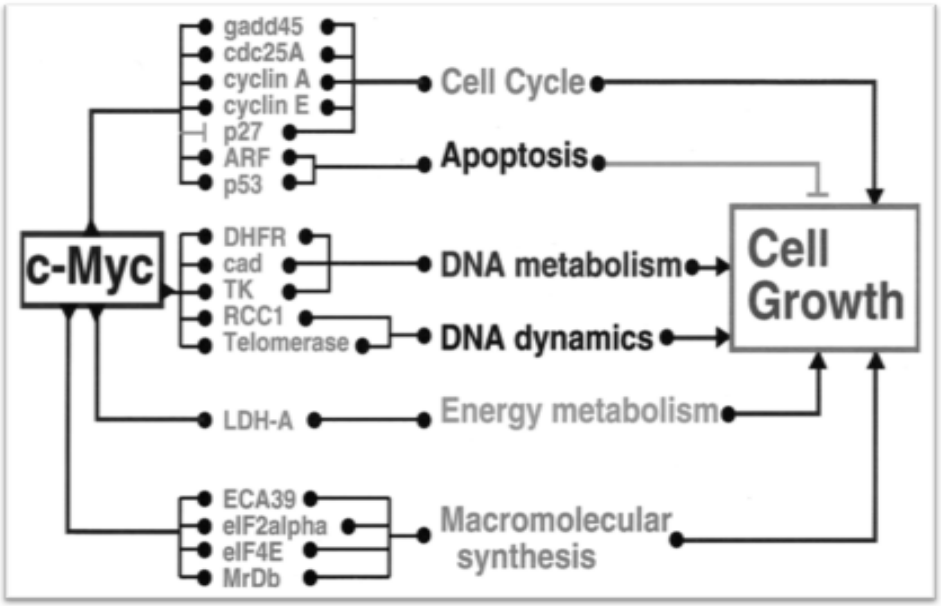

Figure 6. MYC Induces Tumorgenesis Through Transcriptionally Activating A Wide Variety Of Tumor Promoting Genes.

MYC is regulated at the levels of transcription, translation and posttranslational modification (Xu, Chen, and Olopade 2010). Studies showed that any deregulation or mutation in MYC that drives MYC constitutive expression, could result in tumorgenesis (Felsher 2010; Tansey 2014).

MYC mediates tumorgenesis through activating the genes involved in four different cellular functions, namely, cell cycle progression and proliferation, cell metabolism, cell microenvironment and cell growth (Figure 7) (Tansey 2014). The changes in the above-mentioned cellular functions along with disturbance of genome stability, results in aberrant proliferation, promotes cell to proliferate and switches the cell from normal state to the cancerous one, thus initiating tumorgenesis.

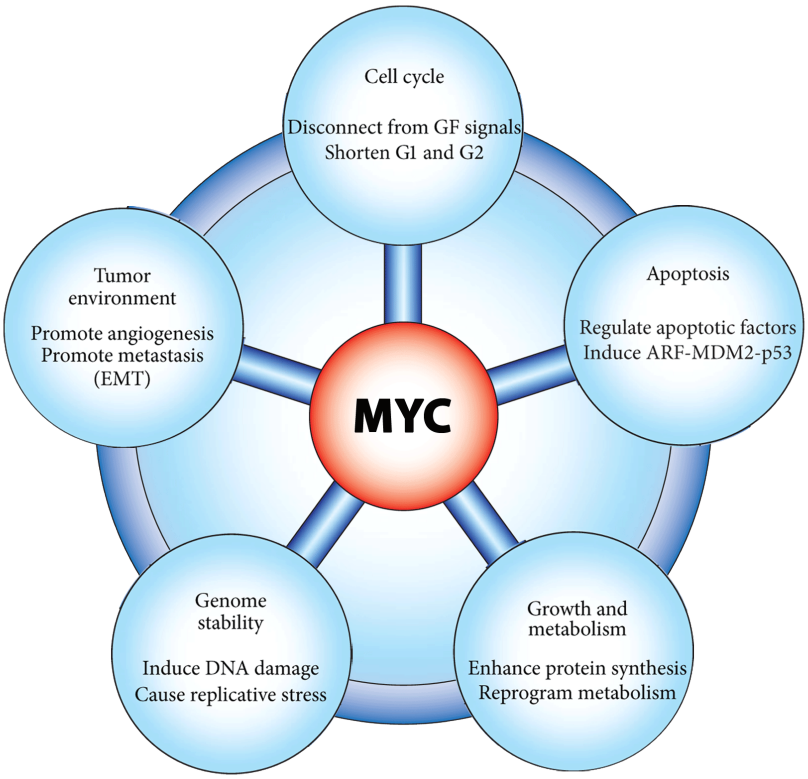

Figure 7. MYC Activated Cellular Functions Contribute To Tumor Development (Tansey 2014).

Overexpression of c-MYC is broadly observed in distinct types of tumors including solid and blood-borne tumors (Tansey 2014). Two other types of MYC are also frequently expressed in different types of cancers; n-MYC is highly expressed in solid tumors originating from neural system (Strieder and Lutz 2002). MYC is predominantly expressed in small lung cancers (Tansey 2014).

The role of c-MYC in tumorigenesis and tumor progression has been widely shown in a wide variety of cancer types (Efstratiadis, Szabolcs, and Klinakis 2007; Dang et al. 2006). Goga's lab recently showed that that c-MYC gene expression and its signaling is significantly increased in TNBC compared to receptor positive subtypes

(Figure 8) and is associated with triple negative breast cancer's poor prognosis (D. Horiuchi et al. 2012). Concluding that c-MYC overexpression in mammary tissue plays a crucial role in TNBC tumorgenesis, suggesting this molecule as an interesting target candidate for TNBC therapy.

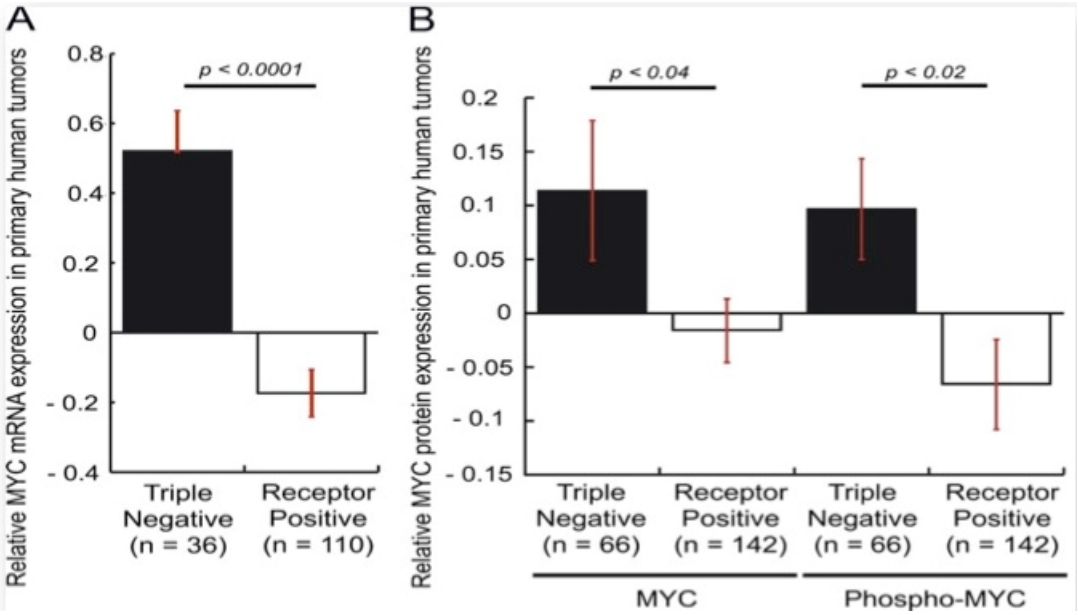

Figure 8. MYC Overexpressed In Human TNBC Versus Receptor Positive Ones. (A) qPCR on 146 primary patients' tumor samples has shown that MYC mRNA expression is significantly higher in triple-negative versus receptor-positive primary breast tumors. The samples were collected through the I-SPY TRIAL (Investigation of Serial Studies to Predict Your Therapeutic Response with Imaging and Molecular Analysis). (B) Quantitative reverse-phase protein arrays on 208 breast cancer patients showed that MYC and phospho-MYC (T58/S62) protein expression increased in triple-negative primary tumors compared to receptor positive. Error bars represent means ± SEM. P-values were calculated by two-tailed Student's *t* test (D. Horiuchi et al. 2012).

Although the role of MYC in cancer development is widely studied, targeting this protein in MYC overexpressed cancer patients is problematic. Considering the fact that MYC is a transcription factor who's activated signaling pathways drives cell cycle progression from G1 to S cell cycle phases, targeting MYC can impact the rapidly dividing normal cell cycle and result in toxicity. Moreover, due to the MYC specific structure for which no active site sequence has been identified yet, finding a MYC-specific targeted inhibitor has remained a challenge (Dai Horiuchi, Anderton, and Goga 2014).

All mentioned reasons, along with many other unknown MYC-mediated molecular pathways, which act in parallel with MYC, have shifted focus from this oncogene as a therapeutic target to research on factors downstream of the MYC-mediated pathway as a therapeutic target for TNBC treatment.

1.3 Cancer Immunotherapy

Cancer immunotherapy is the harnessing of the immune system to treat cancer. The capability of the immune system to fight and eradicate cancer, however, was not illuminated for many years. It was Anton Chekhov whom first showed a strong connection between tumor regression and bacterial/viral infection in 1884. His study began a new era of efforts in applying bacterial infections for cancer treatment, which was effective to some extent (Lizée et al. 2013). The most compelling evidence which illuminates the antitumor ability of the immune system is referred to the successful tumor

regression trials in late 1980s using immune cell activator, IL-2, in both melanoma and renal cell cancers (Lamm et al. 1990; Coley 1910; Gressor 1987).

Antitumor-immune response is a cyclic process of seven events. 1) neoantigens are released by cancer cells into the microenvironment 2) neoantigenes later are captured and displayed by dendritic cells (DCs). DCs are specialized immune cells that capture, process and then present antigens on their surfaces through binding them to major Histocompatibility class I (MHC I) molecules. 3) Cytotoxic T cells are primed and become activated through receptor-ligand binding communication between DCs and T cells. 4) Activated T cells traffic to the cancer site. 5) T cells infiltrates into the tumor, 6)T cells recognize tumor cells via binding their T cell receptor (TCR) with displayed neoantigen. 7) This cell-cell communication results in activation and release of cytokines. The secreted cytokines activate intracellular pathways within tumor cells, which lead to cell cycle arrest, apoptosis and angiostasis, a regulatory mechanism to inhibit further vascularization of tissue or tumor to form new blood vessels (Lizée et al. 2013; Smyth, Dunn, and Schreiber 2006). As the tumor cells are killed, more neoantigen is released which results in re-initiation of this antitumor response cycle and the increase of depth and extent of the response (Figure 9).

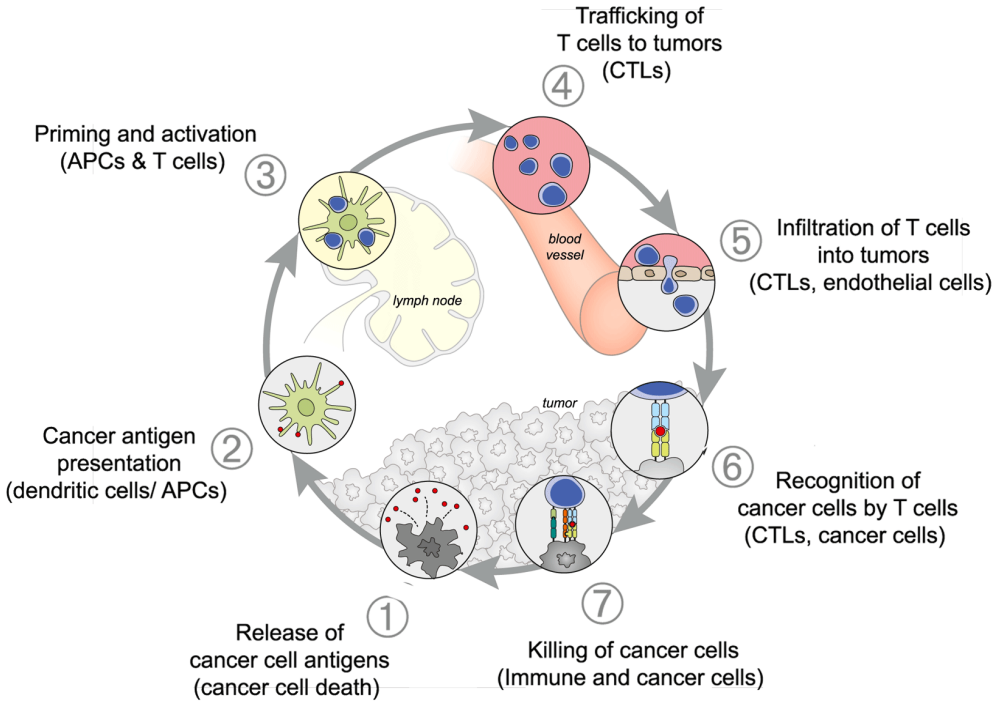

Figure 9. Cancer-Immunity Cycle. The cancer immune response is a cyclic event consisting of seven steps that continuously repeat. Briefly, the cycle is initiated through cancer neoantigen release into the microenvironment. These antigens are captured and displayed by dendritic cells (DCs) at their surface. DCs presenting neoantigens prime and activate naïve T cells. T cells migrate to the tumor sites, infiltrate the tumor and recognize cancer cells through their TCR receptors. The interaction of these cancer-specific T cells activates T cells to kill tumor cells through releasing antitumor factors and cytokines (Chen and Mellman 2013).

In addition to cytotoxic T cells, $CD4^+$ T helper cells also provide an immune response indirectly by activating both macrophages to become tumoricidal and $CD8^+$ cells to proliferate, traffic and secret more cytokines against tumor cells. B lymphocytes also elicit an immune response by producing antibodies against these antigens as well (Lizée et al. 2013).

T cells that contribute in the cancer-immunity cycle get activated at two time points throughout this cycle; in the beginning of the cycle when naïve T cells interact with antigen presenting DCs and at the end of the cycle when T cells bind to tumor cells through their TCR receptors. These interactions are required for initiating intracellular signaling pathways within T cells leading to their proliferation and cytokine release (Figure 10).

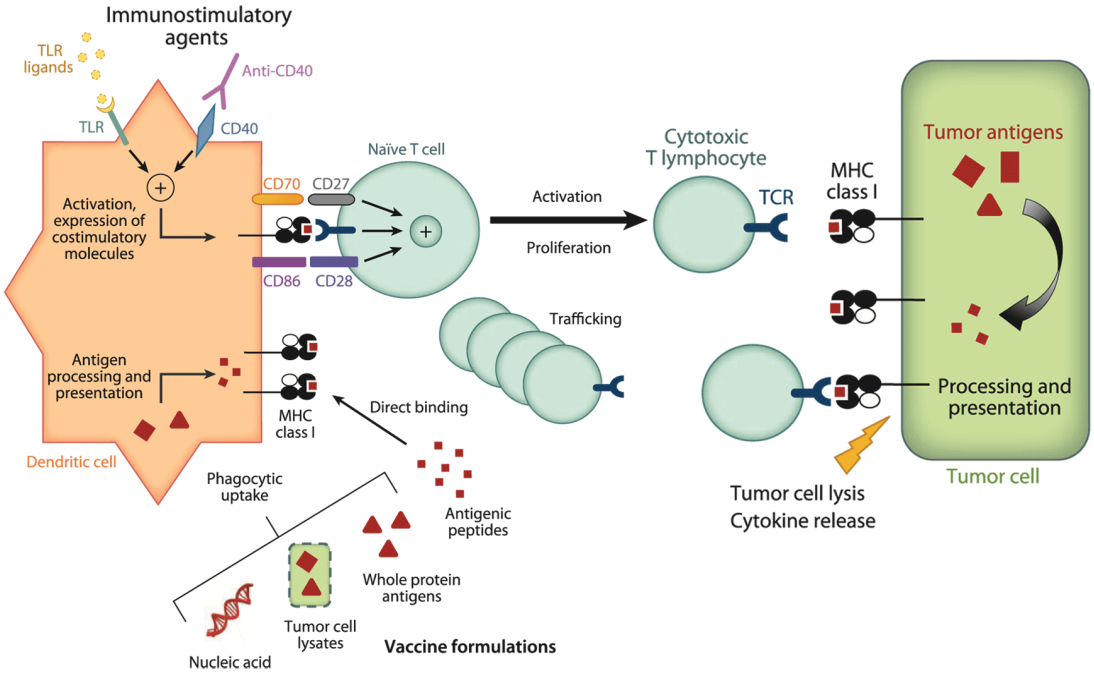

Figure 10. Effector T Cells Activation Upon Tumor Antigen Stimulation And Their Antitumor Immune Response. Throughout this process, T cells are activated at two points in time. One is mediated by interaction with antigen presenting cells and another is mediated by interaction of TCR with MHC: peptide complex. Note: MHC, major histocompatibility complex; TCR, T-cell receptor. TLR: Toll-like receptor (Lizée et al. 2013).

Considering the fact that the human immune system is highly elaborate in detecting and fighting against foreign and abnormal cells, why then is one still diagnosed with cancer? A myriad of studies have shown that the tumor-specific T cells activation could be tightly regulated through inhibitory signals from internal or external sources. The external immuninhibitory factors are either cytokines such as IL-10 or immunosuppressive cells including T regulatory cells or macrophages. The internal inhibitory signals are mediated through immune checkpoint molecules, the ligands that expressed by tumor cells, which bind to their corresponding receptors on T cells (Chen and Mellman 2013; Motz and Coukos 2013).

1.3.1 Immune Checkpoints

Immune checkpoints are receptors expressed on the surface of immune cells. They are classified into two groups based on their effects on the functionality of immune cells: the inhibitory receptors and co-stimulatory receptors. Immune inhibitory checkpoints can control the function of immune cells through two mechanisms: 1) exhibit inhibitory effect on T cells through sequestering the ligands of co-stimulatory receptors, which is required for complete activation of T cells. 2) Exhausting immune response through interaction of these immune inhibitory receptors to their ligands expressed on tumor cells, immune inhibitory receptors contain an immunoreceptor tyrosine-based inhibition motif (ITIM) conserved sequence. Upon inhibitory receptors-ligand interaction, ITIM motif becomes phosphorylated. The phosphorylated motif recruits other

enzymes including the phosphotyrosinephosphatases SHP-1 and SHP-2, or the inositol-phosphatase called SHIP. These phosphatases dephosphorylate signaling molecules downstream of the TCR receptor that lead to down-regulation of T cells' activation-induced genes and their attenuation (Figure 11) and the last mechanism is the inducing T cells exhaustion through up-regulating the gene that is involved in inhibiting T cells function (Odorizzi and Wherry 2012).

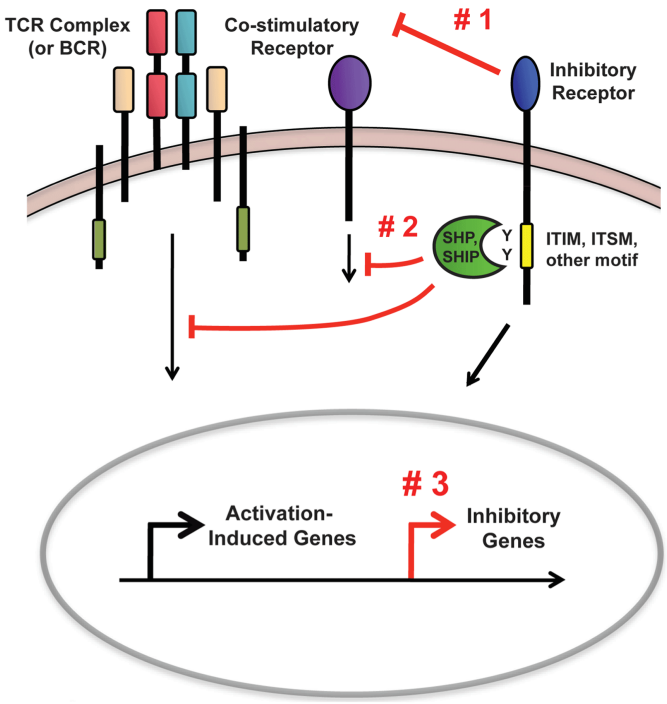

Figure 11. Immune Inhibitory Receptors Inhibit T Cells' Function Through Two Mechanisms (Odorizzi AndWherry 2012).

Inhibitory immune checkpoint receptors are widely expressed throughout a variety of cancer types. Programmed Cell Death 1 (PD1), Cytotoxic T Lymphocyte-Associated Protein 4 (CTLA-4) as well as co-inhibitory molecules of T cell

Immunoglobulin and Mucin domain-containing protein3 (TIM3), B and T Lymphocyte Attenuator (BTLA), T cell Immunoglobulin and Immunoreceptor Tyrosine-based Inhibitory Motif (ITIM) domain (TIGIT), Lymphocyte Activation Gene 3 (LAG3) and V-domain Immunoglobulin Suppressor of T cell Activation (VISTA) are several of the most well-known immune inhibitory receptors which are expressed at the surface of T cells and regulates their function (Figure 12) (Peggs, Quezada, and Allison 2009).

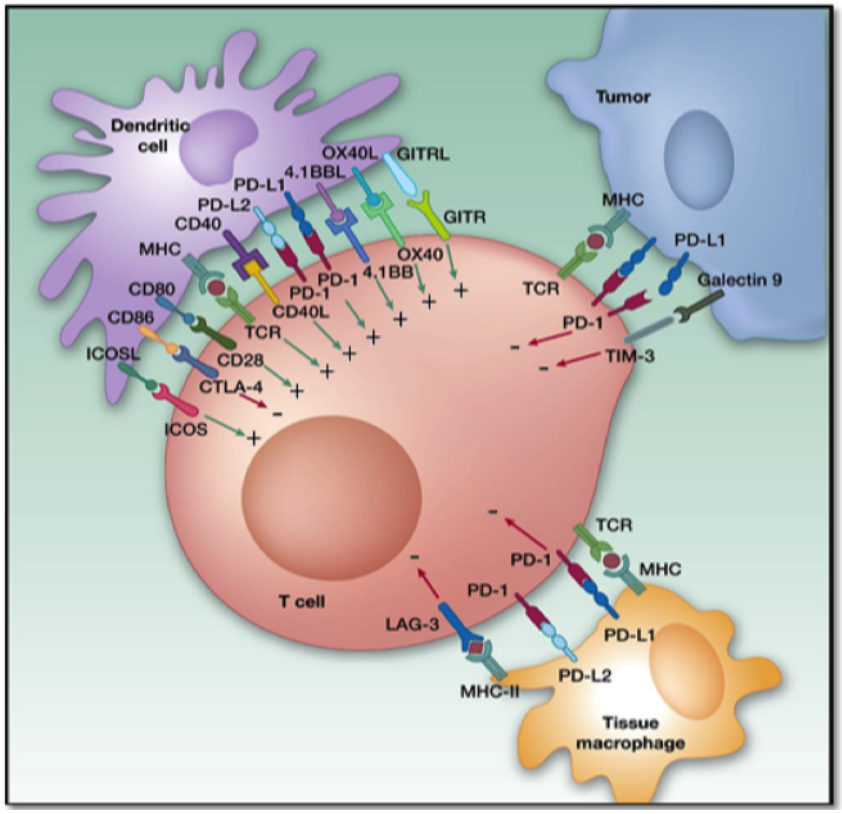

Figure 12. Immune Inhibitory And Stimulatory Receptors' Interaction With Their Ligands. Both Immune inhibitory and stimulatory ligands can express at the surface of both tumor cells and myeloid cells and interact with their corresponding immune inhibitory receptors on T cells.

1.3.1.1 PD-L1 and Its Role in Immune Tolerance

B7-HA so called PD-L1 is a ligand, which is constrictively expressed on the surface of both immune and normal cells. T and B cells, Dendritic cells (DCs), macrophages, mesenchymal stem cells, bone marrow-derived mast cells and non-hematopoietic cells are several of the most important cells that display this protein ligand on their surface (Yamazaki et al. 2002). In addition, many studies have shown that this protein is significantly expressed at the surface of a wide variety of cancer cells including breast and melanoma cancers.

According to The Cancer Genome Atlas (TCGA), an RNA sequence database, this ligand is expressed in TNBC (Figure 16). This ligand could bind to a receptor called PD1, which is expressed on the surface of most immune cells including activated T-lymphocytes ($CD4^+$, $CD8^+$), B cells, natural killer cells, activated monocytes and dendritic cells (DCs). This ligand competes with PD-L2 (B7-DC) to bind to the PD1 receptor. In contrast to PD-L1, PD-L2 is expressed only on DCs, macrophages and bone marrow-derived mast cells (Zhong et al. 2007). Notably, PD-L1 is expressed at higher levels in both human and mice, compared to PD-L2 (Keir et al. 2008).

Upon interaction of PD-L1 on tumor cells with PD1 on the immune cells, an intracellular signaling pathway is initiated which results in the inhibition of the immune response. The release of interferons (IFNs) by T- cells promotes the expression of PD-L1 on the tumor cells(Keir et al. 2008). Following the interaction of PD1 with PD-L1, an immunosuppressive signaling pathway initiates in which cytoplasmic tyrosine residues of

PD1 phosphorylate in T-cells. In the next step, SH1 and SH2 (both phosphatases) are recruited by PD1 through their ITIM motif. SH2 dephosphorylates PI3 kinase-signaling cascade and blocks it. This further inhibits the downstream AKT pathway (Figure 13).

The AKT pathway is responsible for controlling several critical activities of T-cells including cytokines release (IL-2, INF-γ), proliferation, protein synthesis, and metabolite transportation and cell survival (Chemnitz et al. 2004; Parry et al. 2005). Thus, the interaction of PD1-PD-L suppresses T-cell function, survival and proliferation while promoting apoptosis and attenuation. Moreover, altering cytokine levels themselves further controls T-cell function. Overall, this T-cell attenuation provides immune tolerance for tumor cells, enabling them to evade immune response and sustain progression (Chen and Mellman 2013; Callahan, Wolchok, and Allison 2010).

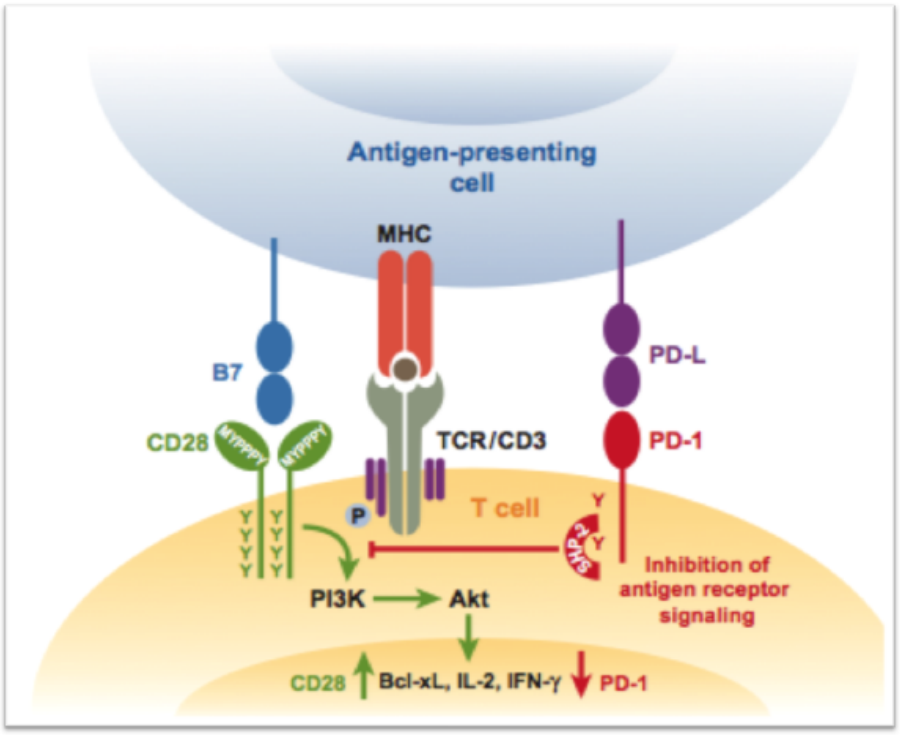

Figure 13. PD1-PDL Mediated Pathway Induces T-Cell Attenuation And Immune Tolerance. Once PD-L1 binds to its corresponding receptor (PD1) on the surface of lymphocytes, a series of downstream signaling cascades, which are responsible for T-cell function, will be blocked resulting in impairment of T-cells functionally (Chen and Mellman 2013).

Cancer immunotherapy using monoclonal antibodies to block immune checkpoints is widely used for various types of cancers including melanoma, Renal Cell Cancer (RCC) and Non-Small Cell Lung Cancer (NSCLC). In these clinical trials PD-L1, PD1 or even both particularly are targeted (Brahmer et al. 2012). In many patients, this targeted therapy is sufficient and exerts durable and rapid response inhibits cancer progression while, in some, monotherapy is not enough and combinational therapy is required. Combinational therapies using either antibodies against other

immunosuppressive proteins or T-cell activator proteins, along with the PD-L1 antibody, have been tested in other types of cancer (Sharma et al. 2011).

1.3.2 Immune Checkpoints Blockade

Among the four most effective immunotherapeutic approaches namely cancer vaccines, immune checkpoint blockade, adaptive T-cell transfer and immune stimulatory agents, the immune checkpoints blockade agents have appeared to effectively control tumor progression or even cancer eradication in a wide variety of cancer patients including NSCLC, prostate and pancreatic cancers, melanoma, breast and renal cell carcinoma. Thus, harnessing immune system through inhibiting Immune checkpoints becomes a promising anti-cancer therapy technique with more durable and objective response, higher efficacy, low toxicity and lower risk of recurrence (Lizée et al. 2013).

Through the binding of these immune checkpoint molecules on T cells with their ligands expressed on the surface of tumor cells, T cells become exhausted so that their proliferation capacity and antitumor function are remarkably impaired. Previous studies on different types of cancer have shown that blocking these immune inhibitory checkpoints could restore function to the exhausted T cells and reactivate T cell-mediated tumor cell killing (Figure 14 and Figure 15) (Chen and Mellman 2013).

CTLA-4 is one of the immune inhibitory receptors expressed by $CD4^+$ and $CD8^+$ cells upon T cell activation. Ipilimumab, the CTLA-4 blocking antibody, was recently been developed and its clinical trial on melanoma patients has been initiated (Figure 14).

Phase I and II clinical trials of this antibody produced successful results significantly. The phase III clinical trial in patients with metastatic melanoma showed 3.7 months improvement in median overall survival (P-value: 0.003). Strikingly, approximately 23% of the advanced melanoma patients survived more than four years. This successful trial resulted in FDA approval of this immune checkpoint blockade antibody for metastatic melanoma patients (Hodi et al. 2010; O'Day et al. 2010; Wolchok et al. 2010; Robert et al. 2011).

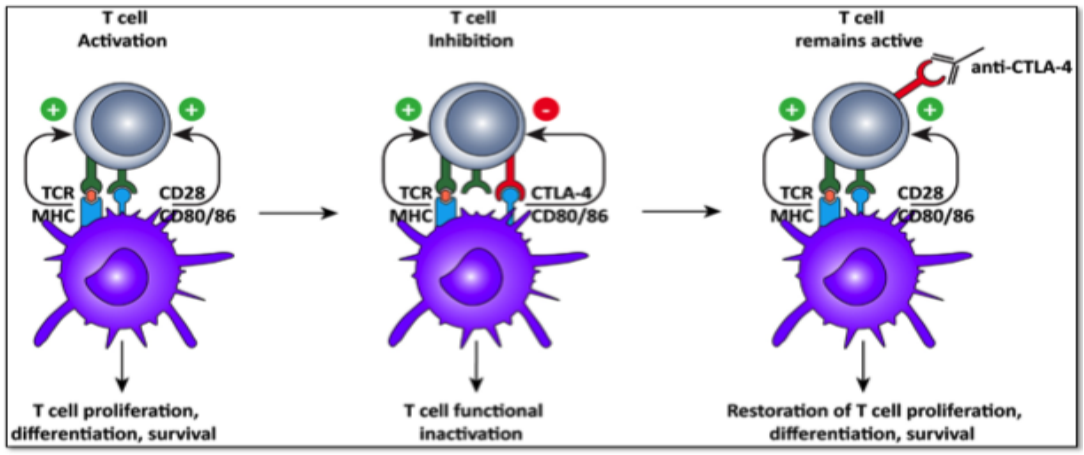

Figure 14. The CTLA-4 Immunosuppressive Pathway And The Effect Of Its Blockages On Reactivation Of T Cells' Function. Tumor cells and T cells communicate through interaction of their surface molecules A) TCR recognizes tumor cells through binding to their MHC: peptide complex at their surface. However, this interaction is not enough for T cell activation and a secondary signal is required which is provided through interaction of co-stimulatory molecules of CD28 to its CD80/86 ligand so that T cells get activated and provide immune response. B) Immune inhibitory checkpoint of CTLA-4 competes with CD28 and sequesters CD80/86. This interaction not only interrupts the secondary signal for T cell activation but also inhibits T cell function and proliferation. C) The interaction of CTLA-4 with CD80/86 can be blocked via administration of anti CTLA-4 antibody. Thus, the co-stimulatory receptor CD28 can bind to its ligand on tumor cells and activate T cell function which leads to proliferation of tumor-specific T cells and their antitumor response. Note: MHC, major histocompatibility complex; Ag, antigen; CTLA-4, cytotoxic leukocyte antigen 4; TCR, T-cell receptor (Vasaturo et al. 2013).

LAG3, also known as CD223, is another immune inhibitory receptor which is currently tested in a phase I clinical trial of solid tumors including NSCLC, melanoma and head and neck squamous cell carcinomas (Woo et al. 2012). The administration of anti-LAG3 antibody, either alone or in combination with a second immune-checkpoint blocker, has been shown to enhance antitumor response in animal models of cancer (Drew M. Pardoll 2012).

PD-L1 is another immune-inhibitory checkpoint whose expression has been found recently on a wide variety of cancers. This motivates many researches to test the therapeutic approach of immune-checkpoint blockade of PD-L1 for cancer treatment. In 2012, one phase I clinical trial of monoclonal antibody of anti-PD-L1 has been undertaken in several types of cancer: melanoma, NSCLC, RCC and ovarian cancer (Figure 15). This trial results in a durable objective clinical response in 17%, 12%, 10% and 6% in cancer patients of melanoma, RCC, NSCLC and ovarian respectively (Brahmer et al. 2012). Furthermore, PD-L1 based immunotherapy on different types of cancer including metastatic melanoma and lung cancer has been successful so far.

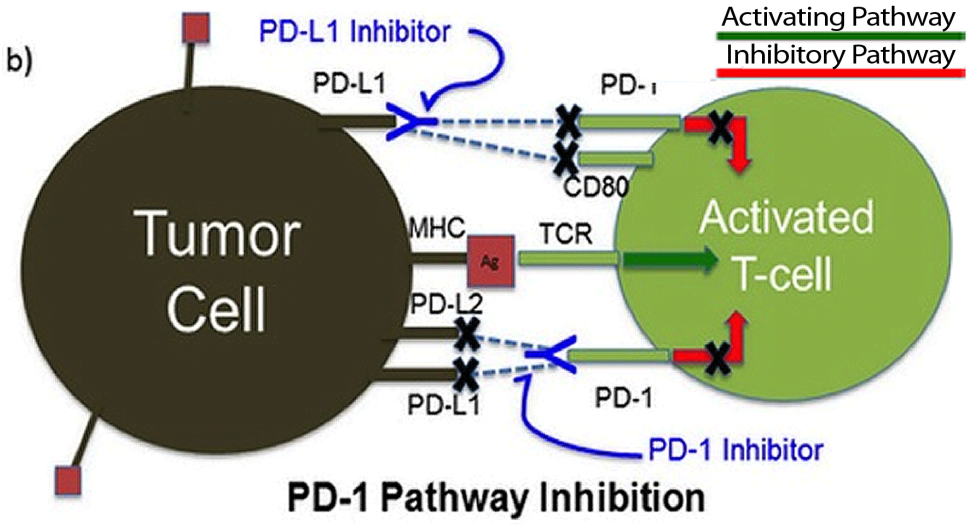

Figure 15. Targeting PD-L1 To Reactivate T Cells. The monoclonal antibody inhibits tumor mediated CD8+ T cell exhaustion and restores T cell function. The interaction of PD1 on activated T cells with PD-L1 expressed on tumor cells suppress the $CD8^+$ T cell function through activating an inhibitory pathway. The activation of this inhibitory pathway results in T cell exhaustion and tumor immune resistance. Administration of monoclonal antibodies against either PD1 or PD-L1 can block this inhibitory pathway and result in the restoration of T cells and their anti-tumor immune response. Note: MHC, major histocompatibility complex; Ag, antigen; TCR, T-cell receptor; PD, programmed cell death (Godwin et al. 2015).

Our preliminary data also has shown that according to TCGA database, PD-L1 is one of the immune inhibitory checkpoints that is expressed significantly higher in TNBC tumors compared to other subtypes of breast cancer (n=716; $P < 0.001$) (Figure 16).

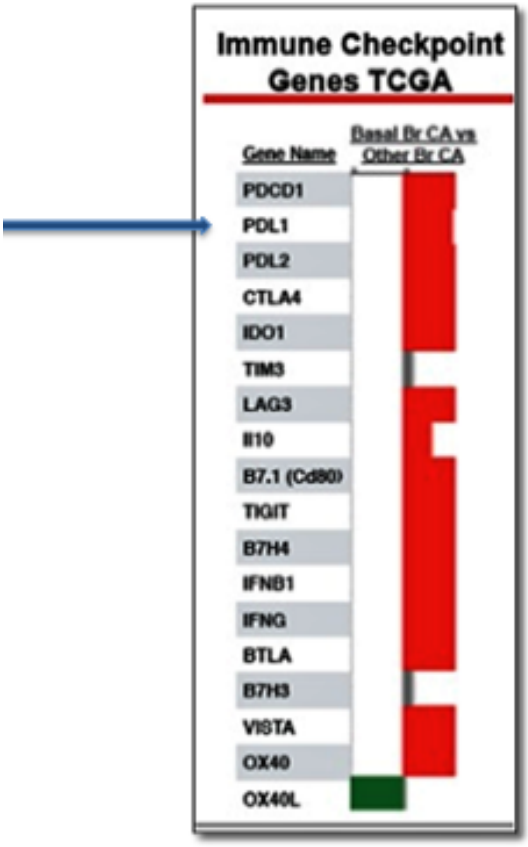

Figure 16. TCGA Database Of Immune Inhibitory Checkpoints Ligands mRNA Expression In TNBC Versus Other Subtypes Of Cancer. Moreover, a recent immunohistochemistry (IHC) study on 44 breast cancer specimens shows that PD-L1 was expressed in both epithelium and TILs in 22 of 44 studied samples (34% of tumor cells and 41% of TILs). Strikingly, the PD-L1 expression was significantly associated with TNBC phenotype (Ghebeh et al. 2006). In addition, a microarray analysis on breast tumor samples shows that PD-L1 is expressed in 19% of TNBC specimens (Mittendorf et al. 2014).

Taking all of this preliminary data together, we hypothesize that PD1-PD-L1 immunosuppressive pathway may contribute to T cell exhaustion and tumor immune tolerance in a TNBC mouse model. Hence, blocking of this pathway could preclude its

inhibitory effects and results in tumor attenuation and prolonged antitumor response. To test this hypothesis, we pursue three aims including

1) Determine whether the PD-L1 expression, if there is any, is regulated by MYC

2) Targeting PD-L1 ligand through anti-PD-L1 antibody therapy to study the effect of PD1-PDL mediated immunosuppression pathway on TNBC tumor progression and recurrence

3) Widely studying other immune checkpoint candidates that were found on most recent immunotherapy literatures and their expression on TNBC was detected. We focus on the expression of these candidate molecules on both immune cells and tumor cells in this tumor model through FACS to investigate other immune checkpoints to be targeted in MYC-driven TNBC.

In addition to this effort, we also followed a forth aim that will help us to expand our knowledge about this tumor model and will become the preliminary data for the future experiments. We found that two available MYC-driven breast cancers tumor models in our laboratory bear two different mutations. We also demonstrated that these two tumor models differ in their growth rate *in vivo*. Thus, we were interested to know if the difference in tumor growth is due to the secondary mutations or to the differences in antitumor-immune response. This study can further reveal the effect of the type of mutation on personalized medicine and used as the biomarker to evaluate the efficacy of treatment. To address this hypothesis, we embarked on characterization of tumor growth and tumor-infiltrating immune cells of the two types of MYC driven breast tumors at both the progression and recurrence stages.

Chapter Two

Background Data

2.1 MYC-Driven MTB/TOM Mouse Model

MTB/TOM is a widely used model system for breast cancer studies which is constructed by mating two transgenic mouse lines namely, MTB and TOM. The MTB is a transgenic mouse expressing a construct in their mammary epithelial cells which contains mouse mammary tumor virus (MMTV) long terminal repeat (LTR) region upstream of the Reverse **t**etracycline-controlled **T**rans**A**ctivator (rtTA) followed by SV40 poly A. The rtTA is subsequently expressed but won't be activated in the tetracycline deprivation. TOM, the second transgenic mouse, expresses human c-MYC under the control of tetracycline operator (tetO). This operator can be recognized by the complex of tetracycline bound to rtTA (rtTA+Tet) (Figure 17).

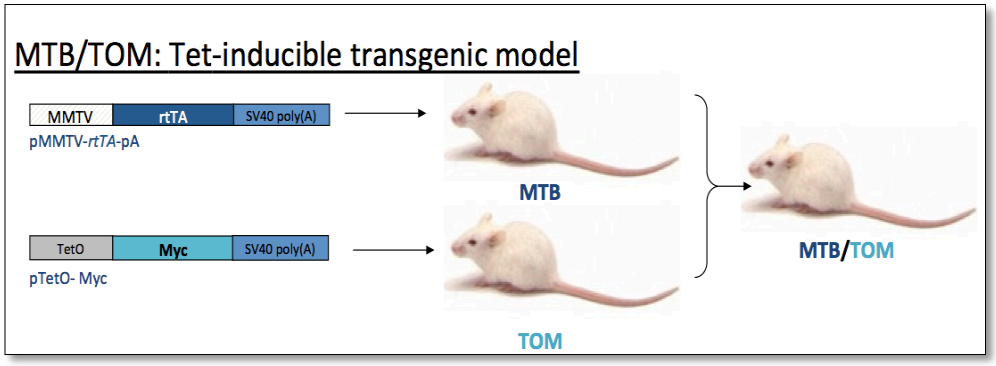

Figure 17. Schematic Showing The Procedure To Develop Tet-Inducible MTB/TOM Transgenic Mouse Model.

In the presence of tetracycline, rtTA+ Tet complex can be formed and bind to TetO, inducing human c-MYC expression in the mammary epithelial cells. Consequently, upon mating these two mouse lines, a MTB/TOM transgenic mouse will be developed expressing human c-MYC only in the breast tissue upon administration of tetracycline (Figure 18) (D'Cruz et al. 2001; Gossen and Bujard 1992; Yao et al. 1998).

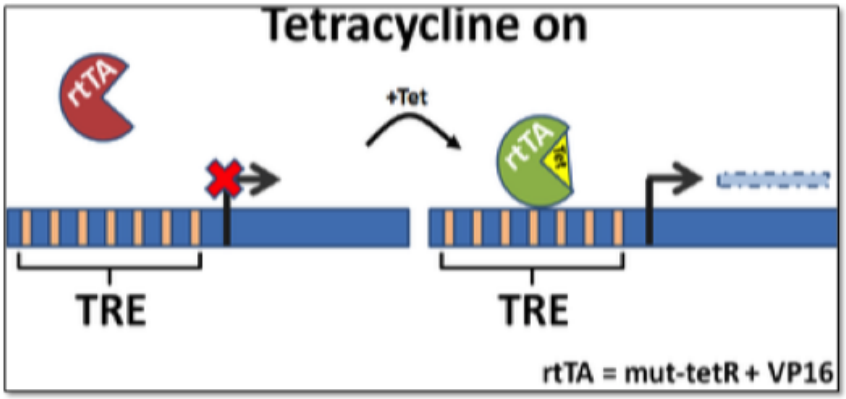

Figure 18. MYC Inducible MTB/TOM Mouse Model. MYC is only expressed in the presence of tetracycline. rtTA binds to tetracycline making a complex which initiates MYC expression.

2.2 MTB/TOM Tumor Development

After developing the MYC driven MTB/TOM transgenic mouse model, the pups were fed with Doxycycline, a member of tetracycline class of antibiotics (Barza and Schiefe 1977). 86% of Mice developed tumors after approximately 22 weeks on Doxycline (D'Cruz et al. 2001). The growth of the tumor was monitored and each mouse that developed tumor was named alphabetically in an orderly manner. Through this avenue, more than 26 tumor lines were generated and their growth rate and tumor behavior were studied. Among all lines, line A and B were the fastest growing tumors according to their tumor progression graphs.

2.3 MYC Expression Upon MYC Withdrawal

Western blot analysis on MYC expression in line A MTB/TOM tumor, showed that 12 hours after Dox removal, the MYC protein expression was shut down (Figure 19). β- actin was used as the loading control (unpublished data, Alicia Zhou, 2015).

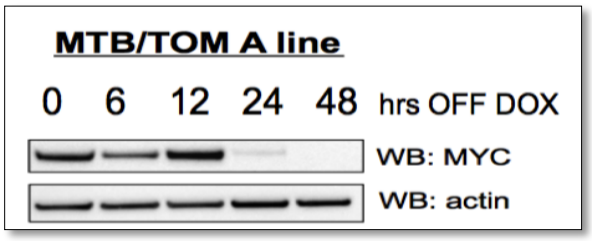

Figure 19. MYC Expression In The Beast Tumor Of MTB/TOM Mouse Model. MYC protein expression decreases over time after Dox removal.

2.4 Tumor Growth Study in Lines A and B.

Tumor progressions studies on both A line and B line showed significant difference in growth pattern. The growth rate in Line A was significantly higher than line B. Studying the tumor growth pattern showed that while the tumor size in Line A sharply increased over one week, tumor B had a steady slope with a delay in the fourth week. Tumors grew with the approximate average rate of 283 mm^3/day in A line while the average growth rate in B line was much slower, around 53 mm^3/day. Both tumors also showed differences in terms of take rate, the percentage of mice with a palpable tumor after transplantation. The take rate was slightly higher in A line compared to B line, 90% versus 80%. They also show some differences in their Time to First Tumor (TFT), the required time for the tumor to grow to the detectable size after transplantation. Tumors in Line A can be detected two weeks after transplantation while it takes 3-5 weeks for the B line (Figure 20) (unpublished data, Alicia Zhou, 2015). In general, Line A appeared to be more aggressive than line B.

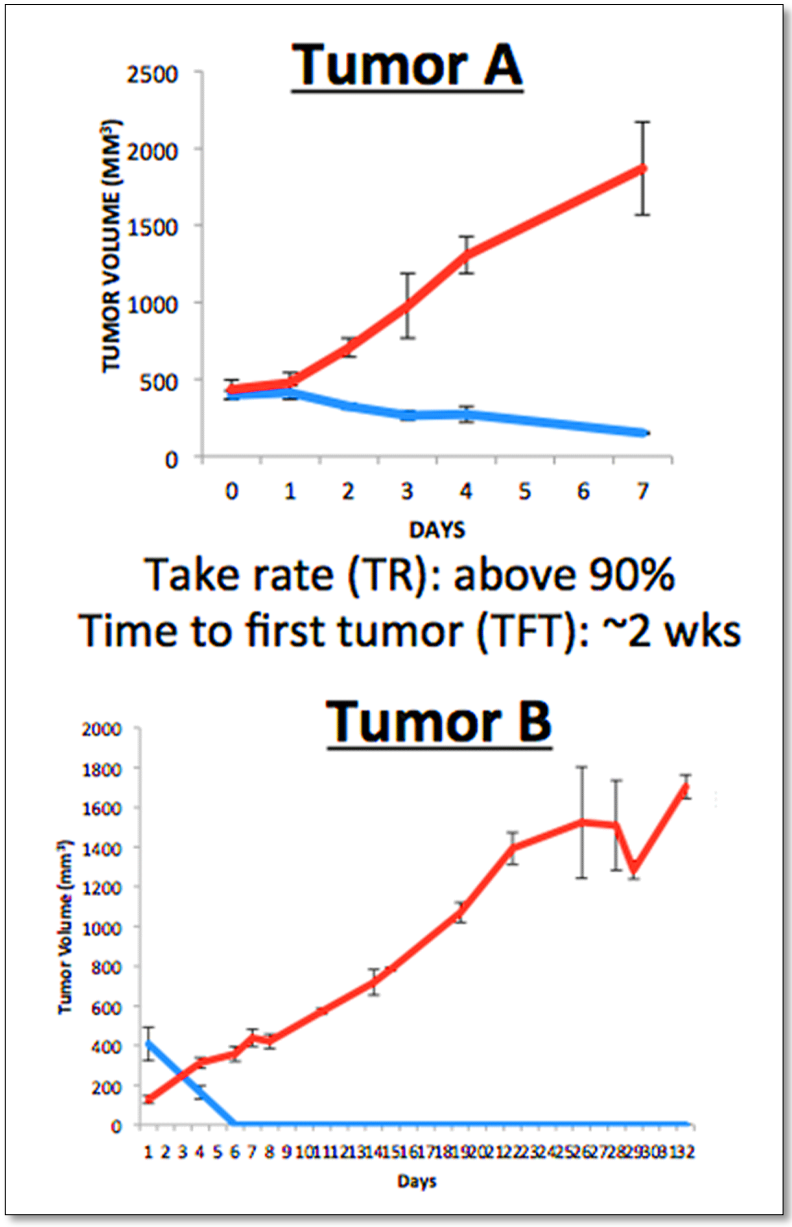

Figure 20. Tumor Progression Graphs Of Line A And B. Red line: the tumor growth graph of mouse fed with Dox. Blue line: the tumor growth graph of mouse fed with normal food (without Dox).

2.5 Sequence Analysis

To study the possibility of bearing a secondary mutation in these tumor models, next generation sequencing was performed on 265 cancer genes using Illumina Solexa HiSeq 2000 sequencer. Data showed that each of these lines contains a different secondary mutation (see Table 1). A frame shift mutation of S460 in PIK3R1 gene in Line A and a hotspot mutation of Q61L in Kras gene was detected (unpublished data, Alicia Zhou and Meng Li, 2014).

Table 1. Next Generation Sequencing Data Analysis Of Lines A And B. A frame shift mutation of S460 in PIK3R1 gene was detected in Line A and a hotspot mutation of Q61L in Kras gene was found in line B

Tumor Line	Chr	Begin Pos	End Pos	Ref	Obs	Freq	Depth	cytoBand	Gene	Annotation
MT-A	chr13	101688679	101688679	-	T	0.36	651	13qD1	Pik3r1	S460, fs mutation
MT-B	chr6	145234356	145234356	T	A	0.64	1787	6qG3	Kras	Q61L, hotspot mutation

PIK3R1 is the eleventh most mutated gene across the entire TCGA (>4000 tumor samples across 20 disease). It is mutated or altered in 9% of breast TCGA samples.

PIK3R1 encodes PI3K regulator subunit p85α (Carpenter et al. 1990; Cancer Genome Atlas Network and Cancer Genome Atlas Research Network 2012). *p85α* is a tumor progression gene that negatively regulates p110α. It also can bind to

PTEN, which in turn inhibits PIP3 receptor activation. PIP3 receptors play a major role in PI3K-AKT signaling pathways. Upon its activation, the AKT protein is recruited and activated which mediates downstream responses, namely cell proliferation, cell survival, growth and angiogenesis. Upon p85α mutation, PTEN cannot inhibit PIP3 receptors activation, which leads to AKT signaling pathway activation that promotes cell cycle progression and growth (Figure 21).

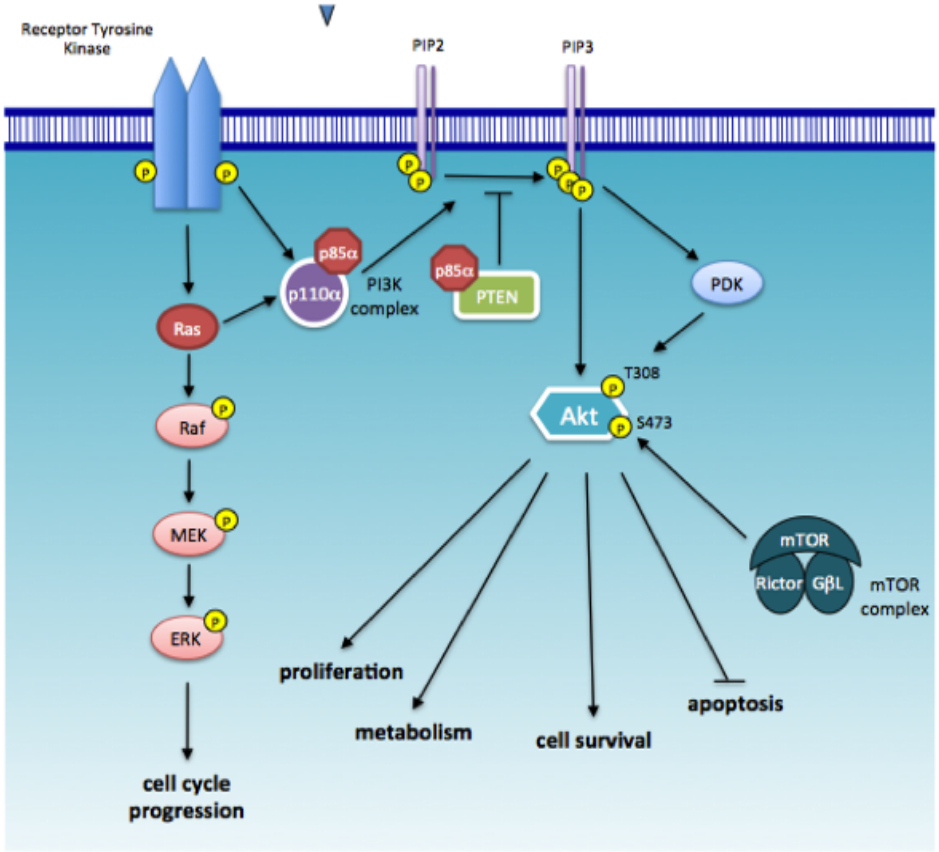

Figure 21. **PI3k / Akt Signaling Pathway**

V-Ki-Ras2 Kirsten rat sarcoma viral oncogene homolog, known as *KRAS*, is a proto-oncogene encodes a GTPase. This protein can be found in two forms of cytoplasm, the active form when bound to GTP and the inactive conformation when bound to GDP. The exchange of GDP with GTP switches this protein from inactive to the active state facilitated by guanine nucleotide exchange factors (GEFs). GTPase-activating proteins (GAPs), conversely mediate KRAS inactivation through inducing hydrolysis of GTP (Pylayeva-Gupta, Grabocka, and Bar-Sagi 2011; Eser et al. 2014). GEFs that are bound to the intracellular domain of the transmembrane growth factor receptors are activated through extracellular signals. Upon activation, GEFs induce conformational changes in GTPase bound GDP and make GDP dissociated.

KRAS has many downstream intracellular signaling pathway targets including; mitogen-activated protein (MAP) kinase cascade (McGrath et al. 1983; Popescu et al. 1985). These targeted pathways contribute in essential cellular processes including cell differentiation and proliferation, cytoskeletal organization, vesicle trafficking, and nuclear transport (Figure 22) (Alberts et al. 2008).

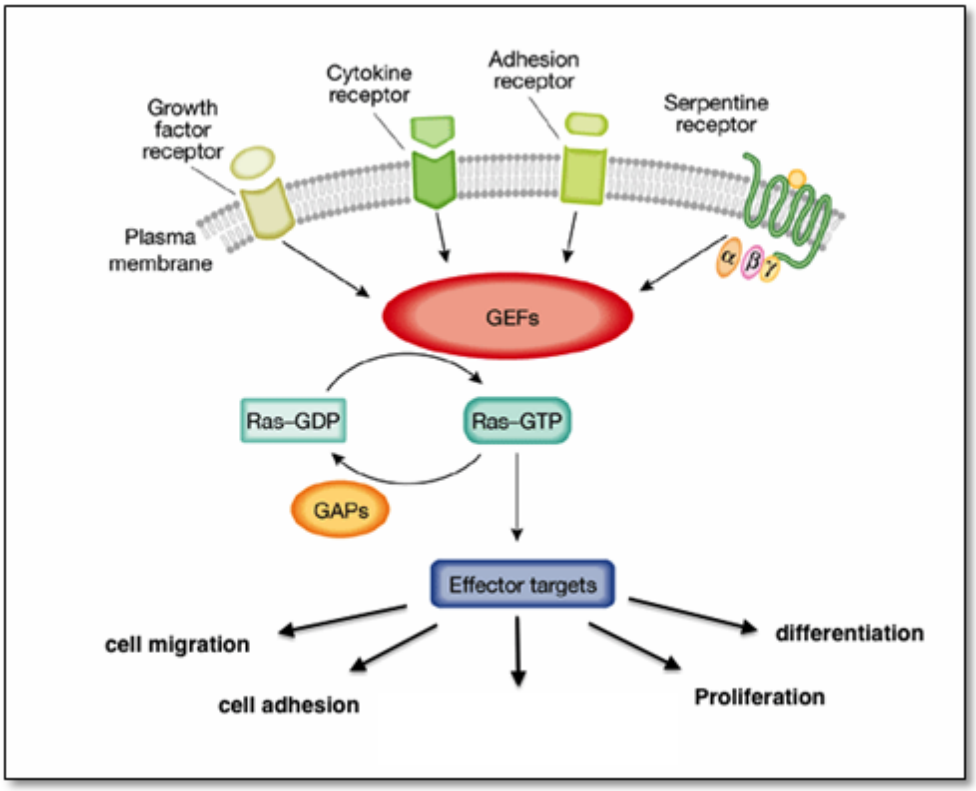

Figure 22. Kras-Mediated Signaling Pathway

Mutations in the Ras family of proto-oncogenes are very common, and cause 20% to 30% of all human tumors including non-small cell lung cancer, pancreatic and colorectal cancer (Bos 1989; Downward 2003).

Chapter Three

Materials and Methods

3.1 Studying The Tumor Progression And Recurrence of MTB/TOM Tumor Breast-Transplanted Mouse Models

3.1.1 Line B Tumor Recurrence

To study the tumor recurrence of line B, one cohort of four FVN/NJ female mice (*Mus musculus*) was employed. Four FVN/NJ mice strains were purchased from Jackson Laboratory (Bar Harbor, ME) and transplanted with approximately 1mm^3 tumor chunks of line B in the mammary fat pads of their right side. The growth of the transplanted tumors was controlled through Dox-induced MYC expression by oral administration of Doxycycline (Dox).

Once the tumor reached the volume of 1.5 mm^3, all mice were taken off Dox. The Mice were ear tagged and the growth of the tumor was measured using a caliber. The tumor volume was determined using the following formula: 1/2 ($width^2$ * length). The tumor-growth and survival curves were drawn using GraphPad software, Prism 6 for Mac.

3.2 Leukocyte Isolation From Tumor-Burden Mice

3.2.1 Line A Tumor Progression and Recurrence upon Anti-PD-L1 Antibody Treatment

To study the effect of anti-PD-L1 antibody on tumor progression, tumor growth was monitored by measuring the size of the tumor over time in the absence and presence of anti-PDL1 antibody treatment. Two cohorts of five FVN/NJ female mice (*Mus musculus*) at the same age (age 3-4 weeks) were subjected for this study. Five mice were designated as experimental group and five mice used as control group. FVN/NJ mice strains were purchased from Jackson Laboratory (Bar Harbor, ME). Mice were transplanted with approximately 1mm^3 tumor chunks of line A, derived from the MTB/TOM transgenic mice breast tumors, in the right side of their mammary fat pads (Figure 23). The growth of the transplanted tumors was initiated through Dox-induced MYC expression by placing the mice on food containing Doxycycline (Dox).

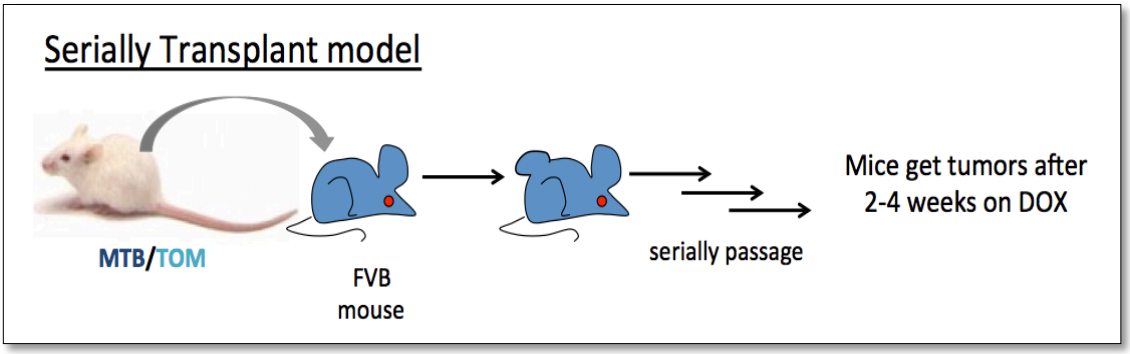

Figure 23. Developing Breast Tumor In FVB Mouse Through Serial Transplantation Of MTB/TOM Breast Tumor Line A/B Into Their Mammary Fat Pad.

The take rate of transplantation is more than 90%. Thus, at least four mice per group with a tumor should be available for this study. Once the tumor reached to the volume of 1.5 mm^3, all mice received treatment either the anti-PD-L1 antibody or isotype control antibody. The treatment group was injected with anti-mouse PD-L1 antibody (200 µg, BioXcell) intraperitoneally every two days for ten days. The Control group was treated with a monoclonal rat IgG2a isotype control; anti Trinitrophenol (200 µg, BioXcell) in PBS. After 10 days, mice were treated once a week until the tumors reached the end point (2 cm by any side). The mice were ear tagged and the growth of the tumor was measured using a caliber. The tumor volume was determined using the following formula: 1/2 ($width^2$ * length). The tumor-growth and survival curves were drawn using GraphPad software, Prism 6 for Mac.

To study the effect of anti-PD-L1 antibody treatment on tumor recurrence, two FVN/NJ mice cohorts of the same age consisting of five mice per group were transplanted with MTB/TOM tumor chunks. Once the tumor reached a volume of 1.5 mm^3, the treatment group was given anti-mouse PD-L1 antibody (200 µg, BioXcell) intraperitoneally every two days for 10 days. Both cohorts were taken off Doxycycline a day after beginning treatment. Tumor growth was measured using a caliber until the tumors reached an end point of 2 cm at any sides. At the endpoint, the mice were euthanized and tumors were processed for FACS analysis, mRNA extraction, protein isolation, and histological analysis. The tumor volume that was measured using the above formula was used to draw tumor growth and survival curve using Prism 6.

3.2.2 Tumor-Infiltrating Leukocyte Isolation From MYC-Induced Breast Tumors Using Density Gradient Centrifugation Technique

To characterize the immune infiltrating cells in terms of their distribution in tumor and their inhibitory receptor expression, the leukocytes of both the tumor and spleen were isolated, stained and analyzed by FACS.

Once the tumors reached the end point (1.5 mm^3), the mice were euthanized and both their tumors and spleens were removed. Tumor chunks of 0.9 g and whole spleens were placed in RPMI media (Gibson, life biotechnologies), supplemented with 2% fetal bovine serum (FBS) (Gibson, life biotechnologies). Samples were kept on ice for the next step.

Tumors were minced into 2-4 mm chunks using a razor blade. For enzymatic digestion, 5 ml of enzymatic mixture consisting of 1mg/ml collagenase type II (125 units/mg, Worthington,), 40 ug/ml DNase (20 mg/ml, Sigma crude) was added to the minced tumors and the mixture transferred into the gentle MACS tube. Tumor chunks were dissociated in Gentle MACS tubes using gentle MACS™ Onto Dissociate (Miltonic Biotic). The Dissociation step was followed by a 30 min incubation at 37º C on shaker at speed of 250 rpm for further enzymatic digestion. 100µl of 0.5 M EDTA pH 7.2 were added and tumor tissue was dissociated further using gentle MACS™ Octo Dissociator (Miltenyi Biotec).

To separate the dissociated cells from aggregated ones, the cell suspension was passed through a 40-μm filter. The filter was washed several times using RPMI growth

media (Gibco, life biotechnologies) supplemented with 2% FBS and transferred into a 15 ml conical tube. Dissociated cells were centrifuged for 7 min at 1200 rpm. Supernatant was aspirated and the cells re-suspended in final volume of 1ml of RPMI growth media (Gibco, life biotechnologies) supplemented with 2% FBS (Gibco, life biotechnologies) . Cells were counted using Vi-Cell XR cell viability analyzer (Bekman coulter).

Adequate amount of complete media of RPMI (Gibco, life biotechnologies) supplemented with 2% FBS (Gibco, life biotechnologies) were added to the re-suspended cells reaching the cell suspension to the final volume of 6 ml. The viable mononuclear cells were isolated from this cell suspension, which contains both dead cells and viable cells, using Histopaque gradient centrifugation technique. Steps were performed as follows: The tube was inverted gently to re-suspend the cells evenly. Then 4 ml of Histopaque-1083 (Sigma), kept at RT, were added gently to the bottom of the tube and spun at 2500 rpm at RT for 15 min with brake disengaged. Dead cells were pelleted down and separated from viable cells which moved to interface of histopaque–medium. This layer of viable cells containing both tumor cells and leukocytes was collected and diluted in 15 ml RPMI complete media. The cell suspension was washed and centrifuged for 7 min at 1200 rpm, followed by two more steps of re-suspending and spinning down using RPMI complete medium. Then the cells were re-suspended in the desired volume and counted using Vi-Cell XR cell viability analyzer (Bekman coulter). These cells were kept on ice for immune cell staining.

3.2.3 Spleen Leukocytes Isolation

Spleen cells were used as a control for compensation and FACS data analysis. To isolate immune cells from spleen, the spleen was pushed through 70 μm filter. The filter was washed several times using RPMI complete media. Washed dissociated spleen cells were transferred into a 15 ml conical tube and centrifuged at 1200 rpm for 7 min. The supernatant was aspirated and the pellet was re-suspended with 2ml red blood cells lysis buffer (17 mM Tris base, 139 mM NH_4CL, pH 7.2). Cells were lysed at RT for 2 min then diluted in 13ml RPMI complete media. One-step centrifugation was performed at 1200 rpm for 7 min to pellet the spleen cells. The Supernatant was aspired and the pellet was re-suspended in the desired volume and subjected for counting using Vi-Cell XR cell viability analyzer (Bekman coulter). The spleen cells were kept on ice for immune cell staining.

3.3 Immunoinhibitory Ligands and Receptor Staining of Myeloid Cells

To study both the immune inhibitory ligands and immune inhibitory receptors involved in the T cell attenuation pathway, two different sets of staining were performed. For each sample $1x10^6$ spleen cells and $5\ x10^6$ isolated tumor cells were seeded into a round bottom 96-well plate (three wells per cell type) in FACS buffer (D-PBS w/o calcium and magnesium salts (1X), 1 mM EDTA, 2% Fetal Calf Serum (FCS), 0.1% NaN_3) and then centrifuged for 1 min at a speed of 2100 rpm. The plate was then flicked

to remove the supernatant and tapped to re-suspend the cells. The seeded wells were then stained as follows.

3.3.1 Isotype Control Antibody Staining

Two wells, one seeded with tumor immune cells and one containing spleen immune cells, were dedicated for isotype antibody staining (see Table 2). The isotype antibody mixture contained isotype control antibodies against each of the myeloid cell surface markers. These isotope antibodies have no specificity against the corresponding immune cell markers and were used as a negative control to discern background signals over specific antibody signals. After washing the cells with FACS buffer, 25 µl of the isotope control antibody mixture was added to the wells. The Isotype control antibody mixture contains: Ly6C-FITC (1:100), rat IgG2b-PE (1:100), Rat IgG2a-PECy7 (1:100), Epcam-PerCPCy5.5 (1:100), CD11c-APC (1:100), CD11b-BV605 (1:200), CD45-PacBlue (1:100), and Ly6G-BV510 (1:100) antibodies. All antibodies were purchased from BioLegend Company. The Antibodies were diluted with 1X Phosphate Buffered Saline (PBS) (137 mM NaCl, 2.7 mM KCl, 10 mM Na_2HPO_4, 1.8 mM KH_2PO_4, pH 7.4).

3.3.2 Immune Inhibitory Ligands' Antibody Staining

Two wells containing isolated immune cells of tumor and spleen were designated for immune inhibitory ligand antibody staining (see Table 2). The immune inhibitory ligands' antibody staining set contained antibodies against various myeloid cell surface markers and immunoinhibitory ligands of PD-L1 and PVR. Each of these fluorescently labeled antibodies recognizes one specific type of either myeloid cells or their displayed immunoinhibitory molecules of PD-L1 and PVR. For example, ly6C^{low} and Ly6C^{hi} are specifically expressed at the surface of monocytes. CD45 is expressed at the surface of hematopoietic cells (CD4/CD8). CD326 (Epcam) is used as an antibody against Epcam, expressed at the surface of tumor cells. CD11b is a marker for myeloid cells. CD11c is dominantly expressed at the surface of dendritic cells. Ly6G is expressed mostly at the surface of polymorphonuclear neutrophils (PMN).

After washing these cells with FACS buffer, 25 µl of immune inhibitory ligands' antibody mixture was added to designated wells containing immune cells of both spleen and tumor. The immune inhibitory ligands antibody mixture contains Ly6C-FITC (1:100), PD-L1-PE (1:100), PVR-PECy7 (1:100), Epcam-PerCPCy5.5 (1:100), CD11c-APC (1:100), CD11b-BV605 (1:200), CD45-PacBlue (1:100), and Ly6G-BV510 (1:100). This antibody mixture also contained Fc-block (anti-CD16/CD32) at 1:100 and 2% normal rat serum. The purpose of Fc-block is to prevent the anti-PD-L1 or anti-PVR to bind through the Fc receptor to myeloid cells and other cells that express the Fc receptor. All antibodies were purchased from BioLegend Company and diluted with 1X PBS.

3.3.3 Immune Inhibitory Receptors' Antibody Staining

Two wells were dedicated for this set of staining. One well was already seeded with an adequate number of spleen immune cells and one seeded with isolated tumor immune cells (see Table 2). After washing these wells with an adequate amount of FACS buffer, 25 µl of the immune inhibitory receptors stains was added to each well. The immune inhibitory receptors' antibody staining set contained antibodies against immune inhibitory receptors expressed on the surface of T cells, $CD4^+$ and $CD8^+$. These immune inhibitory receptors include PD1, TIM3, LAG3 and TIGIT. Antibodies against $CD8^+$, $CD4^+$, CD44 and TCR-β were also used to detect these cell populations. The antibody mixture for the inhibitory receptor experiment contains CD44-FITC (1:200), TIM3-PE (1:100), PD1-PECy7 (1:100), LAG3-PerCPCy5.5 (1:100), TIGIT-APC (1:100), $CD4^+$-BV605 (1:100), TCR-β-PacBlue (1:100), and $CD8^+$-V500 (1:100).

After adding the antibody mixtures of the above-mentioned staining sets, isotype staining, immune inhibitory receptors and ligand staining cells were incubated for 20 min on ice, in darkness. Each well was washed with FACS buffer and centrifuged for 1 min at 2100 rpm. The plate was flicked and tapped to re-suspend the pellets. The re-suspended cells were washed with 1X PBS and centrifuged for 1 min at 2100 rpm. The plate was flicked and tapped again. 25 µl of e780 viable dye (diluted 1:1000 in 1X PBS) were added to re-suspended cells and were incubated for 10 min on ice, in darkness.

The cells were then washed with 1X FACS buffer and spun down for 1 min at 2100 rpm. The plate was then flicked and tapped again for cell suspension. Finally, re-

suspended cells were fixed by adding 100 µl of FACS fix buffer (1% paraformaldehyde (16%, Electron Microscopy Science) in D-PBS w/o calcium and magnesium salts (1X)) and stored in 4ºC to be acquired by a flow cytometer. Stained samples were analyzed on BD LSRfortessa flow cytometer machine and data collected using BD FACSDiva software. The acquired flow data were analyzed using Flowjo X 10.0.7 software.

Table 2. Schematic Shows The Wells With Seeded Cells And Their Applied Antibody Staining Per Sample

Spleen cells stained with Isotype Control antibody mixture	Tumor cells stained with Isotype Control antibody mixture
Spleen/ cells stained with Immune Inhibitory Ligand antibody mixture	Tumor cells stained with Immune Inhibitory Ligand antibody mixture
Spleen cells stained with Immune Inhibitory Receptors' antibody mixture	Tumor cells stained with Immune Inhibitory Receptors' antibody mixture

3.3.4 Compensation

Each fluorochrome emits light in a certain range of wavelengths called emission spectrum. Band pass filters are used to narrow down the range of emitted light to a certain wavelength that is assigned to that fluorochrome that later is detected by photo detectors. The emission spectrum of a fluorochrome can cover a broad range of wavelengths that can be passed through and detected by more than one band pass. In that

case, for one fluorochrome more than one wavelength is detected. A correction is required to ensure that the fluorescence detected by a particular detector emitted by a single fluorochrome. This correction is called compensation. To compensate a fluorochrome, single color staining was done. Each well was stained with single-color antibody and was run through flow cytometer. The positive and negative peaks were determined. Then, Flow cytometer software BD FACS Diva was utilized to carry out compensation through an automatic calculation.

3.3.4.1 Single-Color Antibody Staining for Compensation

To do staining, 1 x 10^6 spleen cells seeded in 96-well plates, cells were washed with FACS buffer, centrifuges for 1 min at 2100 rpm, flicked and tapped to re-suspend the cells. To each well containing re-suspended cells 25 µl of fluorescently labeled antibody was added (See Table 3). The antibody mixture for compensation contains Ly6C-FITC (1:100), Ly6G-PE (1:200), CD11c-PECy7 (1:100), CD8-PerCPCy5.5 (1:100), CD11b-APC (1:200), CD4-BV605 (1:200), CD45-PacBlue (1:100), and e780-dye (1:1000). All antibodies were purchased from BioLegend Company and diluted with 1X PBS.

One well designated as negative control and labeled as no stain. The last well also designated for e780 dye antibody. Only FACS buffer was added to these two wells at this step. The rest of the well containing cells were incubated in single color stain for 20 min on ice then all wells were washed with FACS buffer. Cells then centrifuged for 1 min at

2100 rpm, flicked and re-suspended by tapping. PBS (1X) was added to each well followed by one step centrifugation at 2100 rpm for 1 min, flicking and tapping. 25 µl of FACS buffer or e780 dye were added to the well dedicated for e780 dye antibody. Cells Incubated on ice for 10 min, washed with FACS buffer, centrifuged for 1 more min at 2100 rpm. Re-suspended cells were fixed by adding100 µl of 1% paraformaldehyde in PBS, stored in 4º C and ran on Flow cytometer. BD FACSDiva software was used for compensation.

Table 3. The Order Of Single-Color Antibody Staining Of Spleen Cells For Compensation In 96-Well Plate

Comp1	Comp2	Comp3	Comp 4	Comp 5	Comp 6	Comp7	Comp 8	Comp 9
No stain	Ly6C-FITC	Ly6G-PE	CD11c-PECy7	CD8-PerCPCy5.5	CD11b-APC	CD4-BV605	CD45-PacBlue	e780-dye

Chapter Four

Results

4.1 Aim 1: Determine Whether The PD-L1 Expression, If There Is Any, Is Regulated By MYC

4.1.1 Tumor Cells (Both A Line And B Line) Do Not Express PD-L1 And The Expression Of PD-L1 Is Not Regulated By Transcription Factor MYC

To investigate whether PD-L1 is expressed on MYC-driven tumor cells, we employed FACS. FACS studies can provide us with very detailed information in regards to the types of cell that express PD-L1 as well as the level of its expression.

The histogram graph of PD-L1 expression on Epcam positive and negative cells stained with anti-PD-L1 was at the same level and close to the MFI of the isotype control stained cells (Figure 24). The quantified level of expression of PD-L1 have also shown that the expression of PD-L1 on the Epcam positive and negative cells do not show a significant difference compared to the ones stained with isotype control antibody on both primary tumor cells of line A and B (Figure 25A). We also observed that, if we take the mice off Dox, the tumor regressed but then several weeks after it recurred. Studying the PD-L1 expression on recurred tumors of line A and B also gave usthe same results as the

progressed tumors (Figure 25B); both tumor lines do not express PD-L1 on Epcam positive as well as Epcam negative cells.

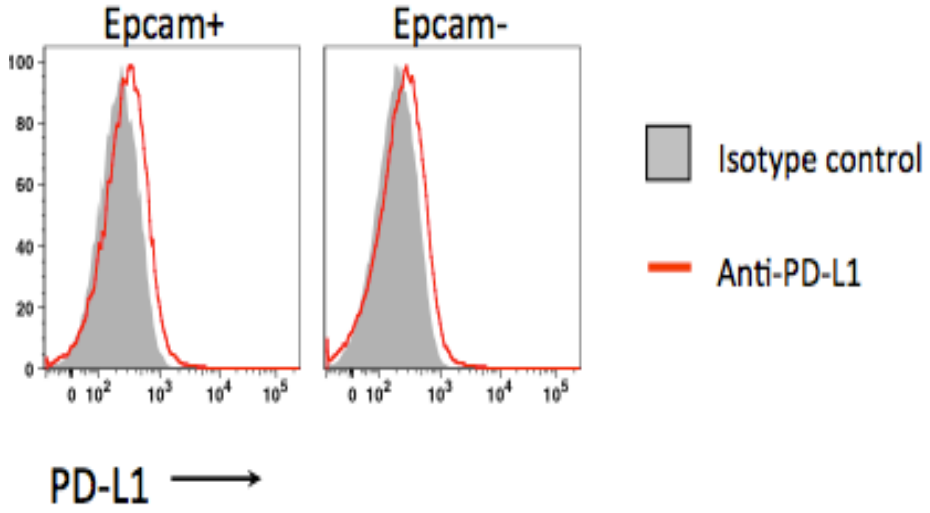

Figure 24. Flow Cytometry Histograms Representative Of PD-L1 Expression On Epcam$^+$ And Epcam$^-$ Cells Of Line A Recurred Tumor Stained By Anti-PD-L1 (Red) And Isotype Control Antibody (Grey). PD-L1 is not expressed on both Epcam$^+$ and Epcam$^-$ cells in the recurred tumor.

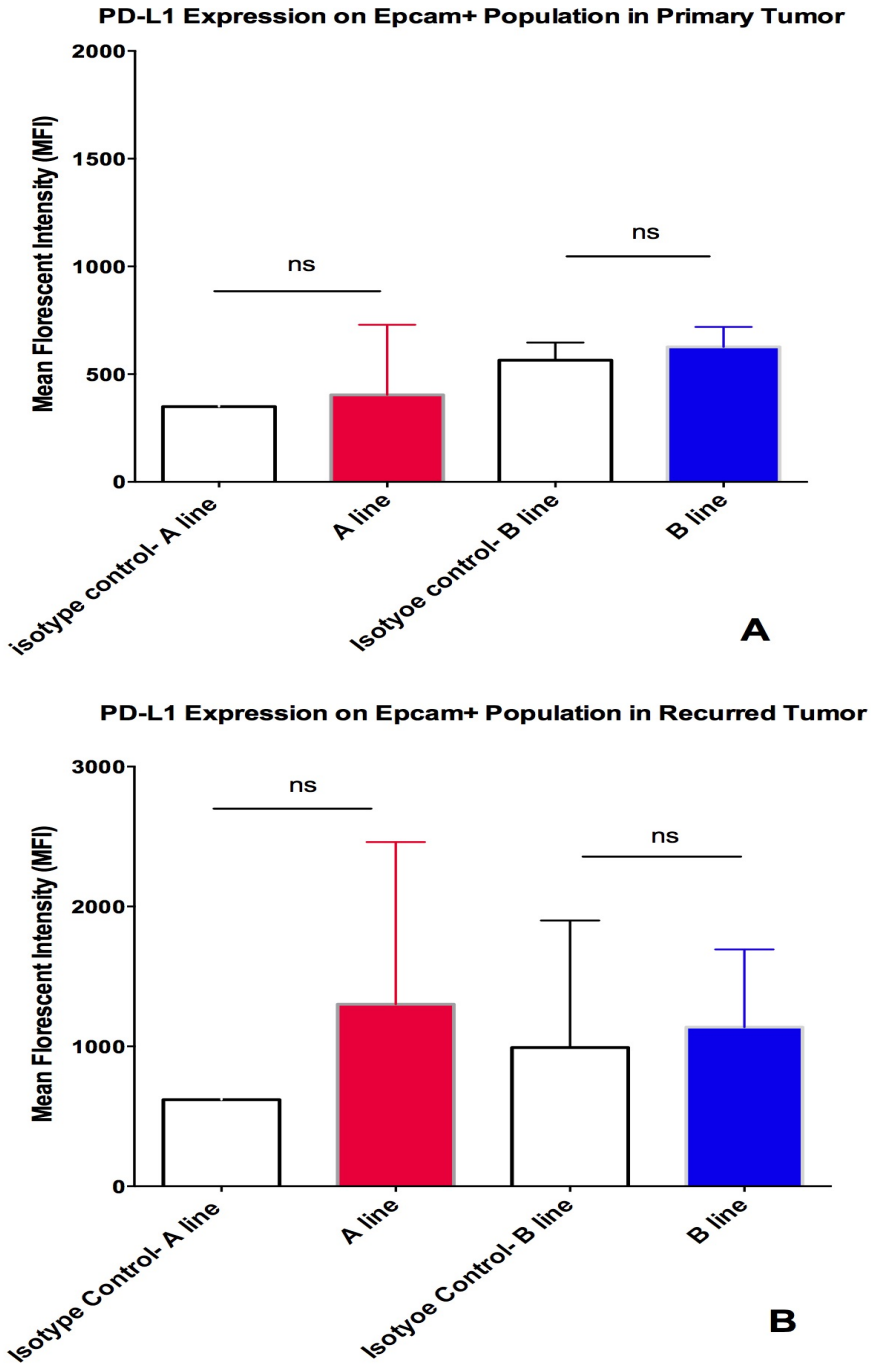

Figure 25. The Quantified MFI Of PD-L1 Expression On Epcam$^+$ Cells Of Both A Line And B Line. A: the primary tumor, B: the recurred tumor. Regardless of the stage of the tumor growth, primary or recurred, and the type of the tumor, Line A vs. Line B, PD-L1 is not expressing on both Epcam$^+$ cells (ns: P> 0.05).

To study if MYC can negatively regulate PD-L1 expression, we did also a FACS analysis of PD-L1 expression on the on-Dox tumor (Figure 26A), regressed tumor two days off-Dox (Figure 26B), and regressed tumor four days off-Dox (Figure 26C, D). Our data indicated that PD-L1was not expressed on tumor cells even after MYC withdrawal. Considering whether the MYC was expressed by tumor cells or not, PD-L1 was still not expressed by tumor cells, we conclude that MYC cannot negatively regulate the PD-L1 expression. On the four day off Dox samples, a new population was detected that express low (lo) to intermedium (int) amount of Epcam, this population was named as $Epcam^{lo\text{-}int}$ cells. Surprisingly, this population was expressed minute amounts of PD-L1 ligand (Figure 26A-D).

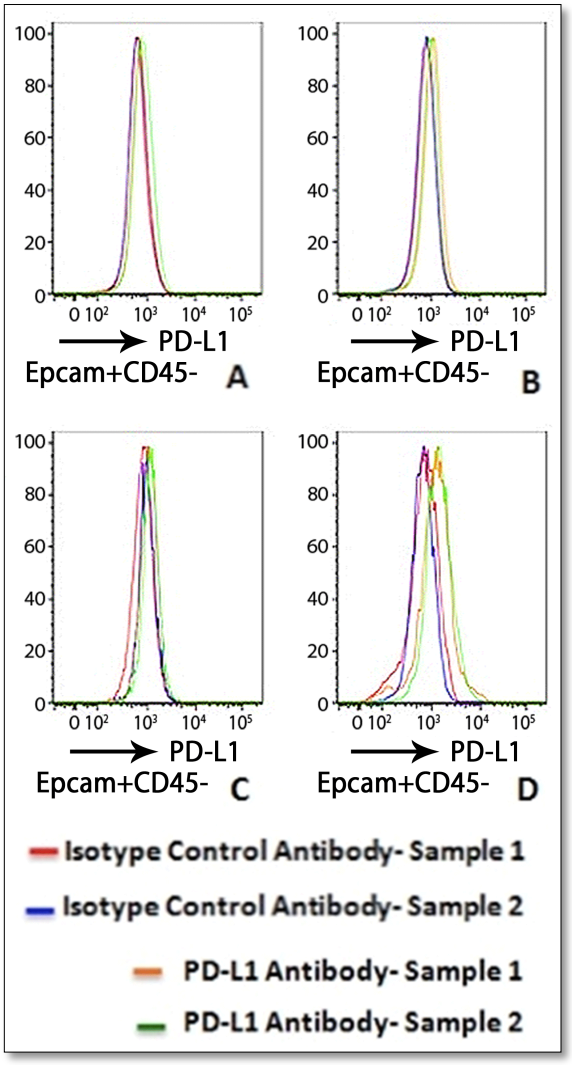

Figure 26. Flow Cytometry Histogram Representative Of PD-L1 Expression On Epcam^{+} CD45^{-} And Epcam$^{lo\text{-}Int}$ CD45^{-} Cells Of Line A Regressed Tumor Stained By Anti-PD-L1 (Green And Orange) And Isotype Control Antibody (Blue And Red). A: MYC driven tumor, B: Regressed Tumor, off Dox for two days, C and D: Regressed Tumor, off Dox for four days.

4.2 Aim 2: Targeting PD-L1 Ligand Through Anti-PD-L1 Antibody To Study The Effect Of PD1-PD-L1 Mediated Immunosuppression Pathway On TNBC Tumor Progression And Recurrence

4.2.1 Anti-PD-L1 Therapy Slowed MYC-Driven Breast Tumor Growth

PD-L1 has been diagnosed as an immune inhibitory ligand in which the RNA expression significantly increased in triple-negative versus receptor-positive human breast tumors, according to TCGA database (Preliminary data). Moreover, the microarray studies done on breast tumors have shown that 19% of the TNBC samples do express PD-L1 at some level (Mittendorf et al. 2014). The initial phase one trial of pembrolizumab (MK-3475), a highly selective, humanized IgG4/kappa monoclonal antibody designed to block PD1-PDL interaction, showed that out of 32 studied patients with advanced (recurrent/metastatic) TNBC, no patient had a complete response. About 16.1% had a partial response, 9.7% had stable disease and 64.5% had progressive disease. This small study suggested the anti-PD-L1 antibody as a well-tolerated and effective treatment with significant therapeutic activity in recurrent/metastatic TNBC patients (Balko et al. 2015).

All of these data together lead us to study the effect of immune checkpoint inhibitor of PD-L1 on MYC-driven tumor growth. To address this question, we embarked on blocking the PD1-PD-L1 immune checkpoint pathway in solid tumor of TNBC through targeting PD-L1.

Tumor progression study showed that the tumor grew slower in mice cohort that received two-weeks anti-PD-L1 antibody treatment compared to the one that did not receive treatment (Figure 27). Anti-PD-L1 treatment caused an average delay of approximately 14 days in tumor progression. The average speed of growth dropped from 143 mm^3 in the untreated group to 87 mm^3 per day in the treated group. Day 0 is the day that the treatment was started (Figure 27A-B). Besides, treated cohort has longer progression-free survival compared to the untreated group. Progression-Free Survival (PFS) refers to the time from treatment initiation to disease progression or death (Hill 2001).

Considering the tumor size of 2500 mm^3 as the end point for the life of the mouse, this time point was used to calculate survival time after treatment using the Kaplan-Meier survival algorithm by Prism software. The Kaplan-Meier survival curve showed a significant difference in percent survival of the treated group compared to the untreated one (Figure 28). Treatment cause an approximately 10-12 days delay in reaching the endpoint in treated group compared to untreated group. P-value was tested using Gelsen-Breslow-Wilcoxon test (P-value: 0.0066).

These two graphs together proved that, anti-PD-L1 treatment could slow down the MYC-driven tumor growth.

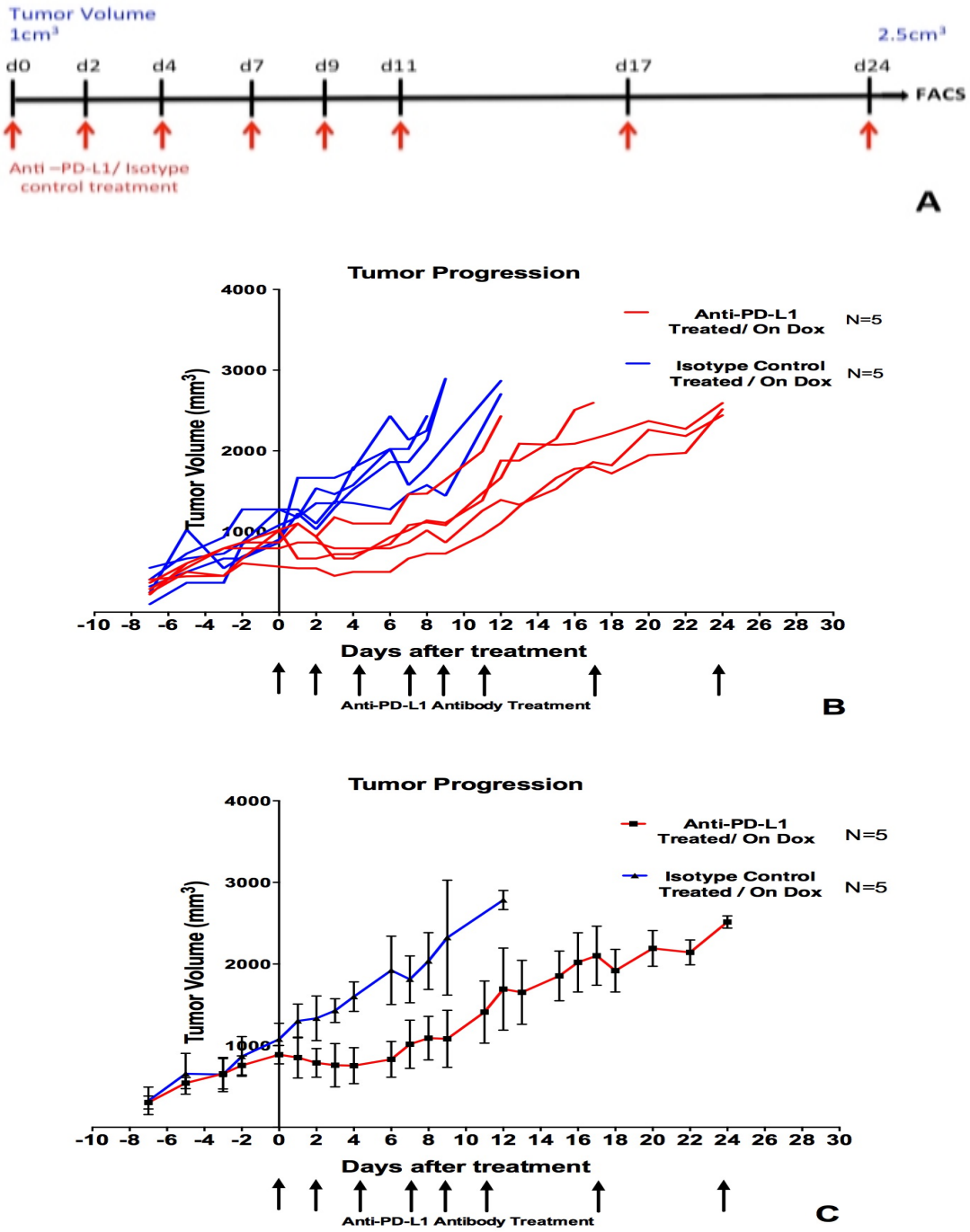

Figure 27. Growth Curve Of Primary Tumor Of Line A. A: treatment regimen. B: growth curve of each sample. C: growth curve of mean data. Red: primary tumor of A line treated with anti PD-L1. Blue: primary tumor of A line treated with isotype control antibody. Little arrows indicated the days of treatment.

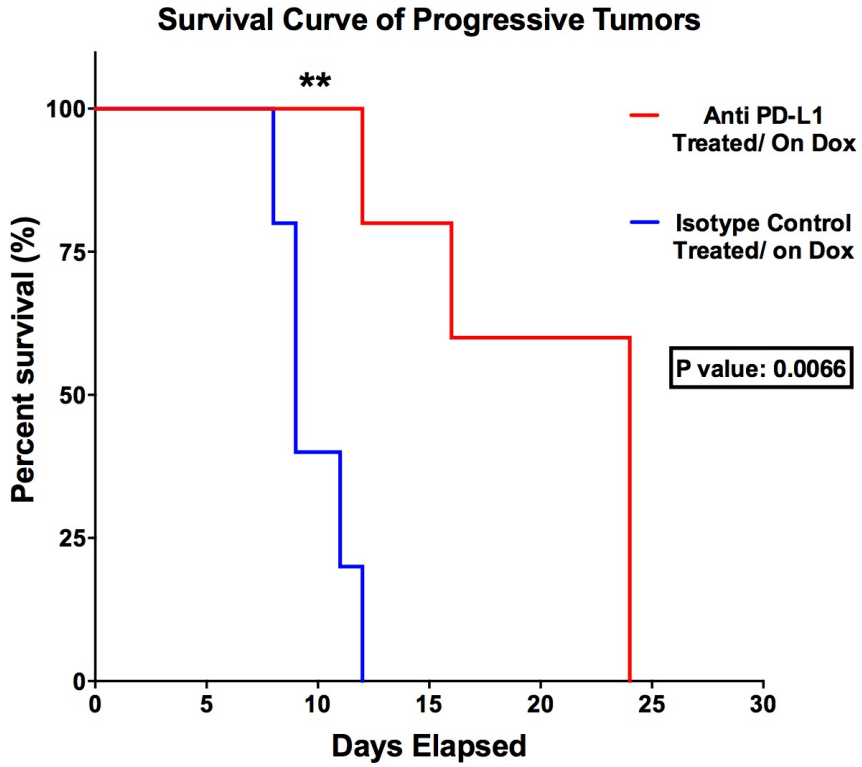

Figure 28. Survival Curve Of Primary Tumor-Bearing Mice. Red: primary tumor of A line treated with anti-PD-L1. Blue: primary tumor of A line treated with isotype control antibody. Day zero is the first day of treatment. There was a significant difference in the survival of treated group compared to untreated one (**: P≤ 0.01)**.**

4.2.2 Anti-PD-L1 Therapy Delayed Recurrence Of MYC-Driven Breast Tumor Growth

Tumor recurrence is one of the known characteristics of this MYC-driven breast cancer mouse model. Previous studies have shown that the tumor starts regressing after taking the primary tumor off Dox and then it goes into latency stage (Figure 29 B). Notably, the tumor recurs several weeks later; the time of recurrence varies from sample to sample and is regardless of primary size upon taking off Dox. The reasons underlying

tumor recurrence haven't been discovered yet. However, some studies in our lab have shown that the endogenous mouse MYC was turned on in this tumor model, which possibly could drive tumor growth at the recurrence stage (data not shown).

Considering the fact that recurrence is one of the important characteristics of TNBC, in this study we also became interested in knowing whether the anti-PD-L1 treatment can delay the recurrence. Studies on two cohorts of mice, one received anti-PD-L1 antibody treatment and one received isotype control antibody have shown that anti-PD-L1 antibody treatment also could result in delay in recurrence. Despite some mice recurred earlier in treated group compared to untreated, the treated group recurred later in general compared to untreated. The difference in recurrence is also not related to the time or speed of regression. There were some samples that regressed at the same time as others but recurred later. Consequently, anti-PD-L1 also could cause a delay in tumor recurrence in MYC-driven TNBC mouse model.

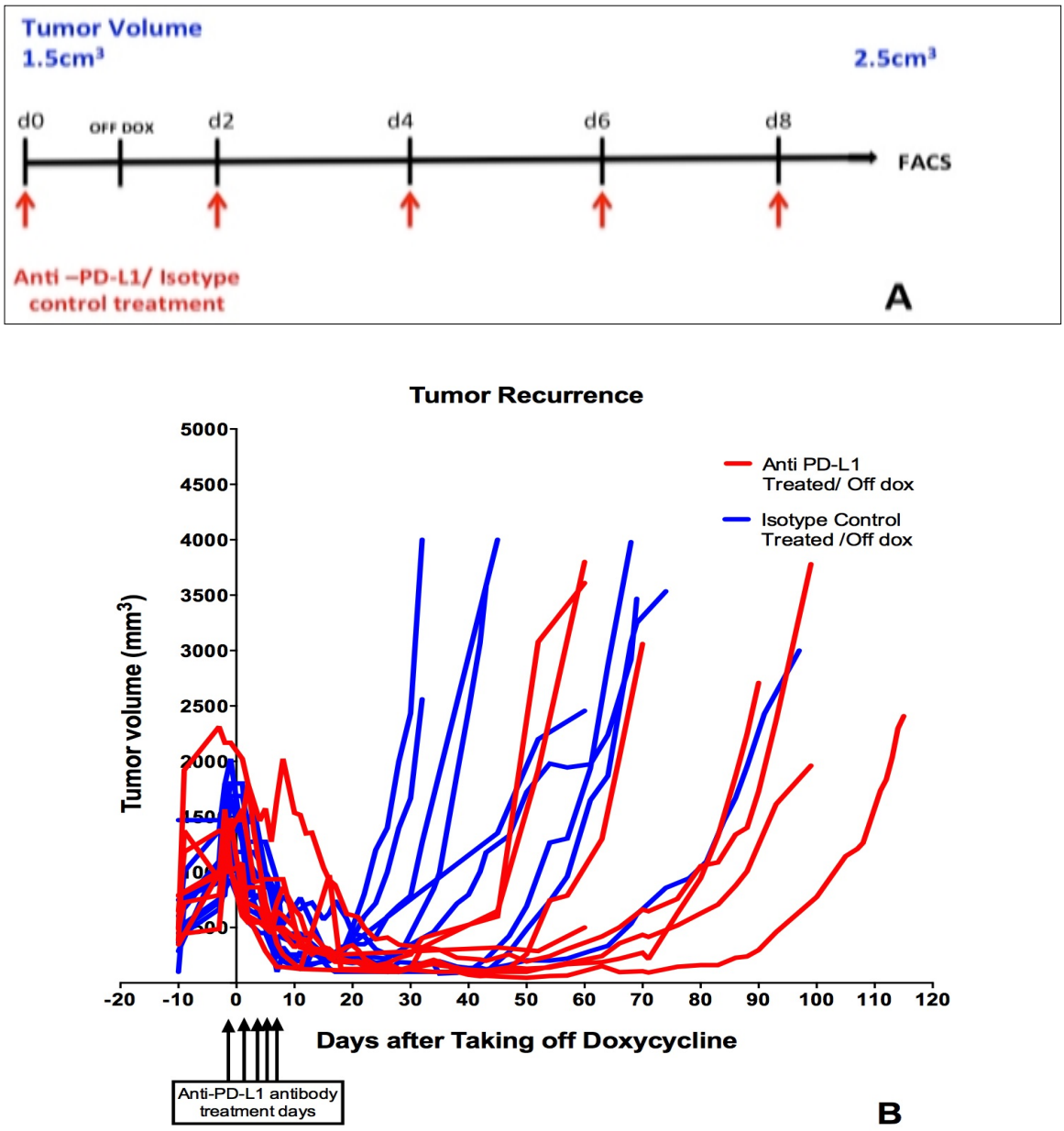

Figure 29. Growth Curve Of Primary Tumor Of Line A Upon MYC Withdrawal. A: Treatment regimen. B: Growth curve of each tumor sample. Red: Primary tumor of A line treated with anti PD-L1. Blue: Primary tumor of A line treated with Isotype control antibody. Little arrows indicated the days of treatment.

The total size of 2500 mm^3 in the recurred tumor burden was used as the end point to calculate the survival time after Doxycycline removal. The Kaplan-Meier

survival curve of the recurrence also shows that the anti-PD-L1 treated ones had delayed in recurrence compared to the treated group (Figure 30). There is a significant delay, the average of 25 days, to reach to the end point in treated group compared to untreated one, which results in prolonged survival of the recurred tumor-bearing mice that received treatment. P-value was tested using Gelsen-Breslow-Wilcoxon test (P-value: 0.0283).

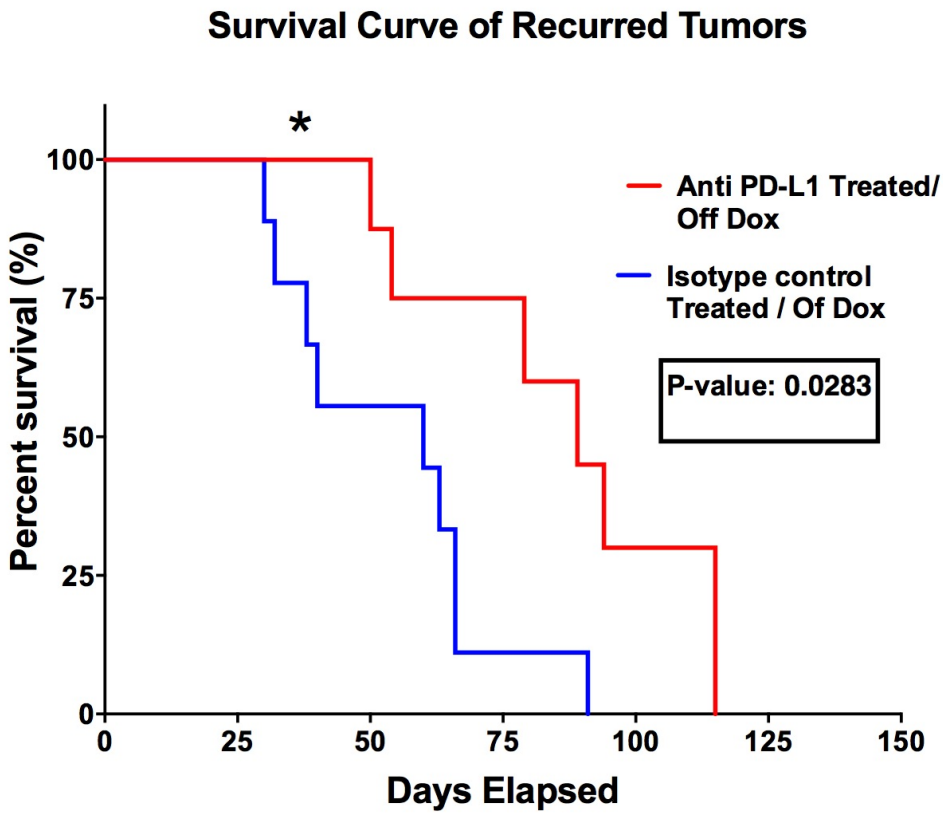

Figure 30. Survival Curve Of Recurred Tumor-Bearing Mice. Red: primary tumor of A line treated with anti-PD-L1. Blue: primary tumor of A line treated with isotype control antibody. Day zero is the first day of treatment (*: $P \leq 0.05$).

4.2.2.1 PD-L1 Was Expressed On Tumor-Associated Myeloid Cells Of Both Primary Tumors And Recurred Tumors But NOT On The Tumor Cells

Western blot studies together with FACS data analysis of isolated tumor cells of Line A have shown that the tumor cells do not express PD-L1. However, targeting this immune inhibitory ligand did delay tumor progression at both the primary tumor and recurred tumor. Consequently there should be cells other than tumor cells than can bind to tumor-specific lymphocytes and impair their antitumor response. This immune response attenuation has to be mediated through PD-L1. Previous data have shown that myeloid cells of mouse can express PD-L1 (Keir et al. 2008). We used flow cytometry to determine which immune cells expressed the immune inhibitory ligand PD-L1. Considering that PD-L1 is on the surface of both immune cells as well as tumor cells, through FACS, we not only can identify the specific cells that express PD-L1 but also we can quantify the level of PD-L1 expression.

In this study we focused on expression of PD-L1 on immune cells found in both primary and recurred tumors of line A. Cells of line A tumor and spleen were isolated, stained according to the protocol outlined above and analyzed on a flow cytometer. According to the level of expression of each of the cell specific surface proteins, each cell population were gated to define specific population of immune cells and their PD-L1 expression was determined as Mean Fluorescent Intensity (MFI) of the channel for the PD-L1 fluorochrome by using Flowjo software (Figure 31).

Since myeloid cells are so called sticky, meaning that they can bind easily to many antibodies nonspecifically, we used a population of myeloid cells that were stained with isotype control as the negative control and compared their PD-L1 expression with the population stained with actual antibody.

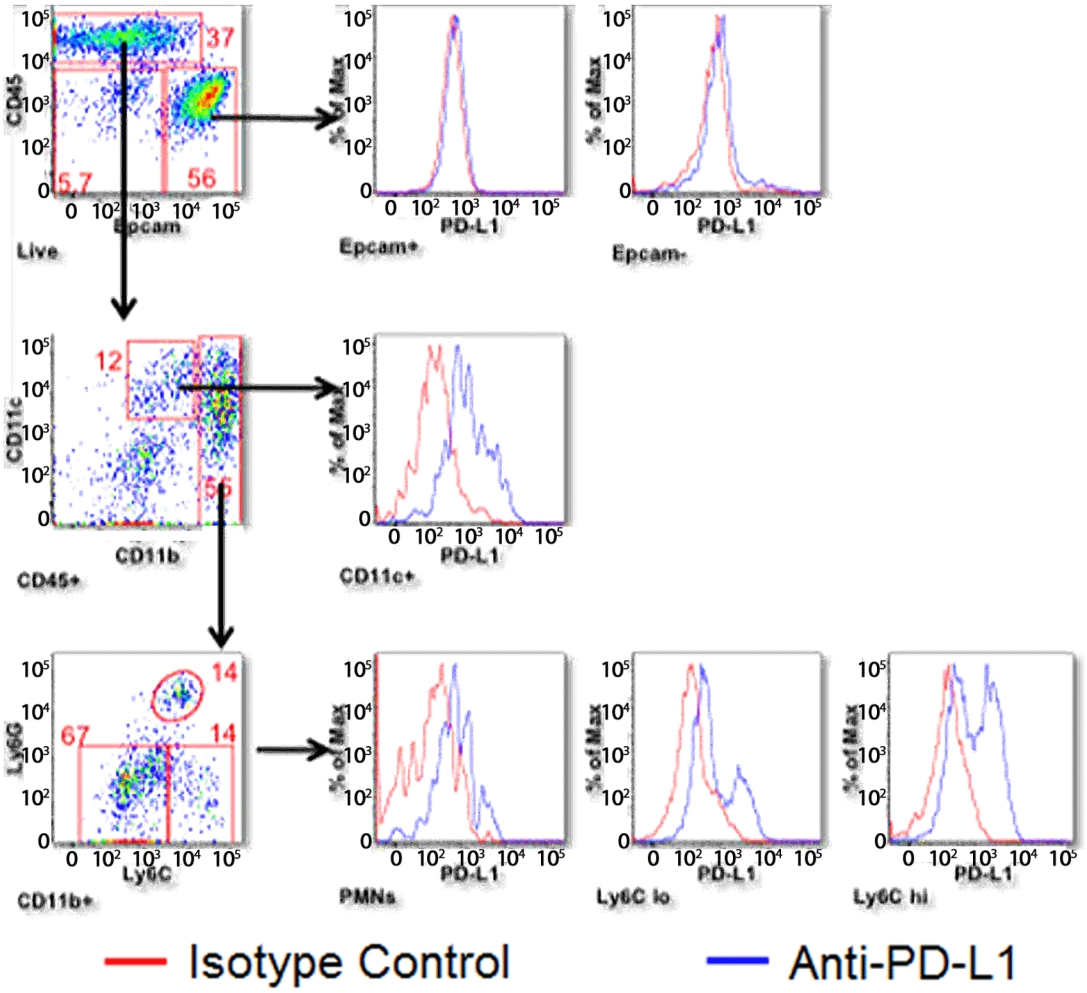

Figure 31 Gating Procedure And Flow Cytometry Histogram Representative Of PD-L1 Expression On Different Myeloid Cell Populations As Well As Epcam^{+} And Epcam$^{lo\text{-}Int}$ Cells. Cells were isolated from primary tumor of line A and stained by anti PD-L1 (Blue) and Isotype control (Red).

We found that PD-L1 was expressed significantly on all four studied myeloid subpopulations of PMN, CD11c, Ly6C^{lo} and Ly6C^{hi} in naïve spleen (Figure 32 A-D). This means that all myeloid population predominantly expresses immune inhibitory ligand, PD-L1 in the spleen. Consequently, we used the myeloid population of naïve spleen as the positive control. As the myeloid population entered within the tumor they cannot leave the microenvironment. In the microenvironment there are many factors including the tumor that myeloid cells interact with. This interaction may result in changing the myeloid cell's PD-L1 expression. Thus, in addition to tumor-infiltrated myeloid cells, we also studied the population of the cells in the spleen comparing the effect of tumor on the expression of this ligand.

Studies of PD-L1 expression on all four myeloid subpopulations of both spleen and tumor have shown that this ligand was expressed on all four myeloid subpopulations significantly at both spleen and tumor regardless of the stage of the tumor (Figure 32A-D). But the level of PD-L1 expression varied from one subpopulation to one another.

The level of PD-L1 expression remained almost the same between the spleen of naive and primary tumors except on CD11c populations whose PD-L1 expression increased in the tumor-bearing mice spleens compared to the naïve spleens. Comparing the fold increase of the level of PD-L1 expression from isotype control-stained cells to anti-PD-L1-stained cells has shown that the level of PD-L1 expression in the CD11c subpopulation is much higher in the spleen of tumor-bearing mice than the naïve spleen. Conversely, at the recurred stage, all four subpopulations of myeloid cells demonstrated elevated PD-L1 expression in the spleen of the tumor-bearing mouse compared to the one

in naïve spleen (Figure 33A-D). The reason underlying such increase in these selective populations is not clear; but these changes demonstrates that how tumors could affect the level of PD-L1 expression on these immune subpopulations at secondary lymphoid organ of spleen.

The level of expression of this ligand on myeloid subsets infiltrated the tumor at both stages (recurred and primary) has been changed as well. Comparing the fold change of the quantified PD-L1 expression between tumors and spleens demonstrated that in the primary tumors, PMN and Ly6C^{hi} subpopulations of myeloid cells showed approximately the same level of PD-L1 expression compared to myeloid population in naïve spleen and their own spleen. In contrast to Ly6C^{hi} and PMN, the expression of PD-L1 on the CD11c and Ly6C^{lo} was lower compared to the one in naïve spleen and tumor-bearing mice's spleen (Figure 32, 33).

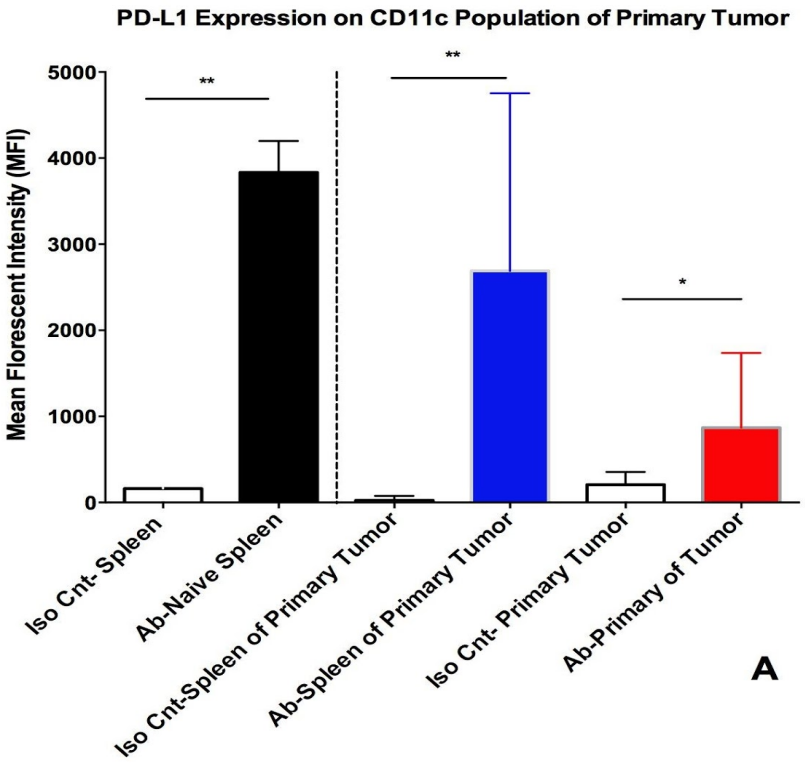
PD-L1 Expression on CD11c Population of Primary Tumor
Mean Florescent Intensity (MFI)
5000
4000
3000
2000
1000
0
**
**
*
Iso Cnt- Spleen
Ab-Naive Spleen
Iso Cnt-Spleen of Primary Tumor
Ab-Spleen of Primary Tumor
Iso Cnt- Primary Tumor
Ab-Primary of Tumor
A

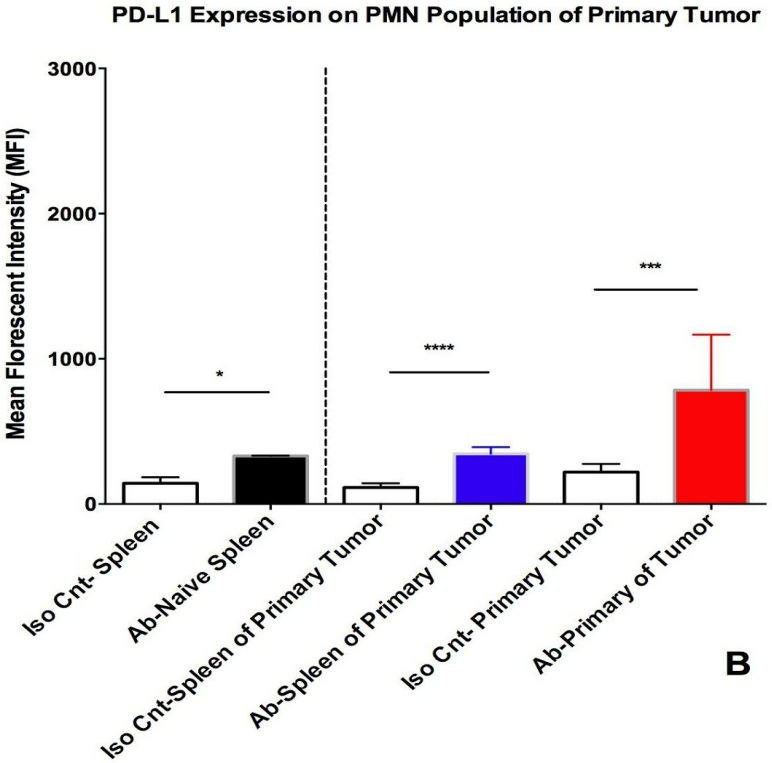
PD-L1 Expression on PMN Population of Primary Tumor
Mean Florescent Intensity (MFI)
3000
2000
1000
0
*
****
***
Iso Cnt- Spleen
Ab-Naive Spleen
Iso Cnt-Spleen of Primary Tumor
Ab-Spleen of Primary Tumor
Iso Cnt- Primary Tumor
Ab-Primary of Tumor
B

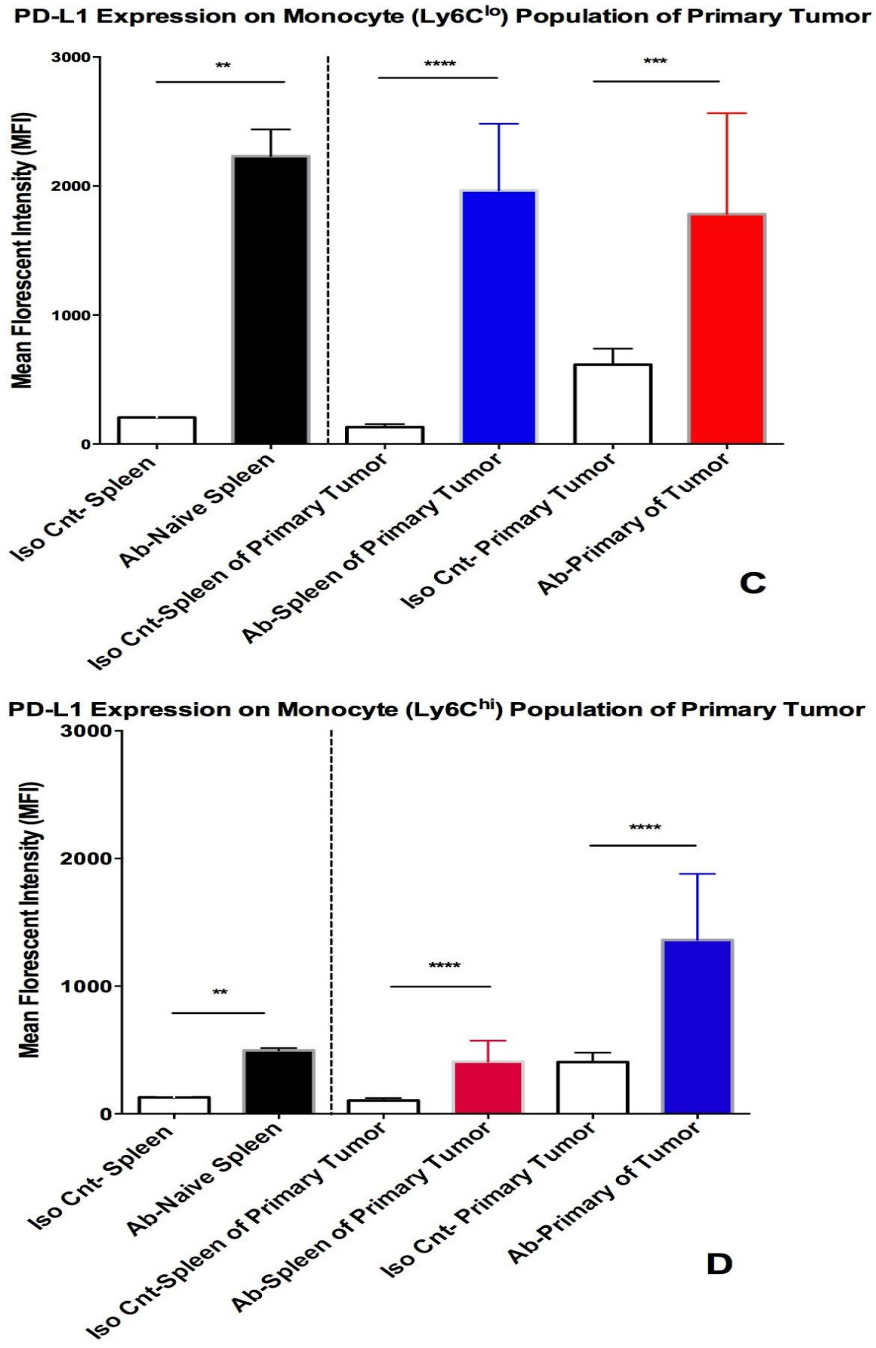

Figure 32. Comparison Of The quantified Level Of PD-L1 Expression On Myeloid Subpopulations Between The Naïve Spleen, Spleen Of Primary Tumor And Primary Tumor Of Line A. A: CD11c population. B: PMN population. C: Monocytes (Ly6C^{hi}) population. D: Monocytes (Ly6C^{lo}) population. Iso. Cnt.: Isotype control antibody. Ab.: antibody. (ns: P> 0.05, *: P ≤ 0.05, **: P≤ 0.01,***:P≤ 0.001, ****: P≤ 0.0001).

At the recurred stage, similar to the primary tumors, the expression of PD-L1 in CD11c and $Ly6C^{lo}$ subpopulations decreased in the tumor compared to the spleens but the expression of PD-L1 significantly increased in the tumor-associated $Ly6C^{hi}$ and PMN compared to the one in the spleen. Despite the fact that the statistical analysis has shown that there is not a significant difference between the PD-L1 level of expression of $Ly6C^{lo}$ in the tumor with the spleen, looking at raw data indicated that the quantified PD-L1 expression of each tumor samples significantly increased from the isotype control stained samples to the anti-PD-L1 stained samples (5-12 fold increase). Thus, we can conclude that this not significant result is a false negative and the PD-L1 was still significantly expressed on this population in the tumor. The abnormally high expression of PD-L1 on one of those samples might be the reason for this false negative.

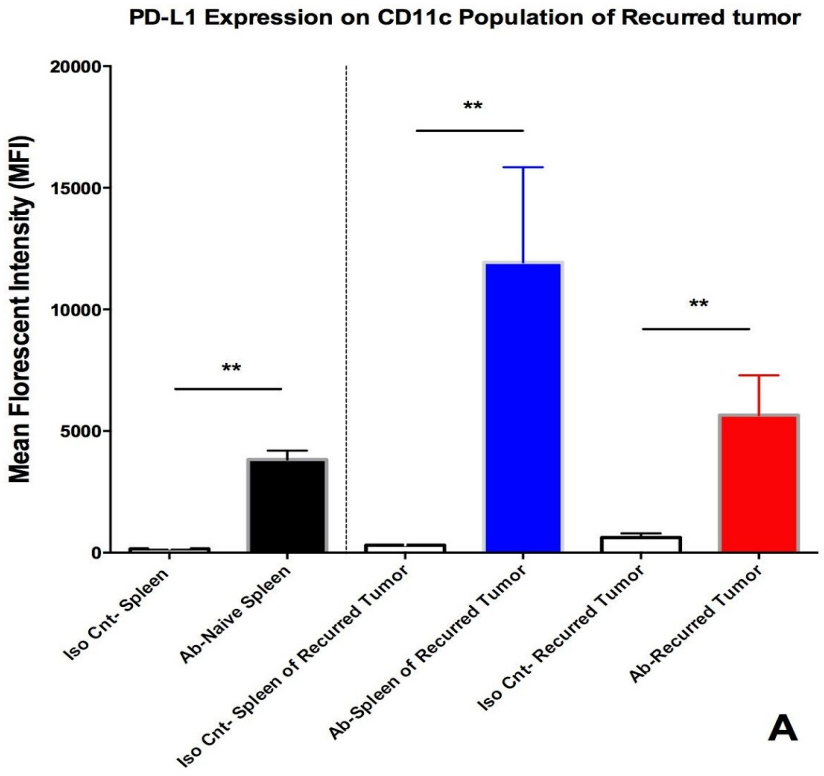
PD-L1 Expression on CD11c Population of Recurred tumor
Mean Florescent Intensity (MFI)
20000
15000
10000
5000
0
**
**
**
Iso Cnt- Spleen
Ab-Naive Spleen
Iso Cnt- Spleen of Recurred Tumor
Ab-Spleen of Recurred Tumor
Iso Cnt- Recurred Tumor
Ab-Recurred Tumor
A

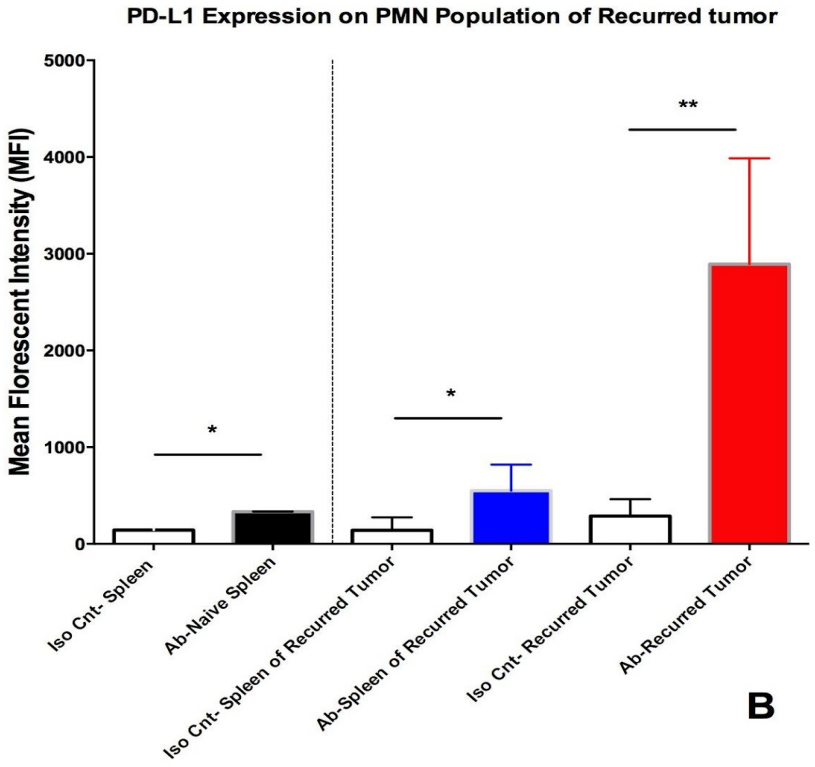
PD-L1 Expression on PMN Population of Recurred tumor
Mean Florescent Intensity (MFI)
5000
4000
3000
2000
1000
0
*
*
**
Iso Cnt- Spleen
Ab-Naive Spleen
Iso Cnt- Spleen of Recurred Tumor
Ab-Spleen of Recurred Tumor
Iso Cnt- Recurred Tumor
Ab-Recurred Tumor
B

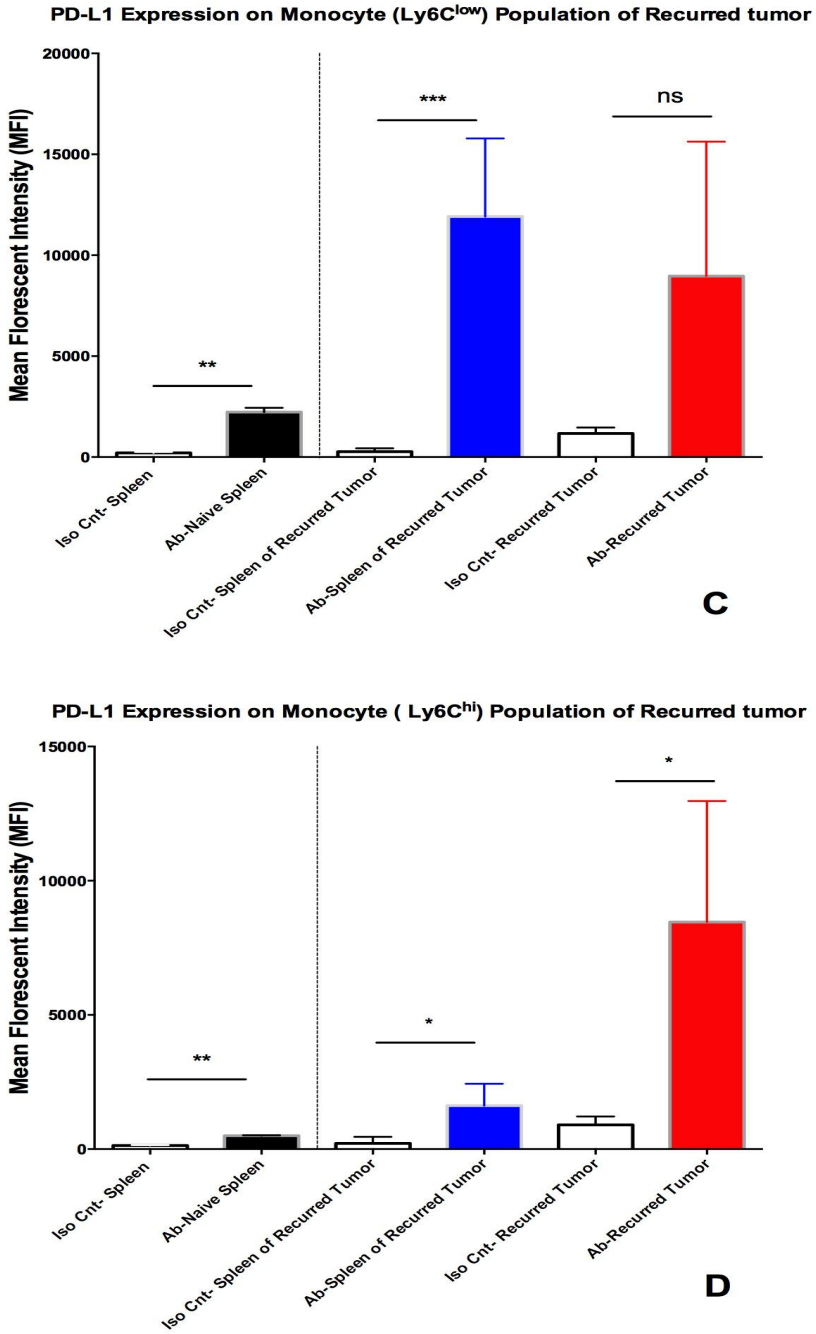

Figure 33. Comparison Of The quantified Level Of PD-L1 Expression On Myeloid Subpopulations Between The Naïve Spleen, Spleen Of Recurred Tumor And Recurred Tumor Of Line A.A: CD11c population. B:PMN population. C: Monocytes (Ly6C^{hi}) population. D: Monocytes (Ly6C^{lo}) population. Iso Cnt: Isotype control antibody. Ab: antibody. (ns: $P > 0.05$, *: $P \leq 0.05$, **: $P \leq 0.01$,***:$P \leq 0.001$, ****: $P \leq 0.0001$).

4.2.2.2 Collagenase Treatment Had No Effect On Detected PD-L1 Expression On Tumor Cells

To ensure the lack of PD-L1 expression on tumor cells was not due to its degradation by the collagenase enzyme treatment throughout the isolation procedure, we isolated the myeloid cells of spleen with and without collagenase treatment. The immune cells were stained and analyzed by FACS according to the procedures described before.

The MFI of PD-L1 on all four myeloid subpopulations namely PMN, CD11c, $Ly6C^{hi}$ and $Ly6C^{lo}$ were stained with anti-PD-L1 was significantly higher than those stained with isotype control antibody regardless of collagenase treatment. These data suggest that collagenase treatment had no effect on the level of PD-L1 expressed on tumor infiltrating myeloid cells (Figure 34).

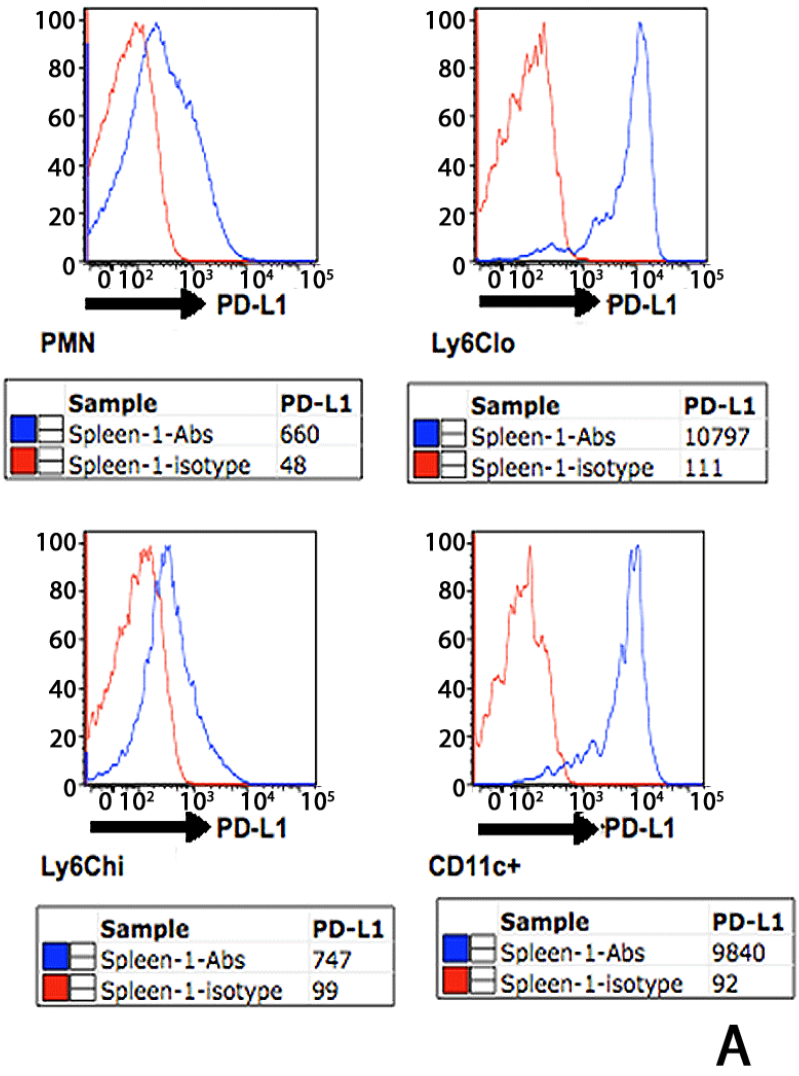
100
80
60
40
20
0
0 10² 10³ 10⁴ 10⁵
PD-L1
PMN
Sample PD-L1
Spleen-1-Abs 660
Spleen-1-isotype 48
Ly6Clo
Sample PD-L1
Spleen-1-Abs 10797
Spleen-1-isotype 111
Ly6Chi
Sample PD-L1
Spleen-1-Abs 747
Spleen-1-isotype 99
CD11c+
Sample PD-L1
Spleen-1-Abs 9840
Spleen-1-isotype 92
A

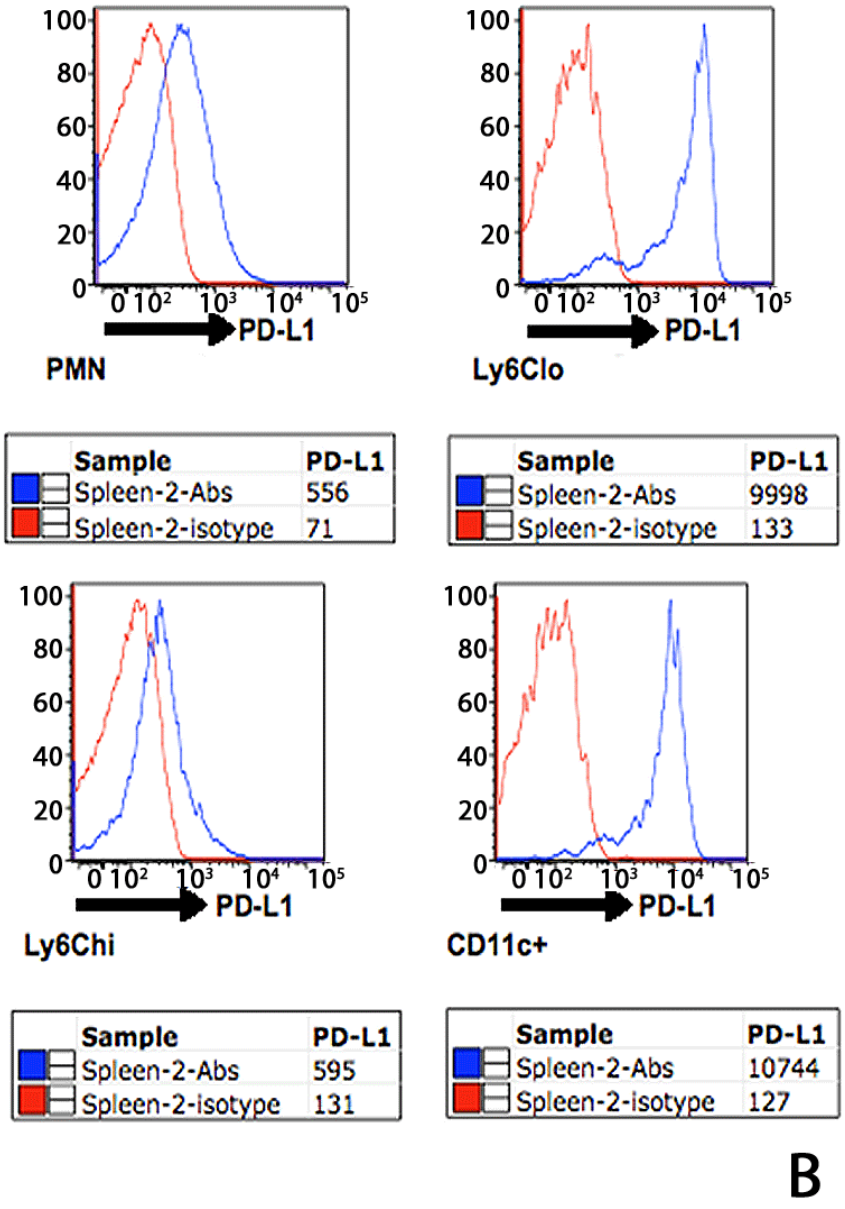

Figure 34. Effect Of Collagenase Treatment On PD-L1 Expression On Different Myeloid Subpopulations. Cells were isolated from spleen and stained by anti PD-L1 (Blue) and is Isotype control (Red). A: the MFI of PD-L1 expression on myeloid subpopulations of spleen isolated without collagenase. B: the MFI of PD-L1 expression on myeloid subpopulations of spleen isolated with collagenase.

4.2.3 Kinetics Of The Immune Response Upon Acute MYC Withdrawal

To study the kinetics of the immune response upon regression, both the distribution of immune cells and immune inhibitory molecules' expression were studied on tumor cells before and after MYC withdrawal. Three aspects of the immune response were subjected for this study; the lymphocyte ($CD4^+$ T cells/$CD8^+$ T cells) population, myeloid cell population and the immune inhibitory receptors and ligand expression on lymphocytes and myeloid cells respectively.

Considering that the tumor is most likely recurred, knowing the kinetics of the immune response upon regression may help to know how we can harness or boost this antitumor immune response to clear up tumor cells from the microenvironment more affectively at the regression stage. This, in turn, may cause a longer delay in tumor recurrence and increase the overall five-year survival rate.

4.2.3.1 FACS Data Analysis Showed Tumor Regression Four Days After MYC Withdrawal

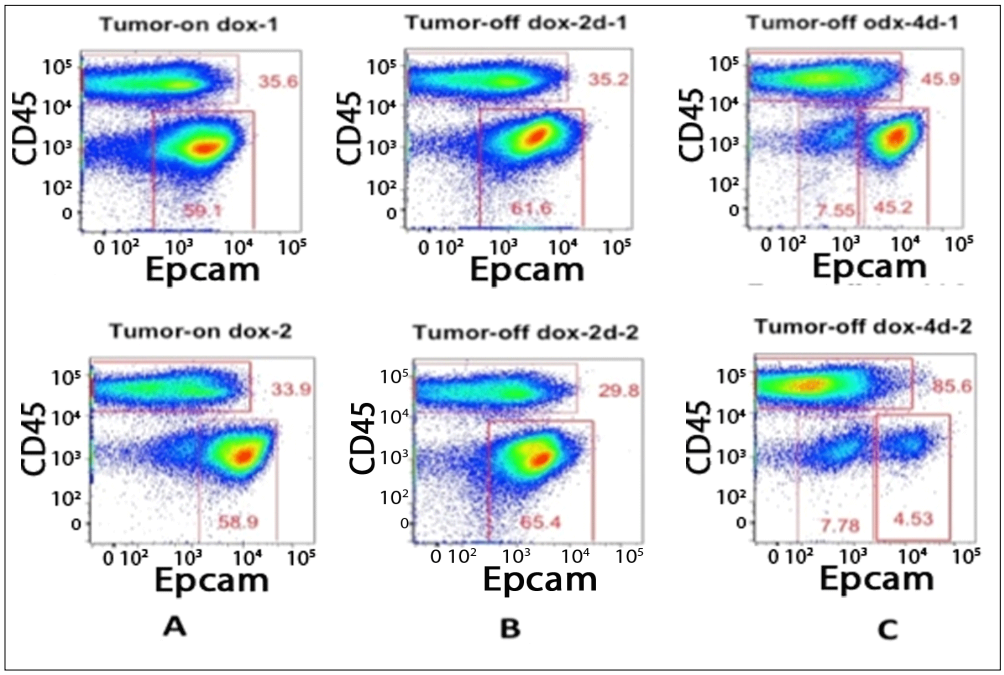

Figure 35. FACS Gating On Tumor Infiltrated Immune Cells, CD45+, And Tumor Cells, Epcam+, And Their Percentage On Primary Tumor And Regressed Tumor. A: The percentage of tumor-associated immune cells and tumor cell of On Dox tumor. B: The percentage of tumor-associated immune cells and tumor cell of regressed tumor (two days off Dox). C: Tumor-associated immune cells and tumor cell of regressed tumor (four days off Dox). FACS data shows the kinetics of tumor regression.

The FACS data analysis showed a sharp drop in the total population of Epcam positive cells four days after Dox removal (~25% and 91%), proving that the MYC-driven tumor cells are dying (Figure 35C). Notably, four days after Dox removal, a new population that expressed lower level of Epcam was detected. This population constitutes approximately 8% of the whole population. Recent studies have already shown that

normal epithelial cells can express Epcam at a variable level but generally lower level than cancer cells (Trzpis et al. 2007). This population could also be the differentiated progenitor epithelial cells isolated along with immune and tumor cells (Stingl 2002) ; the population whose abundance was covered with the Epcam positive cells when the tumor was on Dox.

The populations of both immune infiltrating cells and tumor cells did not change two day after Dox removal compared to the ones in the growing tumor (Figure 35 B). But the FACS data analysis showed that the abundance of immune cell population increased dramatically on day four upon MYC withdrawal when compared to growing tumor (from 35% to ~46% in one sample and 85% in the other) (Figure 35A-C). This change in the abundance of immune cells could be either due to the decrease in the abundance of tumor cells or be a result of the recruitment of immune cells including macrophages and lymphocytes due to increase in the number of tumor antigen and dead tumor cells left behind.

The On-Dox tumor almost showed the same phenotype as the two-day off Dox tumor in terms of tumor-infiltrating immune cell population and $Epcam^{+}$ population. This similarity and delay in response in MYC-starved group for two-days could be due to the fact that while tumor cells stopped their proliferation, they went into the senescence step before dying or because of the remaining Dox in their system (Felsher 2010).

4.2.3.2 Immune Cell Population Is Dynamic Within The Body And There Is A Correlation Between Lymphocyte Populations Of Spleen And Tumor: As One Change, The Other Changes

Studying the spleen's immune subpopulation within each cohort of naïve (no tumor mice), on Dox, two-day off Dox and four-day off Dox has shown that the population of spleen's lymphocytes changed from one cohort to the other. This proves the fact that the immune cell populations in different parts of the body are connected. It also proves how antitumor-immune responses in one part of the body could affect immune cell populations in other sites of the body.

The spleen is the largest secondary immune organ affected by this effect as well. The population of $CD4^+$ T cells and $CD8^+$ T cells within the naïve spleen was $4x10^7$ and $0.7x10^7$ respectively with the $CD4^+$ T cells more abundant than $CD8^+$ T cells. The spleen of tumor-bearing mice in general has a higher lymphocyte population compared to the spleen of naive mice; $CD4^+$ T cell population is much higher in all tumor-bearing cohorts (Figure 36 A-B).

Lymphocyte cell populations, both $CD4^+$ T cells and $CD8^+$ T cells, of spleen increased two days after Dox removal compared to the On-Dox tumor despite Dox withdrawal (Figure 36 A-B). This increase was followed by a sharp decrease (into half) of the number of $CD4^+$ and $CD8^+$ T cells in the spleen of mice that were kept four days off Dox. Comparing both $CD4^+$ T cell and $CD8^+$ T cell populations of tumor-bearing mice with the naïve spleen showed that the overall number of $CD4^+$ T cells and $CD8^+$ T cells

are much higher compared to the number of $CD4^+$ T cells and $CD8^+$ T cells that is expected to be found within the non-tumor spleen. This increase showed how the tumor could change the immune cell population of the tumor-bearing mouse and how the tumor shrinkage leads the immune population toward the normal state.

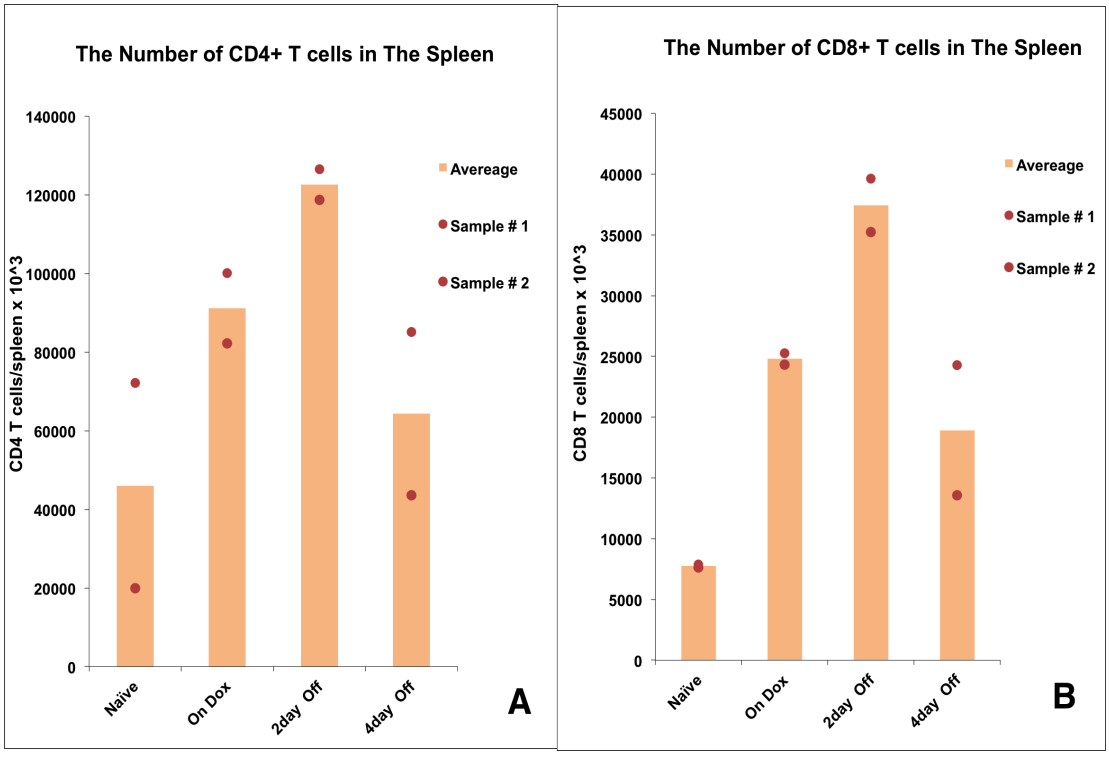

Figure 36. The Total And Average Number Of Spleen Lymphocytes In The MYC-Driven Tumor And Regressed Tumor (Two Days And Four Days After MYC Withdrawal). A: Spleen $CD8^+$T Cells, B: Spleen $CD4^+$T Cells.

In the absence of the oncogene driver of MYC, the overall number of the infiltrated $CD4^+$ T cells population increased in tumors over time (Figure 36A). This

increase could be because of the increase in the number of T regulatory cells (Tregs), the cells that modulate the immune system, as the tumor cells died and immune cells left.

The average population of infiltrated $CD8^+$ T cells didn't change two days after Dox removal in comparison to the growing tumor (Figure 37B). Moreover, the population of $CD8^+$ T cells increased significantly in one sample while remaining at the same level in the other one within the four days off Dox cohort. Due to the inconsistency in the $CD8^+$ T cells population that changed between these samples, no conclusion can be made from the data of the samples that were taken off Dox for four days. More samples are required to make a reliable conclusion in regards to the effect of MYC-off tumor on $CD8^+$ T cells population in tumor.

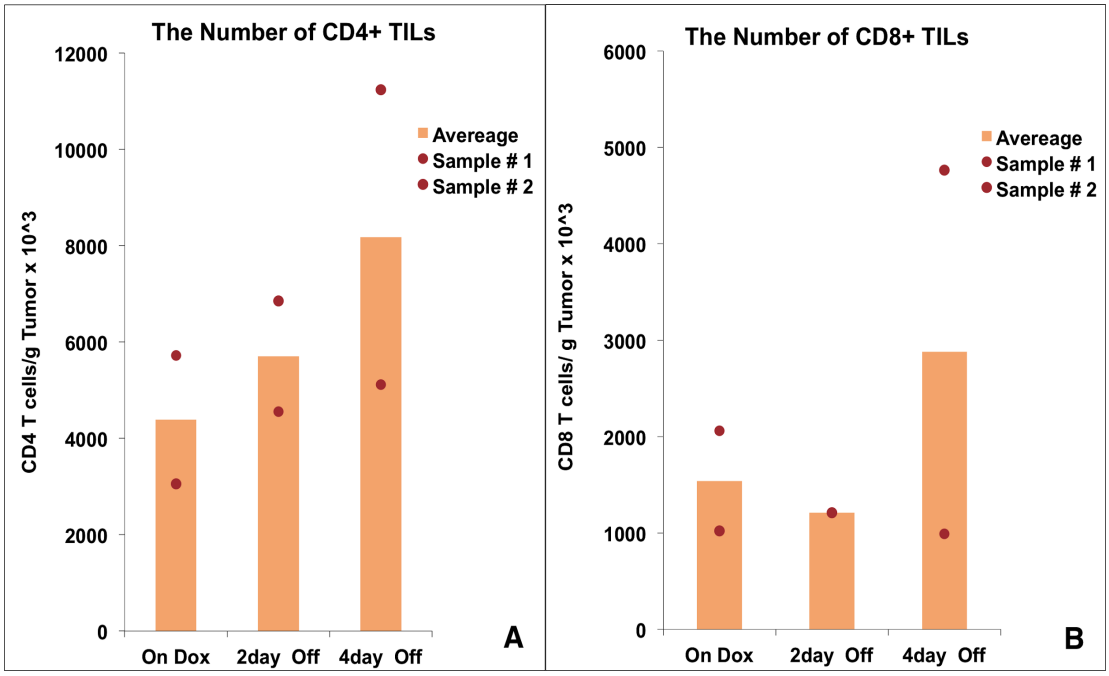

Figure 37. The Total And Average Number Of Tumor-Infiltrating Lymphocytes In The MYC-Driven Tumor And Regressed Tumor (Two Days And Four Days After MYC Withdrawal). A: $CD8^+$ T Cells Of Spleen, B: $CD4^+$ T Cells Of Spleen.

Taken together, upon MYC withdrawal as the tumor cells dying, the $CD4^+$ T cells population increased in the distant secondary lymphoid organ-the spleen of two-day off Dox tumors. Then, this $CD4^+$ T cell population might recruit to the tumor on the fourth day. We assume that might be because of the increase in the amount of released tumor antigen into the tumor microenvironment and myeloid cells recruitment. This population of $CD4^+$ T cells, which is predominantly made of Tregs, then regulates and suppresses the cytotoxic $CD8^+$ T cell function within the tumor that results in attenuation of the immune response. The presence of $CD4^+$ T cells refrain $CD8^+$ T cells to effectively remove tumor cells and provide immune response upon regression.

Studying the change in the myeloid cell subpopulations upon regression showed that monocyte cell numbers also changed after MYC withdrawal. The number of macrophages almost doubled two days after MYC withdrawal, which followed by a decrease in their numbers four days after MYC withdrawal (two days after). The tumor-infiltrated PMN slightly increased two days after Dox removal but then its population within the tumor dramatically decreased four days after MYC withdrawal. Tumor-infiltrated CD11c population did not change between the primary tumor and regressed tumor samples two days and four days after MYC withdrawal (Figure 38). This population is the less abundant population among all the studied myeloid subsets.

PMN and macrophages are have the highest abundance in the on-Dox tumor samples, but after the regression only the number of macrophages stayed high and became the dominant population in the tumor (Figure 38).

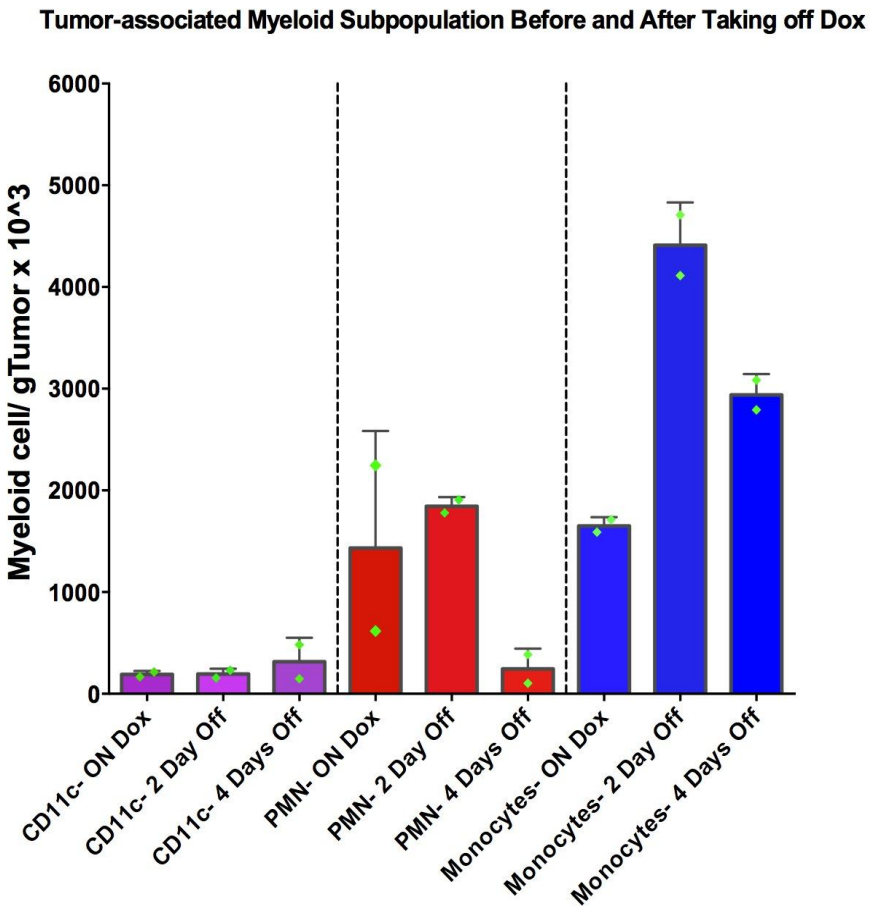

Figure 38. Total Number Of Tumor-Infiltrating Myeloid Populations In The Primary Tumor And Regressed Tumor, Two Days And Four Days After MYC Withdrawal.

4.2.3.3 Both PD1 And TIGIT Are Significantly Expressed On Tumor-Infiltrating $CD8^+$ T Cells But Only The Level Of PD1 Expression Elevated In The Infiltrated $CD8^+$ T Cell Subset Upon Regression

To study how MYC withdrawal could affect the immune response in terms of the expression of immune inhibitory molecules on lymphocytes and myeloid populations, the level of expression of the immune inhibitory receptors of PD1, TIGIT and TIM3 were studied using FACS.

PD1 expression almost doubled on tumor-infiltrated $CD8^+$ T cells of four-days off Dox samples compared to On-Dox and two-day off Dox groups (Figure 39A). Several different hypotheses may be formed for this observation: for instance, we can speculate that this increase may be controlled indirectly by MYC. Once MYC is on, it refrains from expressing PD1 on $CD8^+$ T cell populations through stimulating the expression of factors and releasing them into the microenvironment that down-regulate the expression of PD1. As it shuts off, the $PD1^+CD8^+$ T cell subsets start expressing these molecules over. There is also high possibility that as the tumor dies, more antigens were released into the tumor microenvironment. This recruits more lymphocytes, particularly $PD1^{hi}$ $CD8^+$ T cells subset within the tumor. There is also a possibility that the expression of PD1 in the $PD1^+CD8^+$ T cells subset down regulates through the macrophages or neutrophils in the microenvironment, as the tumor regresses, fewer neutrophils or macrophages are present, so this subset won't be down regulated anymore which revives the PD1 expression.

No changes were observed in the expression of PD1 in the $CD4^+$ T cells population between all three cohorts (Figure 39B). Similarly, no significant changes were detected in the expression of other immune inhibitory receptors of interest in the tumor infiltrating $CD4^+$ T cells/$CD8^+$ T cells populations between three cohorts. This proves that MYC-driven tumor microenvironment cells do not affect the expression of TIGIT or TIM3 receptors on TILs. In other words, only PD1 immune inhibitory receptor expressions on $CD8^+$ T cells are affected by the tumor microenvironment in the tumor regression stage. Whether this elevation in PD1 expression is due to the migration of $CD8^+$ T cell subsets that express PD1 at a high level or it is controlled indirectly by MYC or other infiltrating myeloid cells we are not sure. Nor do we know if this elevation is due to micro environmental factors and whether this T cell subset is a single PD1 subset or express TIGIT and TIM3 as well, we do not know. We still also do not know if this subset, $CD8^+PD1^+$ T cells, is functional or exhausted.

Furthermore, considering that the expression of any of TIGIT, TIM3 have not changed significantly in both MYC on/off systems, no correlation was found between the MYC and the expression of these immune inhibitory molecules (data not shown).

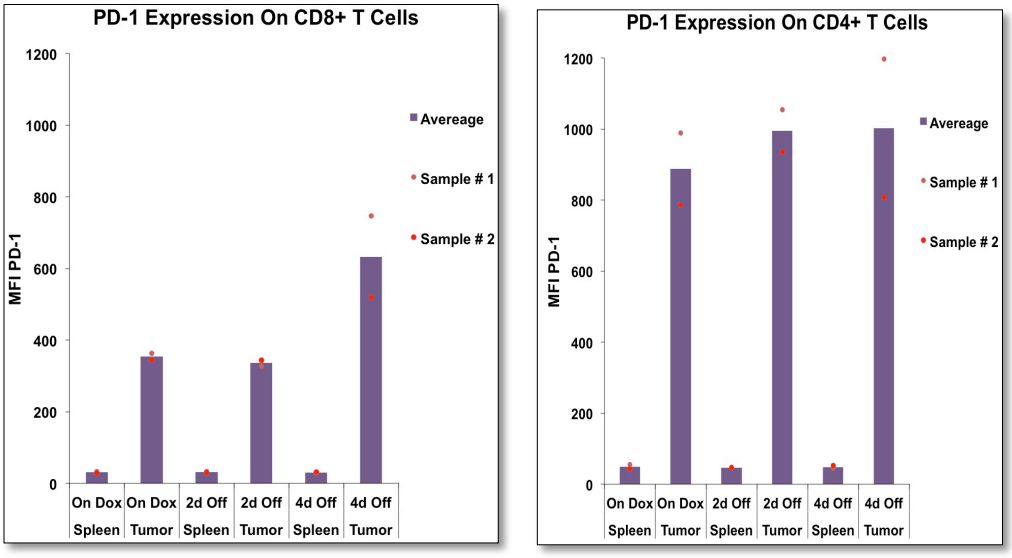

Figure 39. The quantified PD1 Expression On Spleen/Tumor Infiltrating Lymphocytes On MYC-Driven Tumor And Regressed Tumor (2 Days And Four Days After MYC Withdrawal). Purple: Tumor Orange: Spleen. A: The PD1 Expression On $CD8^+$ TILs. B: PD1 Expression On $CD4^+$TILs.

Studying the expression of immune inhibitory ligand of PD-L1 in all three cohorts, on the other hand, has shown that within four days of MYC withdrawal, the expression of this inhibitory ligand increased in myeloid populations, particularly monocytes, compared to the MYC-driven growing tumor (Figure 40). This high expression level of PD-L1 on myeloid cells could be because of the induction of $PD1^{hi}$ $CD8^+$ T cells that up regulate PD-L1 expression on myeloid cells. It is also could be due to the inhibitory effect of tumor MYC or MYC-induced tumor microenvironment factors on the PD-L1 expression of myeloid cells. Alternatively, this high level of PD-L1 on myeloid cells might be due to the recruitment of $PD\text{-}L1^{hi}$ myeloid cells upon regression in response to the tumor antigens or T cells' cytokines.

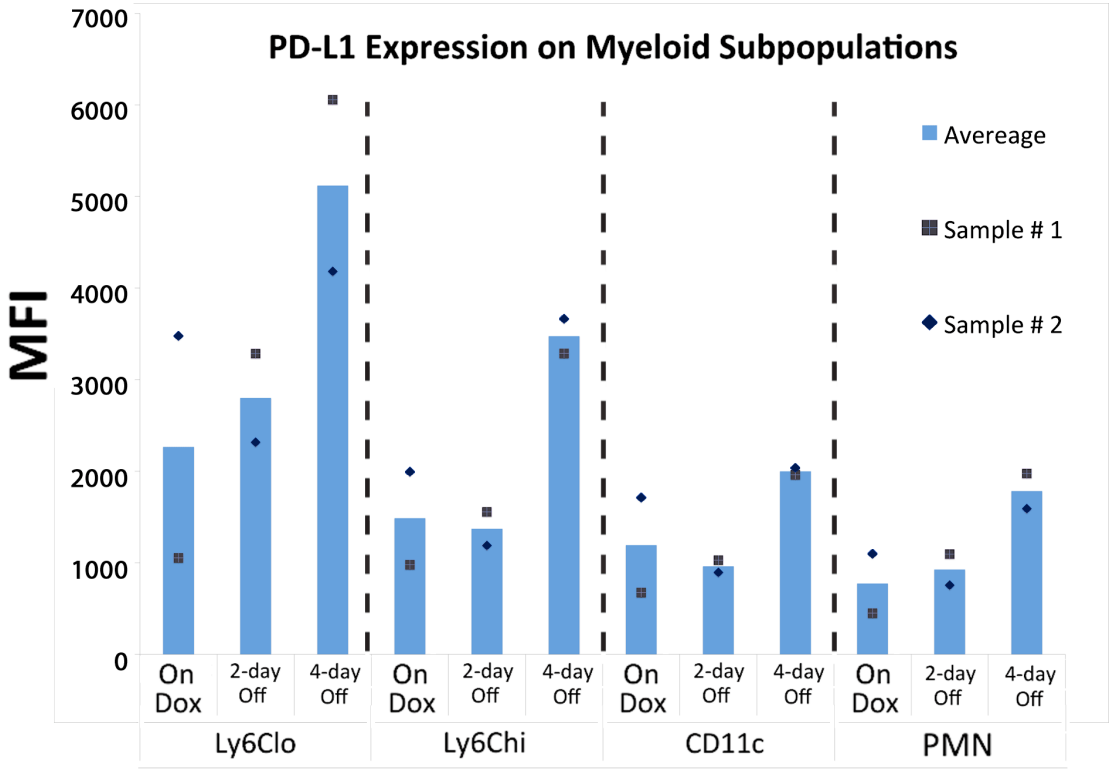

Figure 40. The Quantified MFI Of PD-L1 Expression On Tumor-Infiltrating Myeloid Populations At The Primary Tumor And Regressed Tumor, Two Days And Four Days After MYC Withdrawal.

4.3 Aim 3: Investigating Other Immune Checkpoints Expressed On Tumor Cells To Target In MYC-Driven TNBC.

4.3.1 PVR Is Highly Expressed On Tumor-Associated Myeloid Cells As Well As On The Tumor Cells

The immune kinetics studies of regression have shown that TIGIT, an immune inhibitory receptor of PVR, was expressed on immune cells of both spleens and tumors.

Thus, besides PD-L1 we also focused on PVR and studied the expression level of this ligand on different immune populations of both lines. Since this molecule was found in the middle of the study, we failed to study the expression of this molecule on the primary tumors of line A and B. Thus, all the data in regards to PVR expression on tumor cells were limited to the recurred tumors.

FACS data analysis of PVR expression on $Epcam^{+}$ cells, tumor cells, showed that PVR, the ligand of immune inhibitory receptor TIGIT, is expressed significantly in both recurred line A and B tumor compared to the stained cells with isotype control antibody for this ligand (P-values: 0.002 and 0.0139 respectively) (Figure 41 and 42). Similarly, $CD45^{-}$ $Epcam^{-}$, which may represent epithelial progenitor cells or $Epcam^{lo}$ tumor cells, also express PVR (Figure 42).

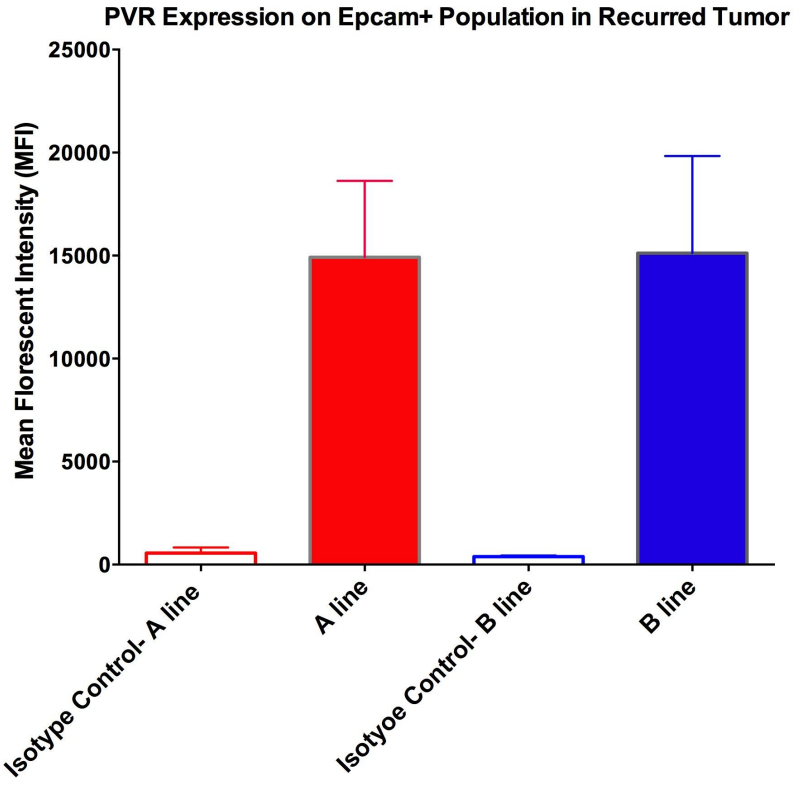

Figure 41. The Quantified MFI Of PVR Expression On Epcam^{+} Cells Of Both A Line And B Line At Their Recurred Stage Stained With Isotype Control Antibody And PVR Antibody. PVR significantly express on Epcam positive cells of recurred tumor of line A and B at the almost same level.

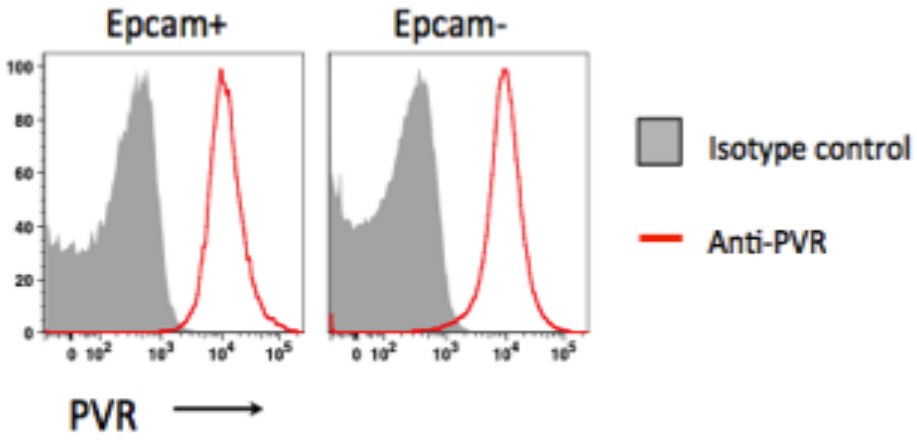

Figure 42. Flow Cytometry Histogram Representative Of PVR Expression On Epcam$^+$ And Epcam$^-$ Cells Of Line A Recurred Tumor Stained By Anti-PVR (Red) And Isotype Control Antibody (Grey).

4.3.2 PVR Expression On Tumor Cells Is Not Regulated By MYC Induction *In Vitro*

We were interested to know if this PVR expression on Epcam$^+$ cells were regulated by MYC induction. To address this question, we isolated MMTV/MYC cells and kept them in DMEM media supplemented with 10% FBS (Gibco, life biotechnologies) and 1% penicillin-streptomycin MYC in (Gibco, life biotechnologies) with and without Dox. Cells were then submitted for FACS analysis. Results showed that both isolated cells grown with and without Dox are positive for Epcam (Figure 43C-D). FACS analysis for PVR expression also showed that both on/off Dox samples do express PVR significantly compared to the cells stained with isotype control antibody and their

MFIs are almost close to each other. This data suggests that PVR expression level is not regulated by MYC induction (Figure 43A-B).

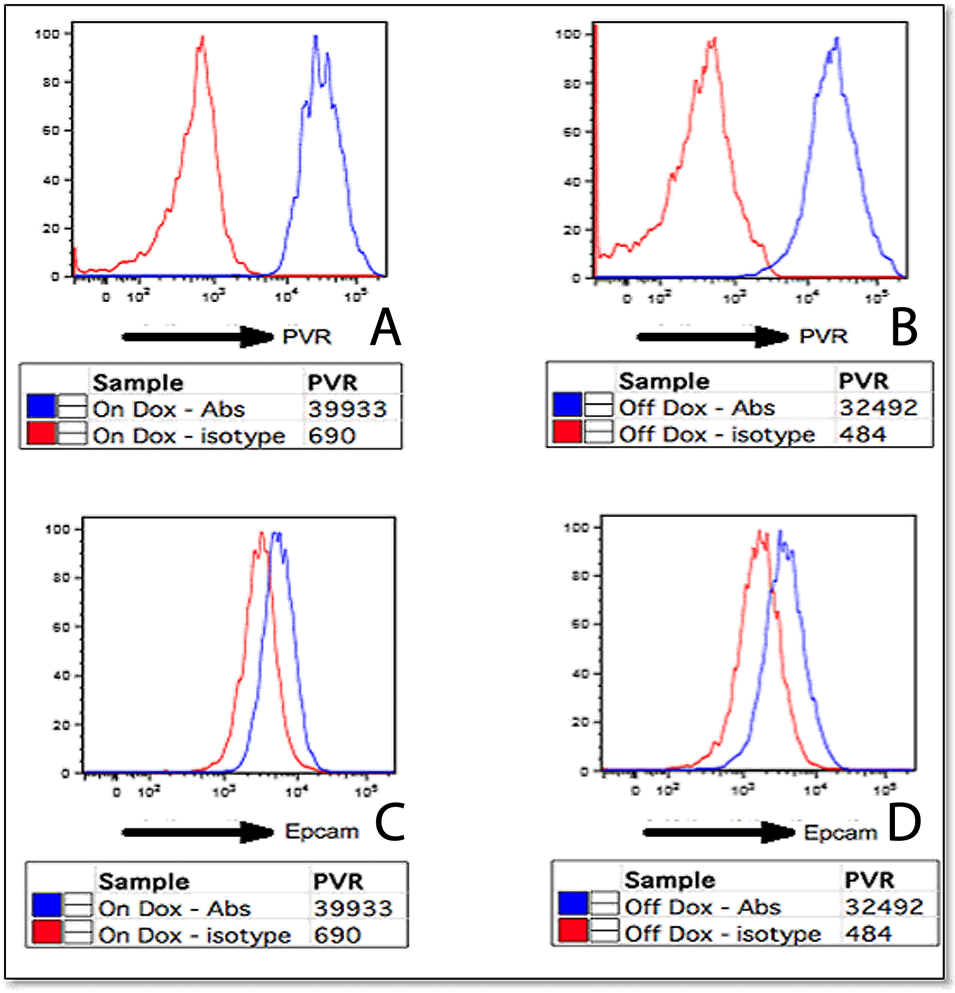

Figure 43. Flow Cytometry Histogram Representative Of Epcam And PVR Expression On Isolated Tumor Cells Grown In Culture. Cells were treated with and without Dox. Cells stained with isotype control antibody (Red) and cells stained with PVR antibody (Blue). A: PVR expression on the on-Dox tumors cells. B: PVR expression on the off-Dox tumor cells. C: Epcam expression on the on-Dox cells. D: Epcam expression on the off-Dox cells.

4.3.3 PVR Was Also Expressed On Tumor-Associated Myeloid Cells Of Recurred Tumor Regardless Of The Tumor Type

To further study if immune cells also express the immune-inhibitory ligand of PVR, we performed a FACS analysis on tumor-associated myeloid cells (Figure 44). We determined PVR expression in both tumor lines.

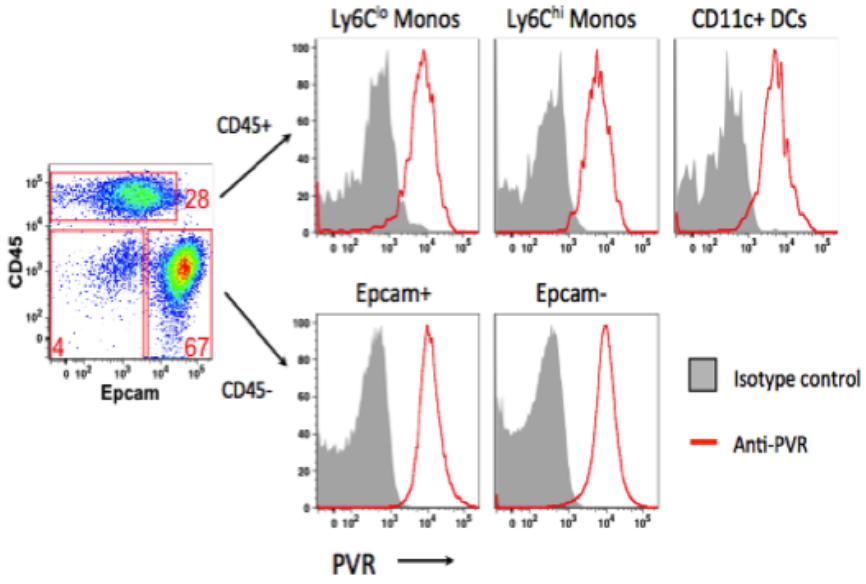

Figure 44. Representative Flow Cytometry Histograms Of PVR Expression Of Tumor-Infiltrating Myeloid Cells (Monocytes And Dendritic Cells). Cells stained with anti-PVR (red) and isotype control (Gray). Tumor cells, $Epcam^{+}$, as well as $Epcam^{-}$ cells also overexpress this ligand significantly (over 10 fold).

We found that PVR was expressed in all four tumor-associated myeloid subpopulations and its expression is higher on all four subpopulations within the tumor compared to the one in the spleen in both lines (Figure 45A-D). This ligand was also

expressed on the CD11c population of line B samples but due to the depletion of this population in some samples of line B, the statistical analysis showed a false negative expression of this molecule on CD11c population overall (Figure 44A).

CD11c had the highest level of PVR expression in line A tumors which was followed with monocytes.

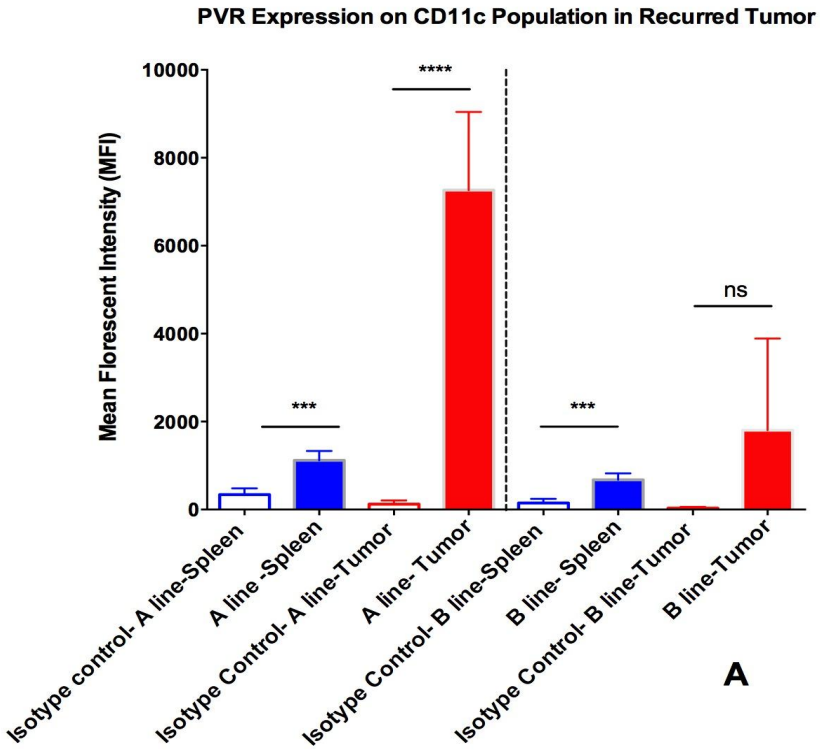
PVR Expression on CD11c Population in Recurred Tumor
Mean Florescent Intensity (MFI)
10000
8000
6000
4000
2000
0
****
***
***
ns
Isotype control- A line-Spleen
A line -Spleen
Isotype Control- A line-Tumor
A line- Tumor
Isotype Control- B line-Spleen
B line- Spleen
Isotype Control- B line-Tumor
B line-Tumor
A

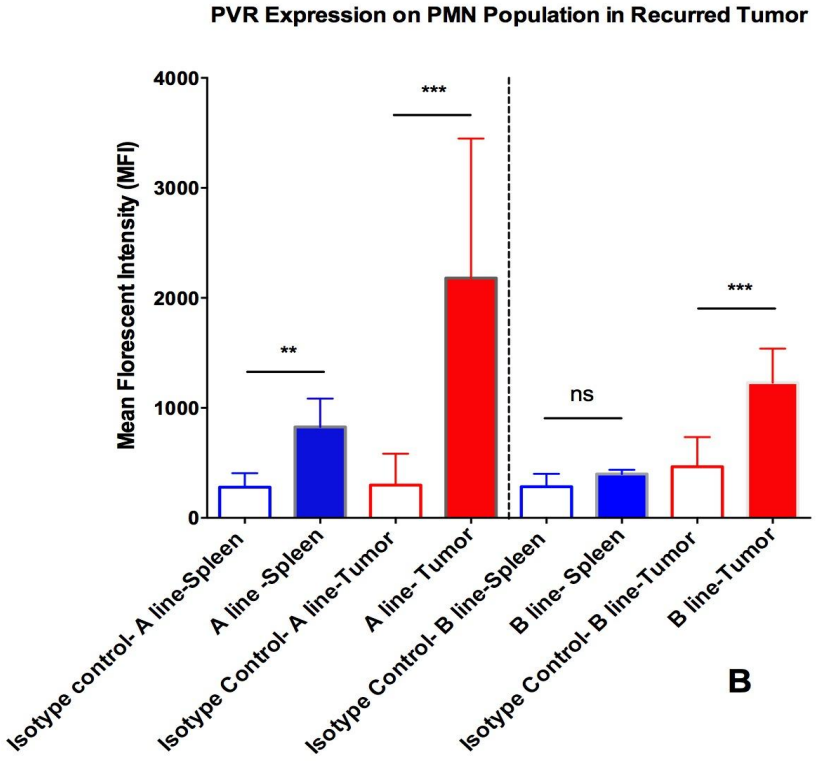
PVR Expression on PMN Population in Recurred Tumor
Mean Florescent Intensity (MFI)
4000
3000
2000
1000
0
***
**
ns
***
Isotype control- A line-Spleen
A line -Spleen
Isotype Control- A line-Tumor
A line- Tumor
Isotype Control- B line-Spleen
B line- Spleen
Isotype Control- B line-Tumor
B line-Tumor
B

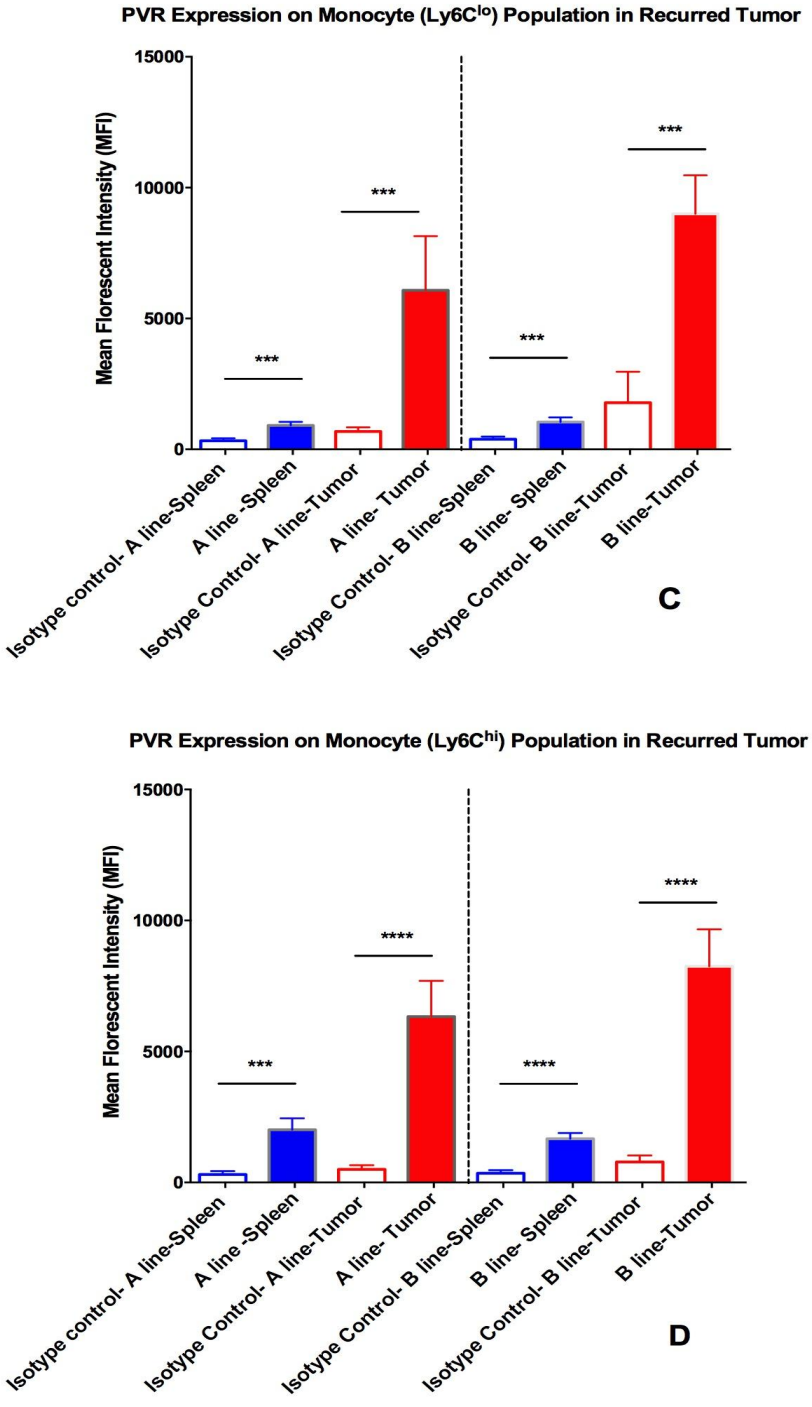

Figure 45. The Quantified MFI Of PVR Expression On Tumor-Infiltrated Myeloid Cells of Both A Line And B Line at Their Recurrent Stage Only. A: CD11c population. B: PMN population. C: Monocytes (Ly6C^{hi}) population. D: Monocytes (Ly6C^{lo}) population (ns: P> 0.05, *: P ≤ 0.05, **: P≤ 0.01,***:P≤ 0.001, ****: P≤ 0.0001).

4.4 Aim 4: Can Secondary Mutation In Primary Tumors Cooperate With MYC And Alter Immune Response To The Both Primary And Recurred Tumor?

Tumor progression studies in line A and B demonstrated that these tumors exhibited two different growth curves. Moreover, sequence data analysis had shown that each line bears a secondary mutation that can be correlated to the observed differences in the growth rate between lines. The effect of immune response to the tumor should not be ignored. We are trying to see if the observed differences between the growth curves of these two lines are a result of the effect of secondary mutation on tumor growth rate or the effect of this mutation on antitumor immune response. These finding enable us to better find the right immunotherapeutic approach for the cancer treatment.

To address this question, we first need to know how the antitumor response is different between these two lines, if there is any. To do so, we embarked on a comprehensive immune response characterization of these two lines both at primary tumor and recurred tumors. Moreover, we studied the tumor growth curve at the recurred stage to see if there are any differences in the growth rate and pattern of these two tumor models at the recurred stage.

Throughout the whole project, we used the spleen as a source of immune cells to study and compare their immune inhibitory molecules' expression with the tumor. Notably, we observed some changes in the size of the spleen. Thus, we also decided to characterize the spleen between these two lines.

4.4.1 Tumor Recurrence Pattern Was Different Between Line A And B

Preliminary data of tumor growth patterns of primary tumors showed some differences in the rate of growth. To further characterize tumor behavior in both line A and B, tumor growth at the recurred stage was also studied. Once the tumor reached above one centimeter on any side, all mice were taken off Dox. Immediately afterwards, tumors from both lines started to shrink dramatically. The rate of the shrinkage was almost the same in both lines. However, some differences in the duration of latency were observed between these two lines. In both lines, the recurrence growth rate and latency duration varied from tumor to tumor and is independent on the primary size before being taken off Dox (Figure 46).

Overall, Line A recurred much earlier compared to line B. It takes approximately a couple of days to 30 days for line A tumors to recur. While for line B, it took approximately 40-100 days to come back. In terms of the morphology at the latency stage, also some differences were observed. For example, tumors in line A were palpable and they never shrunk entirely after shrinkage in Line A. On the contrary, the line B tumors were completely gone and even no trace of the presence of tumor nodules could be detected under the skin of the mice. In line B, two out of four tumors showed a delay in growth at the recurred stage while two others grew at the same speed.

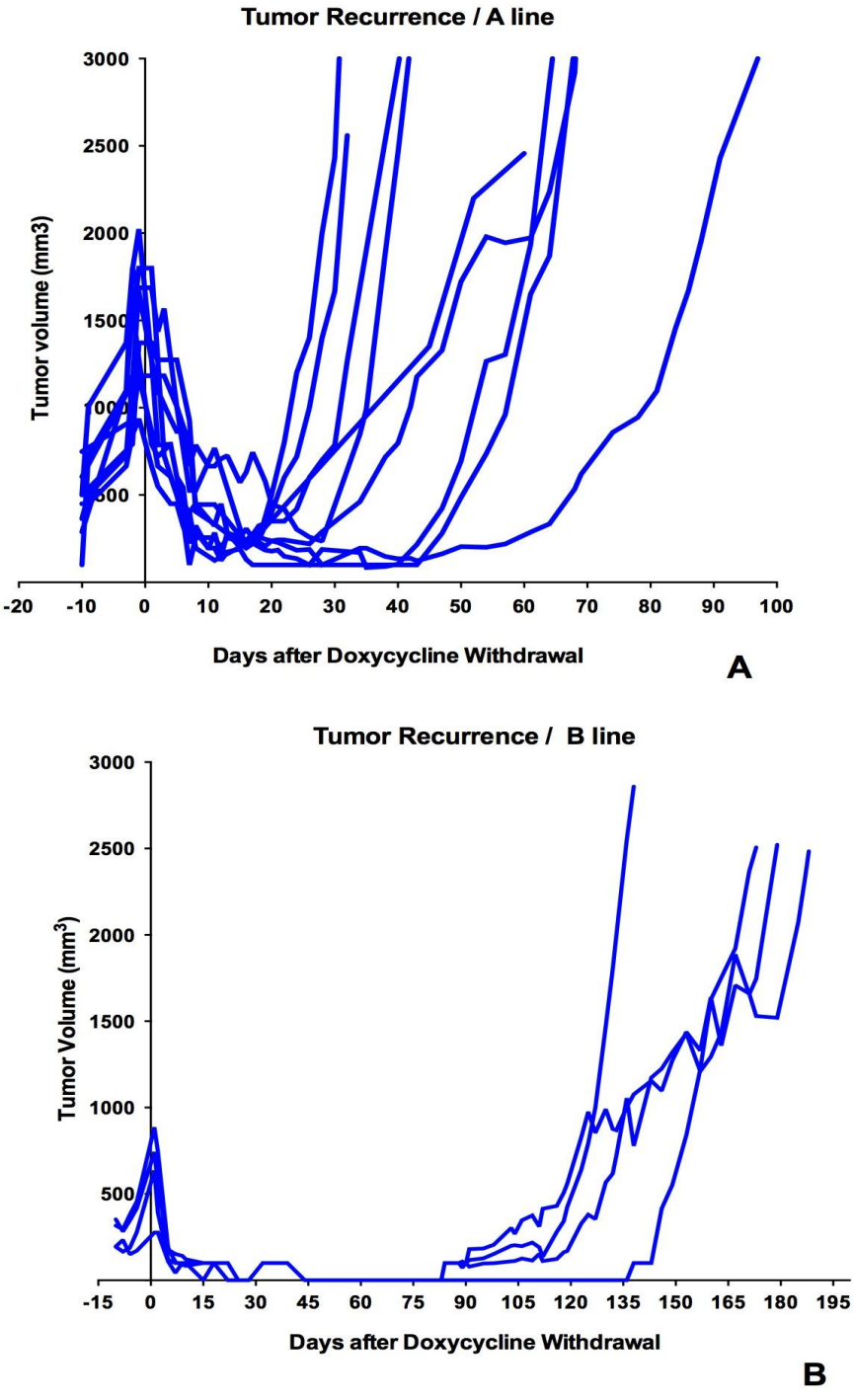

Figure 46. Tumor Recurrence of Lines A And B After Dox Withdrawal

4.4.2 The Spleen In Line A And B Was Different In Terms Of Size And Total Number Of Immune Cells

The spleen is considered to be the largest secondary immune organ in the body and is responsible for initiating immune response to antigens and for filtering the blood of foreign cells and old or damaged red blood cells. It also serves as a large reservoir of red blood cells, monocytes and lymphocytes (Pearse 2006).

Studying the spleen as one of the major organs of immune system also showed a significant difference in the size and total number of cells in the spleens in Line A compared to line B regardless of the stage of tumor growth (Figure 47, 48 and 49). The spleen in Line A was much bigger than the spleen of line B, particularly at the recurred stage (Figure 47). No significant differences in the physical characteristics of lymph nodes were observed.

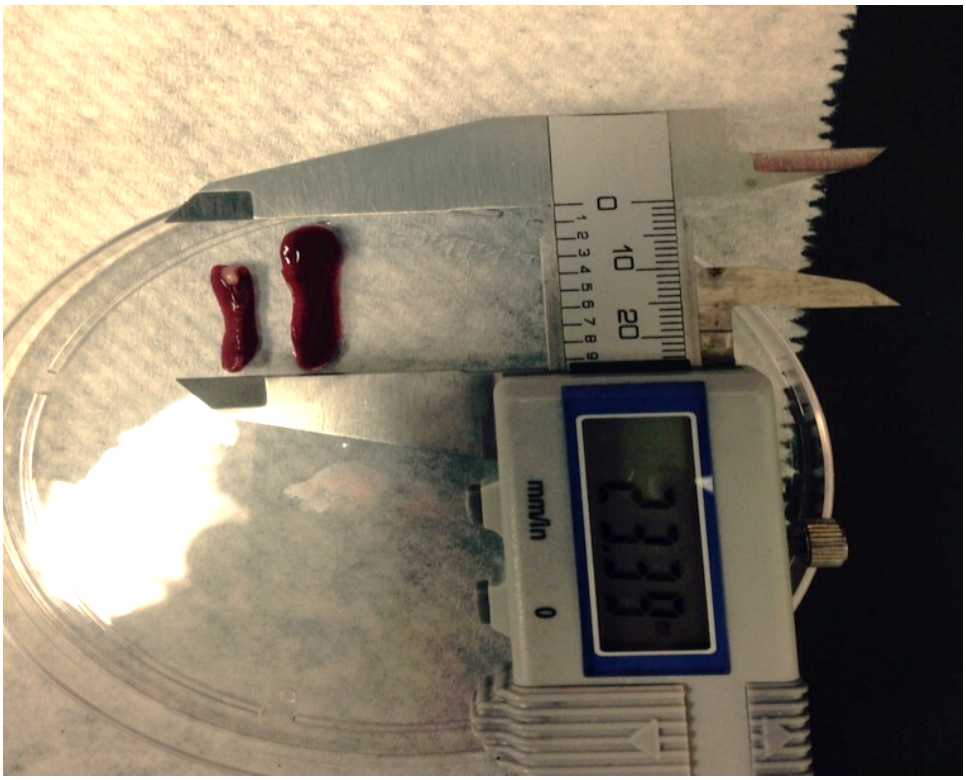

Figure 47. Spleens Of Tumor-Bearing Mice Of Line A And B At Their Recurred Stage. (Left: Spleen Of Line B, Right: Spleen Of Line A).

To further study the reasons behind the spleen enlargement in recurred line A, the total number of viable cells isolated from the spleen of tumor-bearing mice at their recurrence stage were counted. No significant difference was observed between the total viable cells of the spleen in line B compared to the naïve spleen, the spleen of non-tumor bearing mice (Figure 48). On the contrarily, studies showed a significant increase in the total number of viable cells in Line A compared to line B though (P-value <0.0001). Notably, on the average, the A line spleen has approximately three times more viable cells as line B at its recurrence stage.

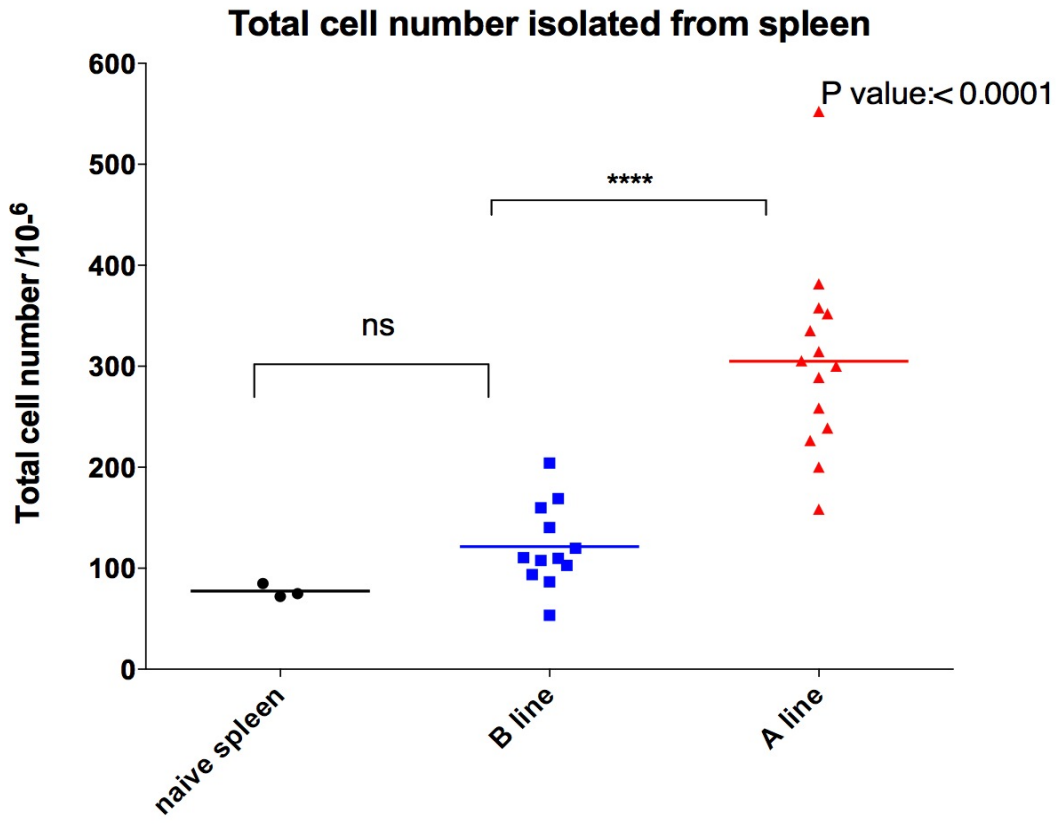

Figure 48. Total Number Of Viable Cells In The Spleen Of Recurred Tumor Line A And B. Each dot represents the total viable cells of one studied mouse sample. (Blue: total cell number of Line B spleen, Red: total cell numbers of line A spleen). P-values were calculated by two-tailed Student's *t* test (P-value< 0.0001).

While no significant differences were observed in the physical size of spleen in the mice with primary tumors, studying the total number of spleen isolated cells of the primary tumor showed increase in the line A compared to the one isolated from the naïve spleen (P value <0.05) (Figure 49). No such differences, however, were observed between the viable cell number of line B and naïve spleen. The total number of viable cells in Line A was nearly two times more than line B. Considering the fact that spleen is made of immune cells mainly, the increase in the total cell number and size in Line A

could possibly be because of the accumulation of immune cells within the spleen which become higher at the recurred stage.

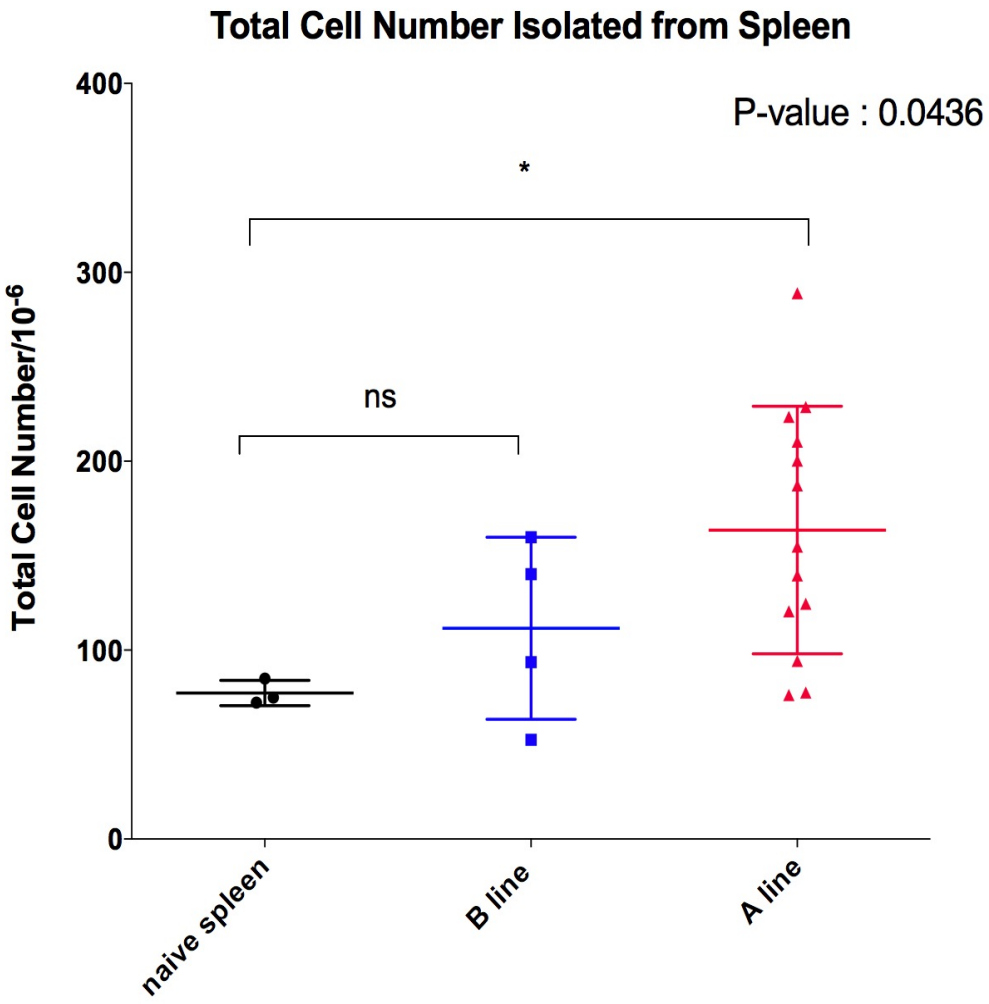

Figure 49. Total Number Of Viable Cells In The Spleen Of Recurred Tumor Line A And B. Each dot represents the total viable cells of one studied mouse sample. (Blue: total cell number of Line B spleen, Red: total cell numbers of line A spleen). P-values were calculated by two-tailed Student's *t* test (P-value< 0.0436).

4.4.3 Immune Phenotype Of Both Spleen And Tumor Of These Two Lines Showed Some Differences That Can Be Associated With Differences In The Immune Response

To further investigate the reason of spleen enlargement in line A, the percentage and total numbers of each immune cell type in the naïve spleen, line A spleen and line B spleen were studied. To do this, first we need to study the population of both myeloid cells and lymphocytes using FACS.

Furthermore, to characterize the myeloid cell population of the tumors from these two lines, immune cells of both spleens and tumors were isolated using the technique that was described in methods (See Chapter Three-Materials and methods page 54). Isolated cells of both spleen and tumor were stained by the antibodies against each of the myeloid cells' specific surface markers and analyzed by FACS.

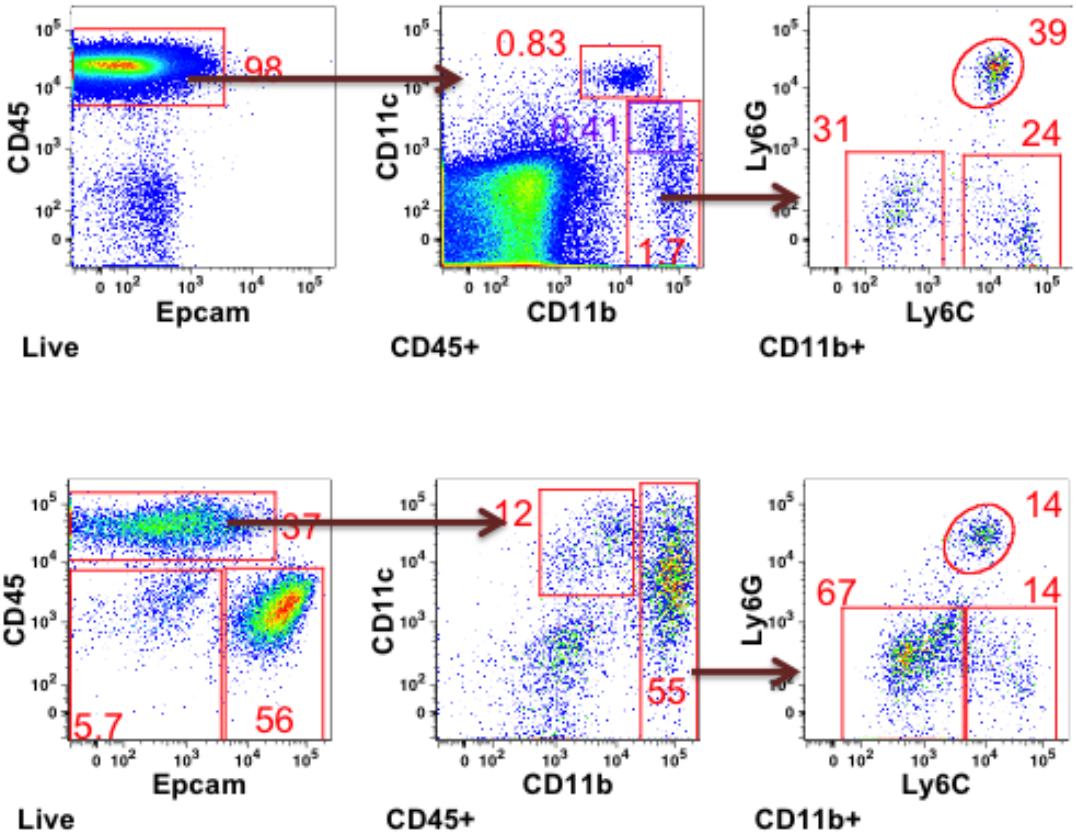

Figure 50. Gating Procedures to Detect Myeloid Subsets of Spleen and Tumor on FACS (Top Row: Spleen, Bottom Row: Tumor)

Cells are usually gated according to their physical characteristics. For instance, size is a good characteristic through which subcellular debris and clumps can be distinguished from single cells. Granulocytes, monocytes and lymphocytes have different physical characteristics that let us to distinguish from one to the other. To distinguish myeloid cells from the rest of the immune cells, we used the physical characteristics of size. Myeloid cells have the bigger nucleus than lymphocytes so scatter the emitted light at higher range. The density plot was used to depict these populations. In the density plot, each dot represents an individual cell that has passed through the FACS machine. Each

dot in FACS terminology is called an event. As the abundance of each cell type increases, the color of events changes from blue to yellow, and then green and eventually red which gives the graph a three-dimensional feel.

After gating a cell population with the size of interest, we studied the different subpopulations of that gate. Each myeloid cell population constitutes several known and unknown subpopulations. To distinguish these subpopulations, using cell surface markers is the best approach. Each subpopulation expresses a specific protein on their surface abundantly which is used as the marker of that population. The expression of each specific cell surface on the population of interest was depicted by showing the symbols of positive and negative at the top right of the primaries of the marker; for instance: the population which expresses the CD4 protein marker at their surface is called $CD4^+$ T cells. Subpopulations of myeloid cells can be easily identified by studying the level of expression of each of these cell surface markers,

Based on the cell surface marker, a plot was set on the CD45 cells vs. Epcam to only analyze cells that express $CD45^+$ $Epcam^-$ and $CD45^-$ $Epcam^+$ (Figure 50). CD45, or Protein Tyrosine Phosphatase, Receptor type, C (PTPRC), is the hematopoietic cell surface marker that specifically expresses on the surface of hematopoietic cells including immune cells. Epithelial Cell Adhesion Molecule (Epcam), on the other hand, is a cell surface marker of breast cancer cells (Osta et al. 2004). The resulted display would reflect two populations in spleen immune cells and three populations in tumor-isolated cells. Three populations detected on the tumor isolated cells are namely $CD45^+$ $Epcam^-$, which contain mainly the immune cells, $CD45^-$, $Epcam^-$ cells (in fact this is a population that

expresses a low to intermedium level of Epcam), which may contain epithelial progenitor cells or $Epcam^{lo}$ cells and $Epcam^{+}$ $CD45^{-}$ cells, which are the tumor cells. Only $CD45^{+}$ cells, $Epcam^{-}$and $CD45^{-}$ $Epcam^{-}$ were detected in the spleen-isolated cells.

After gating each population on the density plot, a percentage appears close to that population in the plot. This percentage represents the percentage of the gated population in that plot. Comparing the abundance of each of these three populations has shown that, $CD45^{+}$ cells are more abundant in spleen while the tumor is dominant with the Epcam positive tumor cells. Since we were interested in myeloid cells that express the $CD45^{+}$ protein marker, a gate was opened on the $CD45^{+}$ cell population in both spleen and tumor. The opened plot on the gated $CD45^{+}$ cells was set on CD11c vs. CD11b (Figure 50).

CD11b or Cluster of Differentiation Molecule 11b (CD11b) that is specifically expressed on the surface of many leukocytes including monocytes, granulocytes, macrophages, and natural killer cells (Solovjov, Pluskota, and Plow 2005). CD11c is a cell surface protein used as a marker to detect, dendritic cells mostly (Steinman, Pack, and Inaba 1997). CD11b is the cell surface marker of myeloid cells.

Three populations were detected in both tumors and spleens, namely $CD11c^{+}$, $CD11b^{+}$ and $CD11b^{-}$ $CD11c^{-}$. In both spleens, the population of CD11b is higher than CD11c. In spleens we have a significant population of $CD11c^{-}$ $CD11b^{-}$, which is made mainly from immune cells other than myeloid cells and dendritic cells including lymphocytes. This population is smaller in tumor cells as the tumor is made mainly of tumor cells as opposed to spleen, which is made mainly of immune cells. It was much

harder for us to discern the CD11b and CD11c cell population within the tumor than it was in the spleen. It may be because of the changes in the cell surface marker level of expression of this subset of immune cells as they infiltrated within the tumor.

As we are interested in the myeloid cells which are $CD11b^{+}$, a gate was opened on this population in both spleen and tumor panel. The opened plot that was gated on CD11b was set on Ly6C and Ly6G cell surface markers (Figure 50). Lymphocyte Antigen 6 Complex Locus G6D (Ly6G) is the surface marker of polymorphonuclear neutrophils (PMN) (Rose, Misharin, and Perlman 2012) and Ly6C is a marker of monocyte/macrophage (Jutila, M. A. et al).

Similar to CD11b-CD11c plot, the Ly6C-Ly6G plot consists of three populations in both spleens and tumors; Ly6G positive, the population of cells that express this protein marker significantly at the high level on their surface (From now on we'll refer to it here as $Ly6C^{hi}$ positive), Ly6C positive cell population that express this marker but at the lower level, so called Ly6C low, and Ly6G positive, which contains mainly PMNs. While the percentage of monocytes has been higher in tumors compared to spleen, more PMN was detected in spleen. Consequently, spleen and tumor showed two different phenotypes for myeloid cell population. Each panel of FACS data for the tumor was analyzed together with the spleen of their own respective mouse.

To study the population of lymphocytes in the tumor, the same approach used to detect the population of myeloid cells was followed on FACS data. Similarly, isolated cells of both spleen and tumor were stained by the antibodies against each of the lymphocytes specific surface markers, namely $CD4^{+}$ and $CD8^{+}$, then analyzed by FACS.

Spleen, again, was used as the control to detect and open the gate on the right population in the detected events.

Lymphocytes, T cells, was detected based on their size and was gated on the analyzed cells (Figure 51). After opening a gate on the cell population with the size of interest, we studied the different subpopulations of that gate. Among different subpopulations of lymphocytes we were interested in T cells, as they play a main role in antitumor immune repose. This subpopulation of lymphocytes expresses TCR-β significantly.

Two subtypes of T cells that express TCR-β are; T effector cells, which express CD8 cell surface marker, and T helper cells and T regulatory cells, which express Cluster of Differentiation 4 (CD4) marker predominantly (Bernard, Boumsell, and Hill 1984; Bernard et al. 2013). Cluster of Differentiation 8 (CD8) is the other T cell surface marker, which predominantly express on the T effector cells. However, other immune cells including natural killer cells, cortical thymocytes, and dendritic cells also can express it (Leong et al. 2003). T effector cells play a critical role in antitumor immune response by attacking the tumor directly.

Consequently, to study both lymphocytes populations ($CD4^+$ and $CD8^+$ T cells), a plot that was opened on gated lymphocytes was set on $CD4^+$ and TCR-β cell surface markers (Figure 51). One more plot was also opened on the gated lymphocytes and was set on $CD8^+$ and TCR-β (Figure 51). After gating the populations that are positive for both markers a percentage appears on the plot, which is designated for the percentage of

the gated population on that plot. Consequently, through this way, we can estimate what percentage of the lymphocytes are $CD4^+$ and $CD8^+$ T cells.

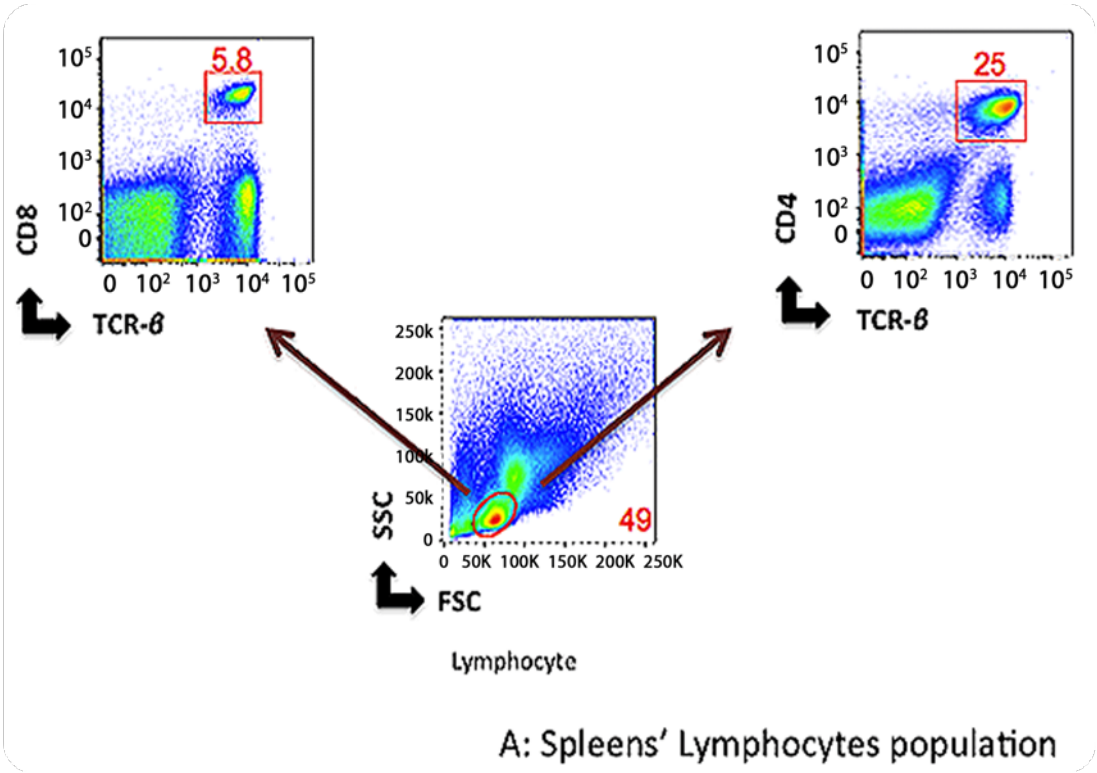

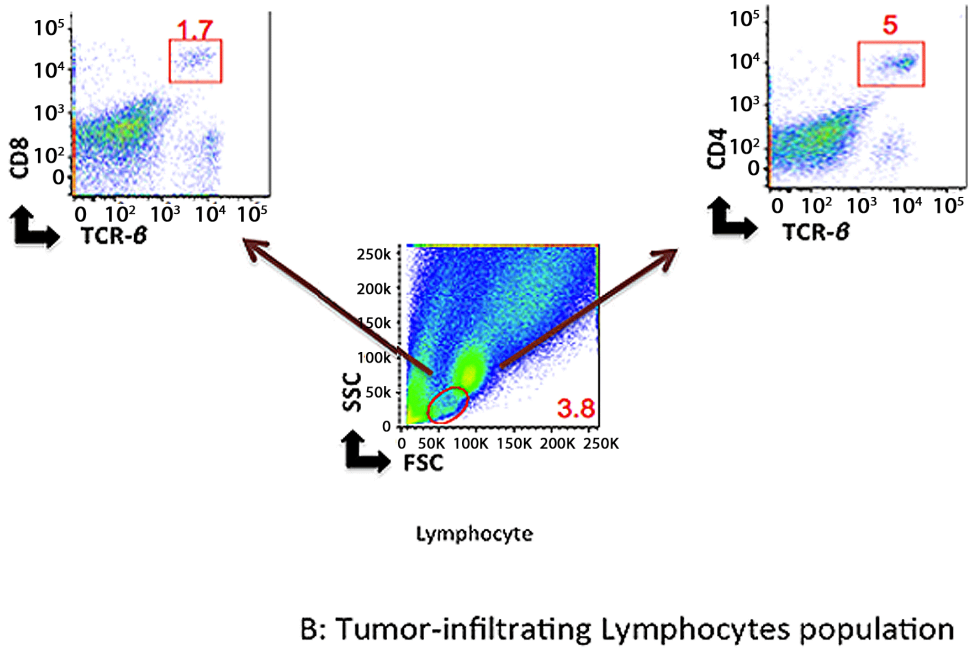

Figure 51. Gating Procedures To Detect Lymphocytes Subpopulations Of Spleen And Tumor On FACS. A: Spleen, B: Tumor.

4.4.3.1 Immune Cell Composition Within The Spleen Changed Upon Tumor Response. These Changes Differed From Line To Line.

FACS data analysis of the spleen immune cells provides the necessary information in regards to the percentage of immune cell population of naïve spleen, line A spleen and line B spleen. This acquired data was used to calculate the total number of each cell subtype as well as the percentage of the total number of each immune cell population over the total detected immune cells within each spleen type.

The graphed data showed that out of the total isolated cells from naïve spleen, the $CD4^+$ T cells and $CD8^+$ T cells were the dominant population. This was followed by PMN, monocytes and CD11c respectively (Figure 52 A and B). Interestingly, the growth of tumor changed this composition entirely. The total percentage of all populations of myeloid cells increased while the total percentage of $CD4^+$ T cells, $CD8^+$ T cells and CD11c decreased. Notably, these observed changes were consistent in both lines and was not dependent to the stage of growing tumor.

Comparing the spleen immune population of line A with line B, CD11c was the smallest population in the spleens of both samples. The population of PMN was significantly increased in the spleen of both lines but this increase was much higher in the spleen of line A compared to line B such that the myeloid cell together, including PMNs, constituted the half of the population of spleen in line A (Figure 52A and B). As opposed to the PMN population, the percentage of the population of both $CD4^+$ T cells and $CD8^+$ T cells dropped in both lines. The observed reduction in both populations was much higher in line A versus line B.

Interestingly, in the spleen of three groups of samples, including naïve spleen, spleen of line A and spleen of line B, a new unidentified myeloid population appeared that we didn't detect. The abundance of this unidentified population increased in line A specifically and might play a role in immune response.

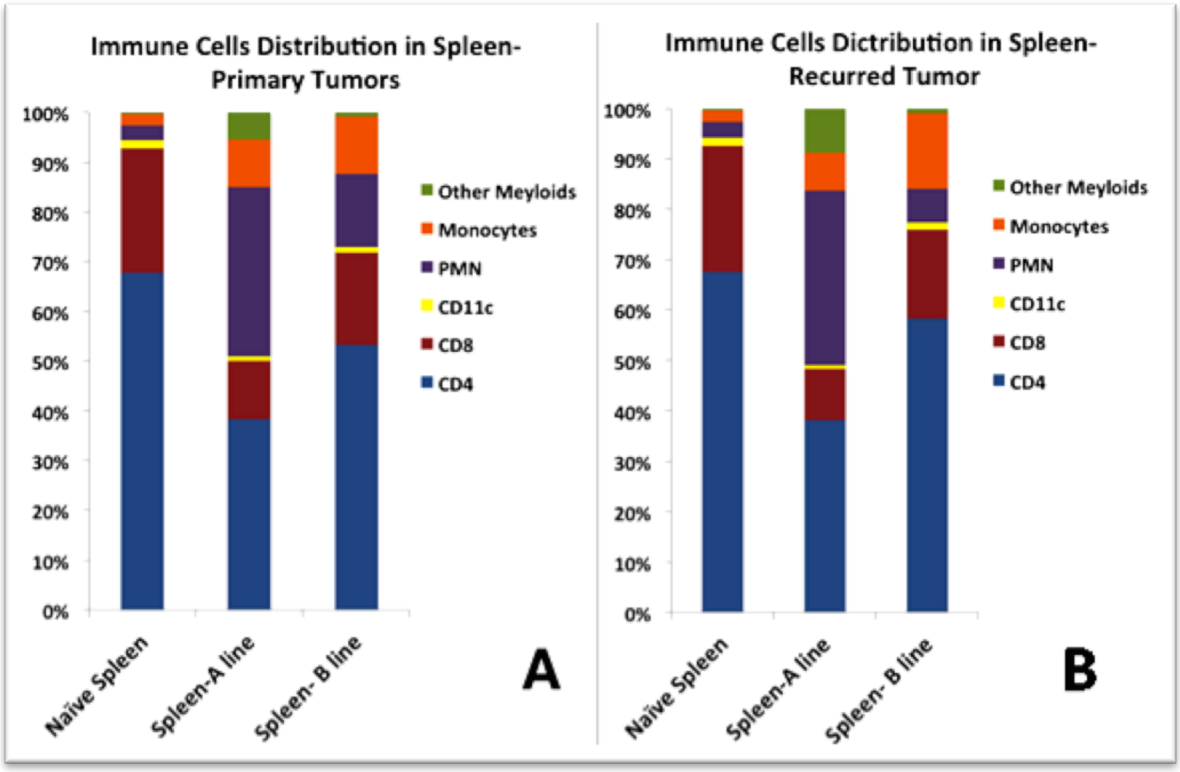

Figure 52. The Comparison of The Distribution of Immune Subpopulations in The Spleens. A: Spleen of primary tumors of Line A And B burdening mice, B: Spleen of recurred tumors of Line A And B burdening mice.

These changes could be due to the recruitment of the spleen $CD4^+$ T cells, $CD8^+$ T cells and CD11c cell populations by tumors, which results in a decrease of the population of $CD4^+$ and $CD8^+$ T cells as well as CD11c in the spleen of both lines.

The impact of the tumor on the myeloid cell population particularly PMNs were striking. These two myeloid populations increase in the spleen of both primary tumors and recurred tumors of both lines. This increase was much higher in line A compared to line B.

Together, these changes in the spleen immune cell compositions definitely correlate to the tumor response. These changes were almost the same in the spleens of both recurred and primary tumors. However, if the differences in immune composition of spleens between lines is dependent on the secondary driver mutation in tumor or if they are in the favor of tumor growth or resulted by the immune system response against the tumor, is a question, which hasn't been illuminated yet.

4.4.3.2 The Spleen Enlargement In Line A Is Due To The Increase In The Total Number Of All Immune Cells But Mostly PMNs And $CD4^+$ T Cells

Despite the decrease observed in the percent population of $CD4^+$ T cells in the spleens of tumor-bearing mice of both primary and recurrence groups of line A and B, the total number of $CD4^+$ T cells within the spleen increased in both line A and B compared to the naïve spleen (Figure 53A, C). This average increase was also much higher in A line compared to B line which could be associated to spleen enlargement in this group. This increase could possibly have been because of the increase in the number of Treg, which is responsible for modulating the immune response and suppressing the activity and proliferation of $CD8^+$ T cells, which results in impairment of antitumor response and in tumor progression.

In the primary tumor, despite the decrease in the percentage of $CD8^+$ T cells population in spleen of both lines compared to the naïve spleen, both lines showed an

average increase in the number of $CD8^+$ T cells in their spleens (Figure 53B). In some samples, the number of $CD8^+$ T cells increased significantly compared to the $CD8^+$ population of naïve spleen but in other samples (two out of eight), the number remained at the same level as in naïve spleens or decreased slightly. This variation in the total number of $CD8^+$ T cells might be due to the technical error, which caused $CD8^+$ T cells lost or due to failure in their infiltration. Those samples that showed increase in the number of $CD8^+$ T cells also might be exhausted. Overall, we are not certain about the functionality of them at the time of experiment. In addition, due to the small number of studied samples, no statistical analysis can be made to ensure if this increase was significant.

The graph data of $CD8^+$ T cells of the line A spleen have shown that at the recurrence, the average number of $CD8^+$ T cells population almost doubled compared to those within the naïve spleen (5 out of 8 samples) (Figure 53D). Furthermore, the average number of $CD8^+$ T cells slightly increased in the line B sample.

Despite the average increase in the total number of $CD8^+$ T cells in the spleen of both lines, the samples in both lines showed an extensive variation in the number of $CD8^+$ T cells. On the other hand, the cohort of the naïve spleen samples consisted of only two samples and this population in line B increase in two samples while decrease in two others, it was impossible to do any type of statistical analysis to determine whether or not this increase or decrease was significant. Thus, using the data of total number of $CD8^+$ T cells is not conclusive and to have been able make a promising conclusion out of this data, more samples were in need.

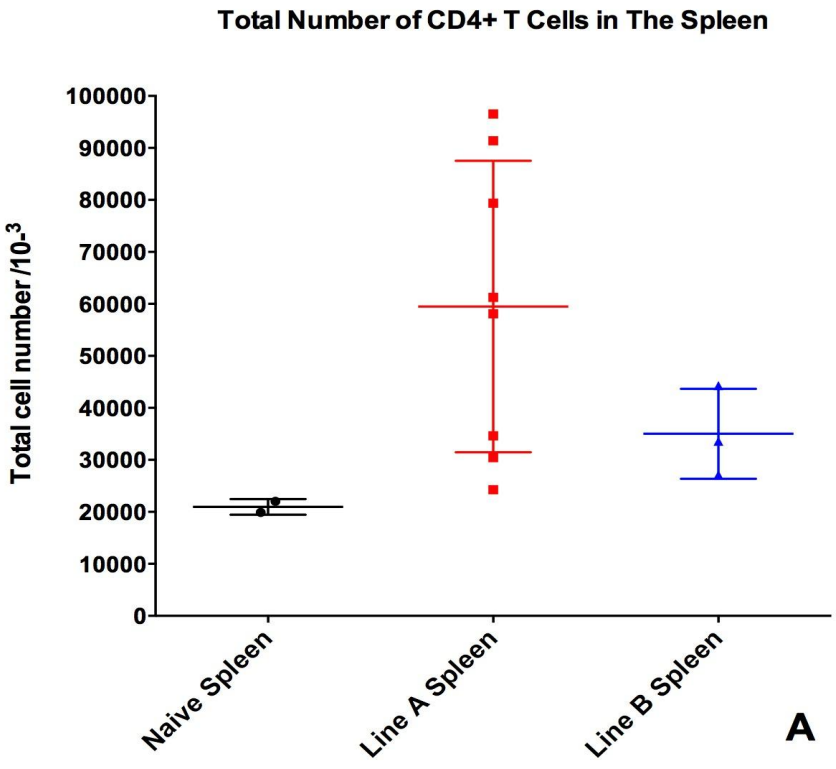
Total Number of CD4+ T Cells in The Spleen
Total cell number /10-3
100000
90000
80000
70000
60000
50000
40000
30000
20000
10000
0
Naive Spleen
Line A Spleen
Line B Spleen
A

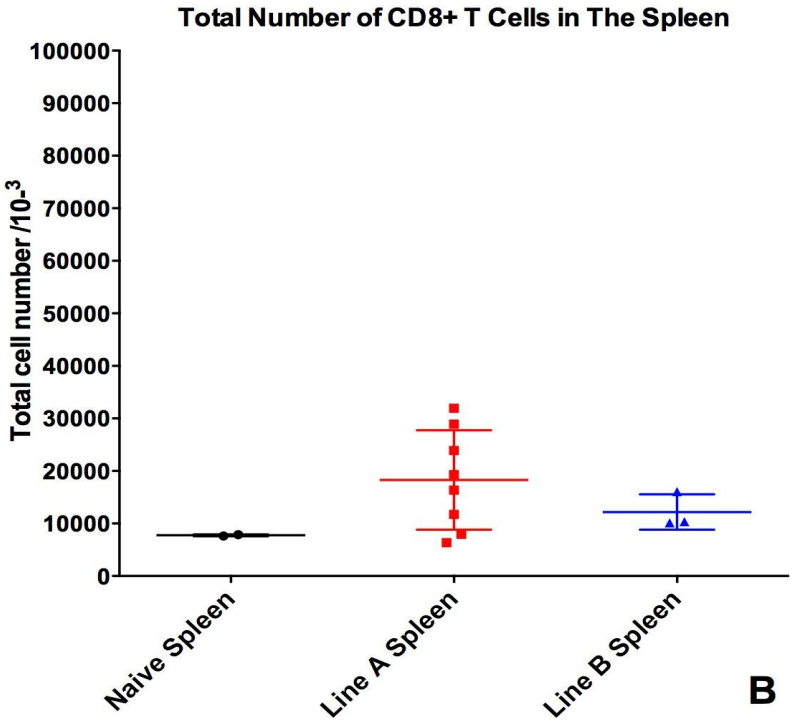
Total Number of CD8+ T Cells in The Spleen
Total cell number /10-3
100000
90000
80000
70000
60000
50000
40000
30000
20000
10000
0
Naive Spleen
Line A Spleen
Line B Spleen
B

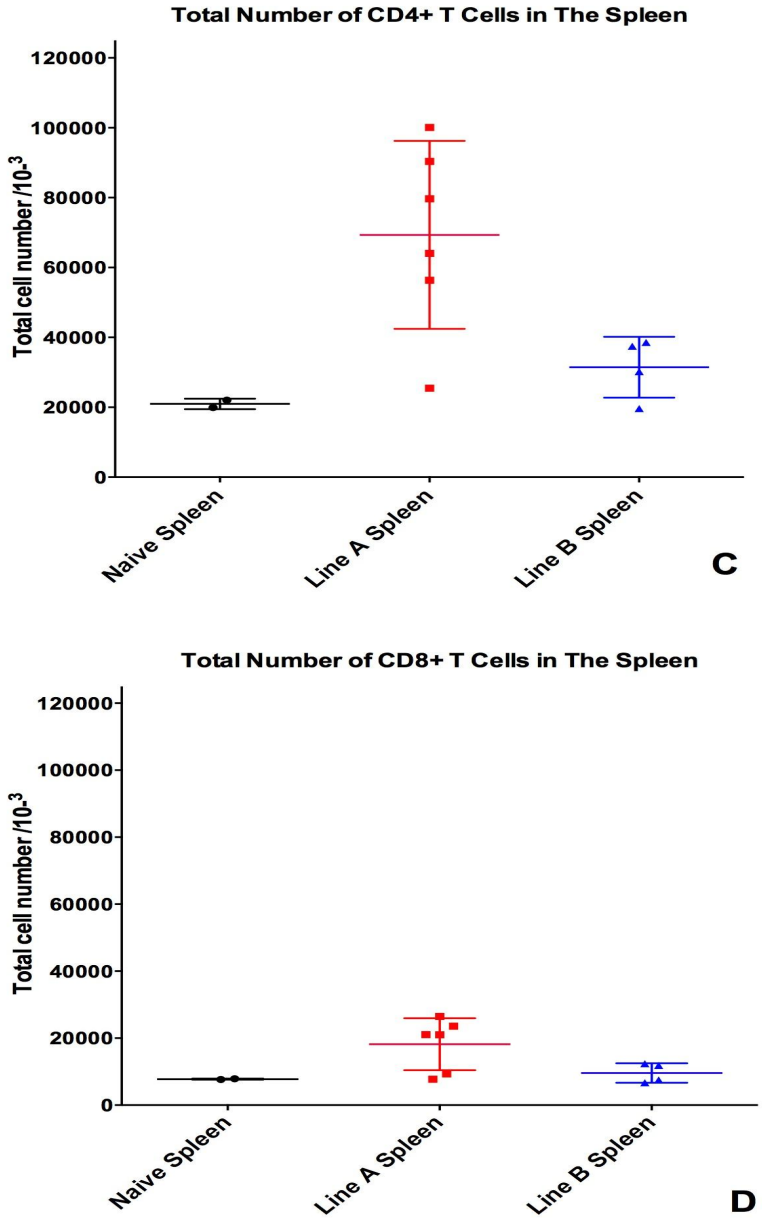

Figure 53. Total Number Of $CD4^+$ And $CD8^+$ T Cells Isolated From Spleens Of Both A Line And B Line Tumor-Bearing Mice At Both The Recurred Stage And Primary Stage Of Tumor Growth. Each dot represents one spleen sample. The horizontal bars depict mean values ± SEM (Standard Error of Mean) A: Total number of spleen's $CD4^+$ T cells at the primary stage. B: Total number of spleen's $CD8^+$ T cells at the primary stage. C: Total number of spleen's $CD4^+$ T cells at the recurred stage. D: Total number of spleen's $CD8^+$ T cells at the recurred stage.

Despite the variation in the total number of CD11b cells, both the average number of CD11b cells in all samples as well as the percentage of CD11b populations increased in both lines compared to the naïve spleen samples at both the recurrence stage as well as primary tumor (Figure 54). This increase in both the average number and percentage is much higher in line A compared to line B. Such a high increase in CD11b population of line A spleens could possibly be the result of specifically the line A tumor effect on these populations causing myeloid cells to recruit and accumulate within the spleen. These cells also may play a role upon infiltration within the tumor. So far, various roles have been prescribed to the tumor-infiltrated myeloid cells (i.e. pro-tumorigenic or antitumor). More studies need to be performed in order to further understand their function.

Notably, at both tumor recurrence and progression step, CD11c constitutes the smallest population in the all three types of spleen with the lowest number compared to other studied immune populations. Despite the decrease in the percentage of CD11c cells in the spleens of both lines, the average number of CD11c cells increased compared to the naïve spleen (Figure 54B, D). The average increase in line A is much higher than line B with both recurrent and primary tumor. However, at the recurrence stage, this increase varies from sample to sample; in some line A samples it increased 6 fold while in other it stays the same (Figure 54D). More samples needed to be studied to make a conclusion.

Strikingly, in two out of four line B samples in the recurred tumors, the CD11c cells were completely depleted within the spleen (Figure 54D). Two other samples, one from the primary tumors and one from other line B studied cohorts also showed that the CD11c cells were depleted. Thus, overall, among nine line B samples that have been

studied, four of them were shown to have no CD11c cells within the spleen (Data not present).

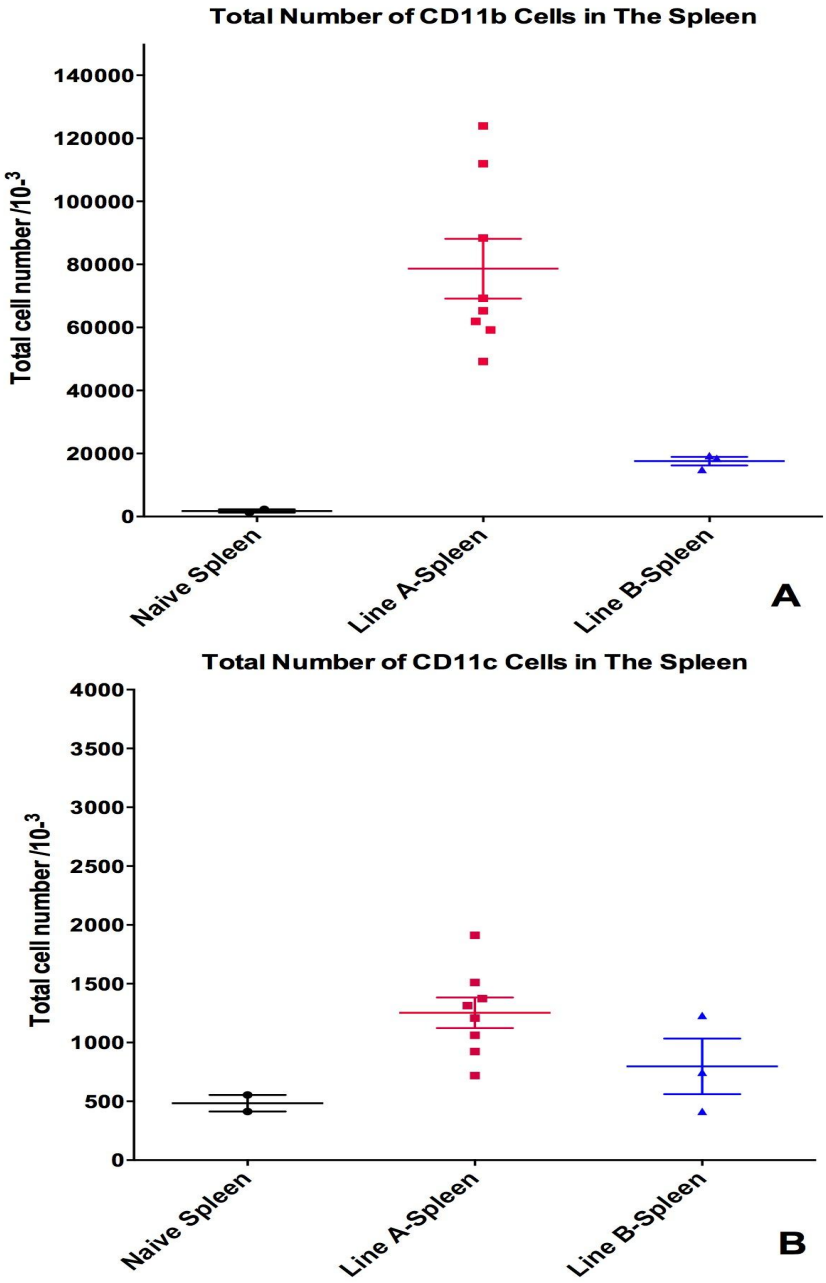

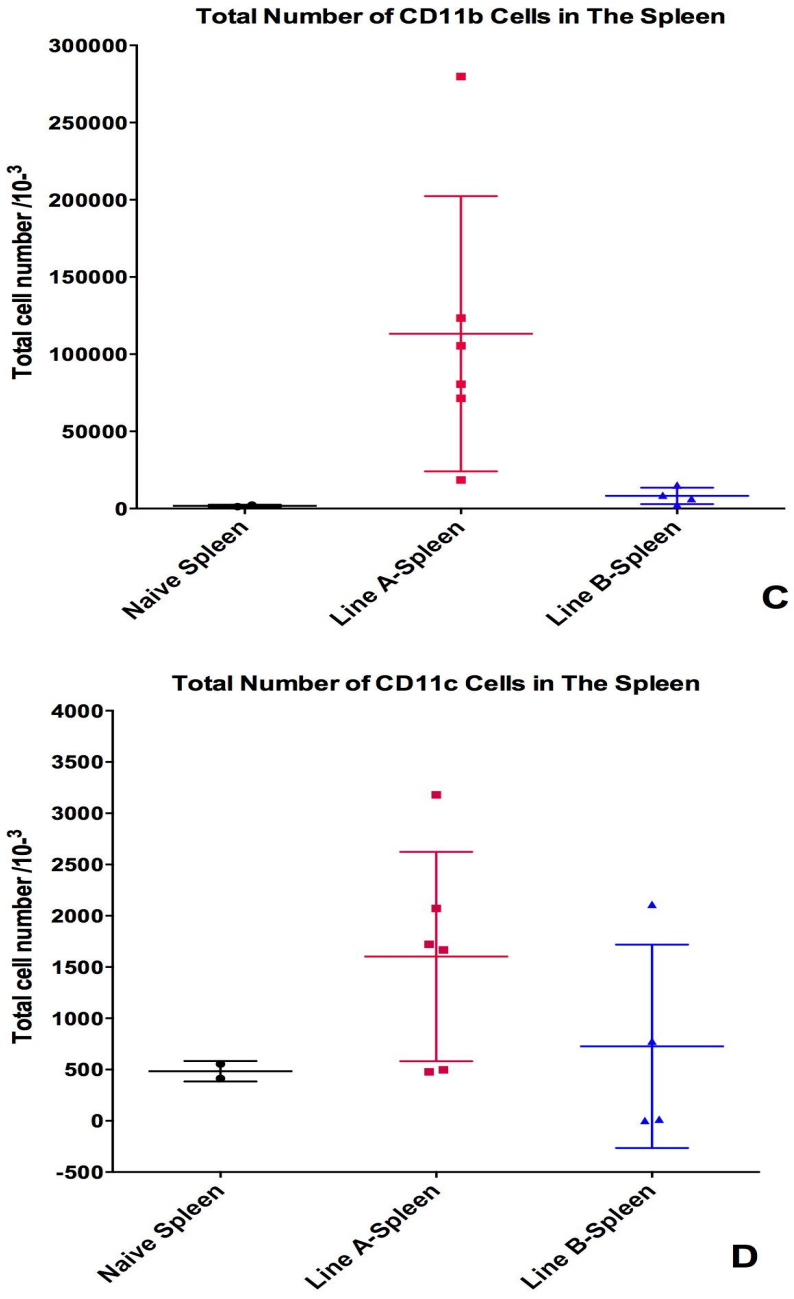

Figure 54. Total Number Of CD11b And CD11c Cells Isolated From Spleens Of Both A Line And B Line Tumor-Bearing Mice At Both The Recurred Stage And Primary Sage Of Tumor Growth. Each dot represents one spleen sample. The horizontal bars depict mean values ± SEM. A: Total number of spleen's CD11b cells at the primary stage. B: Total number of spleen's CD11c cells at the primary stage. C: Total number of spleen's CD11b cells at the recurred stage. D: Total number of spleen's CD11c cells at the recurred stage.

The data analysis of three main populations of CD11b namely PMN, Ly6C^{hi} and Ly6C^{lo} at both step of tumor growth, progression and recurrence, showed that the overall increase in the number of CD11b is due to the increase in the population of all three studied cells (Figure 55). This increase was observed in both lines compared to the naïve spleen and is regardless of the stage of the tumor growth.

These data show that regardless of the type of tumor, upon tumor stimulation, myeloid cells population increased in spleen, although, the level of increase was different from line to line and also dependent of the stage of the tumor growth. The fold increase in all three myeloid subpopulations was much higher in line A compared to line B at both stages which could possibly explain the reason for spleen enlargement in this group.

Amongst all three myeloid subpopulations at both primary tumor and recurred tumor, the highest fold increase in line A was observed in the PMN population (56 and 77 fold increase respectively compare to naïve spleen) (Figure 55B, D). This fold increase varied in the myeloid population of Line B spleen depends on the stage of the tumor growth. For instance, the highest fold increase was observed in both PMN and monocytes at the primary tumor (10 fold) and the highest fold increase was observed in the monocytes only at the recurred tumor (3 fold) (Figure 55B, D).

The accumulation of almost all immune cells in line A spleen would result in spleen enlargement. However, according to the studies on immune cell demographics, these immune cells did not increase proportionally in the spleen. Line A tumor recruited a huge population of PMN which resulted in their excessive accumulation within the spleen and spleen's enlargement.

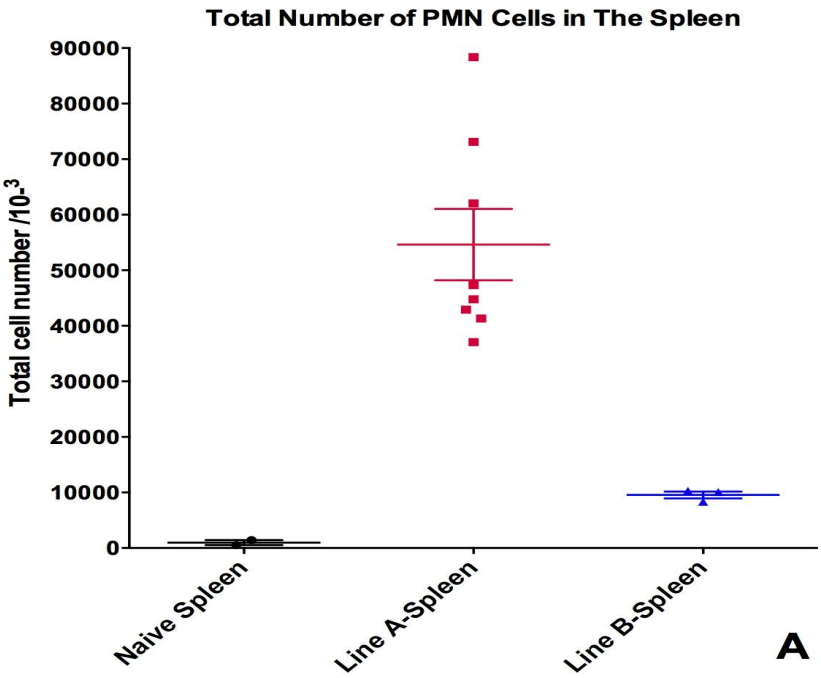
Total Number of PMN Cells in The Spleen
Total cell number /10-3
90000
80000
70000
60000
50000
40000
30000
20000
10000
0
Naive Spleen
Line A-Spleen
Line B-Spleen
A

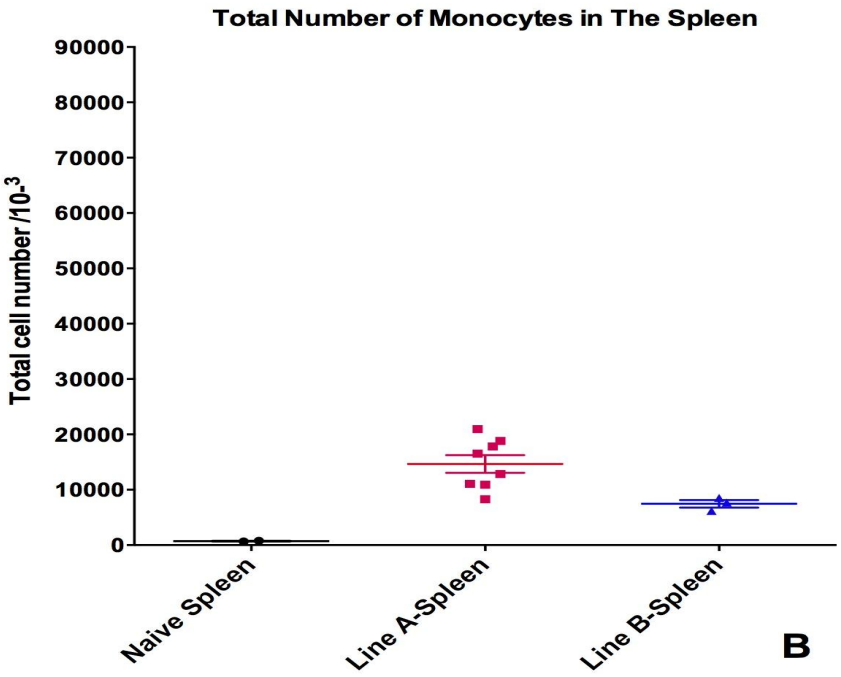
Total Number of Monocytes in The Spleen
Total cell number /10-3
90000
80000
70000
60000
50000
40000
30000
20000
10000
0
Naive Spleen
Line A-Spleen
Line B-Spleen
B

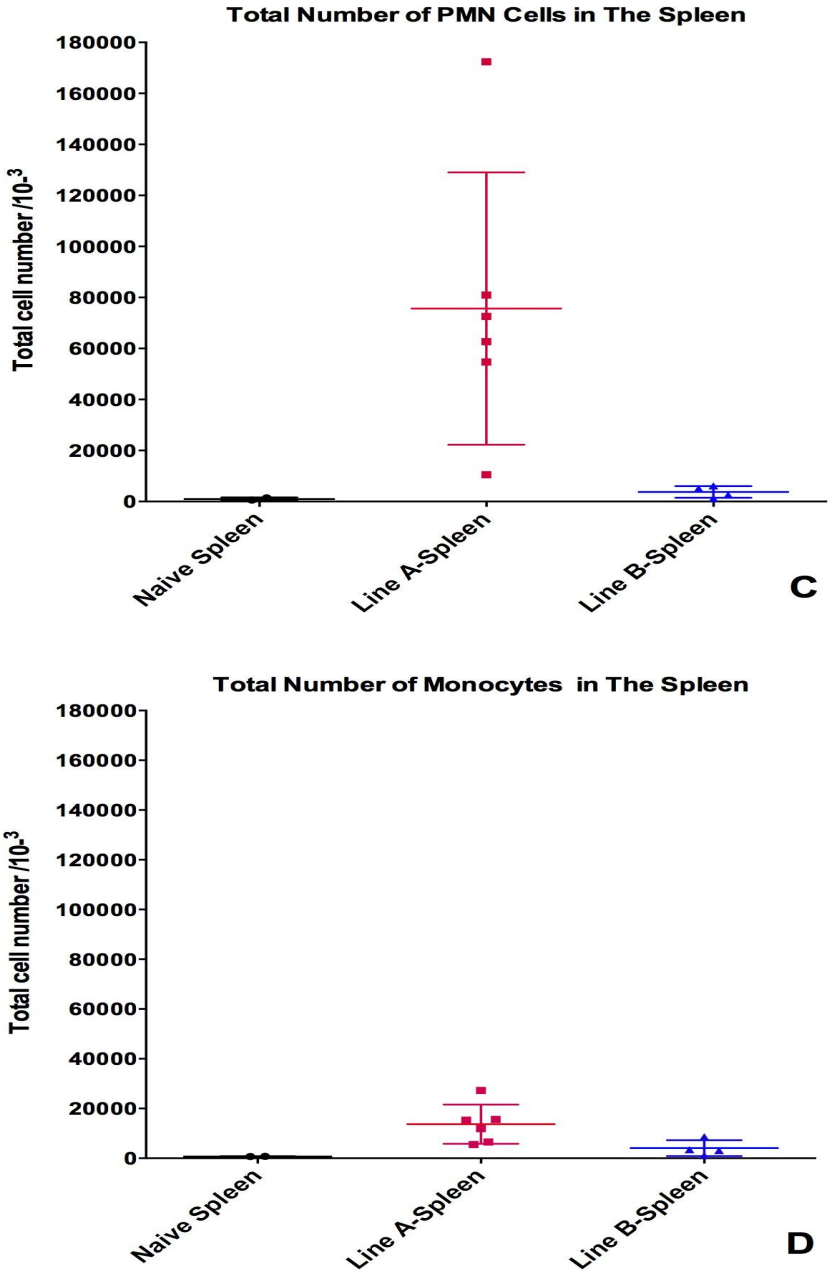

Figure 55. Total Number Of PMN And Monocytes Isolated From Spleens Of Both A Line And B Line Tumor-Bearing Mice At Both The Recurred Stage And Primary Sage Of Tumor Growth. Each dot represents one spleen sample. The horizontal bars depict mean values ± SEM. A: Total number of spleen's PMN cells at the primary stage. B: Total number of spleen's monocytes at the primary stage. C: Total number of spleen's PMN cells at the recurred stage. D: Total number of spleen's monocytes at the recurred stage.

4.4.4 Line A/B Tumor-Associated Myeloid Cells

Considering the previous studies, which have shown that the density of tumor-infiltrated immune cells, particularly T cells, is correlated with better prognosis (Dunn, Old, and Schreiber 2004; Clark et al. 1989; Clemente et al. 1996; Scanlan, Simpson, and Old 2004), this analysis helps us know, firstly, how differently the immune cells can infiltrate the tumors and, thus, determine which tumor is more likely to respond to therapeutics. Secondly, we gain a better understating of the mechanism of the immune response in the tumor microenvironment of these two tumor models. To do so, both the total percentage population and total cell number was determined and the population of myeloid cells as well as T cells that infiltrated the tumor characterized and compared between Line A and Line B.

4.4.4.1 Depending On The Stage Of The Growth And The Type Of The Tumor, Tumors Displayed Different Infiltrating Immune Cells Phenotypes. Line A Attracts PMNs More Than Line B At The Primary Stage

Data analysis of tumor-infiltrating immune cells have shown that almost all four main groups of immune cell namely, $CD4^+$ T cells, $CD8^+$ T cells, CD11b and CD11c cells, infiltrated within the tumor of both primary tumor and recurred tumor (Figure 56).

While in the primary stage, the population of CD11c, CD11b, mainly PMNs, constitute the higher percentage in line A compared to line B, the percentage of $CD8^+$ T cell population is much lower in the primary stage. Considering that high immune infiltration is one of the significant features of TNBC, the low abundance of CD8s in this tumor model might be due to some factors that hold $CD8^+$ T cells back and avoid them to infiltrate significantly or due to the inability of the $CD8^+$ T cells to detect tumor cells or being recruited by tumor cells. This could be caused by impairment of CD11c in activating tumor-specific $CD8^+$ T cells. The high percentage of myeloid cells population, over 60% of the infiltrated cells, as opposed to the low abundance of $CD8^+$ T cells in line A is more likely to lead to poor prognosis and aggressiveness of this tumor compared to B.

In terms of the demography of immune infiltrated cells, both lines at the recurred stage behave similarly, meaning that the abundance of immune infiltrating populations are almost the same at the recurred tumors regardless of their line type. The only population that showed any sort of variation was myeloid cells. This difference could be associated to the type of the tumor and their different behavior in the tumor microenvironment, which cause a different level of myeloid cells recruitment.

CD11c is the smallest population in both lines of primary tumors, whereas, the highest abundant population among infiltrating immune cells varied from line to line.

Myeloid cells, PMN and monocytes, again are infiltrating within these two lines significantly but at a different level and their abundance is less than T cells. Similar to the

primary tumors, in the recurred tumors, line A recruited higher percentage of PMN compared to line B.

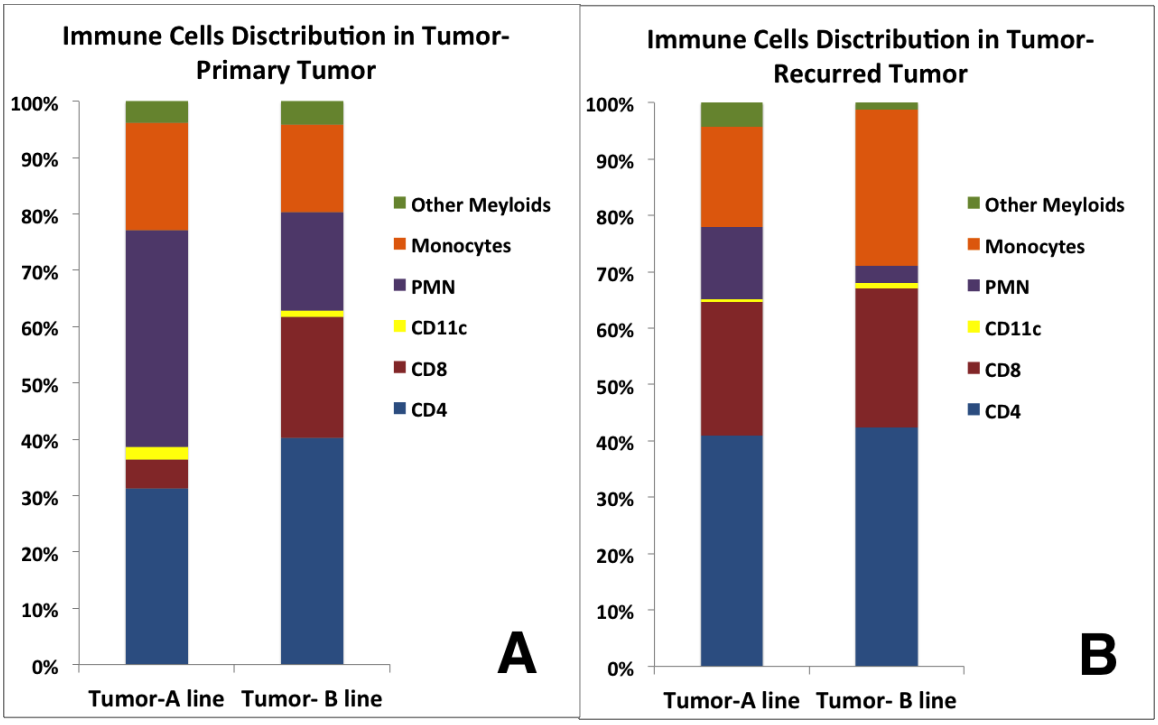

Figure 56. The Comparison Of Demography Of Immune Subpopulations Of Tumors. A: Primary Tumors Of Line A And B, B: Recurred Tumors Of Line A And B.

4.4.4.2 Line A Tumor Constituted Of More Immune Cells, Lymphocytes And Myeloid Cells Compared To Line B, Regardless Of The Stage Of The Tumor Growth. Line A Exclusively Had More PMNs And $CD4^+$ T Cells Than Line B At The Primary Stage.

Despite the fact that the percentage of the $CD4^+$ T cells is the same between lines at both progression and recurrence stage, the percentage of $CD8^+$ T cells shows variation from line to line particularly in the primary tumor (Figure 56 A). Any decrease or increase in the percentage of each immune population does not necessarily represent the actual difference in the number of tumor-infiltrated cells. Thus, besides studying the percentage of each immune cell type, the changes in the total number of each population also needed to be studied.

In terms of the total number of cells infiltrated within the tumor of both primary tumor and recurred tumor, data analysis have shown that in general more cells, regardless of their type, infiltrated within the recurred tumor compared to primary tumor. Considering that MYC is expected to express less at the recurred stage, this low infiltration rate may be related to the MYC and its influence in the tumor microenvironment and immune cells.

In the primary tumor, both the percentage and the average number of $CD8^+$ T cells is much lower in line A compared to B (Figure 57 B). $CD4^+$ T cells' percentage was the same between lines at this stage; however, the average of the total number is higher in line A compared to line B. Since, on the one hand, the total number of both $CD4^+$ and

$CD8^+$ T cells varied from sample to sample and on the other hand, the number of studied samples is relatively small, we cannot study the significance of these differences by statistical analysis. Nor can we make a reliable conclusion in regards to the difference of these lines in terms of the level of infiltration of T cells in the primary tumor.

Despite that the percentages of both $CD4^+$ and $CD8^+$ T cell populations remained the same between lines at the recurred stage, the total number of these cells is higher in line A compared to line B. This shows that there are more T cells present in line A compared to B at this stage, due to either their proliferation or infiltration (Figure 57C, D).

Notably, $CD4^+$ T cells are also the most abundant population in both line A and B at both stages of the tumor growth.

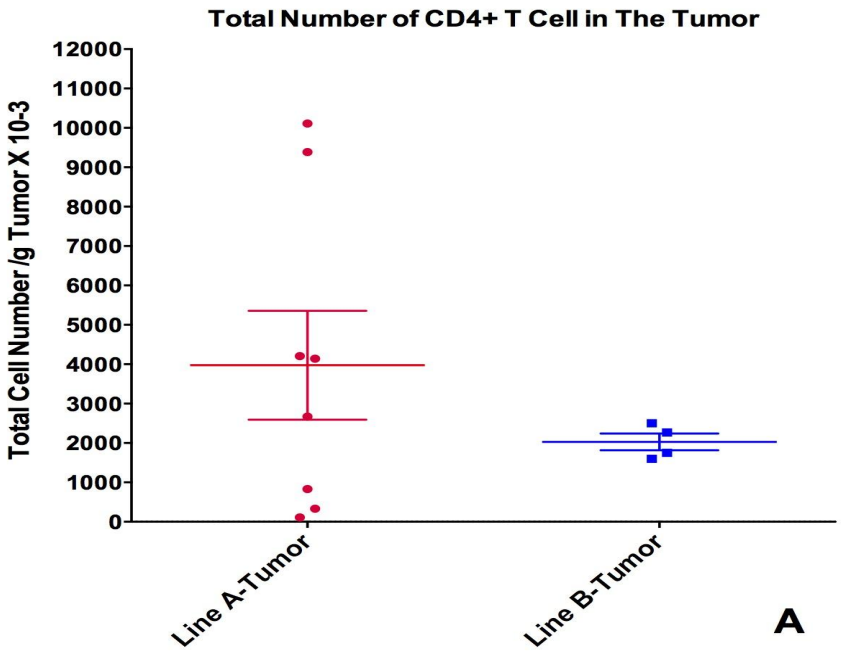
Total Number of CD4+ T Cell in The Tumor
Total Cell Number /g Tumor X 10-3
12000
11000
10000
9000
8000
7000
6000
5000
4000
3000
2000
1000
0
Line A-Tumor
Line B-Tumor
A

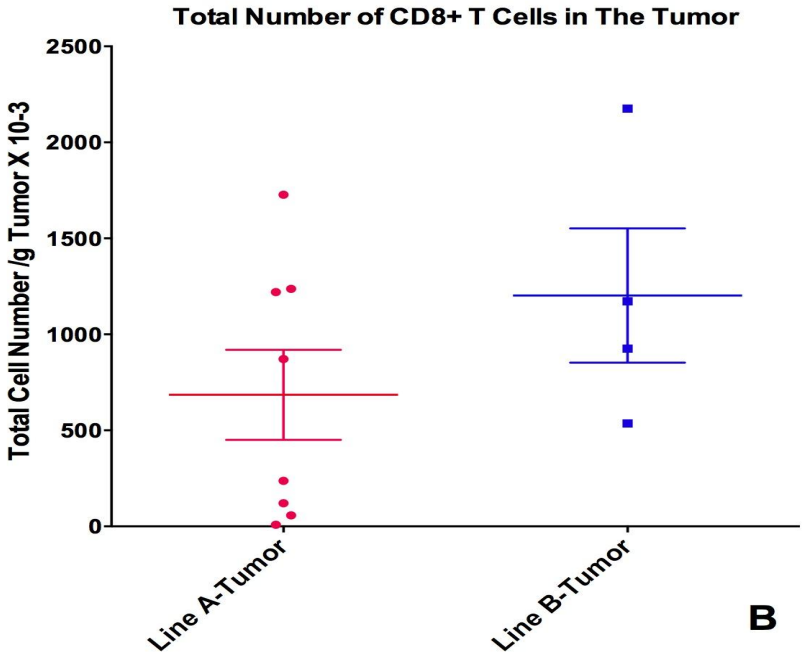
Total Number of CD8+ T Cells in The Tumor
Total Cell Number /g Tumor X 10-3
2500
2000
1500
1000
500
0
Line A-Tumor
Line B-Tumor
B

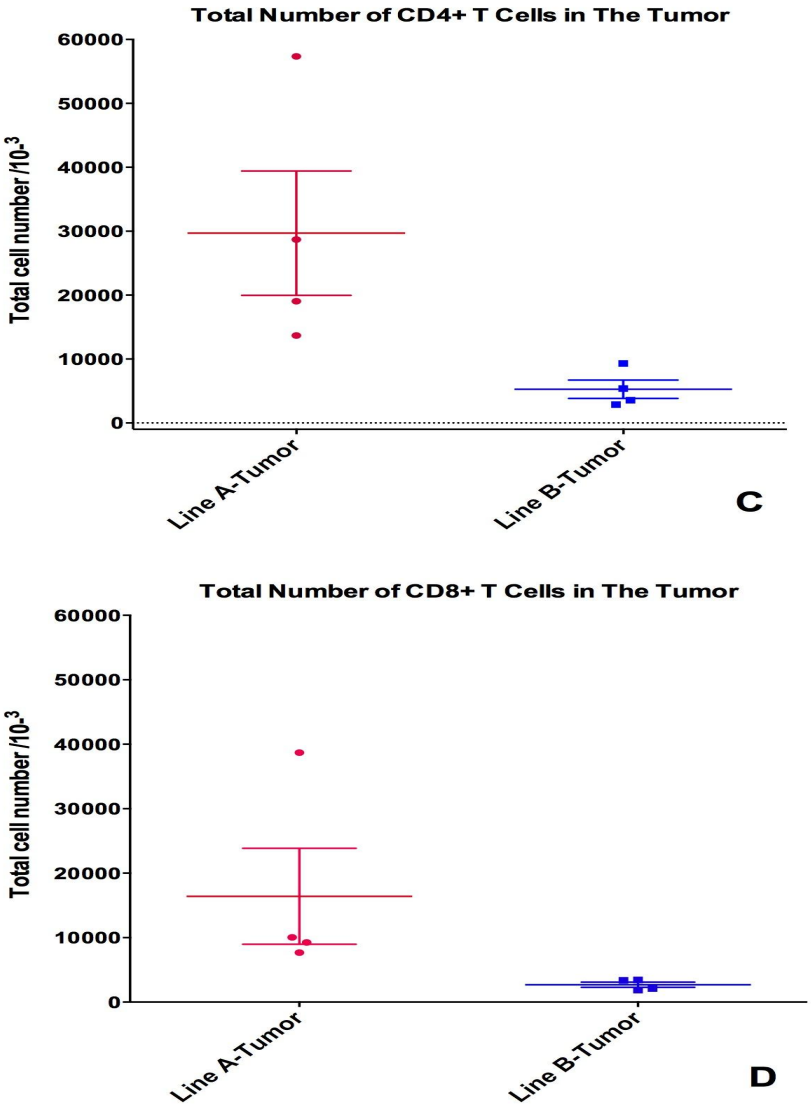

Figure 57. Total Number Of $CD4^+$ And $CD8^+$ T Cells Isolated From Tumors Of Both A Line And B Line Tumor-Bearing Mice At Both The Recurred Sage And Primary Stage Of Tumor Growth. Each dot represents one spleen sample. The horizontal bars depict mean values ± SEM. A: Total number of $CD4^+$ TIL cells at the primary stage. B: Total number of $CD8^+$ TIL cells at the primary stage. C: Total number of $CD4^+$ TIL cells at the recurred stage. D: Total number of $CD8^+$ TIL cells at the recurred stage.

Overall, the average total number of CD11b and CD11c cells is higher in line A compared to Line B in the recurred tumor (Figure 58C-D). The same pattern was observed in the primary tumor. However, due to the limited number of the samples and the variation in the number of CD11b and CD11c cells from sample to sample at the primary stage in both lines, particularly in line A (Figure 58A-B), it is not possible to study the significance of this increase and make a reliable conclusion out this data. Interestingly, the depletion observed in the CD11c population of spleen was also detected in the tumor-infiltrated CD11c as well; half of the samples (two out of four) in line B were depleted from this cell population (Figure 58D).

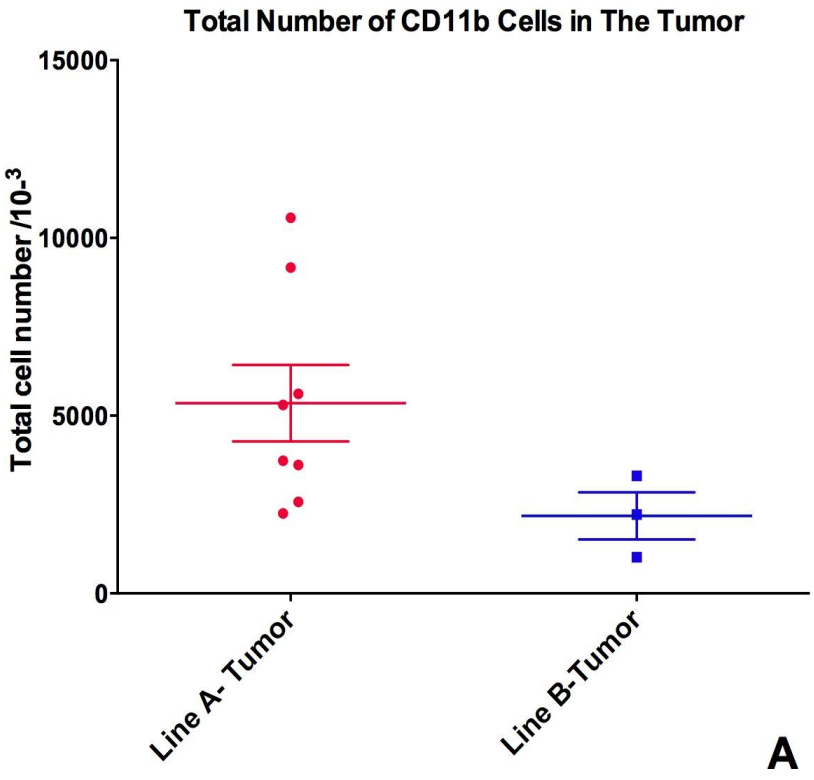
Total Number of CD11b Cells in The Tumor
15000
10000
5000
0
Total cell number /10-3
Line A- Tumor
Line B-Tumor
A

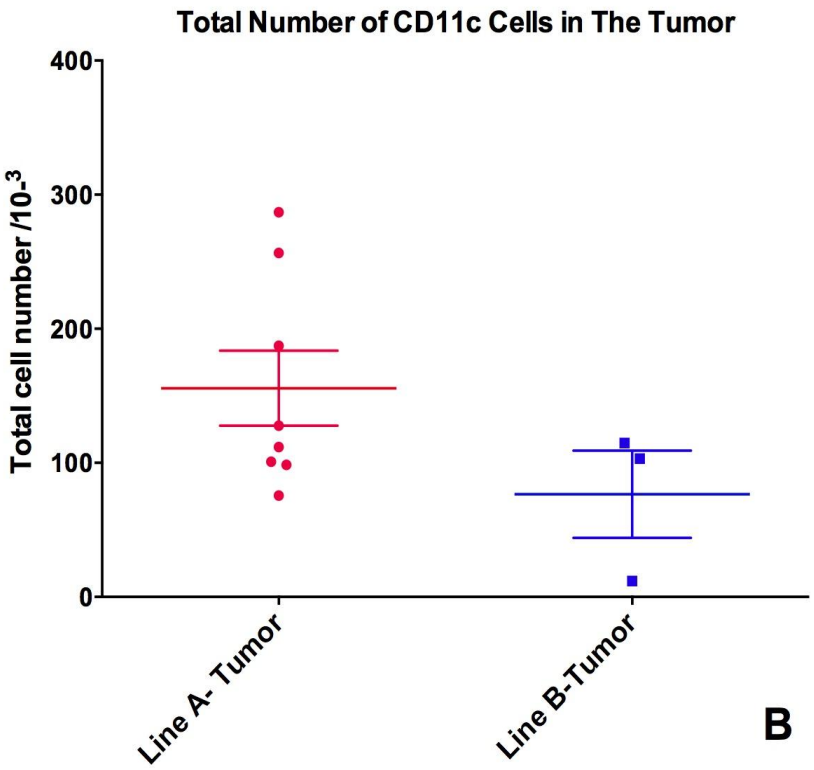
Total Number of CD11c Cells in The Tumor
400
300
200
100
0
Total cell number /10-3
Line A- Tumor
Line B-Tumor
B

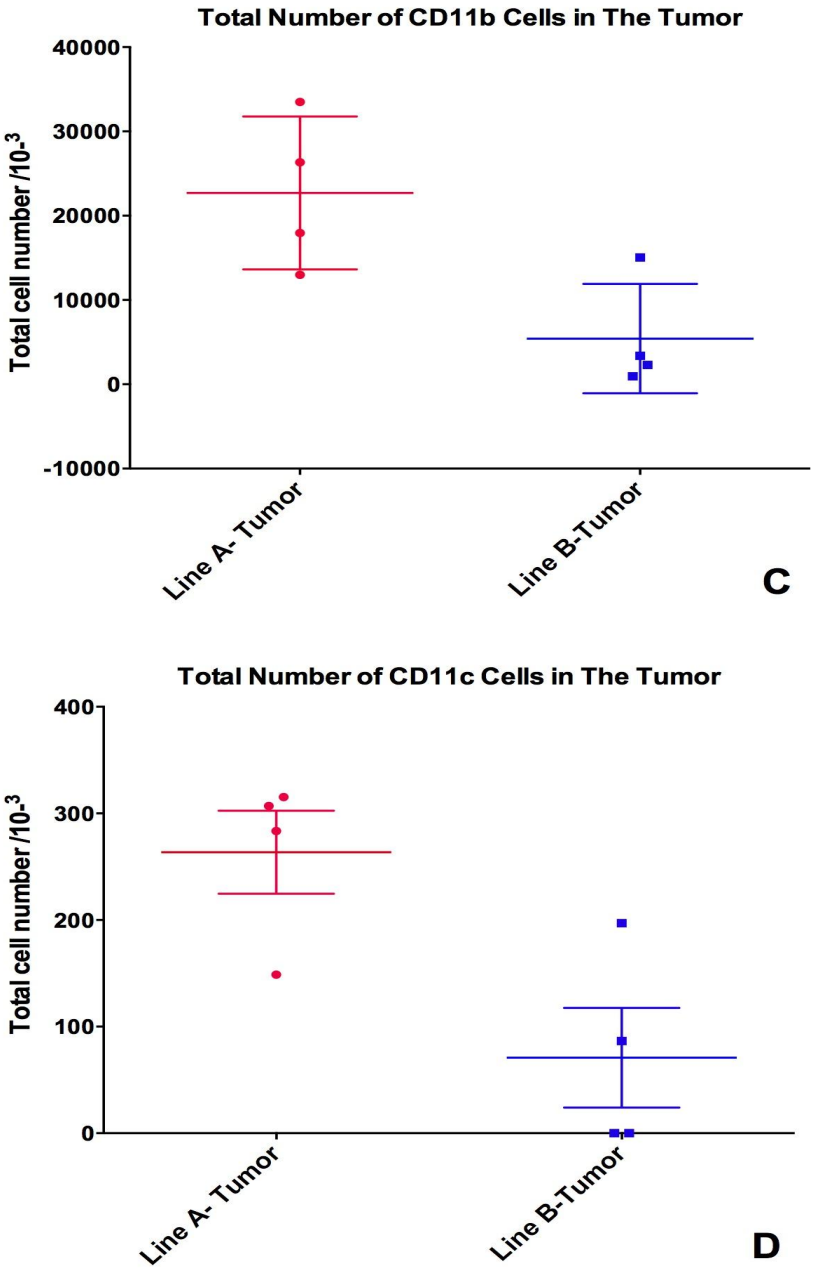

Figure 58. Total Number Of CD11b And CD11c Isolated From Tumors Of Both A Line And B Line Tumor-Bearing Mice At Both The Recurred Stage And Primary Stage Of Tumor Growth. Each dot represents one spleen sample. The horizontal bars depict mean values ± SEM. A: Total number of tumor-infiltrated CD11b cells at the primary stage. B: Total number of tumor-infiltrated CD11c cells at the primary stage. C: Total number of tumor-infiltrated CD11b cells at the recurred stage. D: Total number of tumor-infiltrated CD11c cells at the recurred stage.

More detailed studies of the tumor-infiltrating myeloid cells through determining the total number of myeloid subpopulations showed that the average number as well as the percentage of PMN is higher in both recurred tumor and primary tumor of line A to line B (Figure 59A, C). Likewise, the average number and percentage of monocytes is higher in line A compared to line B in the primary tumor. On the contrary, at the recurred stage, despite the average number of monocytes is higher in line A, the percentage of monocytes in line A is slightly lower than the percentage of line B (Figure 59B, D).

Considering that in general the numbers of studied samples are limited, it is not possible to do any statistical analysis out of the total number of tumor-infiltrated immune cells to study the significance of these differences.

Comparing the average abundances of each immune subpopulation had shown that in the recurred tumor, in both lines $CD4^+$ T cells and monocytes are the dominant populations. While in the primary tumor, this dominant population varied from line to line. In Line A, $CD4^+$ T cells and PMN were dominant while only $CD4^+$ T cells is the dominant population in line B.

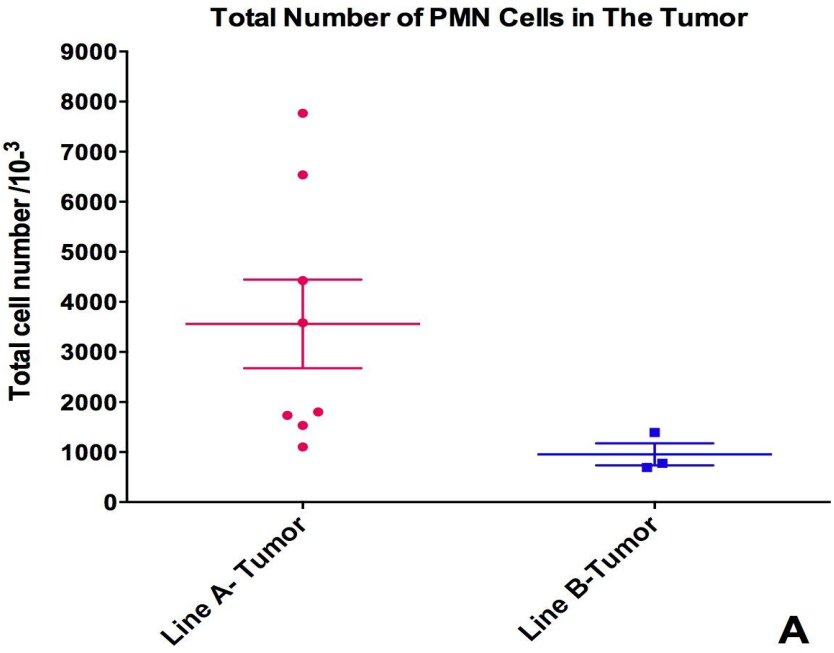
Total Number of PMN Cells in The Tumor
Total cell number /10-3
9000
8000
7000
6000
5000
4000
3000
2000
1000
0
Line A- Tumor
Line B-Tumor
A

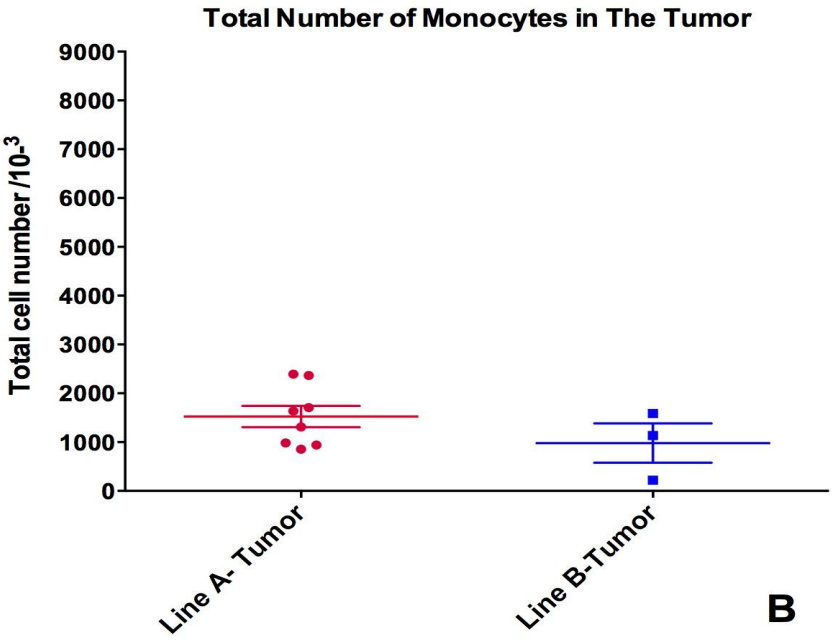
Total Number of Monocytes in The Tumor
Total cell number /10-3
9000
8000
7000
6000
5000
4000
3000
2000
1000
0
Line A- Tumor
Line B-Tumor
B

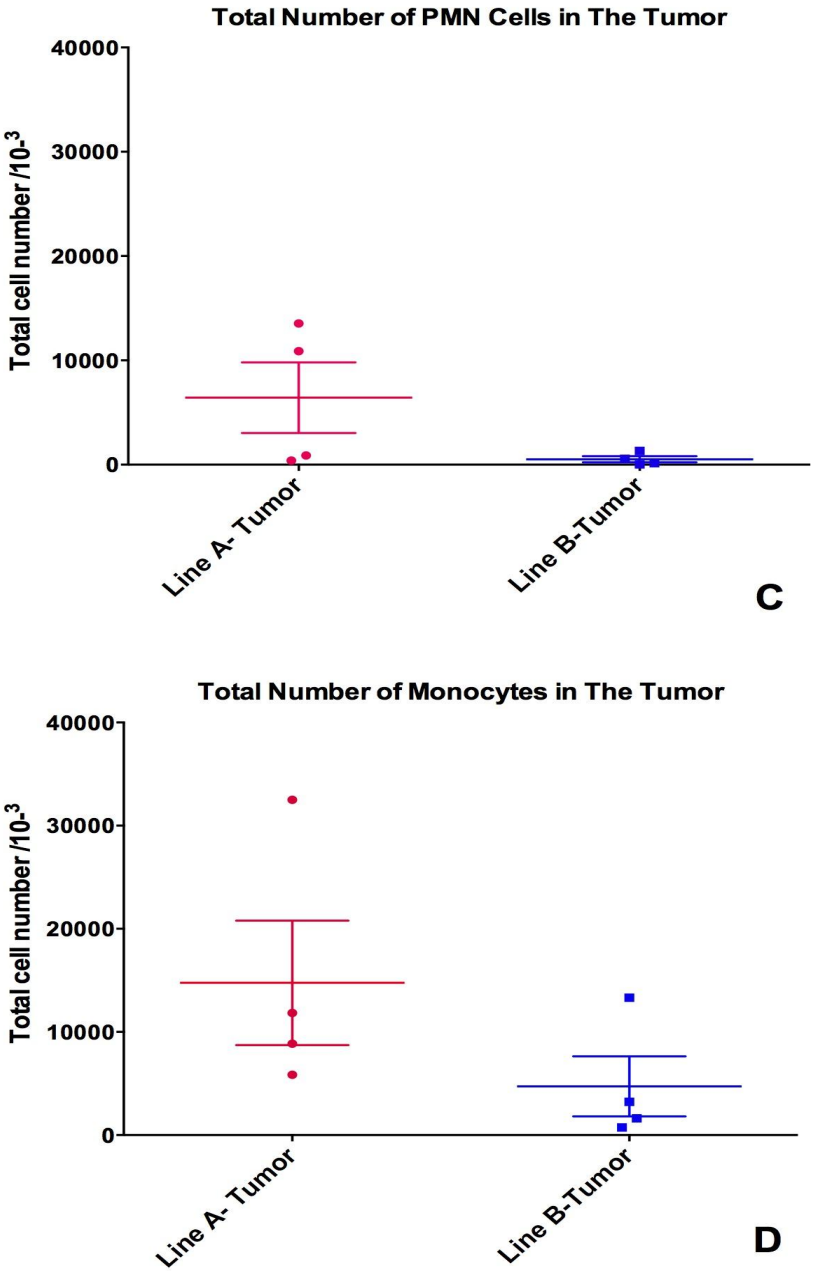

Figure 59. Total Number of PMN and Monocytes Isolated from Tumors of both A Line and B Line Tumor-Bearing Mice at both The Recurred Stage and Primary Stage of Tumor Growth. Each dot represents one spleen sample. The horizontal bars depict mean values ± SEM.A: Total number of tumor-infiltrated PMN cells at the primary stage. B: Total number of tumor-infiltrated monocytes at the primary stage. C: Total number of tumor-infiltrated PMN cells at the recurred stage. D: Total number of tumor-infiltrated monocytes at the recurred stage.

Taken together, we know that at the recurrent tumor, both lines have more infiltrated immune cells regardless of their types compared to the primary tumors. We also realized that PMN population is much higher in line A compared to line B regardless of the stage of tumor growth.

Moreover, we observed a variation in the abundance of myeloid cells, as well as $CD8^+$ T cells but not $CD4^+$ T cells, from line to line regardless of the stage of the growth. It is as if the myeloid abundance, particularly PMNs, is sensitive to the type of the tumor and their recruitment varied depending on the type of tumor. Considering the differences observed between these lines, in terms of their abundance in tumor-infiltrating immune cell types, to make a reliable conclusion from the total number of infiltrated cells is relatively hard or impossible. That is due to the small number of samples, high variation of total number of cells between samples and the difficulty in detecting the population of interest in the FACS analysis of tumor data. This difficulty is a result of our lack of information about the changes in the phenotype of myeloid cells, the continuous changes of the phenotype of the myeloid cells upon infiltrating the tumor microenvironment and difficulty in finding the right antibody to detect these populations.

We still are not sure if this difference in abundance and total number is due to the infiltration of each of these populations or the result of both recruitment and proliferation. We also do not know if infiltrated T cells are functional or exhausted. Also, we need to know what the origin of these infiltrating populations are, as they may change their phenotypes from one type to the other as they stay or infiltrate the tumor. Additionally, we do not know why the population of myeloid cells was sensitive to the type of line and

their abundance also varied between these lines. More detailed experiments, in regards to the functionality and origin of these cells need to be performed in order to further understand the mechanism of immune response.

4.4.5 The Tumor-Infiltrating T Cell Subsets Of Both Lines Displayed The Same Phenotype In Terms Of The Expression Of Immune Inhibitory Molecules Of TIM3, PD1 And TIGIT In The Primary Tumor. Both Lines Are Different At The Recurred Stage In Regards To The Level Of Expression Of These Receptors

Getting back to the antitumor-immune response cycle, the immune response initiated upon releasing tumor antigens. Briefly, the antigens captured and presented by antigen presenting cells (APCs), DCs at the lymphoid organs. Then the naïve T cells interact with the tumor antigen displayed at the surface of APCs. This interaction is essential for the T cell activation and trafficking to the tumor microenvironment. The activated T cells are a subset of $CD8^+$ T cells that are activated and specific to the tumor meaning that they can specifically recognize the tumor antigens and cause antitumor immune response.

Upon T cell activation through interaction with tumor antigens displayed on the surface of APC, the expression of immune inhibitory molecules increase.

Considering that the tumor antigens are the product of mutated genes including Ras and tumor-specific antigen or proto-oncogenes such as MYC, we hypothesized that

this secondary mutation could mediated two different immune responses through activating two different $CD8^+$ T cell subsets. Tumor-antigen specific $CD8^+$ T cells for TNBC haven't been characterized yet. Consequently, we still don't know if there is any difference in the tumor-specific antigen between these two lines. However, we embarked on characterization of TILs subsets according to their immune inhibitory receptor expression and compared them between these two lines using FACS. We were interested to see if there are any differences in the level of expression of these immune inhibitory receptors on the TILs, which might be associated to the effect of secondary mutation on immune response directly or indirectly. This finding also can be employed to find the target candidate molecule for the purpose of cancer immune checkpoint blockade therapy.

To compare the activated TIL subsets in these two lines, the expression of three candidate immune inhibitory receptors of TIM3, TIGIT and PD1 on tumor-infiltrated $CD4^+$ and $CD8^+$ T cell populations were studied. Previous studies have shown that these inhibitory molecules are expressed on infiltrated CD8s T cells in a wide variety of tumors including TNBC (Stagg and Allard 2013). In addition, according to TCGA databases, the ligands of these receptors are expressed relatively more in TNBC subtypes than in other breast cancer subtypes (Figure 60).

To study the expression of immune inhibitory receptors on the surface of lymphocytes ($CD4^+$ T cells/$CD8^+$ T cells), the level of expression of each of immune inhibitory receptor was quantified using Flowjo and compared to the corresponding

population isolated from the spleen of the same mouse. These studies were conducted on both the primary tumors and recurred tumors.

Normally, both $CD4^+$ and $CD8^+$ T cells do express immune inhibitory molecules but at much lower basal levels. This expression is required for lymphocyte hemostasis and regulating immune response (Freeman et al. 2000; Linsley et al. 1992). Thus, we used the immune inhibitory receptor expression of $CD4^+$ and CD^+ T cells of spleen as the negative control.

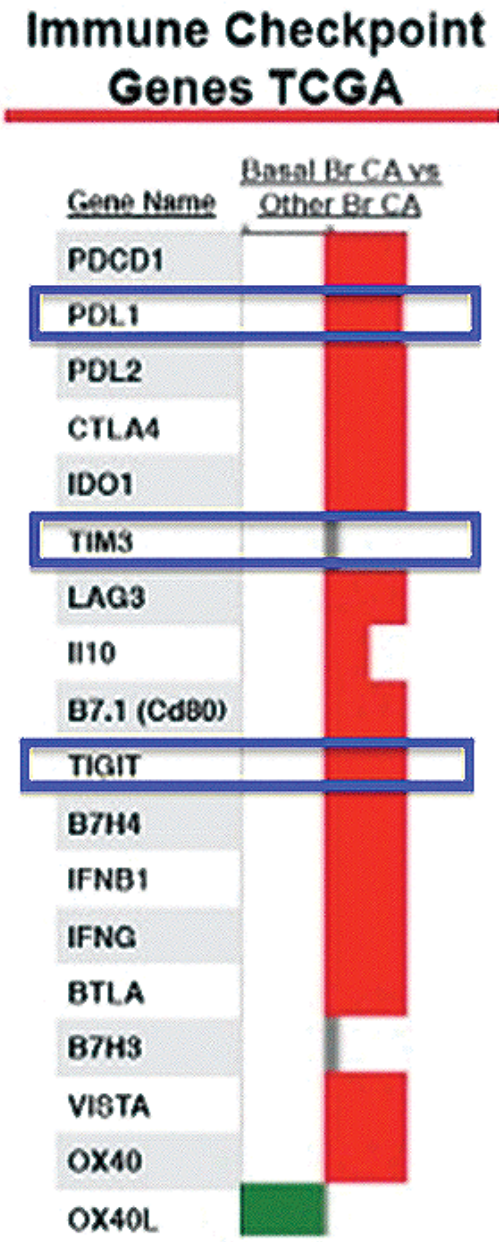

Figure 60. TCGA Database Of Immune-Inhibitory Checkpoints Ligands mRNA Expression In TNBC Versus Other Subtypes Of Cancer.

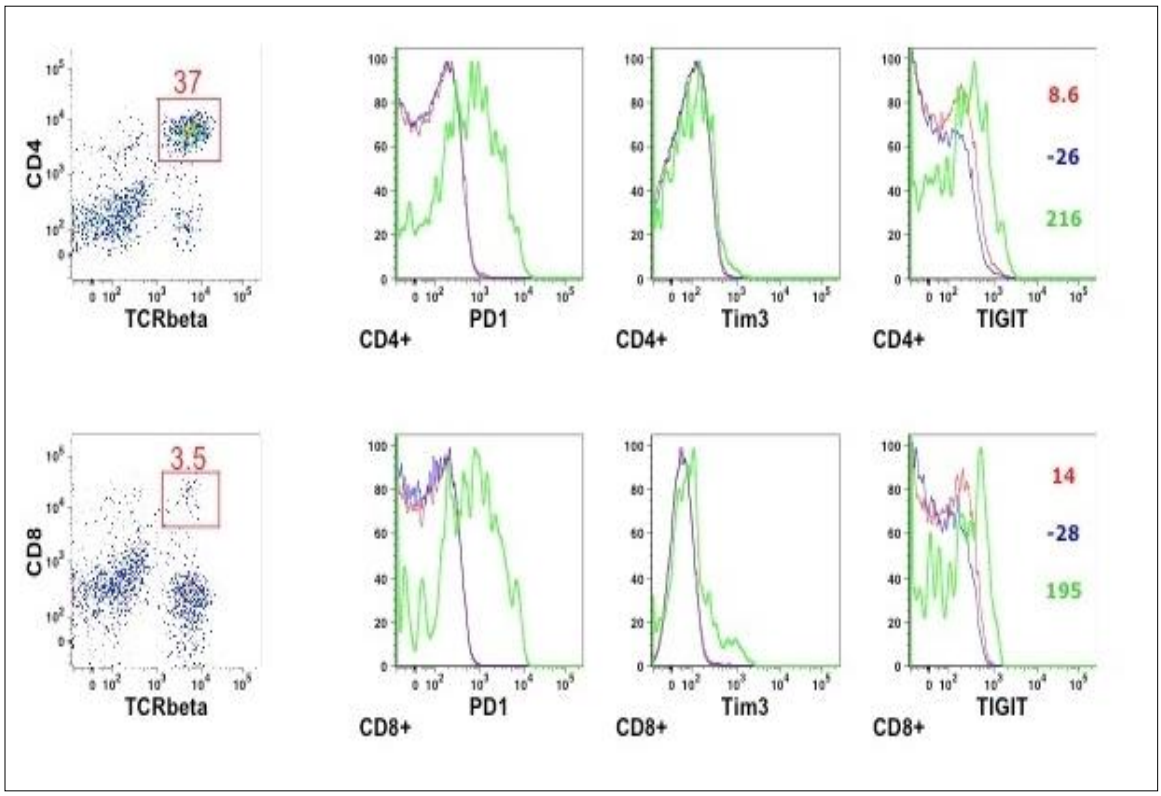

Figure 61. Flow Cytometry Histogram Representative Of PD1, TIM3 And TIGIT Expression On $CD4^+$ T Cells And $CD8^+$T Cells By Anti-PD1, Anti-TIM3 And Anti-TIGIT (Green), Respectively. The naïve spleen used as the negative control (Red). The spleen of tumor bearing mouse (Blue) was used for comparison and data analysis.

Studying the level of expression of the TIGIT in the spleen has shown that there was not a significant difference between Line A and B, in terms of TIGIT expression in $CD4^+$ T cells as well as $CD8^+$ T cells at both recurrence and progression steps (Figure 61, 62); TIGIT was expressed on both tumor-infiltrating T cells, suggesting TILs or probably tumor-antigen specific T cells may be exhausted through their TIGIT receptors.

In the primary tumor, the tumor-infiltrating $CD4^+$ and $CD8^+$ T cells expressed higher level of TIGIT compared to the $CD4^+$ and $CD8^+$ T cells population in the spleen

(Figure 62A, B). Similar to the primary tumor, at the recurred stage, the expression of TIGIT was higher in the $CD4^+$ infiltrated cells of both lines but infiltrated $CD8^+$ T cells showed different phenotype at this stage (Figure 62C, D). $CD8^+$ T cells of the line B expressed higher level of TIGIT while the infiltrated $CD8^+$ T cells of the line A did not express TIGIT significantly (Figure 62C). Is this difference due to the activation and recruitment of different subsets of the T cells or due to the effect of tumor cells or tumor micro-environmental factors on the expression of these immune inhibitory molecules on the infiltrated T cell? All of these questions and many other unknown factors needed to be address to further discover the role of secondary mutation on the antitumor immune response.

The $TIGIT^+$ $CD4^+$ T cell could be either a T helper cell that indirectly contributes in antitumor-immune response through activating APC and releasing stimulatory cytokines such as IL-2 (D.M. Pardoll and Topalian 1998). A tumor extensively inhibits them through binding to their immune inhibitory receptor of TIGIT, or they are Tregs, which regulate the activity of other immune cells.

T cells functional studies need to be done to further clarify the functionality of these cells and the possibility of their role in the antitumor response. More studies also need to be done to ensure that these TIGIT positive $CD4^+$ / $CD8^+$ T cells are tumor specific subsets.

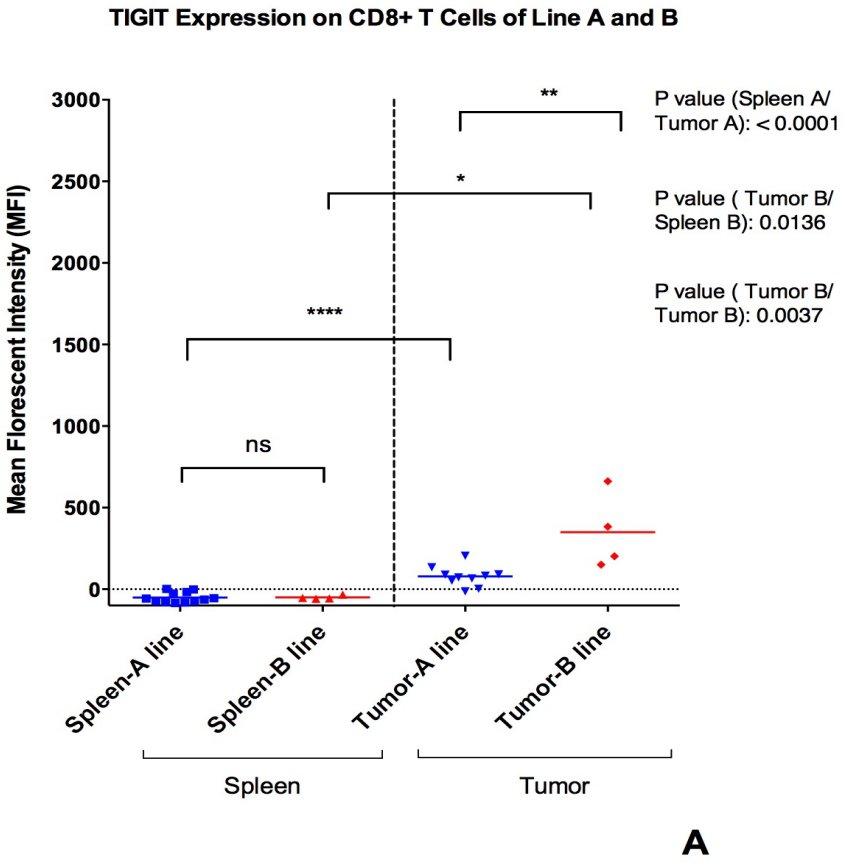
TIGIT Expression on CD8+ T Cells of Line A and B
Mean Florescent Intensity (MFI)
3000
2500
2000
1500
1000
500
0
**
*
****
ns
P value (Spleen A/ Tumor A): < 0.0001
P value (Tumor B/ Spleen B): 0.0136
P value (Tumor B/ Tumor B): 0.0037
Spleen-A line
Spleen-B line
Tumor-A line
Tumor-B line
Spleen
Tumor
A

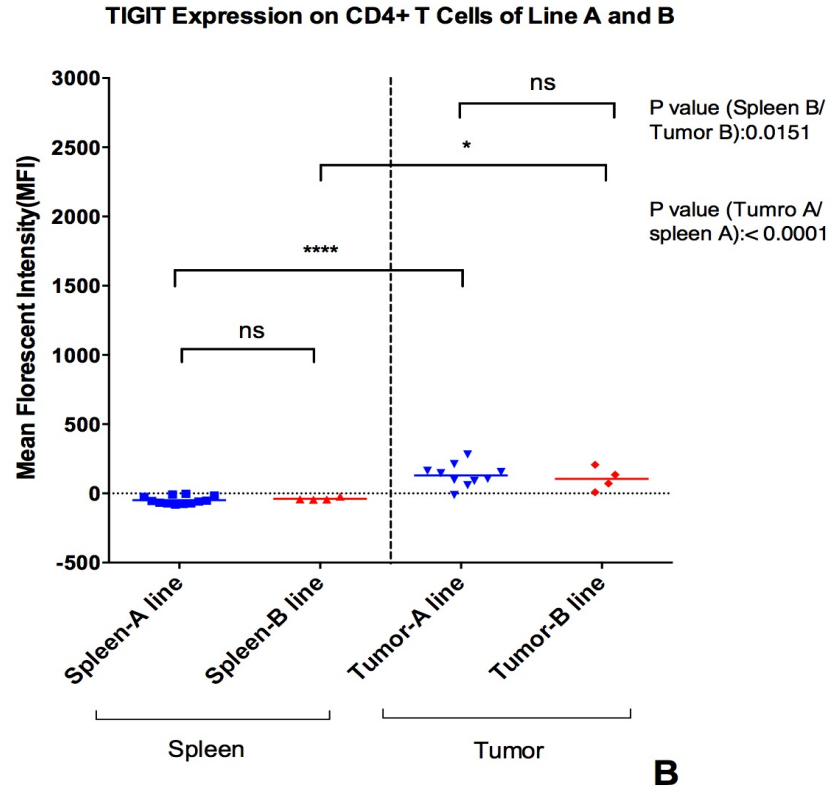
TIGIT Expression on CD4+ T Cells of Line A and B
Mean Florescent Intensity(MFI)
3000
2500
2000
1500
1000
500
0
-500
ns
*
****
ns
P value (Spleen B/ Tumor B):0.0151
P value (Tumro A/ spleen A):< 0.0001
Spleen-A line
Spleen-B line
Tumor-A line
Tumor-B line
Spleen
Tumor
B

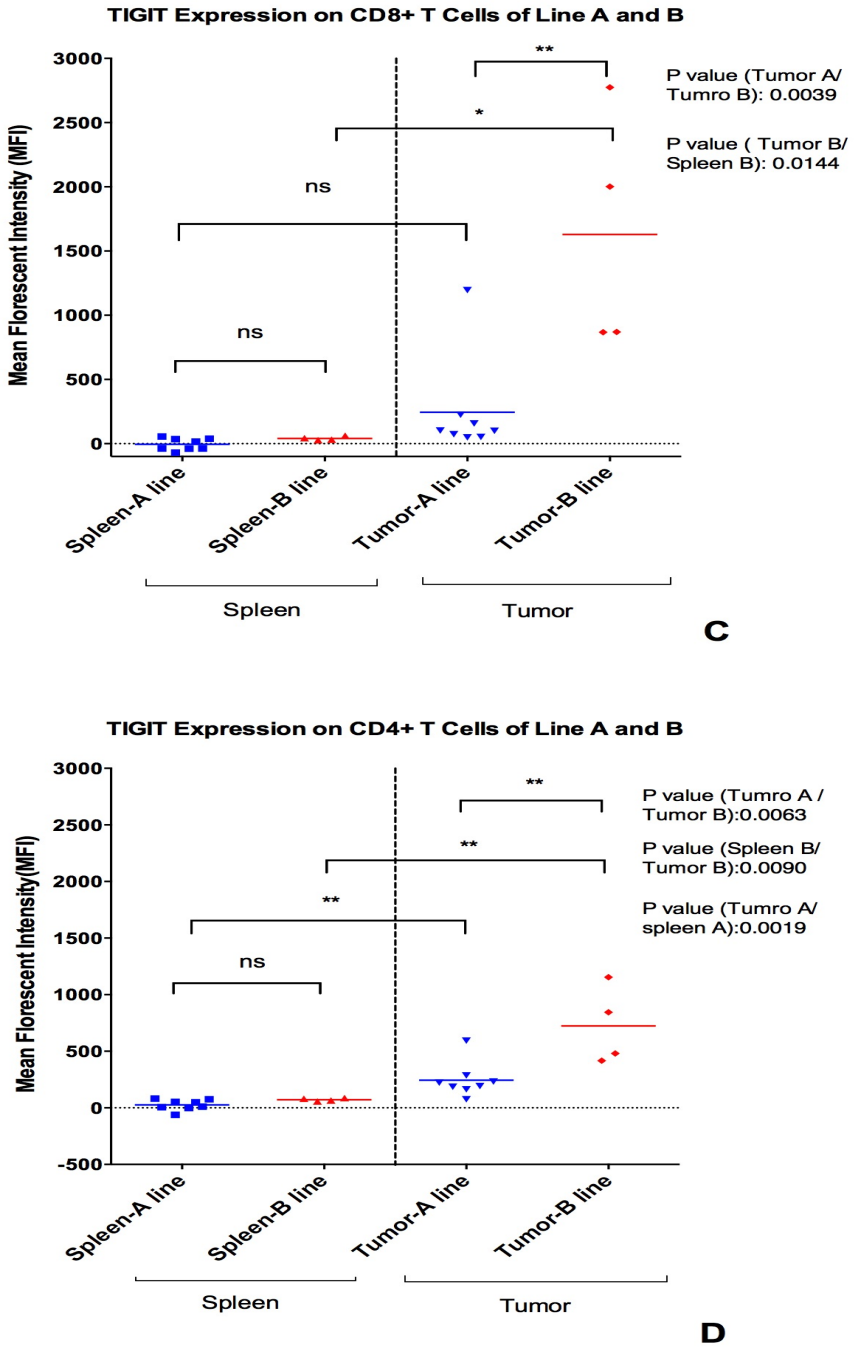

Figure 62. Comparing The TIGIT Inhibitory Receptor Expression On Lymphocytes' Population Of $CD4^{+}$And $CD8^{+}$ T Cells Between Line A And B. A-B: are the primary tumor of both lines, C-D: are the recurred tumor of both lines. P-values were calculated by two-tailed Student's t test. Horizontal bars depict the mean of the quantified TIGIT expression.

The MFI of TIM3 for the $CD4^+$ T cell population of line A and B were sometimes negative (Figure 61, 63B, D). The negative MFI is resulted by the error in measuring the baseline florescent, which usually happened when the MFI of the molecule of interest was pretty low. To solve this problem, the setting of the machine should be manipulated throughout running the samples. In both lines, a small population of $TIM3^+$ $CD4^+$ T cells infiltrate within the tumor. Due to differences in the MFI of spleen in both Line A and B at the recurrence stage, comparing the difference in the expression of TIM3 between these two lines is not conclusive (Figure 63 C, D).

The $CD8^+$and $CD4^+$ T cells of line A expressed TIM3 cells at various levels at both tumor growth stages. In some samples TIM3 did express at relatively high levels while in some other samples this inhibitory molecules expressed at a very low level (close to zero) (Figure 61, 63 A-D). This variation in TIM3 expression was observed in both spleen and tumor. Except in $CD8^+$ T cell population of primary line A tumor which highly expressed TIM3 compared to the spleen, the other T cells at both stages of the tumor growth, did not express TIM3 significantly compared to theirs in spleens (Figure 63A-D). In general TIM3 expression in line A was pretty low on $CD4^+$ and $CD8^+$ infiltrated T cells of line A regardless of the stage of the tumor growth.

In contrast to line A, tumor-infiltrated $CD4^+$ and $CD8^+$ T cells of line B expressed TIM3 at high level in both stages of tumor growth compared to the spleen except on the $CD8^+$ T cells of the primary tumor. However, this high expression of TIM3 in tumors was not as high as other studied immune inhibitory molecules such as PD1 and TIGIT.

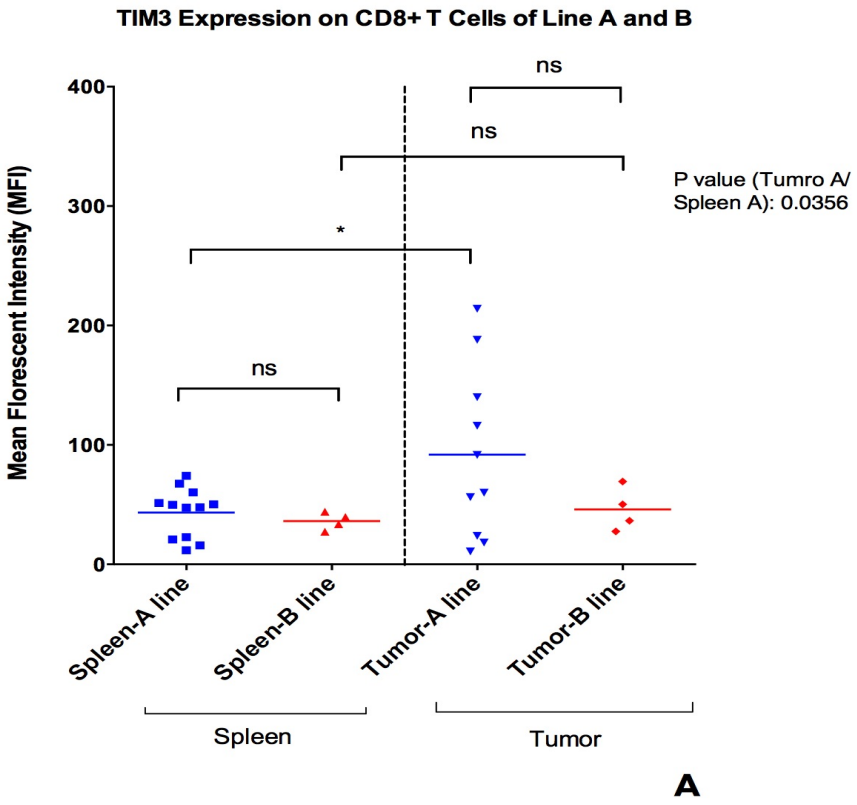
TIM3 Expression on CD8+ T Cells of Line A and B
Mean Florescent Intensity (MFI)
400
300
200
100
0
ns
ns
*
ns
P value (Tumro A/ Spleen A): 0.0356
Spleen-A line
Spleen-B line
Tumor-A line
Tumor-B line
Spleen
Tumor

A

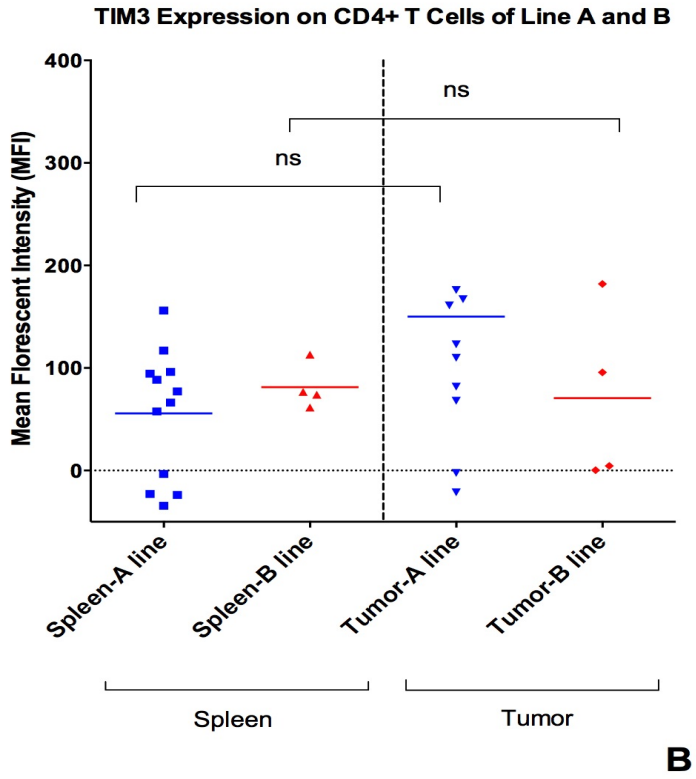
TIM3 Expression on CD4+ T Cells of Line A and B
Mean Florescent Intensity (MFI)
400
300
200
100
0
ns
ns
Spleen-A line
Spleen-B line
Tumor-A line
Tumor-B line
Spleen
Tumor

B

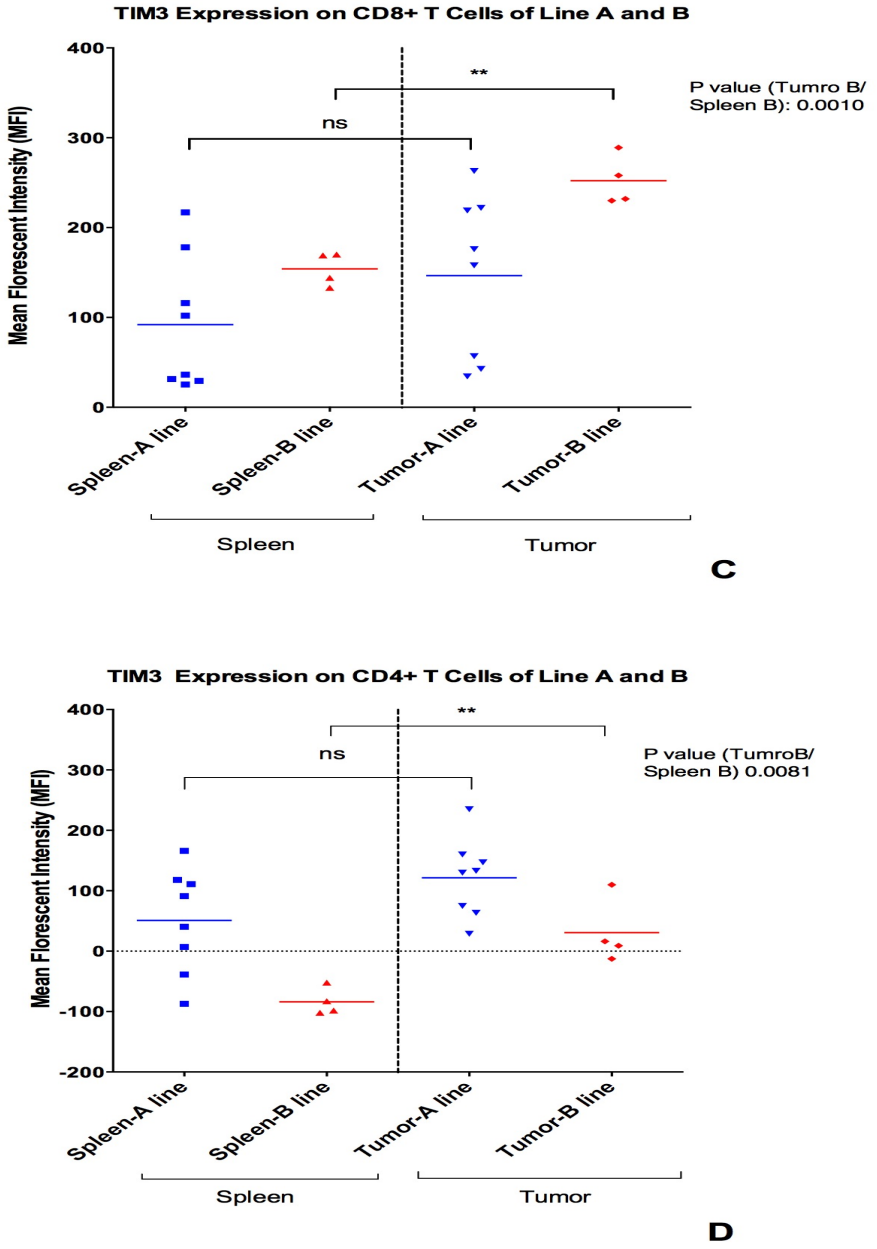

Figure 63. Comparing The TIM3 Inhibitory Receptor Expression On Lymphocytes' Population Of $CD4^+$ And $CD8^+$ T Cells Between Line A And B. A-B: are the primary tumor of both lines, C-D: are the recurred tumor of both lines. P-values were calculated by two-tailed Student's *t* test. Horizontal bars depict the mean of the quantified TIM3 expression.

Tumor-infiltrating $CD4^+$ and $CD8^+$ T cells expressed PD1 at higher level compared to the spleen. This high expression of PD1 in the tumor was observed at both primary tumor and recurred tumor in both lines except on the $CD8^+$ T cells of the line B recurred tumor (Figure 61, 64 A-D).

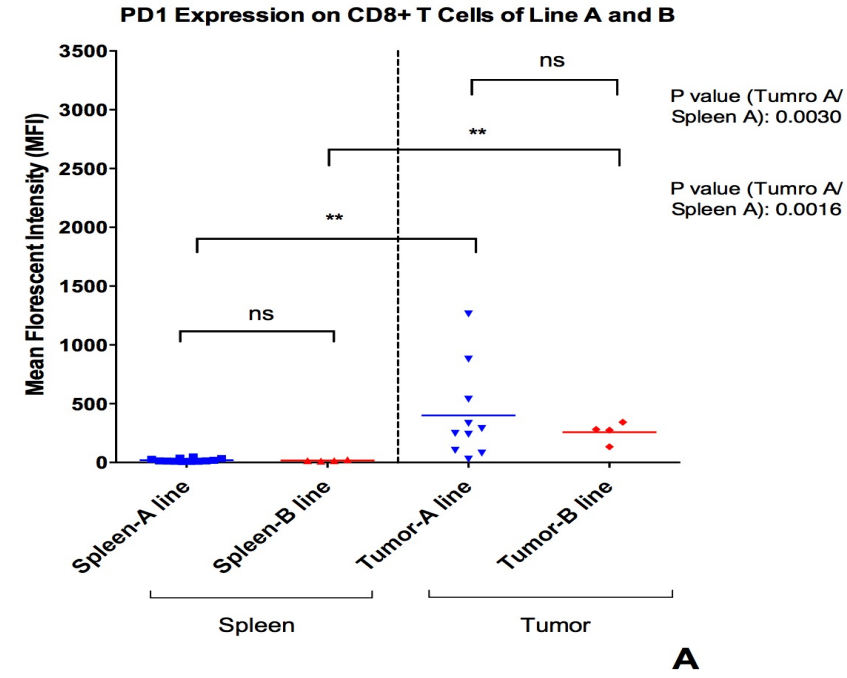
PD1 Expression on CD8+ T Cells of Line A and B
Mean Florescent Intensity (MFI)
3500
3000
2500
2000
1500
1000
500
0
ns
**
**
ns
P value (Tumro A/ Spleen A): 0.0030
P value (Tumro A/ Spleen A): 0.0016
Spleen-A line
Spleen-B line
Tumor-A line
Tumor-B line
Spleen
Tumor
A

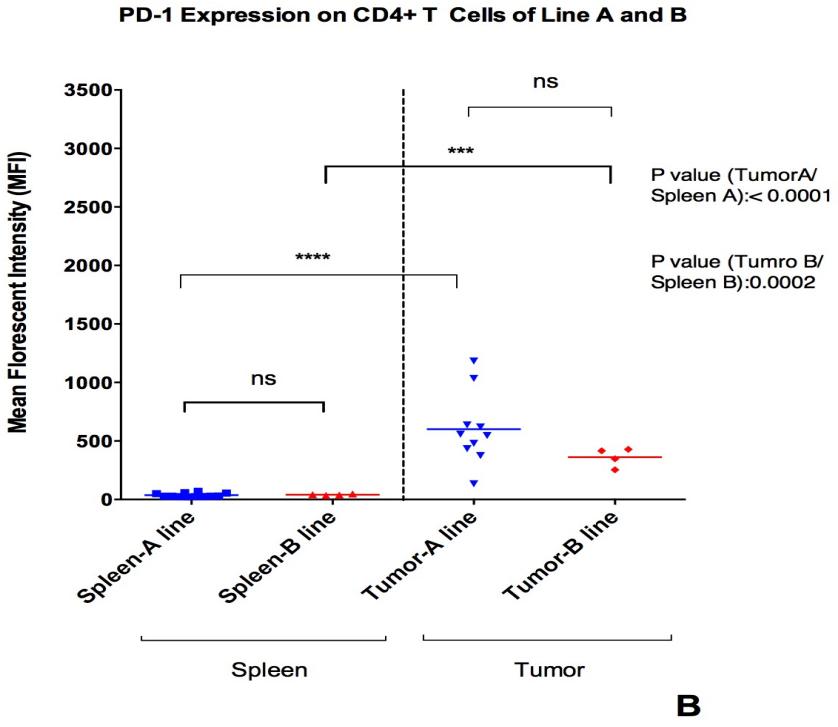
PD-1 Expression on CD4+ T Cells of Line A and B
Mean Florescent Intensity (MFI)
3500
3000
2500
2000
1500
1000
500
0
ns
***
****
ns
P value (TumorA/ Spleen A):< 0.0001
P value (Tumro B/ Spleen B):0.0002
Spleen-A line
Spleen-B line
Tumor-A line
Tumor-B line
Spleen
Tumor
B

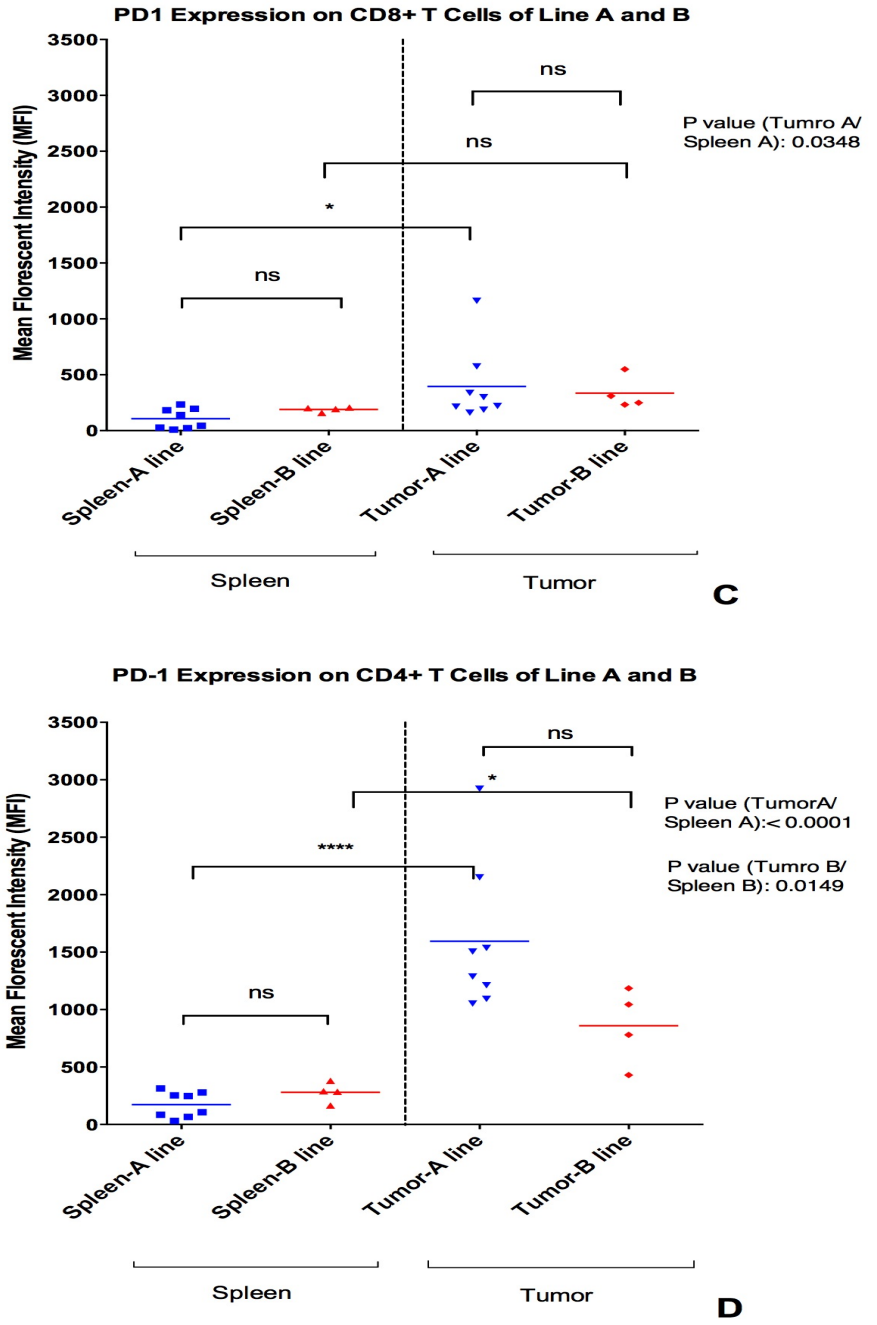

Figure 64. Comparing The PD1 Inhibitory Receptor Expression On Lymphocytes' Population Of $CD4^+$ And $CD8^+$ T Cells Between Line A And B. A-B: are the primary tumor of both lines, C-D: are the recurred tumor of both lines. P-values were calculated by two-tailed Student's *t* test. Horizontal bars depict the mean of the quantified PD1 expression.

In general, the phenotypic characterization of the tumor-infiltrating $CD4^+$ and $CD8^+$ T cells in the primary tumors of line A and B showed almost the same characterization and revealed a higher level of PD1 and TIGIT expression compared to the one on corresponding T cell populations in the spleens of tumor bearing mice. It was also likely that these infiltrating $CD4^+$ and $CD8^+$ T cells were exhausted through TIGIT and PD1 immune inhibitory response mediated pathway.

In the recurred tumors, however, both lines showed different phenotypes in terms of the expression of these immune inhibitory molecules. For instance, in Line A, the only inhibitory receptor, which expressed at a high level in infiltrating $CD8^+$ T cells was PD1. TIGIT and TIM3 were not expressed more when compared to the spleen. $CD4^+$ T cells of this line expressed both PD1 and TIGIT significantly in the tumor. In line B, in contrast, $TIM3^+$ and $TIGIT^+$ highly expressed on $CD8^+$ T cells subsets of tumor compared to $CD8^+$ T cells of spleen while PD1 expression was at the low level and hasn't shown any difference on $CD8^+$ T cell populations between spleen and tumor. All three inhibitory molecules significantly expressed in $CD4^+$ T cells within the tumor.

Chapter Five

Discussion and Conclusion

Triple Negative Breast Cancer is a subtype of breast cancer characterized by its lack of expression of any of the three receptors of progesterone, estrogen and ERBB2. This subtype of breast cancer is also clinically characterized by high metastatic rates, high aggressiveness and also a poor prognosis (Livasy et al. 2006; Sarrió et al. 2008). As the second most common subtype of breast cancer in the U.S., for which no targeted agents are yet available, finding promising therapeutics for such an invasive type of cancer is imperative.

In immunotherapy, particularly targeting immune checkpoints have appeared to effectively control tumor progression or even eradicate cancer in a wide variety of cancer patients including NSCLC, prostate and pancreatic cancers, melanoma, breast and renal cell carcinoma (Lizée et al. 2013). Thus, harnessing the immune system through inhibiting immune checkpoints has become a promising anti-cancer therapy technique with more durable and objective response, higher efficacy, low toxicity and lower risk of recurrence. With our goal of finding an affective targeted agent for TNBC treatment, we reasoned that targeting immune checkpoints, anti-PD-L1, could possibly delay tumor progression and recurrence.

To address this hypothesis, we studied the tumor response to anti-PD-L1 treatment in both the primary tumor and recurred tumor by measuring the size of the tumor before and after treatment. This study showed that anti-PD-L1 treatment on an inducible model of MYC-driven TNBC causes a delay in tumor progression as well as a delay in the initial time point of tumor recurrence in the treated cohort compared to the untreated one. However, in any tumor-bearing mouse, anti-PD-L1 treatment could cause tumor size reduction.

Tumor-bearing mice treated with anti-PD-L1 reached to the end point later compared to untreated ones. Likewise, treatment caused a longer survival for the tumor-bearing mice whose tumor recurred. This data then suggested that anti-PD-L1 treatment could yield response in MYC-driven TNBC mice through extending the Progression Free Survival (PFS) in the treated group.

FACS data analysis of PD-L1 expression on tumor cells has shown that PD-L1 was not expressed on tumor cells at any stage of growth including at the primary stage, at the recurred stage and at regression stage. The PD-L1 expression was negative for both types of the MYC-driven tumor models: line A and line B. This expression was also not regulated by MYC induction.

At the regressed stage, we could detect a population that expressed Epcam at a low to intermedium level. This population constituted ~6-8% of the total population and expressed minimal level of PD-L1. We are still not sure about the identity of this population. Presumably this population was $Epcam^{lo}$ tumor cells. Epcam is also a marker of epithelial progenitor cells and its expression down regulated upon differentiation

(Trzpis et al. 2007). Thus, this tumor model could be a perfect model to study those types of MYC-driven TNBC that has PD-L1^{-} tumor cells but PD-L1^{+} immune cells.

Focusing on PVR as another immune inhibitory checkpoint candidate to target showed that PVR is expressed on the recurred tumor epithelial cells of both line A and B. Notably, the expression of PVR is not dependent on the type of MYC-driven tumor, line A vs. line B. We didn't have the chance to study the expression of PVR on the primary tumors of these lines due to the late discovery of the PVR expression. However, the *in vitro* study has shown that PVR does express on the MYC on Epcam^{+} cells and its expression is not regulated by MYC. We still need to study the expression of PVR on the primary tumor to ensure the expression of this immune checkpoint on tumor cells *in vivo*.

Despite the lack of PD-L1 expression on MYC-driven tumor cells, we observed a delay in tumor recurrence and primary tumor progression upon anti-PD-L1 treatment, we questioned what might be the possible mechanism that inhibits the tumor growth, even for a short amount of time, and which cells might be involved in this mechanism. Considering that PD-L1 could be expressed by other cells including myeloid cells, we looked at the PD-L1 expression on three myeloid subpopulations namely, monocytes, CD11c and PMNs. We inferred that these tumor-associated myeloid cells that express PD-L1 interacted with TILs that express PD1 and exhaust the cytotoxic killer cells and inhibited an effective antitumor response.

We found that in the normal state, when no tumor is growing, all these myeloid populations did express PD-L1 in the spleen. This PD-L1 expression was required for the inhibitory effect of these subpopulations and immune tolerance. Upon primary tumor

growth, while the myeloid cells of both spleen and tumor continue their PD-L1 expression, the tumor-associated myeloid cells showed different levels of PD-L1 expression. The tumor-infiltrated myeloid cells express PD-L1 as high as their spleen myeloid cells or even slightly higher except CD11c subpopulation, which showed lower PD-L1 expression in their tumor compared to the spleens. The highest level of PD-L1 expression belonged to the tumor-associated monocytes, $LY6C^{lo}$.

The other question is how many myeloid cells can infiltrate the tumor? As to exhaust lymphocytes, myeloid cells must first infiltrate within the tumor. The immune cells, in general, constituted about 30-40 % of the whole isolated population, which proved that the immune cells can infiltrate within the tumor in this tumor model. The rest was the tumor cells (60%) and $Epcam^{lo\text{-}int}$ cells (5-8%). Among all tumor-infiltrating immune cells, the myeloid cells constituted the majority of the immune cells (60%) (Mostly PMNs and then monocytes) which was followed by lymphocytes. The detected high PD-L1 expression on triple negative versus receptor positive at TCGA database is more likely associated to these immune cells rather than the tumor cells as TCGA database looked at mRNA expression in total tumor samples which contained both tumor cells as well as immune cells

Taking all of this data into consideration, we can suggest the role of myeloid cells on immune tolerance; tumor-infiltrating myeloid populations might exhaust the tumor-antigen specific $CD8^+$ T cells and inhibited their antitumor response through PD1-PD-L1 pathway.

Based on our observation of the short delay in tumor progression upon anti-PD-L1 treatment, we assumed that anti-PD-L1 treatment targeted PD1-PD-L1 pathway mediated by tumor-infiltrated myeloid cells and impair their immune inhibitory role. We still do not know if these myeloid populations are the reasons for tumor exhaustion and their targeting is the reason for the observe delay in tumor growth. To ensure, we need to study the functionality of the lymphocytes upon treatment to see if these attenuated lymphocytes restored due to the treatment. The reason of the high expression of PD-L1 on the tumor-associated neutrophils and monocytes ($Ly6C^{hi}$) cells is the other question for which the answer needs to be illuminated.

Studying the kinetics of the immune response at tumor regression revealed some facts about the mechanism of immune response upon regression. Upon MYC withdrawal, tumor cells, which require MYC for their growth and proliferation, underwent apoptosis. The tumor cell death would result in an increase in recruiting macrophages, which are responsible for ingesting and removing the dead cells.

As a result of tumor death, a tremendous amount of tumor antigens were released in the tumor microenvironment that primed $CD4^+$ and $CD8^+$ T cells. This increase in the number of immune cells (lymphocytes and macrophages) at the tumor microenvironment upon MYC withdrawal stimulated $CD4^+$ T cells, particularly Tregs, to migrate to the tumor site. The observed increase in the $CD4^+$ TILs might be associated to the Treg's function. In contrast to $CD4^+$ T cells, the number of tumor-infiltrating $CD8^+$ T cells varied from sample to sample at the cohort, which was four days off Dox. Thus, due to

the high variation in data and limited number of studied samples, the determined number of tumor- infiltrated $CD8^+$ T cells was not conclusive.

Upon tumor regression, the expression of immune inhibitory receptor PD1 as well as its ligand, PD-L1, specifically changed; the expression of PD-L1 on all four myeloid subpopulations, particularly macrophages, was elevated. The expression of PD1 on $CD8^+$ T cells was also increased. Many hypotheses may be suggested for this observed increase in PD1 expression on $CD8^+$ TILs. For instance, this increase could be due to the up-regulation of PD1 as a response to the increase in the released tumor antigen by dead tumor cells. This increase in PD1 expression could also be due to the exhaustion of $CD8^+$ $PD1^+$ subsets that highly express PD1and upon regression this subset revived and became active. Alternatively, it was suggested that the recruitment of PD1 high $CD8^+$ T subset to the tumor site after regression resulted in an observed increase in $PD1^+$ expression. Another suggestion is that this elevated PD1 expression on $CD8^+$ TILs was due to the lack of some factors that down regulate the expression of PD1 on $CD8^+$ T cell subsets.

The increase in the PD1 expression accompanied with increase in the PD-L1 expression on myeloid cells. This increase in the myeloid cell PD-L1 expression could be either due to the presence of PD1 high $CD8^+$ T cells in the tumor microenvironment that induce PD-L1 expression on myeloid cells through secretion of cytokines or could be due to up regulation of PD-L1 due to lack of inhibitory factors. Other reasons can also be suggested for this observation. For instance, the migration of myeloid cells that express higher amount of PD-L1 or the lack of factors in the microenvironment that inhibit the expression of PD-L1 on the myeloid cells in the MYC-driven tumor.

Kuang et al. (2009) found that TNF-α and IL-10 secreted by activated monocytes at peritumoral stroma can stimulate PD-L1 expression in tumor associated macrophages in an autocrine manner which suppresses the immune response through reduction of T cell activity (Kuang et al. 2009).

Whatever the reason of the increase in the expression of PD1 or PD-L1 may be, upon regression, this increase in the expression of immune-inhibitory checkpoint of PD1 could result in the further exhaustion of $CD8^+$ T cells, which results in having an ineffective antitumor immune response. Anti-PD-L1 treatment, restores the exhausted tumor-specific T cells through blocking the possible interaction between $CD8^+$ T cells and macrophages in the tumor microenvironment, that results in having more effective antitumor immune response which in turn results in delay in tumor recurrence. To further validate this hypothesis, we need to study the functionality of $CD8^+$ T cells upon regression during treatment to ensure that these cells become activated and effectively attack the tumor. These results also suggest continuing treatment after tumor regression.

We also learned that growing tumor change the immune profile of a distant secondary lymphoid organ, the spleen. Studying the distribution of different types of immune cells in the spleen at different stages of the tumor growth, namely primary tumor, regressed and recurred tumor, and comparing it to the immune profile of the non-tumor spleen showed how the tumor can change the immune profile of the spleen remotely. The presence of tumor causes an overall increase in the number of different types of immune cells, lymphocytes and myeloid cells. This increase was not proportional though. While all immune cell populations increased in the spleen upon

tumor growth, the ratio of their increase was not equal. The population of some cell types including monocytes and neutrophils increased much higher compared to others. This increase in the average number of immune cells was higher in line A compared to line B, which resulted in spleen enlargement, particularly at the recurred stage.

It is generally believed that PD-L1^{+} tumors are more likely to respond to anti-PD-L1 treatment (Topalian et al. 2012). However, in the realm of personalized immunotherapy, according to the most recent data from anti-PD-L1 based therapy, the expression of PD-L1 on tumor-infiltrating immune cells and high TILs density is also associated with better response (Herbst et al. 2014; Gros et al. 2014).

In addition, some recent studies highlighted the fact that when we are seeking for the best immune checkpoint candidate to be targeted in cancer immunotherapy, several factors besides the expression of immune checkpoints on the tumor cells might be considered. The TILs' density and expression of the immune checkpoint of interest on the TILs are two of the most important ones. Recent studies show the effect of suppressive subtype of macrophages, that are positive for PD-L1, so called tumor associated macrophages (TAMs) on tumor progression and tumor resistance to anti-PD-L1 (Ding et al. 2014).

The clinical trial of anti-PD-L1 treatment on TNBC has shown that patients with PD-L1^{-} tumor cells but PD-L1^{+} immune cells would also benefit from therapeutics. According to the most recent study presented at the 2015 San Antonio Breast Cancer Symposium, Avelumab, other PD-L1 inhibitor, tested on metastatic TNBC patients has shown promising objective response rates (ORR) (Balko et al. 2015). According to this

study, 5 patients out of 57 respond partially to the treatment (8.8%). They also found that among TNBC patients, exclusively, the PD-L1 expression by tumor-infiltrated immune cells associated with response to this drug. 44.4% (4 out of 9) of TNBC patients with PD-$L1^+$ tumor-infiltrated immune cells partially respond to the treatment in comparison to 2.6% (1 out of 39) PD-$L1^-$ tumor-associated immune cells. This difference in the response is also significant (44.4% vs. 2.4%; P = 0.001). Together, these studies suggest that Avelumab showed an effective clinical activity in TNBC patients and its response is associated with the PD-L1 expression on tumor-infiltrating immune cells.

These data were consistent with our finding in regards to the role of PD-$L1^+$ immune infiltrating myeloid cells in tumor progression and recurrence. The population, if being targeted through treatment with anti-PD-L1, could result in a delay of tumor progression and recurrence to some extent. Despite the delay in tumor progression and recurrence upon anti-PD-L1 treatment, this treatment failed to cause a long delay or even reduction in tumor growth. Thus, applying a secondary treatment as a combinational therapy is suggested. Furthermore, considering the high density TILs in this tumor model, finding a secondary immune checkpoint that is preferably expressed on tumor cells to co-block with anti-PD-L1 would elicit a more effective cancer treatment strategy (Figure 65).

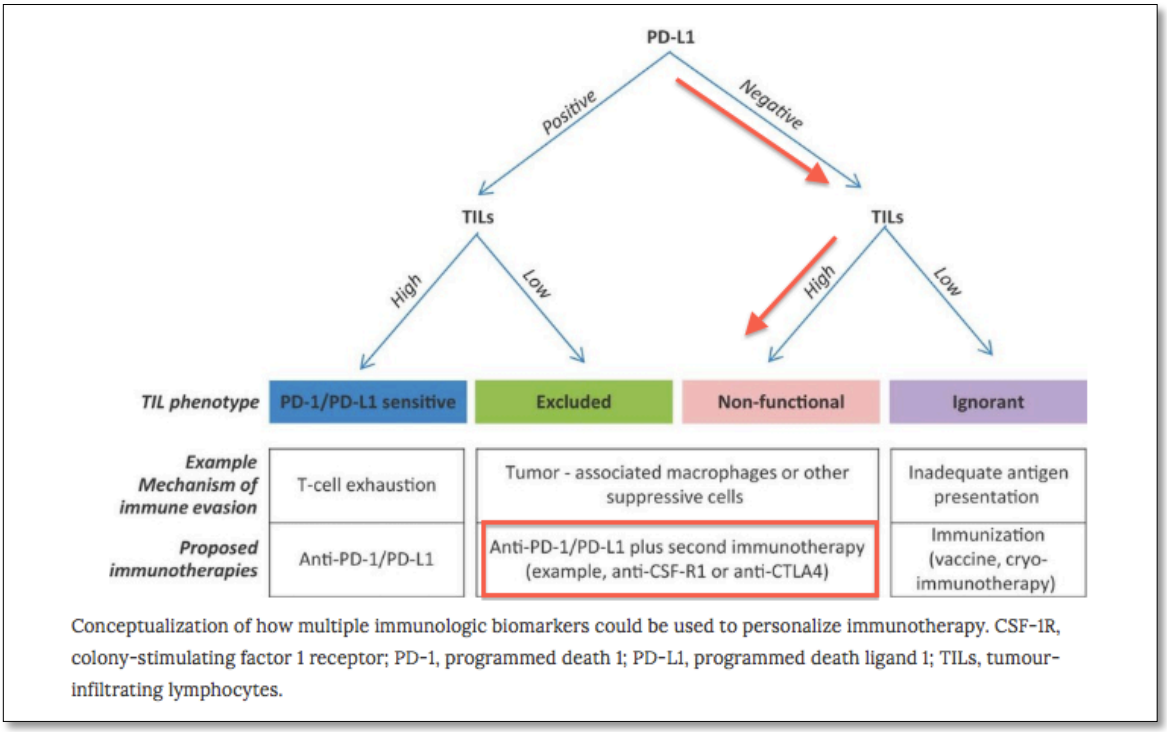

Figure 65. Schematic Of Different Cancer Immunotherapy Approaches According To The Tumor Characteristics. These characteristics are employed as a biomarker for personalized immunotherapy. CSF-1R, Colony-Stimulating Factor 1 Receptor.

Examining PVR expression on immune cells as well as tumor cells at the recurred stage showed that all four myeloid subpopulations as well as Epcam positive and negative cells did express PVR significantly. We also found that PVR expression was much higher on tumor-associated myeloid cells than spleen myeloid cells. This observation was consistent between two MYC-driven TNBC tumor models of line A and B. In addition our studies demonstrated that, TIGIT, the PVR's immune inhibitory receptor, was significantly expressed in $CD4^+$ and $CD8^+$ TILs of both line A and B. Considering that PVR was significantly expressed by tumor cells as well as immune

cells, it is likely that these TILs were exhausted through TIGIT mediated pathways as well. Thus, it is suggested that targeting TIGIT in combination with PD-L1 could significantly break down the inhibitory interaction and stop tumor progression and restore antitumor immune response of lymphocytes.

The dual expression of TIGIT and PD1 on $CD8^+$ TIL and tumor-antigen specific CD8s have been studied recently in various types of cancer (Johnston et al. 2014). These studies have shown that TIGIT was significantly expressed on TILs and it was often co-expressed with PD-1 inhibitory receptors in colorectal cancer. They also found that TIGIT regulates the function of tumor-infiltrating $CD8^+$ T Cells. Despite the overexpression of TIGIT in tumor-infiltrating $CD8^+$ T cells, blockage of TIGIT or PD-1 alone had little effect on inhibiting tumor progression and increased the median survival of tumor-bearing mice for only 3 days. Whereas, the dual blockade of TIGIT and PD1 led to a complete response in the majority of tumor-bearing mice through complete shrinkage of the tumor during and even after the treatment (Johnston et al. 2014).Yet the underlying molecular mechanism behind this synergistic inhibitory effect of PD-L1 and TIGIT remains unclear (Figure 66).

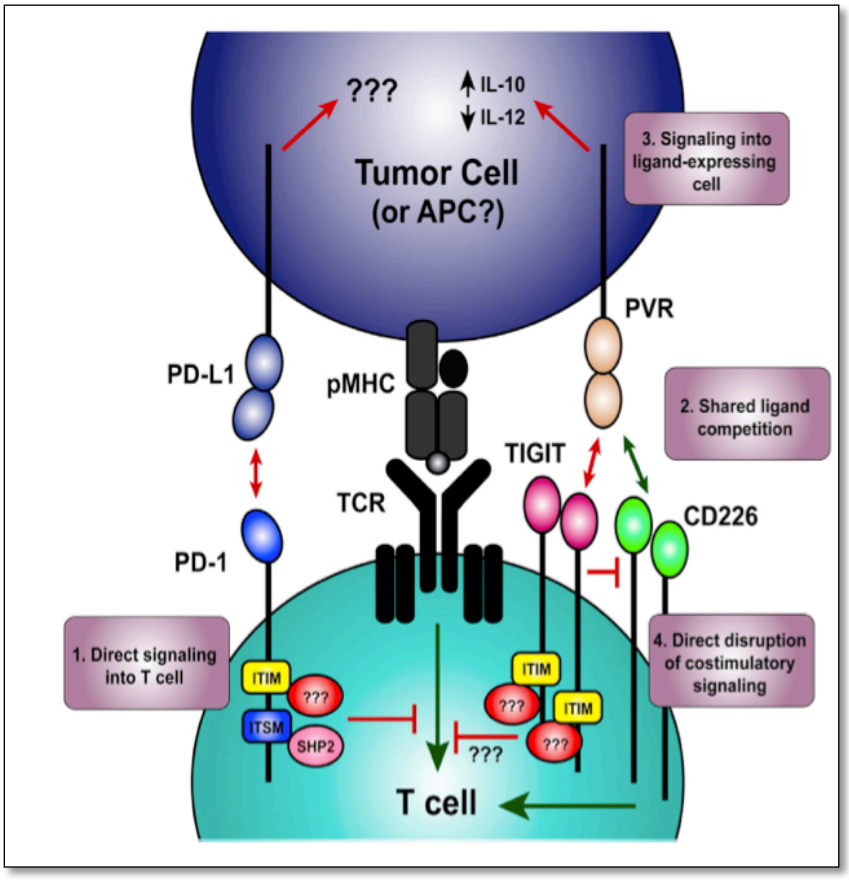

Figure 66. The Suggested Molecular Mechanism Underlying The TIGIT-Mediated TIL Inhibition (Pauken and Wherry, 2014).

In addition, the dual expression of TIGIT and PD1 on tumor-antigen specific $CD8^+$ T cells was found in melanoma (Chauvin et al. 2015). Chauvin et al. (2014) demonstrated that dual blockade, but not single treatment, could exponentially increase the function of both $CD8^+$ TILs and tumor–antigen specific $CD8^+$ T cells.

One of the important immune cell populations in our tumor model, which is speculated to play a role in the tumor progression, is monocytes and macrophages. Blood circulatory monocytes could be recruited to the tumor microenvironment through the

action of a wide variety of signals. Possible signals include cytokines such as Colony-Stimulating Factor-1 (CSF-1), Endothelial Monocyte-Activating Polypeptide II (EMAPII), chemokine's (CCL2, CCL3, CCL4, CCL5, CCL22 and some CXC chemokines, in particular CXCL8), growth factors and lymphokines, a subset of cytokines that produce by lymphocytes and attract other immune cells (Cruse and Lewis 2002). Hypoxia death cells and pathogens are also attract monocytes (Wu et al. 2008; Yoshimura et al. 2013; Milliken et al. 2002; Lin et al. 2001; Zhang, Lu, and Pienta 2010; Roca et al. 2009).

Upon migration of monocytes from blood to the tumor microenvironment, the monocytes differentiate into the mature macrophages, so called tumor-associated macrophages (TAM). These TAMs then polarize into two general different subsets, the classical M1 and the alternative M2 macrophages (2,3,4). These two subsets have different functional phenotype and are driven by different tumor signals; the M1 is driven by the Th1 cytokine interferon-γ, lipopolysaccharide (LPS), and Toll-like receptor (TLR) agonists while the transformation of macrophages to M2 is driven by Th2 cytokines such as IL-4 and IL-13, TLRs and IL-10 (Chanmee et al. 2014).

These two subsets also have different functions as well in the context of tumor immune response. For instance, M1 produces pro-inflammatory factors such as IL-6, IL-12, IL-23, tumor necrosis factor-α (TNF-α) and MHC class I and class II molecules through which they contribute to the inflammatory response and antitumor immunity. M2, on the other hand, exert anti-inflammatory and pro-tumorigenic activities through releasing the immunosuppressive factors (IL-10 and transforming growth factor-beta

(TGF-β) (Sica and Mantovani 2012; Hao et al. 2012; Hiratsuka et al. 2008), angiogenesis factor VEGF and matrix metalloprotease (MMP) protease family proteins (Krecicki et al. 2001). These two TAM phenotypes also have a different effect on angiogenesis. For instance, M1 inhibits angiogenesis and exerts tumor immunity while M2 promotes tumor angiogenesis. In the early stages of tumor growth or in the regression stages, M1 is more dominant in the tumor microenvironment and angiogenesis is inhibited. As the tumor progresses, M1 shift to M2 phenotype, which accelerate tumor angiogenesis and progression (Zaynagetdinov et al. 2011; Gordon and Mantovani 2011).

The polarization of M1 to M2 is regulated by the mixture of signals within the tumor microenvironment, tumor progression stage and hypoxia (Mantovani et al. 2008; Movahedi et al. 2010; Gordon and Taylor 2005; Mantovani et al. 2002; A Sica and Bronte 2007).

Recent studies have shown that solid tumors contain hypoxic areas (Murdoch, Giannoudis, and Lewis 2004). Consistent with these data, we also observed a central necrotic areas in MMTV/MYC tumor models that contain hypoxic areas (C. E. Lewis and Hughes 2007).

Upon migration of macrophages to hypoxic area, the macrophages polarize into the M2. Hypoxia-inducible factor (HIF)-1α is one of the key transcription factors that change the gene expression profile of the macrophages and mediates their transformation to M2 (Burke et al. 2002; Talks et al. 2000) (Figure 67). After migration of M2 to the hypoxic area, their ability to mobilize inhibited and they start accumulating in that area (Grimshaw and Balkwill 2001; Murdoch, Giannoudis, and Lewis 2004).

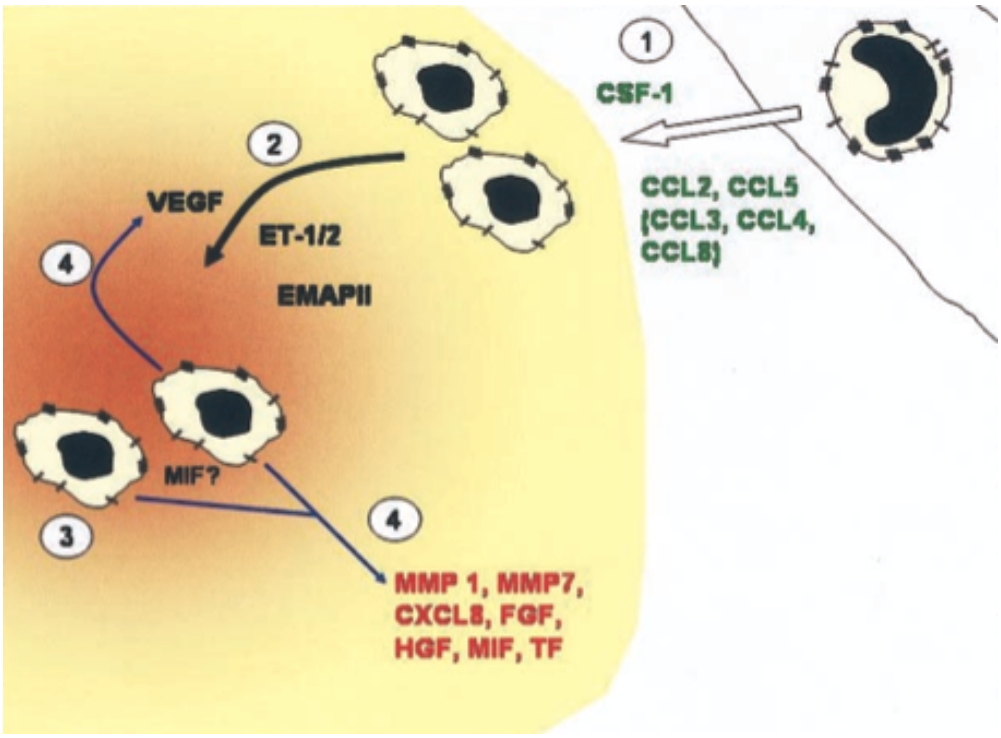

Figure 67. The Model For Monocyte Recruitment To The Solid Tumor Hypoxic Areas. 1) The tumor secreted chemokine attracts monocytes to the tumor microenvironment 2) monocytes differentiate into TAMs and migrate to the hypoxic area upon VEGF-A, endothelin-2 and EMAPII stimulatory signals 3) TAMs are retained in the hypoxic area 4) TAMs produce VEGF and recruit more TAMs which promote angiogenesis and tumor growth (Murdoch, Giannoudis, and Lewis 2004).

A large body of evidence indicates the correlation between the TAM recruitment and polarization with poor cancer prognosis, immune resistance and cancer progression (Fischer et al. 2007; Zhang et al. 2010). Tsutsui et al. (2005), and Zijlmans et al. (2006), have demonstrated that the TAM density is strongly associated with poor prognosis and worst overall survival rate (Zijlmans et al. 2006; Tsutsui et al. 2005). The polarization of macrophages into M2 results in accumulation and interaction of M2 with tumor microenvironment cells which leads to tumor progression and anti-immune responses.

Thus, targeting TAMs appeared to be a potential target in cancer immunotherapy (Fischer et al. 2007; Zhang et al. 2010).

Some of the suggested approaches for TAM-targeting cancer therapy are inhibition of macrophage recruitment through targeting macrophages chemoattractant or VEGFR2 (Gazzaniga et al. 2007) reverting pro-tumorigenic M2 to the antitumor M1 through activation of TLR3/Toll-IL-1 receptor domain-containing adaptor molecule 1 (Shime et al. 2012) and suppression of TAM survival through TAM-specific proteins such as peptide M2pep that selectively kills M2 macrophages (Germano et al. 2013; Cieslewicz et al. 2013).

By studying the growth curve of line A and B tumors, we found that tumors demonstrated a significant difference in terms of tumor growth rate at early stages and their latency duration. Considering that both tumor models are driven by MYC overexpression, the observed differences in growth rate is most likely related to the differences in the secondary mutation(s) that each of these lines are carrying. It also can be due to the different antitumor immune responses, which may somehow be mediated by secondary mutation(s).

In the context of secondary mutations, several hypotheses underlying these observed differences in the tumor growth and recurrence could be made. First, the secondary mutation as the secondary driver genes could possibly cause differences in the growth rate and the latency time before tumor recurrence. Second, this secondary mutation might indirectly change the antitumor immune response resulting in a difference in the ability of the immune system to fight against the tumor leading to changes in the

tumor growth rate. These imposed changes can be mediated through various ways. For instance, secondary mutation could change the tumor antigen, which may result in activating two different tumor-antigen specific $CD8^+$ T cells that respond to the tumor differently. The secondary mutation also could change the immune phenotype of the tumor through producing different signals that lead to recruiting different immune cells or change the TAMs. Third, the secondary mutation could change the tumor growth rate and duration of latency through the combination of both suggested approaches.

To address the question of whether or not a secondary mutation can alter the antitumor immune response, we embarked on a comprehensive characterization of the tumor immune profile on these two different tumor lines. Our study has shown that these two tumor models were different in terms of both the percentage of immune profile of tumor and the number of tumor-infiltrated cells. More immune cells infiltrated in the line A compared to line B and this difference was regardless of the stage of the tumor growth, primary tumor or recurred tumor. However, the number of tumor-infiltrating immune cells was much higher at the recurred stage in both lines. This difference could be associated to differences in signals in the tumor microenvironment such as chemokines that recruit different types of immune cells or to differences in the ability to infiltrate within the tumor (Gajewski et al. 2013).

In general the average number of all tumor-infiltrating immune subsets was higher in line A compared to line B regardless of the stage of the tumor growth. $CD8^+$ T cells were the only population whose average number was lower in line A than line B at the primary stage.

We also found that despite this higher infiltration rate of all immune cells in line A compared to line B, this increase was not proportional. This means that line A was more favorable to $CD4^+$ T cells and PMN and recruited them more compared to other cells. In other words, the rate of the neutrophil and $CD4^+$ T cell infiltration were significantly higher in line A compared to other immune cells at the primary stage. In contrast to neutrophil populations, line A at the primary stage was less favorable for recruiting $CD8^+$ T cells. At the recurred stage, similar to the primary stage, $CD4^+$ T cells recruited at the highest level into the tumor of both lines. But while neutrophils were still recruited more in the recurred line A compared to recurred line B, this population did not one of the dominant populations in the tumor. There were more of monocytes and $CD8^+$ T cells in the tumor compared to neutrophils if this difference was due to the difference in the infiltration rate or due to the differentiation of other infiltrated cells, is needed to be cleared though.

In the line B, tumor demonstrated a specific preference for recruiting $CD4^+$ T cells. In the primary line B, $CD4^+$ T cells have the highest infiltration rate over other immune cells. Other immune cells infiltrated at almost the same level. In contrast, at the recurred stage, besides $CD4^+$ T cells, monocytes recruited into the tumor at the same level.

Studies have shown unique metabolic properties for Tregs. Tregs exhibit high levels of fatty acid oxidation and PPAR-γ expression, a transcription factor, which is activated by environmental fatty acids, and regulates cellular functions including differentiation and metabolism (Berger et al. 2002; Feige et al. 2006). Studies has shown

that increased expression of PPAR- γ promotes fatty acid metabolism in Tregs and stimulates the differentiation of Treg-residing adipose tissue to their suppressive phenotype as well as causing their accumulation. Tregs can be accumulated in adipose tissue through tumor environment factors such as IL-2 and TCR. These factors increase their mTORC1-dependent lipid biosynthesis, which promotes Treg proliferation (Zeng et al. 2014). Considering high dependence of Tregs on fatty acids, the observed abundance of $CD4^+$ T cells in both tumor models particularly in line A can be justified.

While tumor provides a metabolically favorable place for Tregs, it dampens tumor-infiltrating $CD8^+$ T cells function through outcompeting them for essential metabolic nutrient of glucose (Gatenby and Gillies, 2004; Warburg, 1956). This metabolic imbalance has been suggested to be restored through PD-L1 checkpoint blockade therapy (Chang et al.2015).

Besides $CD4^+$ T cells, the presence of neutrophils was observed in a wide variety of human cancers (Eck et al. 2003; Bellocq et al. 1998; Wislez et al. 2003). Neutrophils are recruited to the tumor microenvironment through receiving chemotactic substances including CXC chemokines (e.g., interleukin-8 (IL-8)) (Sparmann and Bar-Sagi 2004).

Traditionally neutrophils are responsible for invading and eliminating pathogens but in the context of cancer, similar to macrophages, neutrophils can be polarized into two different functional phenotypes; protumor neutrophils and antitumor ones (Gregory and Houghton 2011). Each plays a different role in tumor microenvironment.

Little data supports the antitumor effect of neutrophils: Fridlender et al, 2009, describe an antitumor neutrophil population that was recruited to the tumor upon TGF-β

inhibition. This neutrophil population polarized into the tumor cytotoxic phenotype through secreting proinflammatory cytokines (Fridlender et al. 2009; Gregory and Houghton 2011). Conversely, a large body of recent studies indicate a pro-tumor effect for neutrophils; neutrophils can promote tumor progression, metastasis, angiogenesis and surveillance through production of cytokines, chemokines, radioactive oxygen species (ROS) and proteinases into the tumor environment (Nathan 2006; Smith 1994; Pham 2006) (Figure 68).

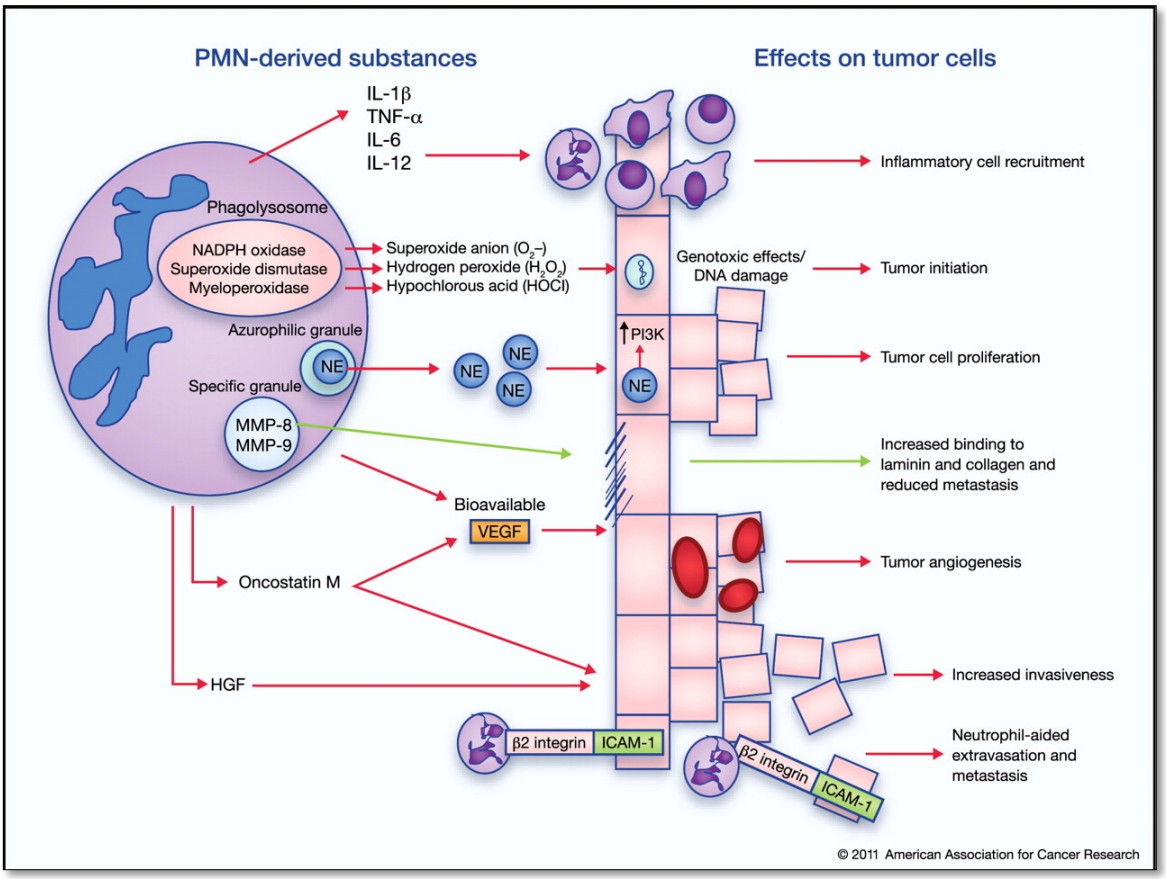

Figure 68. The Mechanism Of Neutrophil-Mediated Tumor Progression And Metastasis. Neutrophils release many substances into the tumor microenvironment that promote tumor progression, metastasis and angiogenesis (red arrows).

Secondary mutation also can change the antitumor immune response through changing the phenotype of TAMS. Considering the fact that TAMs can have two different roles in tumor, antitumor or tumorigenic, further macrophage characterization in terms of their cytokines expression and functional phenotype is required to ensure if these secondary mutations can change the TAM-mediated antitumor-immune response (Lewis and Pollard 2006). Infiltrating neutrophils and tumor microenvironment stimuli are two factors that can change the functional phenotype of TAMs.

Secondary mutations also can affect the activated antigen-specific $CD8^+$ T cell subsets by producing different tumor antigens. We still don't know if this observed difference in tumor growth was due to the differences in activation or function of tumor-antigen specific $CD8^+$ T cells subset. Tumors also can change the functional phenotype of TILs through their physical interaction with the activated $CD8^+$ T cells and the signals in the tumor microenvironment.

Further studies in terms of $CD8^+$ T cell subsets and functional phenotype of TAMs is required to ensure that the observed difference between these two lines in terms of tumor growth rates was associated with the effect of secondary mutation in antitumor immune response.

To study the effect of secondary mutation on tumor growth rate or immune response, it is suggested to transplant these two tumor lines in two immunodeficient mice and monitor their tumor growth curve and recurrence. If the tumors demonstrated the same differences in their rate of growth, then we can conclude that their secondary mutation might not indirectly affect the immune system and the observed difference was

probably due to the secondary mutation driver and its ability to promote tumor growth. But if these two tumor models grew at the same rate in the immunodeficient mice, then we can conclude that the immune system in the immunocompetent mice was affecting the growth rate of them, which can be controlled indirectly by secondary mutations. If secondary mutation can affect both the tumor growth rate and the antitumor response, then slight changes in the tumor growth curve was expected to be observed between immunodeficient mice transplanted with these two lines. Another approach to study the effect of secondary mutation on the tumor growth rate is to target the intracellular pathway activated by these secondary mutations. That way the effect of these mutations on the tumor growth can be studied.

In the era of personalized medicine, we are interested in knowing how slight differences between people can change their ability to respond to drugs. It has already been shown that the type of mutation can determine the patient's response to the drug. For instance, in patients with melanoma bearing different mutations, different immunotherapeutic approaches will be employed. Akbay et al. (2013) showed that EGFR- driven lung tumor bearing different number of mutations in the EGFR gene respond differently to anti-PD1 therapy. Tumors bearing single deletion mutation in exon 19 demonstrate a better response to anti-PD1 therapy compared to other EGFR-driven tumors that bear a secondary mutation in T790M or L858R in combination with exon 19 (Akbay et al. 2013).

Considering that these two tumor models bear two different secondary mutations, we are interested to know how this mutation could change the ability of immune system

to respond to the applied immune checkpoint blockade approach. The answer to this question will enable us to better find the right therapeutic approach for different patients.

Any changes observed in the immune inhibitory receptor expression on TILs could be associated with the tumor's secondary mutations. These mutations can indirectly control the expression of immune inhibitory receptors either through producing different tumor antigens, which activates different $CD8^+$ T cell subsets that express different inhibitory receptors, or through providing different tumor micro-environmental signals, which can change TILs' receptor expression.

To investigate the difference between these lines in terms of immune inhibitory receptor expression, the expression level of the three-candidate immune inhibitory receptors on TILs were studies and compared between these lines. Our studies have shown that these two lines did not exhibit a different pattern in terms of the level of immune inhibitory receptors expression (PD1, TIGIT and TIM3) on their TILs at the primary stage. TIGIT and PD1 expressed at higher level on TILs of both lines compared to spleens. In both lines TIM3 expressed at lower level, if there is any, on TILs compared to PD1 and TIGIT. We, however, observed some differences between these lines at the recurred stage. For example, line B expressed more TIGIT than line A. Due to a technical error we failed to compare these lines in term of TIM3 expression.

Considering the fact that TILs consist of both the tumor-antigen specific $CD8^+$ T cells as well as non-specific $CD8^+$ T cells and we haven't characterized the tumor specific T cells yet, we cannot compare this population in terms of immune inhibitory receptor expression. We need to characterize these tumor-antigen specific $CD8^+$ T

subsets and then compare their immune inhibitory receptor expression to ensure if two different subsets was activated in these two tumor models and if these two tumor models can respond differently to the immune inhibitory chokepoint blockade approach. Alternatively, we can treat the B line with anti-PD-L1 to see if this tumor model can respond to the treatment as well as line A.

5.1 Conclusion

We highlighted the importance of myeloid cell PD-L1 expression in the effectiveness of anti-PD-L1 immune checkpoint therapy. We found that targeting PD1/PD-L1 pathway expressed by myeloid cells, could delay tumor progression and recurrence. Furthermore, we found that this tumor model has a high density of TILs and expresses PVR, another immune inhibitory ligand, on the epithelial tumor cells as well as on myeloid population. We also found that the corresponding immune inhibitory receptors of these ligands, namely PD1 and TIGIT, were expressed on the line A TILs at early stage of tumor growth. Due to the limited effect of anti-PD-L1 treatment on controlling tumor progression and tumor-bearing mouse survival, we postulate that the combination therapy of TNBC using anti PD-L1 and PVR may have a more effective antitumor immune response.

We also demonstrated that two MYC-driven TNBC mouse tumors with different secondary mutations could be different in terms of growth rate, latency duration and recruiting immune cells. We found that line A growth rate was higher and recurred earlier

than line B. We investigated that the average number of tumor-infiltrating immune cells particularly $CD4^+$ T cells and neutrophils were higher in line A compared to line B, which might be associated with the observed difference in the tumor growth rate, latency duration and their secondary mutation(s) and may lead to aggressiveness of this line compared to line B. We also found that the number of tumor-infiltrating immune cells was significantly elevated at the recurred stage in both lines compared to the one in the primary tumors.

5.2 Future Directions

Although we observed some respond in tumor progression and recurrence of MMTV/MYC tumor model upon ani-PD-L1 treatment, the delay in tumor growth was somewhat limited and minimal. Thus, in the next step we are going to optimize the therapies through testing the effect of PD-L1 and TIGIT coblockade on the efficacy of the antitumor-immune response. This enables us to optimize the therapies for improved patients' reposes. In light of the fact that this tumor model is driven by MYC, combining the anti-PD-L1 with MYC-pathway targeted therapies such as PIM inhibitors is another interesting approach for increasing the efficacy of the treatment. Alternatively, we could also target KRAS or PI3K pathways to study their effect on the tumor progression.

We also plan to determine the effects of anti-PD-L1 on the functionality of TILs and ensure that these exhausted TILs get restored upon anti-PD-L1 treatment.

In addition, we will continue treatment after tumor regression to test if sustaining treatment can decrease the chance of recurrence. Moreover, we are interested in addressing our former question in regards to the effect of secondary mutations on the effectiveness of ani-PD-L1 treatment on line B tumor progression. This study can further reveal the effect of the type of mutation on personalized medicine and be used as a biomarker to evaluate the efficacy of treatment.

Further analysis is also required to ensure whether this difference in the neutrophil population is not due to the effect of secondary mutations or another unknown factor.

References

Akbay, E.A., Koyama, S., Carretero, J., Altabef, A., Tchaicha, J.H., Christensen, C.L., …, Wilkerson, M.D., 2013. Activation of the PD-1 pathway contributes to immune escape in EGFR-driven lung tumors. *Cancer discovery*, *3*(12), pp.1355-1363.

Alberts, B., Bray, D., Lewis, J., Raff, M., Roberts, K., Watson, J.D. and Grimstone, A.V., 1995. Molecular Biology of the Cell (3rd edn). *Trends in Biochemical Sciences*, *20*(5), pp.210-210.

Rick, A, Cammie, B., Burke. A., Gansler, T., Gapstur, S., Gaudet, M.,…, Simpson, S., 2014. "Breast Cancer Facts & Figures 2013-2014." *American Cancer Society*: 38. http://www.cancer.org/acs/groups/content/@research/documents/document/acspc-040951.pdf.

Amati, B., Brooks, M.W., Levy, N., Littlewood, T.D., Evan, G.I. and Land, H., 1993. Oncogenic activity of the c-Myc protein requires dimerization with Max. *Cell*, *72*(2), pp.233-245.

Amati, B., Littlewood, T.D., Evan, G.I. and Land, H., 1993. The c-Myc protein induces cell cycle progression and apoptosis through dimerization with Max. *The EMBO Journal*, *12*(13), p.5083.

Balko, J.M., Denkert, C., Salgado, R., O'Hely, M., Savas, P., Beavis, P.A., …, Estrada, M.V., 2015. Abstract S1-08: Reduced tumor lymphocytic infiltration in the residual disease (RD) of post-neoadjuvant chemotherapy (NAC) triple-negative

breast cancers (TNBC) is associated with Ras/MAPK activation and poorer survival. *Cancer Research*, *75*(9 Supplement), pp.S1-08.

Barza, M. and Schiefe, R.T., 1977. Antimicrobial spectrum, pharmacology and therapeutic use of antibiotics. Part 1: tetracyclines. *American Journal of Health-System Pharmacy*, *34*(1), pp.49-57.

Bauer, K.R., Brown, M., Cress, R.D., Parise, C.A. and Caggiano, V., 2007. Descriptive analysis of estrogen receptor (ER)-negative, progesterone receptor (PR)-negative, and HER2-negative invasive breast cancer, the so-called triple-negative phenotype. *Cancer*, *109*(9), pp.1721-1728.

Bellocq, A., Antoine, M., Flahault, A., Philippe, C., Crestani, B., Bernaudin, J.F., …, Cadranel, J., 1998. Neutrophil alveolitis in bronchioloalveolar carcinoma: induction by tumor-derived interleukin-8 and relation to clinical outcome. *The American journal of pathology*, *152*(1), p.83.

Bernard, A., Boumsell, L., Dausset, J., Milstein, C. and Schlossman, S.F. eds., 2013. *Leucocyte Typing: Human Leucocyte Differentiation Antigens Detected by Monoclonal Antibodies. Specification-Classification-Nomenclature/Typage leucocytaire Antigenes de differenciation leucocytaire humains reveles par lesanticorps monoclonaux: Rapports des etudes com*. Springer Science & Business Media.

Bernard, A., Boumsell, L. and Hill, C., 1984. Joint report of the first international workshop on human leucocyte differentiation antigens by the investigators of the

participating laboratories. In *Leucocyte typing* (pp. 9-142). Springer Berlin Heidelberg.

Bhowmick, N.A., Neilson, E.G. and Moses, H.L., 2004. Stromal fibroblasts in cancer initiation and progression. *Nature*, *432*(7015), pp.332-337.

Bos, J.L., 1989. Ras oncogenes in human cancer: a review. *Cancer research*, *49*(17), pp.4682-4689.

Brahmer, J.R., Tykodi, S.S., Chow, L.Q., Hwu, W.J., Topalian, S.L., Hwu, …, Pitot, H.C., 2012. Safety and activity of anti–PD-L1 antibody in patients with advanced cancer. *New England Journal of Medicine*, *366*(26), pp.2455-2465.

Burke, B., Tang, N., Corke, K.P., Tazzyman, D., Ameri, K., Wells, M. and Lewis, C.E., 2002. Expression of HIF-1α by human macrophages: Implications for the use of macrophages in hypoxia-regulated cancer gene therapy. *The Journal of pathology*, *196*(2), pp.204-212.

Callahan, M.K., Wolchok, J.D. and Allison, J.P., 2010, October. Anti–CTLA-4 antibody therapy: immune monitoring during clinical development of a novel immunotherapy. In *Seminars in oncology* (Vol. 37, No. 5, pp. 473-484). WB Saunders.

Cancer Genome Atlas Network, 2012. Comprehensive molecular portraits of human breast tumours. *Nature*, *490*(7418), pp.61-70.

Carey, L.A., Perou, C.M., Livasy, C.A., Dressler, L.G., Cowan, D., Conway, K., …, Deming, S.L., 2006. Race, breast cancer subtypes, and survival in the Carolina Breast Cancer Study. *Jama*, *295*(21), pp.2492-2502.

Carpenter, C.L., Duckworth, B.C., Auger, K.R., Cohen, B., Schaffhausen, B.S. and Cantley, L.C., 1990. Purification and characterization of phosphoinositide 3-kinase from rat liver. *Journal of Biological Chemistry*, *265*(32), pp.19704-19711.

Chanmee, T., Ontong, P., Konno, K. and Itano, N., 2014. Tumor-associated macrophages as major players in the tumor microenvironment. *Cancers*, *6*(3), pp.1670-1690.

Chauvin, J.M., Pagliano, O., Fourcade, J., Sun, Z., Wang, H., Sander, C., …, Zarour, H.M., 2015. TIGIT and PD-1 impair tumor antigen-specific $CD8^+$ T cells in melanoma patients. *The Journal of clinical investigation*, *125*(5), pp.2046-2058.

Cheang, M.C., Chia, S.K., Voduc, D., Gao, D., Leung, S., Snider, J., …, Perou, C.M., 2009. Ki67 index, HER2 status, and prognosis of patients with luminal B breast cancer. *Journal of the National Cancer Institute*, *101*(10), pp.736-750.

Chemnitz, J.M., Parry, R.V., Nichols, K.E., June, C.H. and Riley, J.L., 2004. SHP-1 and SHP-2 associate with immunoreceptor tyrosine-based switch motif of programmed death 1 upon primary human T cell stimulation, but only receptor ligation prevents T cell activation. *The Journal of Immunology*, *173*(2), pp.945-954.

Chen, D.S. and Mellman, I., 2013. Oncology meets immunology: the cancer-immunity cycle. *Immunity*, *39*(1), pp.1-10.

Cheng, N., Chytil, A., Shyr, Y., Joly, A. and Moses, H.L., 2008. Transforming growth factor-β signaling–deficient fibroblasts enhance hepatocyte growth factor signaling in mammary carcinoma cells to promote scattering and invasion. *Molecular Cancer Research*, *6*(10), pp.1521-1533.

Cieslewicz, M., Tang, J., Jonathan, L.Y., Cao, H., Zavaljevski, M., Motoyama, K., .., Pun, S.H., 2013. Targeted delivery of proapoptotic peptides to tumor-associated macrophages improves survival. *Proceedings of the National Academy of Sciences*, *110*(40), pp.15919-15924.

Clark, W.H., Elder, D.E., Guerry, D., Braitman, L.E., Trock, B.J., Schultz, D., Synnestvedt, M. and Halpern, A.C., 1989. Model predicting survival in stage I melanoma based on tumor progression. *Journal of the National Cancer Institute*, *81*(24), pp.1893-1904.

Clemente, C.G., Mihm, M.C., Bufalino, R., Zurrida, S., Collini, P. and Cascinelli, N., 1996. Prognostic value of tumor infiltrating lymphocytes in the vertical growth phase of primary cutaneous melanoma. *Cancer*, *77*(7), pp.1303-1310.

Coley, W.B., 1910. The treatment of inoperable sarcoma by bacterial toxins (the mixed toxins of the Streptococcus erysipelas and the Bacillus prodigiosus). *Proceedings of the Royal Society of Medicine*, *3*(Surg Sect), p.1.

Cooper, G. M., Hausman R. E., 2007. "The Development and Causes of Cancer." *The Cell: A Molecular Approach*: 743. http://www.ncbi.nlm.nih.gov/books/NBK9963/.

Cruse, J.M. and Lewis, R.E., 2002. *Illustrated dictionary of immunology*. CRC Press.

D'Cruz, C.M., Gunther, E.J., Boxer, R.B., Hartman, J.L., Sintasath, L., Moody, S.E., …, Cardiff, R.D., 2001. c-MYC induces mammary tumorigenesis by means of a preferred pathway involving spontaneous Kras2 mutations. *Nature medicine*, *7*(2), pp.235-239.

Dang, C.V., O'Donnell, K.A., Zeller, K.I., Nguyen, T., Osthus, R.C. and Li, F., 2006, August. The c-Myc target gene network. In *Seminars in cancer biology* (Vol. 16, No. 4, pp. 253-264). Academic Press.

DeNardo, D.G., Brennan, D.J., Rexhepaj, E., Ruffell, B., Shiao, S.L., Madden, S.F., …, Rugo, H.S., 2011. Leukocyte complexity predicts breast cancer survival and functionally regulates response to chemotherapy. *Cancer discovery*, *1*(1), pp.54-67.

Dent, R., Trudeau, M., Pritchard, K.I., Hanna, W.M., Kahn, H.K., Sawka, C.A., …, Narod, S.A., 2007. Triple-negative breast cancer: clinical features and patterns of recurrence. *Clinical Cancer Research*, *13*(15), pp.4429-4434.

DeSantis, C., Siegel, R. and Jemal, A., 2013. Breast cancer facts and figures 2013-2014. *American Cancer Society*, pp.1-38.

Ding, Z.C., Lu, X., Yu, M., Lemos, H., Huang, L., Chandler, P., …, Blazar, B.R., 2014. Immunosuppressive myeloid cells induced by chemotherapy attenuate antitumor CD4+ T-cell responses through the PD-1–PD-L1 axis. *Cancer research*, *74*(13), pp.3441-3453.

Downward, J., 2003. Targeting RAS signalling pathways in cancer therapy. *Nature Reviews Cancer*, *3*(1), pp.11-22.

Dunn, G.P., Old, L.J. and Schreiber, R.D., 2004. The immunobiology of cancer immunosurveillance and immunoediting. *Immunity*, *21*(2), pp.137-148.

Eck, M., Schmausser, B., Scheller, K., Brändlein, S. and MÜLLER-HERMELINK, H.K., 2003. Pleiotropic effects of CXC chemokines in gastric carcinoma: differences in

CXCL8 and CXCL1 expression between diffuse and intestinal types of gastric carcinoma. *Clinical & Experimental Immunology*, *134*(3), pp.508-515.

Efstratiadis, A., Szabolcs, M. and Klinakis, A., 2007. Notch, Myc and breast cancer. *Cell Cycle*, *6*(4), pp.418-429.

Eser, S., Schnieke, A., Schneider, G. and Saur, D., 2014. Oncogenic KRAS signalling in pancreatic cancer. *British journal of cancer*, *111*(5), pp.817-822.

Felsher, D.W., 2010. MYC inactivation elicits oncogene addiction through both tumor cell–intrinsic and host-dependent mechanisms. *Genes & cancer*, *1*(6), pp.597-604.

Fischer, C., Jonckx, B., Mazzone, M., Zacchigna, S., Loges, S., Pattarini, L., …, Autiero, M., 2007. Anti-PlGF inhibits growth of VEGF (R)-inhibitor-resistant tumors without affecting healthy vessels. *Cell*, *131*(3), pp.463-475.

Freeman, G.J., Long, A.J., Iwai, Y., Bourque, K., Chernova, T., Nishimura, H., …, Horton, H.F., 2000. Engagement of the PD-1 immunoinhibitory receptor by a novel B7 family member leads to negative regulation of lymphocyte activation. *The Journal of experimental medicine*, *192*(7), pp.1027-1034.

Fridlender, Z.G., Sun, J., Kim, S., Kapoor, V., Cheng, G., Ling, L., Worthen, G.S. and Albelda, S.M., 2009. Polarization of tumor-associated neutrophil phenotype by TGF-β:"N1" versus "N2" TAN. *Cancer cell*, *16*(3), pp.183-194.

Fridman, W.H., Galon, J., Dieu-Nosjean, M.C., Cremer, I., Fisson, S., Damotte, D., …, Sautes-Fridman, C., 2010. Immune infiltration in human cancer: prognostic significance and disease control. In *Cancer Immunology and Immunotherapy* (pp. 1-24). Springer Berlin Heidelberg.

Gazzaniga, S., Bravo, A.I., Guglielmotti, A., van Rooijen, N., Maschi, F., Vecchi, A., …, Wainstok, R., 2007. Targeting tumor-associated macrophages and inhibition of MCP-1 reduce angiogenesis and tumor growth in a human melanoma xenograft. *Journal of Investigative Dermatology*, *127*(8), pp.2031-2041.

Germano, G., Frapolli, R., Belgiovine, C., Anselmo, A., Pesce, S., Liguori, M., …, Nebuloni, M., 2013. Role of macrophage targeting in the antitumor activity of trabectedin. *Cancer cell*, *23*(2), pp.249-262.

Ghebeh, H., Mohammed, S., Al-Omair, A., Qattant, A., Lehe, C., Al-Qudaihi, G., …, Ajarim, D., 2006. The B7-H1 (PD-L1) T lymphocyte-inhibitory molecule is expressed in breast cancer patients with infiltrating ductal carcinoma: correlation with important high-risk prognostic factors. *Neoplasia*, *8*(3), pp.190-198.

Godwin, J.L., Zibelman, M., Plimack, E.R. and Geynisman, D.M., 2014. Immune checkpoint blockade as a novel immunotherapeutic strategy for renal cell carcinoma: a review of clinical trials. *Discovery medicine*, *18*(101), pp.341-350.

Gordon, S. and Mantovani, A., 2011. Diversity and plasticity of mononuclear phagocytes. *European journal of immunology*, *41*(9), pp.2470-2472.

Gordon, S. and Taylor, P.R., 2005. Monocyte and macrophage heterogeneity. *Nature Reviews Immunology*, *5*(12), pp.953-964.

Gossen, M. and Bujard, H., 1992. Tight control of gene expression in mammalian cells by tetracycline-responsive promoters. *Proceedings of the National Academy of Sciences*, *89*(12), pp.5547-5551.

Gregory, A.D. and Houghton, A.M., 2011. Tumor-associated neutrophils: new targets for cancer therapy. *Cancer research*, *71*(7), pp.2411-2416.

Gresser, I., 1987. A. Chekhov, MD, and Coley's toxins. *The New England journal of medicine*, *317*(7), pp.457-457.

Grimshaw, M.J. and Balkwill, F.R., 2001. Inhibition of monocyte and macrophage chemotaxis by hypoxia and inflammation–a potential mechanism. *European journal of immunology*, *31*(2), pp.480-489.

Gros, A., Robbins, P.F., Yao, X., Li, Y.F., Turcotte, S., Tran, E., …, Hanada, K.I., 2014. PD-1 identifies the patient-specific CD8+ tumor-reactive repertoire infiltrating human tumors. *The Journal of clinical investigation*, *124*(5), pp.2246-2259.

Hanahan, D. and Weinberg, R.A., 2011. Hallmarks of cancer: the next generation. *cell*, *144*(5), pp.646-674.

Hao, N.B., Lü, M.H., Fan, Y.H., Cao, Y.L., Zhang, Z.R. and Yang, S.M., 2012. Macrophages in tumor microenvironments and the progression of tumors. *Clinical and Developmental Immunology*, *2012*.

Herbst, R.S., Soria, J.C., Kowanetz, M., Fine, G.D., Hamid, O., Gordon, M.S., …, Kohrt, H.E., 2014. Predictive correlates of response to the anti-PD-L1 antibody MPDL3280A in cancer patients. *Nature*, *515*(7528), pp.563-567.

Green, S., Benedetti, J., Smith, A. and Crowley, J., 2012. *Clinical trials in oncology* (Vol. 28). CRC press.

Hiratsuka, S., Watanabe, A., Sakurai, Y., Akashi-Takamura, S., Ishibashi, S., Miyake, K., …, Maru, Y., 2008. The S100A8–serum amyloid A3–TLR4 paracrine cascade establishes a pre-metastatic phase. *Nature cell biology*, *10*(11), pp.1349-1355.

Hodi, F.S., O'Day, S.J., McDermott, D.F., Weber, R.W., Sosman, J.A., Haanen, J.B., .., Akerley, W., 2010. Improved survival with ipilimumab in patients with metastatic melanoma. *New England Journal of Medicine*, *363*(8), pp.711-723.

Horiuchi, D., Kusdra, L., Huskey, N.E., Chandriani, S., Lenburg, M.E., Gonzalez-Angulo, A.M., …, Yaswen, P., 2012. MYC pathway activation in triple-negative breast cancer is synthetic lethal with CDK inhibition. *The Journal of experimental medicine*, *209*(4), pp.679-696.

Goga, A., 2014. Taking on challenging targets: making MYC druggable. American Society of Clinical Oncology.

Johnston, R.J., Comps-Agrar, L., Hackney, J., Yu, X., Huseni, M., Yang, Y., …, Eaton, D.L., 2014. The immunoreceptor TIGIT regulates antitumor and antiviral CD8+ T cell effector function. *Cancer Cell*, *26*(6), pp.923-937.

Keir, M.E., Butte, M.J., Freeman, G.J. and Sharpe, A.H., 2008. PD-1 and its ligands in tolerance and immunity. *Annu. Rev. Immunol.*, *26*, pp.677-704.

Krecicki, T., Zalesska-Krecicka, M., Jelen, M., Szkudlarek, T. and Horobiowska, M., 2001. Expression of type IV collagen and matrix metalloproteinase-2 (type IV collagenase) in relation to nodal status in laryngeal cancer. *Clinical Otolaryngology & Allied Sciences*, *26*(6), pp.469-472.

Kuang, D.M., Zhao, Q., Peng, C., Xu, J., Zhang, J.P., Wu, C. and Zheng, L., 2009. Activated monocytes in peritumoral stroma of hepatocellular carcinoma foster immune privilege and disease progression through PD-L1. *The Journal of experimental medicine*, *206*(6), pp.1327-1337.

Lamm, D.L., DeHaven, J.I., Shriver, J., Crispen, R., Grau, D. and Sarosdy, M.F., 1990. A randomized prospective comparison of oral versus intravesical and percutaneous bacillus Calmette-Guerin for superficial bladder cancer. *The Journal of urology*, *144*(1), pp.65-67.

Legouy, E., DePinho, R., Zimmerman, K., Collum, R., Yancopoulos, G., Mitsock, L., Kriz, R. and Alt, F.W., 1987. Structure and expression of the murine L-myc gene. *The EMBO journal*, *6*(11), p.3359.

Leong, A.S., Cooper, K., Leong, F. and Joel, W.M., Manual of Diagnostic Cytology 2003. *Greenwich Medical Media, Ltd*, p.73.

Lewis, C.E. and Hughes, R., 2007. Microenvironmental factors regulating macrophage function in breast tumours: hypoxia and angiopoietin-2. *Breast Cancer Res*, *9*, p.209.

Lewis, C.E. and Pollard, J.W., 2006. Distinct role of macrophages in different tumor microenvironments. *Cancer research*, *66*(2), pp.605-612.

Lin, E.Y., Nguyen, A.V., Russell, R.G. and Pollard, J.W., 2001. Colony-stimulating factor 1 promotes progression of mammary tumors to malignancy. *The Journal of experimental medicine*, *193*(6), pp.727-740.

Linsley, P.S., Wallace, P.M., Johnson, J., Gibson, M.G., Greene, J.L., Ledbetter, J.A., Singh, C. and Tepper, M.A., 1992. Immunosuppression in vivo by a soluble form of the CTLA-4 T cell activation molecule. *Science*, *257*(5071), pp.792-795.

Liu, S., Lachapelle, J., Leung, S., Gao, D., Foulkes, W.D. and Nielsen, T.O., 2012. CD8+ lymphocyte infiltration is an independent favorable prognostic indicator in basal-like breast cancer. *Breast Cancer Res*, *14*(2), p.R48.

Livasy, C.A., Karaca, G., Nanda, R., Tretiakova, M.S., Olopade, O.I., Moore, D.T. and Perou, C.M., 2006. Phenotypic evaluation of the basal-like subtype of invasive breast carcinoma. *Modern pathology*, *19*(2), pp.264-271.

Lizée, G., Overwijk, W.W., Radvanyi, L., Gao, J., Sharma, P. and Hwu, P., 2013. Harnessing the power of the immune system to target cancer. *Annual review of medicine*, *64*, pp.71-90.

Mantovani, A., Sozzani, S., Locati, M., Allavena, P. and Sica, A., 2002. Macrophage polarization: tumor-associated macrophages as a paradigm for polarized M2 mononuclear phagocytes. *Trends in immunology*, *23*(11), pp.549-555.

Mantovani, A., Allavena, P., Sica, A. and Balkwill, F., 2008. Cancer-related inflammation. *Nature*, *454*(7203), pp.436-444.

McGrath, J.P., Capon, D.J., Smith, D.H., Chen, E.Y., Seeburg, P.H., Goeddel, D.V. and Levinson, A.D., 1982. Structure and organization of the human Ki-ras proto-oncogene and a related processed pseudogene. *Nature*, *304*(5926), pp.501-506.

Milliken, D., Scotton, C., Raju, S., Balkwill, F. and Wilson, J., 2002. Analysis of chemokines and chemokine receptor expression in ovarian cancer ascites. *Clinical Cancer Research*, *8*(4), pp.1108-1114.

Mittendorf, E.A., Philips, A.V., Meric-Bernstam, F., Qiao, N., Wu, Y., Harrington, S., …, Chawla, A., 2014. PD-L1 expression in triple-negative breast cancer. *Cancer immunology research*, *2*(4), pp.361-370.

Motz, G.T. and Coukos, G., 2013. Deciphering and reversing tumor immune suppression. *Immunity*, *39*(1), pp.61-73.

Movahedi, K., Laoui, D., Gysemans, C., Baeten, M., Stangé, G., Van den Bossche, J., .., Van Ginderachter, J.A., 2010. Different tumor microenvironments contain functionally distinct subsets of macrophages derived from Ly6C (high) monocytes. *Cancer research*, *70*(14), pp.5728-5739.

Murdoch, C., Giannoudis, A. and Lewis, C.E., 2004. Mechanisms regulating the recruitment of macrophages into hypoxic areas of tumors and other ischemic tissues. *Blood*, *104*(8), pp.2224-2234.

Nathan, C., 2006. Neutrophils and immunity: challenges and opportunities. *Nature Reviews Immunology*, *6*(3), pp.173-182.

O'day, S.J., Maio, M., Chiarion-Sileni, V., Gajewski, T.F., Pehamberger, H., Bondarenko, I.N., …, Verschraegen, C., 2010. Efficacy and safety of ipilimumab monotherapy in patients with pretreated advanced melanoma: a multicenter single-arm phase II study. *Annals of Oncology*, p.mdq013.

Odorizzi, P.M. and Wherry, E.J., 2012. Inhibitory receptors on lymphocytes: insights from infections. *The Journal of Immunology*, *188*(7), pp.2957-2965.

Onitilo, A.A., Engel, J.M., Greenlee, R.T. and Mukesh, B.N., 2009. Breast cancer subtypes based on ER/PR and Her2 expression: comparison of clinicopathologic features and survival. *Clinical medicine & research*, *7*(1-2), pp.4-13.

Osta, W.A., Chen, Y., Mikhitarian, K., Mitas, M., Salem, M., Hannun, Y.A., Cole, D.J. and Gillanders, W.E., 2004. EpCAM is overexpressed in breast cancer and is a potential target for breast cancer gene therapy. *Cancer research*, *64*(16), pp.5818-5824.

Pardoll, D.M. and Topalian, S.L., 1998. The role of CD4+ T cell responses in antitumor immunity. *Current opinion in immunology*, *10*(5), pp.588-594.

Pardoll, D.M., 2012. The blockade of immune checkpoints in cancer immunotherapy. *Nature Reviews Cancer*, *12*(4), pp.252-264.

Parry, R.V., Chemnitz, J.M., Frauwirth, K.A., Lanfranco, A.R., Braunstein, I., Kobayashi, S.V., …, Riley, J.L., 2005. CTLA-4 and PD-1 receptors inhibit T-cell activation by distinct mechanisms. *Molecular and cellular biology*, *25*(21), pp.9543-9553.

Pauken, K.E. and Wherry, E.J., 2014. TIGIT and CD226: tipping the balance between costimulatory and coinhibitory molecules to augment the cancer immunotherapy toolkit. *Cancer cell*, *26*(6), pp.785-787.

Pearse, G., 2006. Normal structure, function and histology of the thymus. *Toxicologic pathology*, *34*(5), pp.504-514.

Peggs, K.S., Quezada, S.A. and Allison, J.P., 2009. Cancer immunotherapy: co-stimulatory agonists and co-inhibitory antagonists. *Clinical & Experimental Immunology*, *157*(1), pp.9-19.

Pham, C.T., 2006. Neutrophil serine proteases: specific regulators of inflammation. *Nature Reviews Immunology*, *6*(7), pp.541-550.

Popescu, N.C., Amsbaugh, S.C., DiPaolo, J.A., Tronick, S.R., Aaronson, S.A. and Swan, D.C., 1985. Chromosomal localization of three humanras genes by in situ molecular hybridization. *Somatic cell and molecular genetics*, *11*(2), pp.149-155.

Pylayeva-Gupta, Y., Grabocka, E. and Bar-Sagi, D., 2011. RAS oncogenes: weaving a tumorigenic web. *Nature Reviews Cancer*, *11*(11), pp.761-774.

Robert, C., Thomas, L., Bondarenko, I., O'Day, S., Weber, J., Garbe, C., …, Davidson, N., 2011. Ipilimumab plus dacarbazine for previously untreated metastatic melanoma. *New England Journal of Medicine*, *364*(26), pp.2517-2526.

Roca, H., Varsos, Z.S., Sud, S., Craig, M.J., Ying, C. and Pienta, K.J., 2009. CCL2 and interleukin-6 promote survival of human CD11b+ peripheral blood mononuclear cells and induce M2-type macrophage polarization. *Journal of Biological Chemistry*, *284*(49), pp.34342-34354.

Rose, S., Misharin, A. and Perlman, H., 2012. A novel Ly6C/Ly6G-based strategy to analyze the mouse splenic myeloid compartment. *Cytometry Part A*, *81*(4), pp.343-350.

Sarrió, D., Rodriguez-Pinilla, S.M., Hardisson, D., Cano, A., Moreno-Bueno, G. and Palacios, J., 2008. Epithelial-mesenchymal transition in breast cancer relates to the basal-like phenotype. *Cancer research*, *68*(4), pp.989-997.

Scanlan, M.J., Simpson, A.J. and Old, L.J., 2004. The cancer/testis genes: review, standardization, and commentary. *Cancer Immunity Archive*, *4*(1), p.1.

Sharma, P., Wagner, K., Wolchok, J.D. and Allison, J.P., 2011. Novel cancer immunotherapy agents with survival benefit: recent successes and next steps. *Nature Reviews Cancer*, *11*(11), pp.805-812.

Shime, H., Matsumoto, M., Oshiumi, H., Tanaka, S., Nakane, A., Iwakura, Y., .., Seya, T., 2012. Toll-like receptor 3 signaling converts tumor-supporting myeloid cells to tumoricidal effectors. *Proceedings of the National Academy of Sciences*, *109*(6), pp.2066-2071.

Sica, A. and Bronte, V., 2007. Altered macrophage differentiation and immune dysfunction in tumor development. *The Journal of clinical investigation*, *117*(5), pp.1155-1166.

Sica, A. and Mantovani, A., 2012. Macrophage plasticity and polarization: in vivo veritas. *The Journal of clinical investigation*, *122*(3), pp.787-795.

Sierra, A., Castellsague, X., Escobedo, A., Moreno, A., Drudis, T. and Fabra, A., 1999. Synergistic cooperation between c-Myc and Bcl-2 in lymph node progression of T1 human breast carcinomas. *Breast cancer research and treatment*, *54*(1), pp.39-45.

Smith, J.A., 1994. Neutrophils, host defense, and inflammation: a double-edged sword. *Journal of leukocyte biology*, *56*(6), pp.672-686.

Smyth, M.J., Dunn, G.P. and Schreiber, R.D., 2006. Cancer immunosurveillance and immunoediting: the roles of immunity in suppressing tumor development and shaping tumor immunogenicity. *Advances in immunology*, *90*, pp.1-50.

Solovjov, D.A., Pluskota, E. and Plow, E.F., 2005. Distinct roles for the α and β subunits in the functions of integrin αMβ2. *Journal of biological chemistry*, *280*(2), pp.1336-1345.

Sotiriou, C. and Pusztai, L., 2009. Gene-expression signatures in breast cancer. *New England Journal of Medicine*, *360*(8), pp.790-800.

Sparmann, A. and Bar-Sagi, D., 2004. Ras-induced interleukin-8 expression plays a critical role in tumor growth and angiogenesis. *Cancer cell*, *6*(5), pp.447-458.

Stagg, J. and Allard, B., 2013. Immunotherapeutic approaches in triple-negative breast cancer: latest research and clinical prospects. *Therapeutic advances in medical oncology*, *5*(3), pp.169-181.

Steinman, R.M., Pack, M. and Inaba, K., 1997. Dendritic cells in the T-cell areas of lymphoid organs. *Immunological reviews*, *156*(1), pp.25-37.

Steward, L., Conant, L., Gao, F. and Margenthaler, J.A., 2014. Predictive factors and patterns of recurrence in patients with triple negative breast cancer. *Annals of surgical oncology*, *21*(7), pp.2165-2171.

Strieder, V. and Lutz, W., 2002. Regulation of N-myc expression in development and disease. *Cancer letters*, *180*(2), pp.107-119.

Talks, K.L., Turley, H., Gatter, K.C., Maxwell, P.H., Pugh, C.W., Ratcliffe, P.J. and Harris, A.L., 2000. The expression and distribution of the hypoxia-inducible factors HIF-1α and HIF-2α in normal human tissues, cancers, and tumor-associated macrophages. *The American journal of pathology*, *157*(2), pp.411-421.

Tansey, W.P., 2014. Mammalian MYC proteins and cancer. *New Journal of Science*, *2014*.

Tian, T., Olson, S., Whitacre, J.M. and Harding, A., 2011. The origins of cancer robustness and evolvability. *Integrative Biology*, *3*(1), pp.17-30.

Topalian, S.L., Hodi, F.S., Brahmer, J.R., Gettinger, S.N., Smith, D.C., McDermott, D.F., .., Leming, P.D., 2012. Safety, activity, and immune correlates of anti–PD-1 antibody in cancer. *New England Journal of Medicine*, *366*(26), pp.2443-2454.

Trzpis, M., McLaughlin, P.M., de Leij, L.M. and Harmsen, M.C., 2007. Epithelial cell adhesion molecule: more than a carcinoma marker and adhesion molecule. *The American journal of pathology*, *171*(2), pp.386-395.

Tsutsui, S., Yasuda, K., Suzuki, K., Tahara, K., Higashi, H. and Era, S., 2005. Macrophage infiltration and its prognostic implications in breast cancer: the relationship with VEGF expression and microvessel density. *Oncology reports*, *14*(2), pp.425-431.

Vasaturo, A., Blasio, S.D., Peeters, D.G., Koning, C.C., de Vries, J.M., Figdor, C.G. and Hato, S.V., 2013. Clinical implications of co-inhibitory molecule expression in the tumor microenvironment for DC vaccination: a game of stop and go.

Voduc, K.D., Cheang, M.C., Tyldesley, S., Gelmon, K., Nielsen, T.O. and Kennecke, H., 2010. Breast cancer subtypes and the risk of local and regional relapse. *Journal of Clinical Oncology*, *28*(10), pp.1684-1691.

Wislez, M., Rabbe, N., Marchal, J., Milleron, B., Crestani, B., Mayaud, C., …, Cadranel, J., 2003. Hepatocyte growth factor production by neutrophils infiltrating bronchioloalveolar subtype pulmonary adenocarcinoma role in tumor progression and death. *Cancer Research*, *63*(6), pp.1405-1412.

Wolchok, J.D., Neyns, B., Linette, G., Negrier, S., Lutzky, J., Thomas, L., .., Grob, J.J., 2010. Ipilimumab monotherapy in patients with pretreated advanced melanoma: a randomised, double-blind, multicentre, phase 2, dose-ranging study. *The lancet oncology*, *11*(2), pp.155-164.

Woo, S.R., Turnis, M.E., Goldberg, M.V., Bankoti, J., Selby, M., Nirschl, C.J., …, Liu, C.L. and Tangsombatvisit, S., 2012. Immune inhibitory molecules LAG-3 and PD-1 synergistically regulate T-cell function to promote tumoral immune escape. *Cancer research*, *72*(4), pp.917-927.

Wu, Y., Li, Y.Y., Matsushima, K., Baba, T. and Mukaida, N., 2008. CCL3-CCR5 axis regulates intratumoral accumulation of leukocytes and fibroblasts and promotes angiogenesis in murine lung metastasis process. *The Journal of Immunology*, *181*(9), pp.6384-6393.

Xu, J., Chen, Y. and Olopade, O.I., 2010. MYC and breast cancer. *Genes & cancer*, *1*(6), pp.629-640.

Yamazaki, T., Akiba, H., Iwai, H., Matsuda, H., Aoki, M., Tanno, Y., …, Azuma, M., 2002. Expression of programmed death 1 ligands by murine T cells and APC. *The Journal of Immunology*, *169*(10), pp.5538-5545.

Yao, F., Svensjö, T., Winkler, T., Lu, M., Eriksson, C. and Eriksson, E., 1998. Tetracycline repressor, tetR, rather than the tetR-mammalian cell transcription factor fusion derivatives, regulates inducible gene expression in mammalian cells. *Human gene therapy*, *9*(13), pp.1939-1950.

Yoshimura, T., Howard, O.Z., Ito, T., Kuwabara, M., Matsukawa, A., Chen, K., …, Wang, J.M., 2013. Monocyte chemoattractant protein-1/CCL2 produced by stromal cells promotes lung metastasis of 4T1 murine breast cancer cells. *PloS one*, *8*(3), p.e58791.

Zaynagetdinov, R., Sherrill, T.P., Polosukhin, V.V., Han, W., Ausborn, J.A., McLoed, A.G., …, Yull, F.E., 2011. A critical role for macrophages in promotion of urethane-induced lung carcinogenesis. *The Journal of Immunology*, *187*(11), pp.5703-5711.

Zhang, J., Lu, Y. and Pienta, K.J., 2010. Multiple roles of chemokine (CC motif) ligand 2 in promoting prostate cancer growth. *Journal of the National Cancer Institute*, *102*(8), pp.522-528.

Zhang, W., Zhu, X.D., Sun, H.C., Xiong, Y.Q., Zhuang, P.Y., Xu, H.X., …, Tang, Z.Y., 2010. Depletion of tumor-associated macrophages enhances the effect of sorafenib in metastatic liver cancer models by antimetastatic and antiangiogenic effects. *Clinical Cancer Research*, *16*(13), pp.3420-3430.

Zhong, X., Tumang, J.R., Gao, W., Bai, C. and Rothstein, T.L., 2007. PD-L2 expression extends beyond dendritic cells/macrophages to B1 cells enriched for VH11/VH12 and phosphatidylcholine binding. *European journal of immunology*, *37*(9), pp.2405-2410.

Zijlmans, H.J., Fleuren, G.J., Baelde, H.J., Eilers, P.H., Kenter, G.G. and Gorter, A., 2006. The absence of CCL2 expression in cervical carcinoma is associated with increased survival and loss of heterozygosity at 17q11. 2. *The Journal of pathology*, *208*(4), pp.507-517.

Zimmerman, K., Legouy, E., Stewart, V., Depinho, R. and Alt, F.W., 1990. Differential regulation of the N-myc gene in transfected cells and transgenic mice. *Molecular and cellular biology*, *10*(5), pp.2096-2103.